EurOtop

Manual on wave overtopping of sea defences and related structures

An overtopping manual largely based on European research, but for worldwide application

Second Edition

Errata of November 2019 to **EurOtop 2018**

Page 107. Equation 5.2 should read:

$$\frac{R_{u2\%}}{H_{m0}} = 1.0 \cdot \gamma_f \cdot \gamma_\beta \left(4.0 - \frac{1.5}{\sqrt{\gamma_b \cdot \xi_{m-1,0}}}\right) \qquad 5.2$$

with a maximum of

Page 109, Equation 5.5 should read:

$$\frac{R_{u2\%}}{H_{m0}} = 1.07 \cdot \gamma_f \cdot \gamma_\beta \left(4.3 - \frac{1.5}{\sqrt{\gamma_b \cdot \xi_{m-1,0}}}\right) \qquad 5.5$$

with a maximum of

Pages 142 and 143 should be replaced by the pages 142 and 143 in this errata. The text in red as well as Figures 5.45 and 5.46 have been modified.

Page 178. Last line before Equation 6.9 should read: …increasing angle (compare with Equation 5.29):

Wave wall on top of emerged slope or promenade (non-breaking waves on the slope)

The main improvement, however, in this manual is based on Van Doorslaer *et al.* (2015) and relates to a straight smooth seaward slope of 1:2 or 1:3 with a wave wall or storm wall on top of the slope or somewhere on a promenade, with or without bullnose. In all conditions the waves were not breaking on the slope. In order to give an overall view and an impression of the possible effects of storm walls and a bullnose, Figure 5.45 and Figure 5.46 were produced. The first figure gives all test results with the trend line for a smooth straight 1:2 or 1:3 slope as reference. Equation 5.11 in Section 5.3.1 is the average curve for overtopping, but Van Doorslaer found a little larger overtopping for a smooth slope, represented by Equation 5.44. A reason for this difference has not been established.

Figure 5.45 shows that a smooth slope gave always the largest wave overtopping and that any measure, such as a promenade, a storm wall, with or without a bullnose, reduces wave overtopping. The smallest influences are found for extending the top of the slope with a promenade only (no storm wall) and with a storm wall directly on the slope, without promenade or bullnose. Those data points are closest to the trend line for a smooth slope and mostly within the 90% confidence band. Most effective are a wall with bullnose on a slope or a wall with or without bullnose on a promenade. Those data points give often overtopping that is a factor of 10-100 smaller than for a smooth straight slope, with the same crest level.

If all the reduction factors have been applied that have been described further on in this section, it gives Figure 5.46. The test results have been analysed into great detail, leading to a graph with limited scatter around theVan Doorslaer's fit for a smooth slope. Actually, the scatter for these specific tests is significantly smaller than for the overall Equation 5.11, which is given in the graph by the 5% exceedance lines. Note that the graphs are for non-breaking waves only, as the tested seaward slopes of 1:2 and 1:3 always gave non-breaking waves and the *actual slope* was used to calculate the breaker parameter, $\xi_{m-1,0}$.
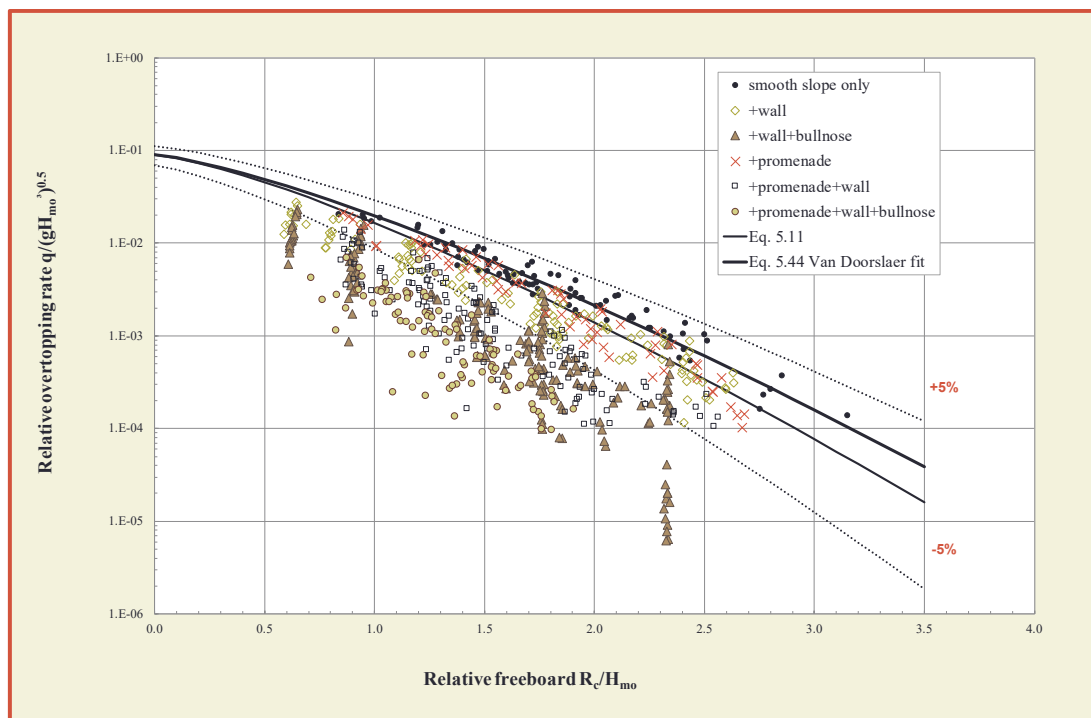

Figure 5.1.   All test results of Van Doorslaer *et al.* (2015) on wave walls with or without bullnose, without applying all reduction factors as described in this section

The range of application of a storm wall on a slope or promenade can be given as follows:
- the foot of the storm wall is above swl
- cot α = 2 - 3 (this could also be an average slope, but without the wall)
- $s_{m-1,0}$ = 0.01 – 0.05
- $\xi_{m-1,0}$ = 2.2 – 4.8 (based on the seaward slope only, this means ***non-breaking waves***)
- R_c/H_{m0} > 0.6
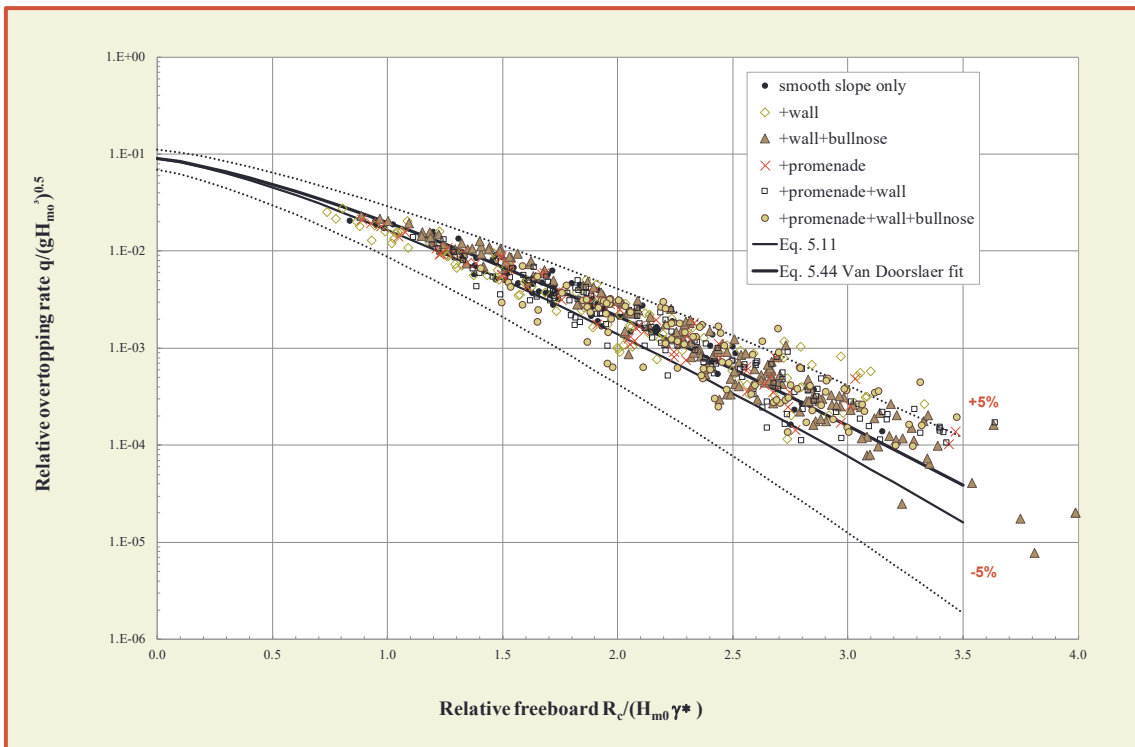- Promenade slope 1% and 2%

Figure 5.2: All test results of Van Doorslaer *et al.* (2015) on wave walls with or without bullnose, applying all reduction factors as described in this section

Influence factors or reduction coefficients are proposed for different geometrical configurations at the top of a smooth sloping dike. Such configurations can be summarized as follows:

a) smooth dike slope + storm wall;
b) smooth dike slope + storm wall and bullnose;
c) smooth dike slope + promenade;
d) smooth dike slope + promenade + storm wall;
e) smooth dike slope + promenade + storm wall and bullnose;

The influence factors are to be included in the denominator of the exponential part of the general formula for non-breaking waves. This would be Equation 5.11 for general application and Equation 5.44 in case Van Doorslaer's fit for a smooth slope is taken as reference.

$$\frac{q}{\sqrt{gH_{m0}^3}} = 0.09 \cdot exp\left(-\left[1.38\,\frac{R_c}{H_{m0}\gamma^*}\right]^{1.3}\right)$$

5.44

where γ^* is the combined influence factor that will be detailed for each configuration a) to e) above. No roughness, obliqueness or presence of a berm was used throughout the model tests. This means that $\gamma_f = \gamma_\beta = \gamma_b = 1$, but these influence factors could be applied in practice, assuming that they are also valid when a wave wall is present.

a) Smooth dike slope + storm wall ($\gamma^* = \gamma_v$)

The case of a smooth dike with a storm wall, Figure 5.47, corresponds to the situation where a vertical wall (with height h_{wall}) is built on the top of the slope of the dike. The height of this storm wall is included in the definition of the crest freeboard R_c ($R_c = A_c + h_{wall}$). The influence factor $\gamma^* = \gamma_v$ is defined as follows:

$$\gamma_v = exp\left(-0.56\,\frac{h_{wall}}{R_c}\right)$$

5.45

The EurOtop team

Authors, in alphabetical order

J.W. van der Meer   Van der Meer Consulting; UNESCO-IHE, NL; co-author and editor
N.W.H. Allsop   HR Wallingford, UK
T. Bruce   University Edinburgh, UK
J. De Rouck   Ghent University, BE
A. Kortenhaus   Ghent University, BE
T. Pullen   HR Wallingford, UK
H. Schüttrumpf   University of Aachen, DE
P. Troch   Ghent University, BE
B. Zanuttigh   University of Bologna, IT

i

Steering group, in alphabetical order

C. Altomare   Flemish Ministry of Works, BE
N. Ely   Environment Agency, UK
L. Franco   University of Roma Tre, IT
B. Hofland   Deltares and Delft University of Technology, NL
A. Tan   Environment Agency, UK
H. van der Sande   Waterschap Scheldestromen, NL
H. Verhaeghe   Flemish Ministry of Works, BE

Funding bodies

Acknowledgements

This manual replaces

EurOtop, 2007. Wave Overtopping of Sea Defences and Related Structures: Assessment Manual.

The manual may also replace sections 5.1.1.1 to 5.1.1.3 in the Rock Manual (2007)

Preferred reference

EurOtop, 2016. Manual on wave overtopping of sea defences and related structures. An overtopping manual largely based on European research, but for worldwide application. Van der Meer, J.W., Allsop, N.W.H., Bruce, T., De Rouck, J., Kortenhaus, A., Pullen, T., Schüttrumpf, H., Troch, P. and Zanuttigh, B., www.overtopping-manual.com.

Version

This version of the manual is: EurOtop 2016 Pre-release October 2016. Chapter 8 and Appendix A will be included in the final version.

Preface

Why is this Manual needed?

This Overtopping Manual gives guidance on analysis and/or prediction of wave overtopping for flood defences attacked by wave action. It is primarily, but not exclusively, intended to assist government, agencies, businesses and specialist advisors & consultants concerned with reducing flood risk. Methods and guidance described in the manual may also be helpful to designers or operators of breakwaters, reclamations, or inland lakes or reservoirs.

Developments close to the shoreline (coastal, estuarial or lakefront) may be exposed to significant flood risk yet are often highly valued. Flood risks are anticipated to increase in the future driven by projected increases of sea levels, more intense rainfall and stronger wind speeds. This risk may also increase by increasing value of assets in flood risk areas or by increasing number of people in such areas. Levels of flood protection for housing, businesses or infrastructure are inherently variable. In the Netherlands, where two-thirds of the country is below storm surge level, large urban and rural areas may presently (2016) be defended to a flood probability of 1:10,000 years or even minimum of 1:100,000 years, with less densely populated areas protected to 1:1,000 years with a minimum of 1:300 years. In the UK, where low-lying areas are much smaller, new residential developments are required to be defended to 1:200 year return.

Understanding future changes in flood risk from waves overtopping seawalls or other structures is a key requirement for effective management of coastal defences. Occurrences of economic damage or loss of life due to the hazardous nature of wave overtopping is more likely, and coastal managers and users are more aware of health and safety risks. Seawalls range from simple earth banks through to vertical concrete walls and more complex composite structures. Each of these require different methods to assess overtopping.

Reduction of overtopping risk is therefore a key requirement for the design, management and adaptation of coastal structures, particularly as existing coastal infrastructure is assessed for future conditions. There are also needs to warn or safeguard individuals potentially to overtopping waves on coastal defences or seaside promenades, particularly as recent deaths in the UK suggest significant lack of awareness of potential dangers.

The first edition of the EurOtop (2007) was well received in the coastal engineering community and has been used as code for many projects. Guidance on wave run-up and overtopping before 2007 have been provided by previous manuals in UK, Netherlands and Germany including the EA Overtopping Manual edited by Besley (EA, 1999); the TAW Technical Report on Wave run up and wave overtopping at dikes by Van der Meer (TAW, 2002); and the German Die Küste (EAK 2002). Significant new information was obtained from the EC CLASH project collecting data from several nations, and further advances from national and other European research projects.

Since EurOtop (2007), new information was established on wave overtopping over very steep slopes up to vertical, on better formulae up to zero relative freeboard, on better understanding of wave overtopping over vertical structures; including the effect of foreshores and storm walls; and on individual overtopping wave volumes. Furthermore, insight can now be given by systematic videos on how a specific overtopping discharge looks like in reality. These videos can be found on the website. This Manual takes account of this new information and advances in current practice. In so doing, this manual will extend and/or revise advice on wave overtopping predictions given in the Rock Manual (2007), the Revetment Manual by McConnell (1998), British Standard BS6349, the US Coastal Engineering Manual (2006), and ISO TC98 (2003).

iii

The Manual, Calculation Tool and Artificial Neural Network ANN

The Overtopping Manual incorporates new techniques to predict wave overtopping at seawalls, flood embankments, breakwaters and other shoreline structures. The manual includes case studies and example calculations. The manual has been intended to assist coastal engineers analyse overtopping performance of most types of sea defence found around Europe. The methods in the manual can be used for current performance assessments and for longer-term design calculations. The manual defines types of structure, provides definitions for parameters, and gives guidance on how results should be interpreted. A chapter on hazards gives guidance on tolerable discharges and overtopping processes, including videos on overtopping discharges. Further discussion identifies the different methods available for assessing overtopping, such as empirical, physical and numerical techniques.

In parallel with this manual, an online Calculation Tool has been developed to assist the user through a series of steps to establish overtopping predictions for: embankments and dikes; rubble mound structures; and vertical structures. By selecting an indicative structure type and key structural features, and by adding the dimensions of the geometric and hydraulic parameters, the mean overtopping discharge will be calculated. Where possible additional results for overtopping volumes, flow velocities and depths, and other pertinent results will be given.

Also in parallel with this manual an Artificial Neural Network, called the EurOtop ANN, will be available that is able to predict mean overtopping discharge for all kind of structure geometries, given by a number of hydraulic and geometrical parameters as input. It is based on a large extended database that contains more than 13,000 tests on wave overtopping. In the course of time other predicting neural networks may also become available.

Intended use

The manual has been intended to assist engineers who are already aware of the general principles and methods of coastal engineering. The manual uses methods and data from research studies around Europe and overseas so readers are expected to be familiar with wave and response parameters and the use of empirical equations for prediction. Users may be concerned with existing defences, or considering possible rehabilitation or new-build.

This manual is not, however, intended to cover many other aspects of the analysis, design, construction or management of sea defences for which other manuals and methods already exist, see for example the CIRIA / CUR / CETMEF Rock Manual (2007), the Beach Management Manual by Brampton et al (2002) and TAW and ENW guidelines in the Netherlands on design of sea, river and lake dikes.

What next?

It is clear that increased attention to flood risk reduction, and to wave overtopping in particular, have increased interest and research in this area. This updated comprehensive manual is an example of that with guidance on many topics related to wave overtopping. We hope that the user may accept and use it with pleasure.

The Authors and Steering Committee
October 2016

Contents

v

vii

1   Introduction

1.1   Background

This manual describes methods to predict wave overtopping of sea defences and related coastal or shoreline structures. It recommends approaches for calculating mean overtopping discharges, overtopping wave volumes and the proportion of waves overtopping a seawall. The manual will help engineers to establish limiting tolerable discharges or overtopping wave volumes for design wave conditions, and then use the prediction methods to confirm that these discharges are not exceeded.

1.1.1   Previous and related manuals

The first edition of the EurOtop (2007) was well received in the coastal engineering community and has now been accepted as industry standard. That manual was developed from, at least in part, three manuals: the (UK) Environment Agency Manual on Overtopping edited by Besley (EA, 1999); the (Netherlands) TAW Technical Report on Wave run-up and wave overtopping at dikes, edited by Van der Meer (TAW, 2002); and the German Die Küste (EAK, 2002) edited by Erchinger. The EurOtop (2007) manual was intended to revise, extend and develop the parts of those manuals discussing wave run-up and overtopping.

Since EurOtop (2007) new techniques were developed on wave overtopping over very steep slopes up to vertical, on improved formulae up to zero relative freeboard, on improved understanding of wave overtopping over vertical structures including the effect of foreshores and storm walls, and on individual overtopping wave volumes. Furthermore, insight can now be given by systematic videos on how a specific overtopping discharge looks like in reality. These videos can be found on the website. This Manual takes account of this new information and advances in current practice. In so doing, this manual will also extend and/or revise advice on wave overtopping predictions given in the Rock Manual (2007), the Revetment Manual by McConnell (1998), British Standard BS6349, the US Coastal Engineering Manual (2006), and ISO TC98 (2003).

1.1.2   Sources of material and contributing projects

In addition to the earlier manuals discussed in Section 1.1.1, new methods and data have been derived from a number of European and national research programmes. The main contributions to the first manual, EurOtop (2007), were from OPTICREST; PROVERBS; CLASH, VOWS and Big-VOWS and partly ComCoast. New information for this second version came through the extended testing with the wave run-up and overtopping simulators in the Netherlands, but also through, sometimes voluntary and not funded, cooperations between the authors. Examples are cooperation between Bruce and Van der Meer on new wave overtopping formulae, and Zanuttigh and Van der Meer on extending the CLASH database and developing a better and extended artificial neural network for prediction of wave overtopping, transmission and reflection. Infram in the Netherlands is acknowledged for providing the systematic videos on wave overtopping discharges, available on the website. Everything given in this manual is supported by research papers and manuals described in the bibliography.

1.2   Use of this manual

The manual has been intended to assist an engineer analyse the overtopping performance of any type of sea defence or related shoreline structure found around the world. The manual uses the results of research studies around Europe and further overseas to predict wave overtopping discharges, number of overtopping waves, and the distributions of overtopping wave volumes. It is envisaged that methods described here may be used for current performance assessments, and for longer-term design calculations. Users may be concerned with existing defences, or considering possible rehabilitation or new-build.

The analysis methods described in this manual are primarily based upon a deterministic approach in which overtopping discharges (or other responses) are calculated for wave and water level conditions

representing an event with a given return period. All of the design equations require data on water levels and wave conditions at the toe of the defence structure. The input water level should include a tidal and, if appropriate, a surge component. Surges are usually comprised of components including wind set-up and barometric pressure. Input wave conditions should take account of nearshore wave transformations, including shoaling and breaking. Methods of calculating depth-limited wave conditions are outlined in Chapter 2.

All of the prediction methods given in this report have intrinsic limitations to their accuracy. For empirical equations derived from physical model data, account should be taken of the inherent scatter. This scatter, or reliability of the equations, has been described where possible or available and often equations for design and assessment use are given where some safety has been taken into account. Still it can be concluded that overtopping rates calculated by empirically derived equations, should only be regarded as being within, at best, a factor of 1 - 3 of the actual overtopping rate. This means that the actual overtopping rate could be three times smaller as well as three times larger than the predicted mean value. The largest deviations will be found for small overtopping discharges. The 90%-confidence band is often given in graphs.

As, however, many practical structures depart (at least in part) from the idealised versions tested in hydraulics laboratories, and it is known that overtopping rates may be very sensitive to small variations in structure geometry, local bathymetry and wave climate. It is generally accepted that empirical methods based upon model tests conducted on generic structural types, such as vertical walls, armoured slopes etc. may lead to large differences in overtopping performance. The methods presented here, in general, will not predict overtopping performance with the same degree of accuracy as structure-specific model tests. In case of very specific structures, Artificial Neural Network Tools may give a fair prediction of overtopping, at least as good as the formulae.

This manual is not, however, intended to cover all aspects of the analysis, design, construction or management of sea defences for which other manuals and methods already exist, see for example the Rock Manual (2007), British Standards BSI (2000), Simm *et al.* (1996), Brampton *et al.* (2002) and TAW or ENW guidelines in the Netherlands on design of sea, river and lake dikes. The manual has been kept deliberately concise in order to maintain clarity and brevity. For the interested reader a full set of references is given so that the reasoning behind the development of the recommended methods can be followed.

1.3   Principal types of structures

Wave overtopping is of principal concern for structures constructed primarily to defend against flooding: often termed sea defence. Somewhat similar structures may also be used to provide protection against coastal erosion: sometimes termed coast protection. Other structures may be built to protect areas of water for ship navigation or mooring: ports, harbours or marinas; these are often formed as breakwaters or moles. Whilst some of these types of structures may be detached from the shoreline, sometimes termed offshore, nearshore or detached, most of the structures used for sea defence form a part of the shoreline.

This manual is primarily concerned with the three principal types of sea defence structures: sloping sea dikes and embankment seawalls; armoured rubble slopes and mounds; and vertical, battered or steep walls.

Historically, sloping dikes have been the most widely used option for sea defences along the coasts of the Netherlands, Denmark, Germany and many parts of the UK. Dikes or embankment seawalls have been built along many Dutch, Danish or German coastlines protecting the land behind from flooding, and sometimes providing additional amenity value. Similar structures in UK may alternatively be formed by clay materials or from a vegetated shingle ridge, in both instances allowing the side slopes to be steeper. All such embankments will need some degree of protection against direct wave erosion, generally using a revetment facing on the seaward side. Revetment facing may take many forms, but may commonly include closely-fitted concrete blockwork, cast in-situ concrete slabs, or asphaltic materials. Embankment or dike structures are generally most common along rural frontages.

A second type of coastal structure consists of a mound or layers of quarried rock fill, protected by rock or concrete armour units. The outer armour layer is designed to resist wave action without significant displacement of armour units. Under-layers of quarry or crushed rock support the armour and separate it from finer material in the embankment or mound. These porous and sloping layers dissipate a proportion of the incident wave energy in breaking and friction. Simplified forms of rubble mounds may be used for rubble seawalls or protection to vertical walls or revetments. Rubble mound revetments may also be used to protect embankments formed from relic sand dunes or shingle ridges. Rubble mound structures tend to be more common in areas where harder rock is available.

Along urban frontages, especially close to ports, erosion or flooding defence structures may include vertical (or battered / steep) walls. Such walls may be composed of stone or concrete blocks, mass concrete, or sheet steel piles. Typical vertical seawall structures may also act as retaining walls to material behind. Another type of vertical structure is the caisson, often used as a breakwater to protect a harbour area. Shaped and recurved wave return walls may be formed as walls in their own right, or smaller versions may be included in sloping structures. Some coastal structures are relatively impermeable to wave action. These include seawalls formed from blockwork or mass concrete, with vertical, near vertical, or steeply sloping faces. Such structures may be liable to intense local wave impact pressures, may overtop suddenly and severely, and will reflect much of the incident wave energy. Reflected waves cause additional wave disturbance and/or may initiate or accelerate local bed scour.

1.4   Definitions of key parameters and principal responses

Overtopping discharge occurs because of waves running up the face of a seawall or dike. If wave run-up levels are high enough water will reach and pass over the crest of the structure. This defines the 'green water' overtopping case where a continuous sheet of water passes over the crest. In cases where the structure is vertical, the wave may impact against the wall and send a vertical plume of water over the crest.

A second form of overtopping occurs when waves break on the seaward face of the structure and produce significant volumes of splash. These droplets may then be carried over the wall either under their own momentum or as a consequence of an onshore wind.

Another less important method by which water may be carried over the crest is in the form of spray generated by the action of wind on the wave crests immediately offshore of the wall. Even with strong wind the volume is not large and this spray will not contribute to any significant overtopping volume.

Overtopping rates predicted by the various empirical formulae described within this manual will include green water discharges and splash, since both these parameters were recorded during the model tests on which the prediction methods are based. The effect of wind on this type of discharge will not have been modelled. Model tests suggest that onshore winds have little effect on large green water events, however they may increase discharges under 1 l/s per m. Under these conditions, the water overtopping the structure is partly spray and therefore the wind is strong enough to blow water droplets inshore.

In the list of symbols, short definitions of the parameters used have been included. Some definitions are so important that they are explained separately in this section as key parameters. The definitions and validity limits are specifically concerned with application of the given formulae. In this way, a structure section with a slope of 1:12 is not considered as a real slope (too gentle) and it is not a real berm too (too steep). In such a situation, wave run-up and overtopping can only be calculated by interpolation. For example, for a cross-section with a part having a slope of 1:12, interpolation can be made between a slope of 1:8 (mildest slope) and a 1:15 berm (steepest berm).

1.4.1 Wave height

The wave height used in the wave run-up and overtopping formulae is the incident significant wave height H_{m0} at the toe of the structure, called the spectral wave height, $H_{m0} = 4(m_0)^{1/2}$. Another definition of significant wave height is the average of the highest third of the waves, $H_{1/3}$. This wave height is, in principle, not used in this manual, unless formulae were derived on the basis of it. In deep water, both

definitions produce almost the same value, but situations in shallow water can lead to differences of 10-15%. There are however not enough tests on overtopping available where there is a large difference in wave heights using both definitions. The choice for H_{m0} was mainly based on the fact that design wave heights are often predicted by numerical models, giving this wave height.

The significant wave height H_s is often used for H_{m0} as well as $H_{1/3}$. In this manual H_{m0} has consequently been used.

In many cases, a foreshore is present on which waves can shoal and break and by which the significant wave height is reduced. There are models that in a relatively simple way can predict the reduction in energy due to breaking and thereby the accompanying wave height at the toe of the structure. The wave height must be calculated over the total spectrum including any long-wave energy present. Based on the spectral significant wave height, it is reasonably simple to calculate a wave height distribution and accompanying significant wave height $H_{1/3}$ using the method of Battjes and Groenendijk (2000).

Recent studies have shown that long waves caused by wave breaking may become very important for wave overtopping prediction. This is certainly the case if the foreshore is relatively steep, say steeper than 1:50, and the water depth at the structure in reality reduces to a few decimetres (prototype). In such a case the short wave spectrum may completely disappear and transform to a long wave spectrum with peak periods of one minute or more. These kind of circumstances are not yet fully understood, not by numerical modelling, nor by wave flume experiments. The manual gives guidance for very shallow water with long waves developing, but one should not rely completely on the given formulae in this manual and consider physical model tests.

1.4.2 Wave period

Various wave periods can be defined for a wave spectrum or wave record. Conventional wave periods are the peak period T_p (the period that gives the peak of the spectrum), the average period T_m (calculated from the spectrum but preferably from the wave record) and the significant period $T_{1/3}$ (the average of the highest 1/3 of the waves). The relationship T_p/T_m usually lies between 1.1 and 1.25, and T_p and $T_{1/3}$ are almost identical.

The wave period used for some wave run-up and overtopping formulae is the spectral period $T_{m-1,0} = m_{-1}/m_0$. This period gives more weight to the longer periods in the spectrum than an average period and, independent of the type of spectrum, gives similar wave run-up or overtopping for the same values of $T_{m-1,0}$ and the same wave heights. In this way, wave run-up and overtopping can be easily determined for bimodal and 'flattened' spectra, without the need for other difficult procedures.

In the case of a uniform (single peaked) spectrum there is a fairly fixed relationship between the spectral period $T_{m-1,0}$ and the peak period. In this report a conversion factor $T_p = 1.1\,T_{m-1,0}$ is given for the case where the peak period is known or has been determined, but not the spectral period.

For very shallow foreshores, where the waves break to a very large extent, the wave period $T_{m-1,0}$ may be largely based on long waves and may become much longer than usual wave periods with less or no breaking (minutes or more).

1.4.3 Wave steepness and breaker parameter

Wave steepness is defined as the ratio of wave height to wavelength (e.g. $s_0 = H_{m0}/L_0$). This will tell us something about the wave's history and characteristics. Generally a steepness of $s_0 = 0.01$ indicates a typical swell sea and a steepness of $s_0 = 0.04$ to 0.06 a typical wind sea. Swell seas will often be associated with long period waves, where it is the period that becomes the main parameter that affects overtopping.

But also wind seas may become seas with low wave steepness if the waves break on a gentle foreshore. By wave breaking the wave period initially does not change much, but the wave height decreases. This leads to a lower wave steepness. A low wave steepness on relatively deep water means swell waves, but for depth limited locations it often means broken waves on a (gentle) foreshore.

The breaker parameter, surf similarity or Iribarren number is defined as $\xi_{m-1,0} = \tan\alpha/(H_{m0}/L_{m-1,0})^{\frac{1}{2}}$, where α is the slope of the front face of the structure and $L_{m-1,0}$ being the deep water wave length $gT^2_{m-1,0}/(2\pi)$. Note that the actual wavelength near the toe of the structure is not used, but the deep water wavelength, using the wave period at the toe of the structure. The calculated wave steepness, therefore, is a notional wave steepness and is used to calculate a "dimensionless wave period", rather than the actual wave steepness.

The combination of structure slope and wave steepness gives a certain type of wave breaking, see Figure 1.1. For $\xi_{m-1,0} > {\sim}2$ waves are considered not to be breaking (surging waves), although there may still be some breaking, and for $\xi_{m-1,0} < {\sim}2$ waves are breaking. For wave run-up on slopes the transition from plunging to surging is given in this manual at $\xi_{m-1,0} = 1.8$, which is very close to a value of 2. Waves on a gentle foreshore break as spilling waves and more than one breaker line can be found on such a foreshore, see Figure 1.2. Plunging waves break with steep and overhanging fronts and the wave tongue will hit the structure or back washing water; an example is shown in Figure 1.3. The transition between plunging waves and surging waves is known as collapsing. The wave front becomes almost vertical and the water excursion on the slope (wave run-up + run-down) is often larger for this kind of breaking. Values are given for the majority of the larger waves in a sea state. Individual waves may still surge for generally plunging conditions or plunge for generally surging conditions.
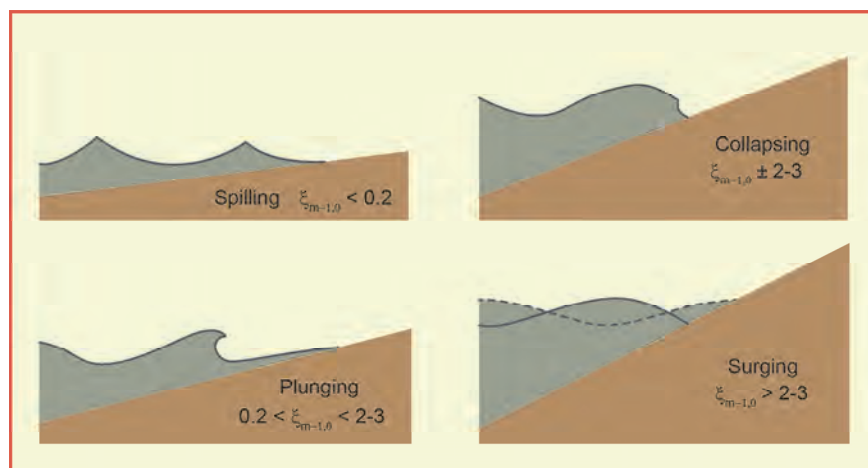
Figure 1.1:   Type of breaking on a slope

Figure 1.2:   Spilling waves on a beach; $\xi_{m-1,0} < 0.2$

Figure 1.3: Plunging waves; $\xi_{m-1,0} < 2.0$

1.4.4 Parameter h*, d* and EurOtop (2007)

EurOtop (2007) used two combination parameters that have been changed in this manual to parameter groups with explicit parameters as water depth, wave height and wave length or even wave steepness. These are the h* and d* parameter. In order to distinguish between non-impulsive waves structure and impulsive waves on a vertical, the parameter h* has been defined and for vertical walls with berms or toe mounds in front, the d*.

$$h_* = 1.35 \frac{h}{H_{m0}} \frac{h}{L_{m-1,0}} \quad \text{and} \quad d_* = 1.35 \frac{d}{H_{m0}} \frac{h}{L_{m-1,0}} \qquad 1.1$$

The parameters describe two ratios together, the wave height and wave length, both made relative to the local water depth h in front of the toe of the structure, or water depth above berm or toe mound, d. Non-impulsive waves predominate when h* or d* > 0.3; impulsive waves when h* or d* ≤ 0.3. Formulae for impulsive overtopping on vertical structures, originally in EurOtop (2007) used these h* or d* parameter to some power, both for the dimensionless wave overtopping and dimensionless crest freeboard. These parameters are no longer used in those predictions, but the parameter groups are still used to identify the switch from non-impulsive to impulsive wave conditions. The parameter groups that are used now in the predictions are $h^2/(H_{m0} L_{m-1,0})$ and $h \cdot d/(H_{m0} L_{m-1,0})$.

1.4.5 Toe of structure

In most cases, it is clear where the toe of the structure lies, and that is where the foreshore meets the front slope of the structure or the toe structure in front of it. For vertical walls, it will be at the base of the principal wall, or if present, at the rubble mound toe in front of it. It is possible that a sandy foreshore varies with season and even under severe wave attack. Toe levels may therefore vary during a storm, with maximum levels of erosion occurring during the peak of the tidal / surge cycle. It may therefore be necessary to consider the effects of increased wave heights due to the increase in the toe depth. The wave height that is always used in wave overtopping calculations is the incident wave height at the toe. This may be different if the toe of the structure is *above* the still water level as a wave height can then not be defined. An example of such a (vertical) structure is given in Section 7.3.2.

1.4.6 Foreshore

The foreshore is the section in front of the breakwater, coastal structure or sea wall and can be horizontal or up to a maximum slope of 1:10. The foreshore can be deep, shallow or very shallow. If the water is shallow or very shallow then shoaling and depth limiting effects will need to be considered so that the wave height at the toe, or end of the foreshore, can be considered as well as the wave period. A foreshore is defined as having a minimum length of one wavelength $L_{m-1,0}$.

A precise transition from a shallow to a very shallow foreshore is hard to give. At a shallow foreshore waves break and the wave height decreases, but the wave spectrum will retain more or less the shape of the incident wave spectrum. At very shallow foreshores the spectral shape changes drastically and hardly any peak can be detected (flat spectrum). As the waves become very small due to breaking many different wave periods arise. Moreover, long waves caused by breaking may result in a spectrum with wave periods of one minute or more. The effect of these kind of conditions on wave overtopping is not yet well understood. Guidance is given in this manual, but there is not much guidance for steep foreshore slopes with very small water depths at the toe of the structure.

In general, the transition between shallow and very shallow foreshores can be indicated as the point where the original incident wave height, due to breaking, has been decreased by 50% or more. The wave height at a structure on a very shallow foreshore is much smaller than in deep water situations. This means that the wave steepness (Section 1.4.3) becomes much smaller, too. Consequently, the breaker parameter, which is used in the formulae for wave run-up and wave overtopping, becomes much larger. Values of $\xi_0 = 4$ to 10 for the breaker parameter are then possible, where maximum values for a gentle slope of 1:3 or 1:4 are normally smaller than say $\xi_0 = 2$ or 3. The wave steepness will then often be smaller than $s_{m-1,0} = 0.01$ and gives a good indication that there might be a shallow or very shallow foreshore.

In Chapter 7 on vertical structures, a division has been made between vertical structures "without an influencing foreshore" and structures with a sloping influencing foreshore. This needs a little more explanation as in principle every coastal structure has a foreshore. A vertical wall may be found at the end of a sloping foreshore and then represent a seawall, often with more or less depth limited waves. A vertical wall with no influencing foreshore is mainly characterised by an (almost) horizontal foreshore and relatively deep water compared to the wave height. In physical models the "foreshore" will then probably be the bottom of the wave flume or basin.

Three examples are given here for situations with a vertical wall without influencing foreshore. First a flood wall in a harbour, where waves are relatively small with respect to the water depth for storm flood situations in the harbour. Secondly, a caisson breakwater founded on a berm, but where the berm is often well below the water level and the berm is too small to affect the waves. Vertical walls may also have some form of bull nose or wave return wall. And as third, lock gates or similar during high water level conditions may also be considered as a vertical wall without influencing foreshore or berm, this is because the wave height may be very small compared to the water depth.

1.4.7 Slope

Part of a structure profile is defined as a slope if the slope of that part lies between 1:1 and 1:8. These limits are also valid for an average slope, which is the slope that occurs when a line is drawn between -1.5 H_{m0} and +$R_{u2\%}$ in relation to the still water line and berms are not included. Here $R_{u2\%}$ is the run-up level on the slope, which is only exceeded by 2% of the incident waves. A continuous slope of between 1:8 and 1:10 can be calculated in first instance using the formulae for simple slopes, but the reliability is less than for steeper slopes. In this case interpolation between a slope 1:8 and a berm 1:15 is not possible as a berm is a gentle slope in between steeper parts and not a continuous slope.

A structure slope steeper than 1:1, but not vertical, can be considered as a battered wall. These are treated in Chapter 7 as a complete structure. If it is only a wave wall on top of gentle sloping dike, it is treated in Chapter 5.

1.4.8 Berm and promenade

A berm is part of a structure profile in which the slope varies between horizontal and 1:15. The position of the berm in relation to the still water line is determined by the depth, d_b, the vertical distance between the middle of the berm and the still water line. The width of a berm, B, may not be greater than one-quarter of a wavelength, i.e., B < 0.25 $L_{m-1,0}$. If the width is greater, then the structure part is considered as a combination of a berm and a foreshore, and wave run-up and overtopping can be calculated by interpolation. Section 5.4.6 gives a more detailed description.

A berm is often situated on a sloping structure like a dike or levee and near design water level, as that is the location where the berm is most effective. A berm creates a gentler "equivalent slope", which may lead to a lower crest level than a similar structure without berm.

Almost horizontal slopes are also found at promenades, such as along the Belgian North Sea coast, and are then situated at a much higher level than a berm in a sloping structure. The promenade itself may actually be the crest level, but if a storm wall is present on top of the promenade, it will be the crest level of the storm wall. Then the promenade is a significant part of the water defence structure and is described by the width G_c. Section 5.4.7 gives examples of promenades with and without storm walls.

1.4.9 Crest freeboard, armour freeboard and width

The crest height of a structure, relative to the water level is defined as the crest freeboard, R_c. It is actually the point on the structure where overtopping water can no longer flow back to the seaside. For rubble mound structures, it is often the top of a crest element and not the height of the rubble mound armour.

The armour freeboard, A_c, is the height of a horizontal part of the crest, measured relative to SWL. The horizontal part of the crest is called G_c. For rubble mound slopes the armour freeboard, A_c, may be higher, equal or sometimes lower than the crest freeboard, R_c, Figure 1.4. For wave overtopping calculations it is best to take the maximum of R_c and A_c, although this may lead to a slight under estimation of the wave overtopping if A_c is larger than R_c as in the graph. This is because some water may go through the upper part of the rock and add. But this is still better than using the smaller R_c as this may lead to quite large over estimation of wave overtopping.
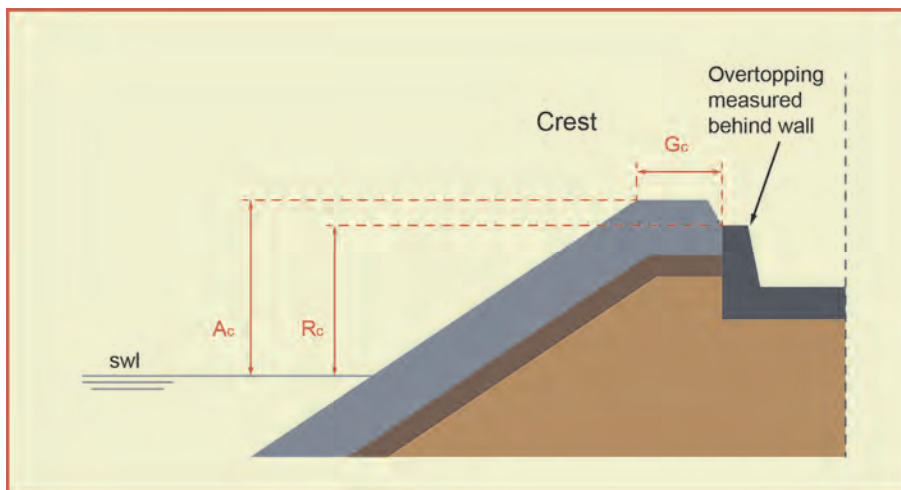
Figure 1.4:   Crest freeboard different from armour freeboard. R_c can also be equal or larger than A_c.

The effect of a permeable crest on wave overtopping is not easy to estimate. Figure 1.5 shows such a crest. The quarry stone armour layer is itself completely water permeable, so that the up-rushing waves may generate wave overtopping over the crest as well as through the permeable layer. The crest height that must be taken into account during calculations for wave overtopping for an upper slope with quarry stone, but without a wave wall, is not the highest level, A_c (that would give too less overtopping), nor the lower level of R_c (that would give too much overtopping). It is proposed to take the average of R_c and A_c for cases as in Figure 1.5 without a wave wall. With wave wall the maximum of R_c and A_c must be taken.
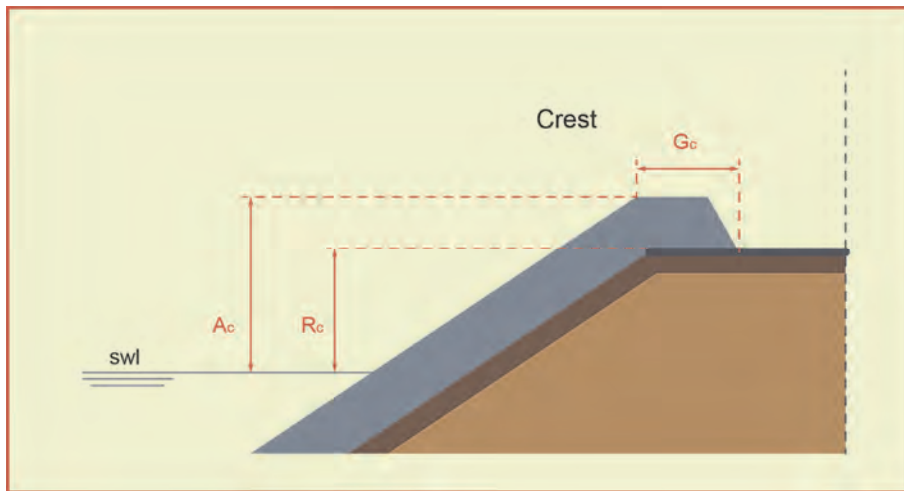
Figure 1.5:   Crest with a permeable layer and no crest element present: take the average of R_c and A_c

The crest of a smooth dike or embankment without any wave wall, is assumed to be horizontal and of limited width. Then the width of the crest has no influence on overtopping discharge. But in reality the crest in many cases is not completely horizontal, but slightly rounded and of a certain width. This is not taken into account for smooth impermeable crests. The crest height at a dike or embankment, R_c, is defined as the height of the seaward crest line (transition from seaward slope to crest). This definition therefore is used for wave run-up and overtopping. In principle the width of the crest and the height of the middle of the crest have no influence on calculations for wave overtopping, which also means that $R_c = A_c$ is assumed (no wave walls) and that $G_c = 0$. Of course, the width of the crest, if it is very wide, can have an influence on the actual wave overtopping. This procedure is of course a little conservative.

If an impermeable slope or a vertical wall have a horizontal crest with at the rear a wave wall, then the height of the wave wall determines R_c and the height of the horizontal part determines A_c, see Figure 1.6. For promenades as well as crests at vertical or sloping structures, the horizontal part is given by G_c.
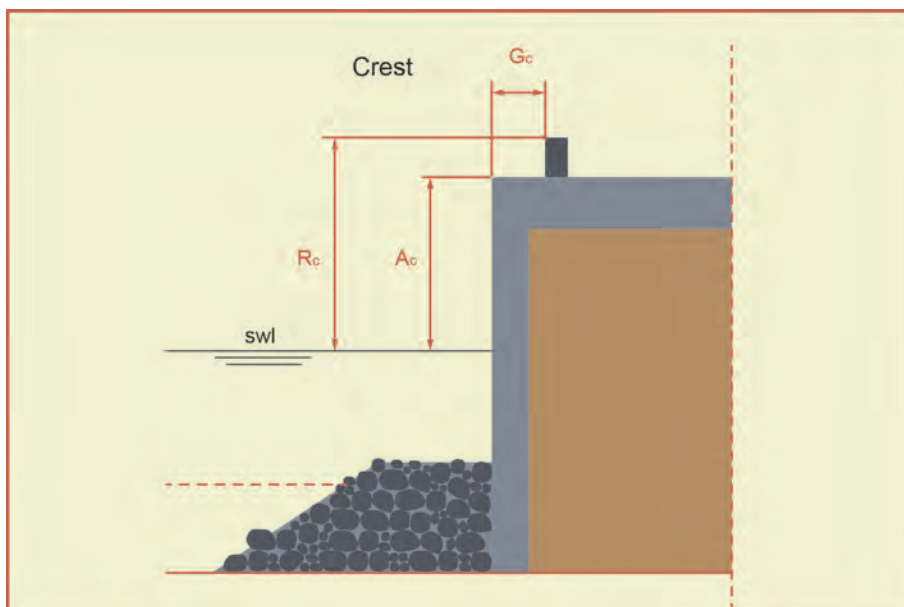
Figure 1.6:   Crest configuration for a vertical wall

1.4.10 Bullnose or wave return wall

Waves at vertical walls may give vertically up-rushing water that then may partly overtop over the crest and partly fall back into the water. In order to decrease the overtopping water often a bullnose/parapet or wave return wall has been designed. It is always a structure that is situated at the top of the vertical wall and the intention is to return the up-rushing wave seawards, decreasing overtopping. There are no real guidelines on how such a structure should geometrically be designed, but the size of the structure has large influence on the effect on wave overtopping.

A bullnose is a relatively small structure compared to the size of the vertical wall and the governing waves. Figure 1.7 gives such an example at a high crest wall on a caisson (at the picture the deck and crest wall of the caisson are under construction). In this particular case there are no impulsive waves and up-rushing water along the vertical wall that reaches the bullnose will be fairly limited and is easily directed seawards. A bullnose may have significant effect on wave overtopping if it is situated fairly high above the water level. If not, a large overtopping wave will easily overtop and will not "feel" the small structure. This manual gives guidance for this type of relatively small bullnose in Section 7.3.6.

Figure 1.7:   A relatively small bull nose on the crest wall of a large caisson. The caisson under construction, Açu, Brasil, is 25 m wide and the crest level is 10 m above sea level

Figure 1.8:   Effective fairly significant bullnose at Cascais, Portugal. Waves are breaking on the foreshore and give impulsive wave conditions. There was no wind. Courtesy L. Franco

A quite significant bullnose is given in Figure 1.8, where impulsive conditions from swell waves jump high into the air and are well returned seawards. A small bullnose like in Figure 1.7 would have a much smaller effect. Section 7.3.6 gives guidance for larger bullnoses, based on basic research.

A very significant wave return wall may also be designed with the purpose of limiting wave overtopping as much as possible, as well as keeping the crest level of the seawall to a minimum. In that case it is not any longer called a bullnose. A good example is shown in Figure 1.9, where a vertical seawall has to protect a city centre against flooding. As the wall is visually already quite high the owner of the seawall wanted to minimise this height. The multi-functional use was created by designing a large, almost horizontal, wave return wall (lower left picture) as part of a promenade (top picture). Even with a high design water level most of the waves could not overtop the structure during model testing (lower right picture).

The manual does not give direct guidance on overtopping for these large wave return walls, but the predicting Artificial Neural Network (Section 4.5) will give a fairly good prediction as the tool was also trained on these kind of structures. One should also note that a wave return wall increases wave forces on the wall.

Figure 1.9:   Large and effective wave return wall at Harlingen (NL). The wave return wall is part of a promenade on top of the wall (picture above). Lower left: the wall with wave return wall in reality; lower right: model testing under design wave conditions

A bullnose may also be applied at a storm wall on a promenade and reduces wave overtopping significantly. Guidance on these kind of structures is given in Section 5.4.7.

1.4.11 Permeability, porosity and roughness

A smooth structure like a dike or embankment is mostly impermeable for water or waves and the slope has no, or almost no roughness. Examples are embankments covered with a placed block revetment, an asphalt or concrete slope and a grass cover on clay. Roughness on the slope will dissipate wave energy during wave run-up and will therefore reduce wave overtopping. Roughness is created by irregularly shaped block revetments or artificial ribs or blocks on a smooth slope.

A rubble mound slope with rock or concrete armour is also rough and in general more rough than impermeable dikes or embankments with artificial roughness elements. But there is another difference, as the permeability and porosity is much larger for a rubble mound structure. Porosity is defined as the percentage of voids between the units or particles. Actually, loose materials always have some porosity. For rock and concrete armour the porosity may range roughly between 30% - 55%. But also sand has a comparable porosity. Still the behaviour of waves on a sand beach or a rubble mound slope is different.

This difference is caused by the difference in permeability. The armour of rubble mound slopes is very permeable and waves will easily penetrate between the armour units and dissipate energy. But this becomes more difficult for the under layer and certainly for the core of the structure. Difference is made between "impermeable under layers or core" and a "permeable core". In both cases the same armour layer is present, but the structure and under layers differ.

12

A rubble mound breakwater often has an under layer of large rock (about one tenth of the weight of the armour), sometimes a second under layer of smaller rock and then the core of still smaller rock. Up-rushing waves can penetrate into the armour layer and will then sink into the under layers and core. This is a structure with a "permeable core".

An embankment can also be covered by an armour layer of rock. The under layer is often small and thin and placed on a geotextile. Underneath the geotextile sand or clay may be present, which is impermeable for up-rushing waves. Such an embankment covered with rock has an "impermeable core". Run-up and wave overtopping are dependent on the permeability of the core.

In summary, the following types of structures can be described:

Smooth dikes and embankments:	smooth and impermeable
Dikes and embankments with rough slopes:	some roughness and mostly impermeable
Rock cover on an embankment:	rough with impermeable core
Rubble mound breakwater:	rough with permeable core

1.4.12 Wave run-up height

The wave run-up height is given by $R_{u2\%}$. This is the wave run-up level, measured vertically from the still water line, which is exceeded by 2% of the number of incident waves. The number of waves exceeding this level is hereby related to the number of incoming waves and not to the number that runs up the slope.

A very thin water layer in a run-up tongue cannot be measured accurately. In model studies on smooth slopes the limit is often reached at a water layer thickness of 2 mm. For prototype waves this means a layer depth of about 2 cm, depending on the scale in relation to the model study. Very thin layers on a smooth slope can be blown a long way up the slope by a strong wind, a condition that can also not be simulated in a small scale model. Running-up water tongues less than 2 cm thickness actually contain very little water. Therefore it is suggested that the wave run-up level on smooth slopes is determined by the level at which the water tongue becomes less than 2 cm thick. Thin layers blown onto the slope are not seen as wave run-up.

Run-up is relevant for smooth slopes and embankments and sometimes for rough slopes armoured with rock or concrete armour. Wave run-up does not have an equivalent parameter for vertical structures. The percentage or number of overtopping waves, however, is relevant for each type of structure.

1.4.13 Wave overtopping discharge

Wave overtopping is the average discharge per linear meter of width, q, for example in m^3/s per m or in l/s per m. The methods described in this manual calculate all overtopping discharges in m^3/s per m unless otherwise stated; it is, however, often more convenient to multiply by 1000 and quote the discharge in l/s per m.

In reality, there is no constant discharge over the crest of a structure during overtopping. The process of wave overtopping is very random in time, space and volume. The highest waves will push a large volume of water over the crest in a short period of time (less than a wave period), whereas lower waves may not produce any overtopping. An example of wave overtopping measurements is shown in Figure 1.10 for a time histories of 30 s. The lowest graph (flow depths) shows the irregularity of wave overtopping, where in this case most waves overtop the crest. The upper graph gives the cumulative overtopping as it was measured in the overtopping tank by a load cell. The graph shows some irregularities due to the dynamic behaviour of overtopping wave volumes that fall into the overtopping tank. Individual overtopping volumes cannot easily be distinguished in this case, as some overtopping waves come in one wave group. The graphs show that at least nine waves gave overtopping and the total overtopping volume was about 15 litres. In order to calculate the average wave overtopping discharge, one should take into account the duration of the measurements and the width of the chute that directs the overtopping water to the tank.
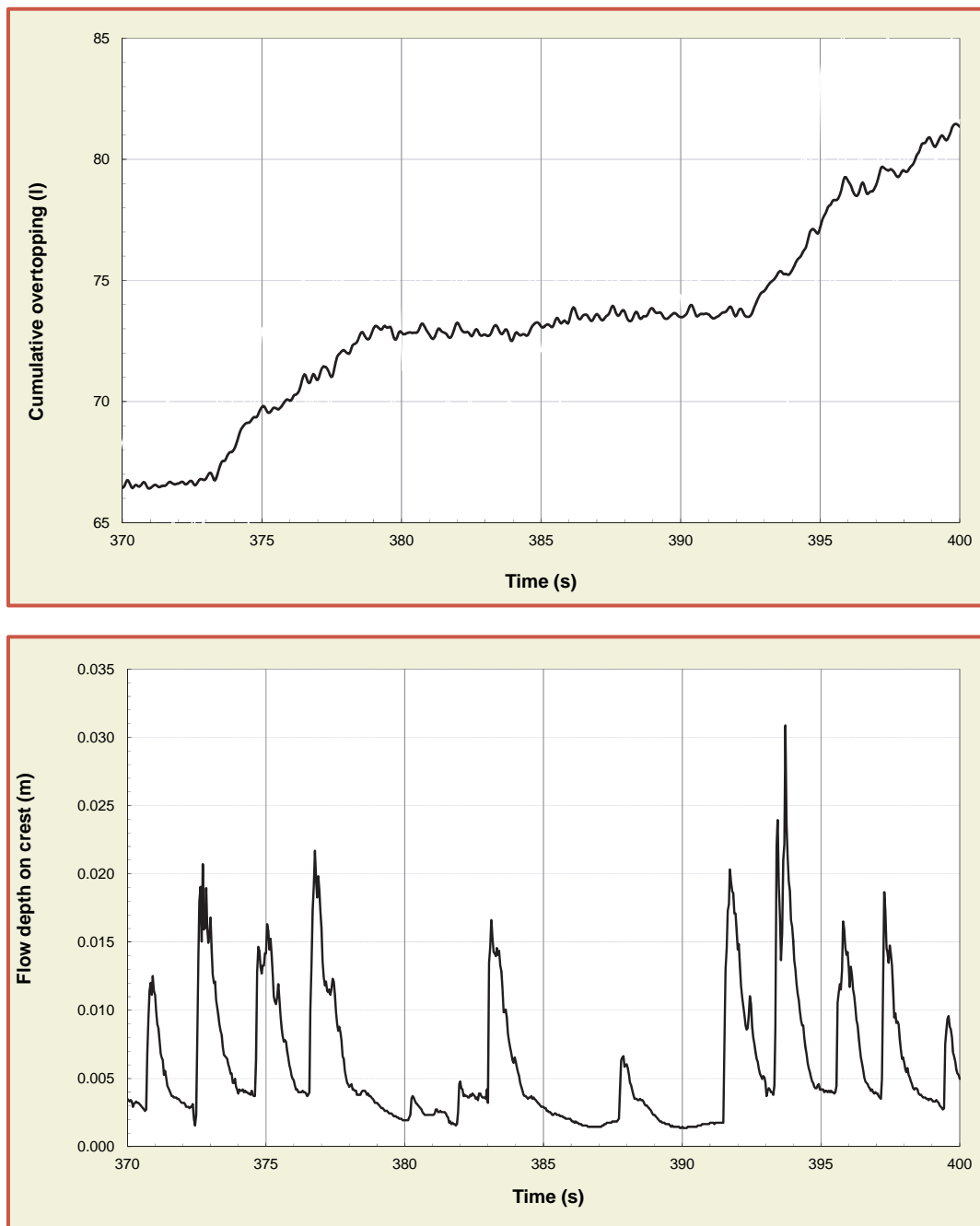
Figure 1.10:   Example of wave overtopping measurements, showing the random behaviour

A mean overtopping discharge is widely used as it can easily be measured and also classified:

- q < 0.1 l/s per m: Insignificant with respect to strength of crest and rear of a structure.
- q = 1 l/s per m: On crest and landward slopes bad grass covers or clay may start to erode. It will not give erosion to rubble mound structures.
- q = 10 l/s per m: Significant overtopping for dikes, embankments. For large wave heights it may lead to severe erosion on the harbour side of rubble mound breakwaters.
- q = 100 l/s per m: Crest and inner slopes of dikes have to be protected by asphalt or concrete; for rubble mound breakwaters transmitted waves may be generated and the armour should cover crest and landward slope.

In fact it is not only the average overtopping discharge that classifies the severity of overtopping, but also the wave height that causes the overtopping. A large wave height gives more severe overtopping than a low wave height, for the same overtopping discharge. More on allowable wave overtopping is given in Chapter 3.

1.4.14 Wave overtopping volumes

A mean overtopping discharge does not yet describe how many waves will overtop and how much water will be overtopped in each wave. The overtopping wave volume, V, that comes over the crest of a structure is given in m^3 per wave per m width. Generally, most of the overtopping waves are fairly small, but a small number gives significantly larger overtopping volumes.

The maximum volume overtopped in a sea state depends on the mean discharge q, on the storm duration and the percentage of overtopping waves. In this manual, a method is given by which the distribution of overtopping wave volumes can be calculated for certain wave condition and average overtopping discharge. A longer storm duration gives more overtopping waves, but statistically, also a larger maximum volume. Many small overtopping waves (like for river dikes or embankments) may create the same mean overtopping discharge as a few large waves for rough sea conditions. The maximum overtopping wave volume will, however, be much larger for rough sea conditions with large waves.

1.5   Description and use of reliability in this manual

This section will briefly introduce the concept of uncertainties and how it will be dealt with in this manual. It will start with a basic definition of uncertainty and after that the various types of uncertainties are explained and more detailed descriptions of parameters and model uncertainties used in this manual will be described. Finally, the methods are given how to include reliability in the application of formulae given in this manual.

1.5.1 Definitions

Uncertainty may be defined as the relative variation in parameters or error in the model description so that there is no single value describing this parameter but a range of possible values. Due to the random nature of many of those variables used in coastal engineering, most of the parameters should not be treated deterministically but stochastically. The latter assumes that a parameter x shows different realisations out of a range of possible values. Hence, uncertainty may be defined as a statistical distribution of the parameter. If a normal distribution is assumed here uncertainty may also be given as relative error, mathematically expressed as the coefficient of variation σ'(x) of a certain parameter x:

$$\sigma'(x) = \frac{\sigma(x)}{\mu(x)}$$

1.2

where σ(x) is the standard deviation of the parameter and μ(x) is the mean value of that parameter. Although this definition may be regarded as imperfect it has some practical value and is easily applied.

A normal distribution is often assumed for the parameter x. But sometimes it is physically not possible that a parameter x becomes negative (for example a thickness) and then the distribution may be changed to a log-normal distribution. Figure 1.11 gives an example where the mean $\mu(x) = 2.0$ and standard deviation $\sigma(x) = 0.75$ for the normal distribution. This normal distribution may become negative, which is not the case for the log-normal. In this case the log-normal distribution gives a slightly skewed distribution. If the mean is quite far from zero and the standard deviation relatively small, then the two distributions show less differences.
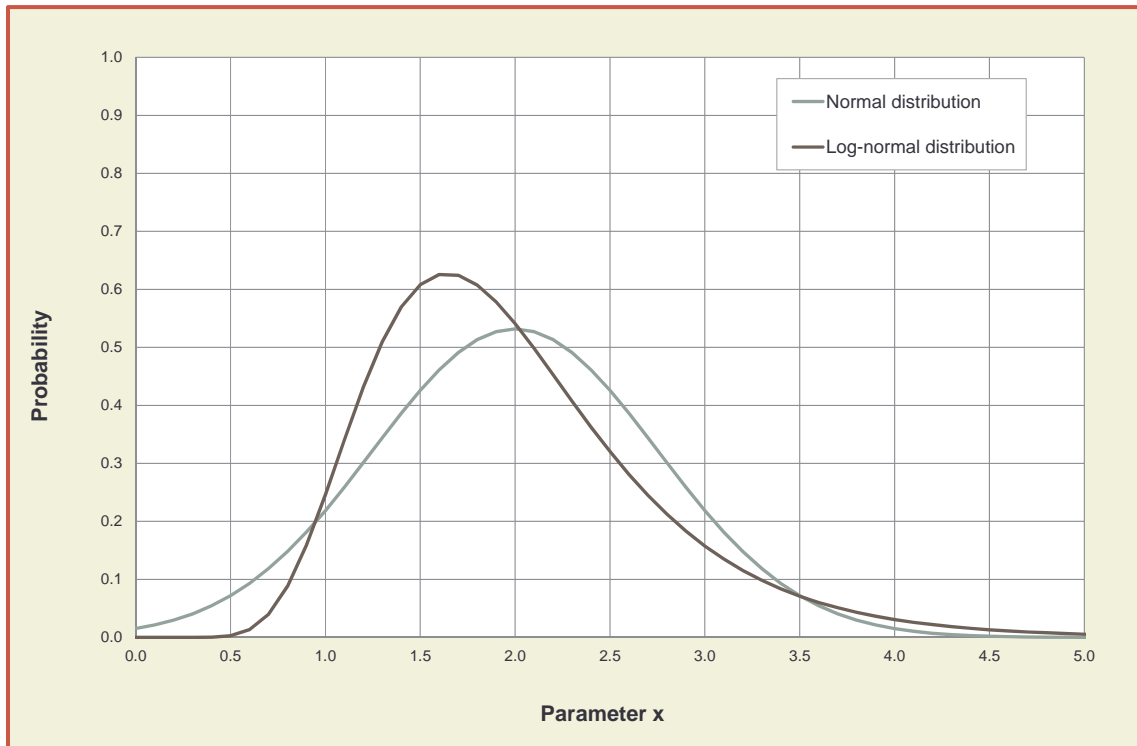
Figure 1.11:   Normal and associated log-normal distribution. For the normal distribution $\mu(x) = 2.0$ and $\sigma(x) = 0.75$.

1.5.2 Background on uncertainties

Many parameters used in engineering models are uncertain, and so are the models themselves. The uncertainties of input parameters and models generally fall into certain categories; as summarised in Figure 1.12.

- Fundamental or statistical uncertainties: elemental, inherent uncertainties, which are conditioned by random processes of nature and which cannot be diminished (always comprised in measured data)

- Data uncertainty: measurement errors, inhomogeneity of data, errors during data handling, non-representative reproduction of measurement due to inadequate temporal and spatial resolution

- Model uncertainty: coverage of inadequate reproduction of physical processes in nature

- Human errors: all of the errors during production, abrasion, maintenance as well as other human mistakes which are not covered by the model. These errors are not considered in the following, due to the fact that in general they are specific to the problems and no universal approaches are available.

If normal or Gaussian distributions for x are used 68.3% of all values of x are within the range of $\mu(x) \pm \sigma(x)$, 95.5% of all values within the range of $\mu(x) \pm 2\sigma(x)$, and almost all values (97,7%) within the range of $\mu(x) \pm 3\sigma(x)$, see Figure 1.13. Considering uncertainties in a design, therefore, means that all input parameters are no longer regarded as fixed deterministic parameters, but can be any realisation of the specific parameter. This has two consequences: Firstly, it has to be checked whether all realisations of

this parameter are really physically sound: E.g., a realisation of a normally distributed wave height can mathematically become negative which is physically impossible. A log-normal distribution can then be used. Secondly, parameters have to be checked against realisations of other parameters: E.g., a wave of a certain height can only exist in certain water depths and not all combinations of wave heights and wave periods can physically exist.

Figure 1.12:   Sources of uncertainties

Figure 1.13:   Gaussian distribution function, variation of parameters and 90%-confidence interval

Another way of looking at uncertainties and this is a method that is often used in this manual, is to give the mean and the 90%-confidence interval or band. This is achieved by giving the 5%-exceedance on both sides of the mean, calculated by $\mu(x) \pm 1.64\sigma(x)$ of a normal distribution. This is also given in Figure 1.13.
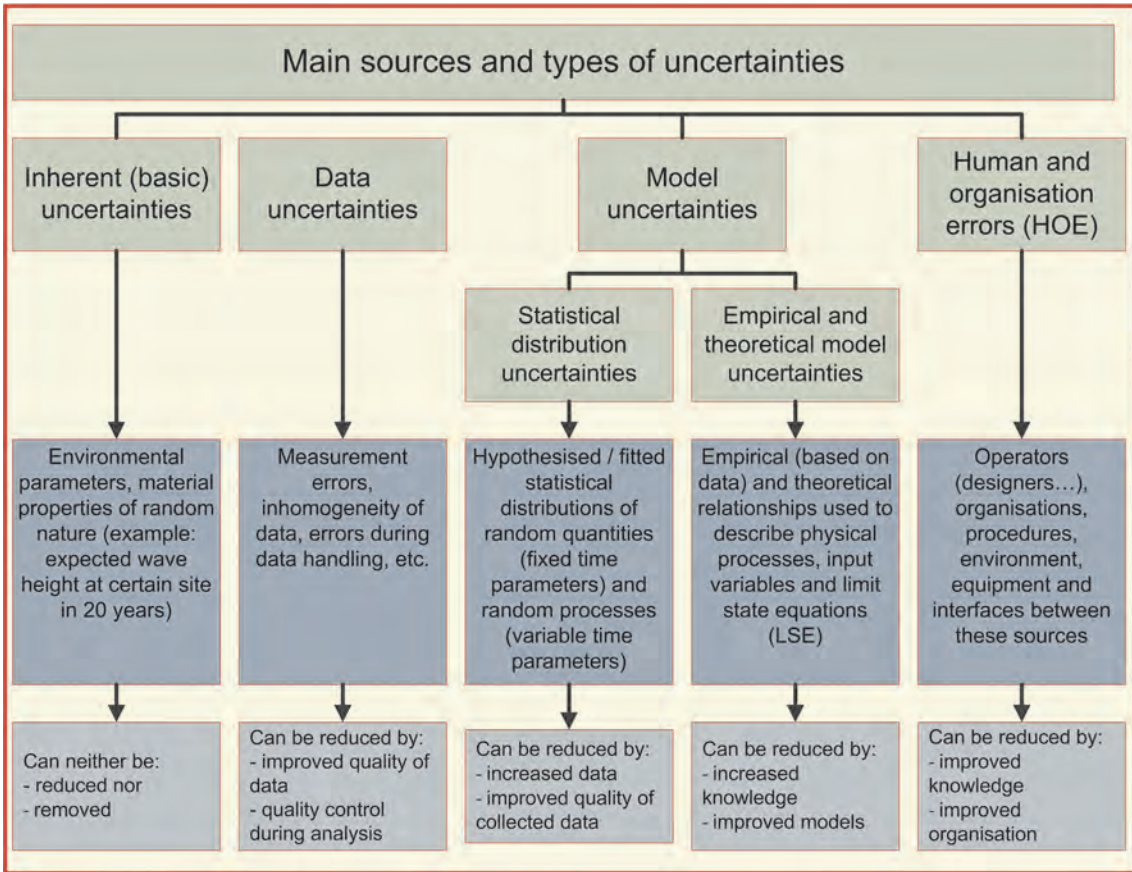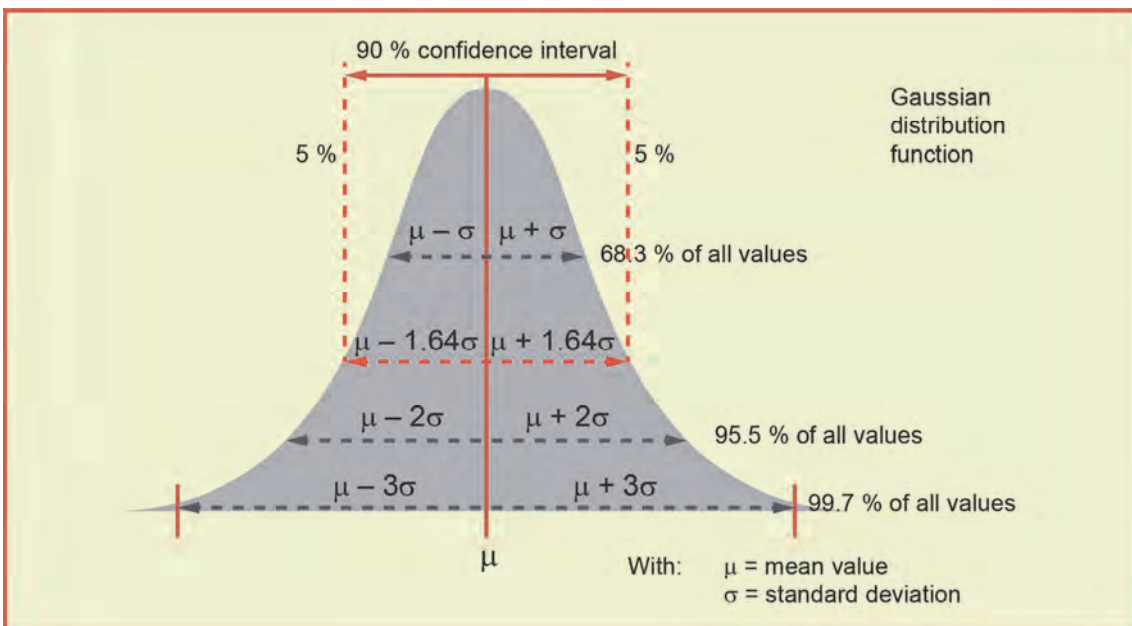
In designing with uncertainties this means that statistical distributions for most of the parameters have to be selected extremely carefully. Furthermore, physical relations between parameters have to be respected. This will be discussed in the subsequent sections as well.

1.5.3 Parameter uncertainty

The uncertainty of input parameters describes the inaccuracy of these parameters, either from measurements of those or from their inherent uncertainties. As previously discussed, this uncertainty will be described using statistical distributions or relative variation of these parameters. Relative variation for most of the parameters will be taken from various sources such as: measurement errors observed; expert opinions derived from questionnaires; errors reported in literature.

Uncertainties of parameters will be discussed in the subsections of each of the following chapters discussing various methods to predict wave overtopping of coastal structures. Any physical relation between parameters will be discussed and restrictions for assessing the uncertainties will be proposed.

1.5.4 Model uncertainty

The model uncertainty is considered as the accuracy, with which a model or method can describe a physical process or a limit state function. Therefore, the model uncertainty describes the deviation of the prediction from the measured data due to this method. Difficulties of this definition arise from the combination of parameter uncertainty and model uncertainty. Differences between predictions and data observations may result from either uncertainties of the input parameters or model uncertainty.

Model uncertainties may be described using the same approach than for parameter uncertainties using a multiplicative approach. This means that:

$$q = m \cdot f(x_i) \hspace{4cm} 1.3$$

where m is the model factor [-]; q is the mean overtopping rate and $f(x_i)$ is the model used for prediction of wave overtopping. The model factor m is assumed to be normally distributed with a mean value of 1.0 and a coefficient of variation specifically derived for the model. It is also possible that m is one of the coefficients in a formula, which is assumed to be a stochastic variable, and that the uncertainty is given by the standard deviation of this coefficient. This procedure is sometimes better than using Equation 1.2, certainly if a process is described in a logarithmic way. For example, a large overtopping discharge is predicted more accurately than a very small overtopping discharge (100-300 l/s per m – a factor or 3 - versus 0.1-0.8 l/s per m – a factor of 8). If a model as in Equation 1.3 is given in a graph, it is very useful to give also the 90%-confidence band or interval by drawing the two 5%-exceedance lines (using $\mu(m) \pm 1.64\sigma(m)$).

These model factors may easily reach coefficients of variations more than 30%, for a predicted overtopping discharge. It should be noted that a mean value of m = 1.0 always means that there is no bias in the models used. Any systematic error needs to be adjusted by the model itself. For example, if there is an over-prediction of a specific model by 20% the model has to be adjusted to predict 20% lower results. This concept is followed in all further chapters of this manual so that from here onwards, and the procedure to account for the model uncertainties is given in Section 4.10.1.

1.5.5 Methodology and application in this manual

All parameter and model uncertainties as discussed in the previous sections are used to apply the formulae and to run the models proposed in this manual. Results of all models will again follow statistical

distributions rather than being single deterministic values. Hence, interpretation of these results is required and recommendations will be given on how to use formulae or outputs of the models.

This manual describes the reliability of the formula often by taking one of the coefficients as a stochastic parameter and giving a standard deviation (assuming a normal distribution). The first EurOtop Manual (2007) gave then a deterministic and probabilistic approach of the prediction formulae, by giving two similar formulae with different coefficients in the formulae. The probabilistic approach used the mean value for the coefficient, where for the deterministic way about one standard deviation was added to the coefficient. The "deterministic way", therefore, included some safety as wave run-up and wave overtopping have a substantial uncertainty.

Actually, the "deterministic design or safety assessment" approach in the first EurOtop Manual (2007) should be termed a semi-probabilistic approach as a partial safety factor of one standard deviation is used. This manual presents the following enhanced approaches:

- **Mean value approach**. Use the formula as given with the mean value of the stochastic parameter(s). This should be done to predict or compare with test data. In a graph also the 5%-exceedance lines or 90%-confidence band could be given to complete the comparison; this was called the probabilistic approach in EurOtop (2007);
- **Design or assessment approach**. This is an easy semi-probabilistic approach with a partial safety factor; this is the mean value approach above, but now with the inclusion of the uncertainty of the prediction. The stochastic parameter(s) become(s) $\mu(m) + \sigma(m)$, where m is given in Equation 1.3; this was called the deterministic approach in EurOtop (2007);
- **Probabilistic approach**. Consider the stochastic parameter(s) with their given standard deviation and assuming a normal or log-normal distribution;
- The 5%-exceedance lines, or **90%-confidence band**, can be calculated by using $\mu(m) \pm 1.64\sigma(m)$ for the stochastic parameter(s).

In this manual, the formulae are given as a **mean value approach**. The formula(e) and 5%-exceedance curves are given in a graphical way. Key coefficients are taken as stochastic variables, and uncertainty is then described by giving the standard deviation, $\sigma(m)$. The coefficient to be used in the formula for the **design or assessment approach** will also be given. An example of this approach is shown next for wave run-up and is followed throughout this manual. The probabilistic approach is not used in this manual, except in an example in Section 5.6.

The formula for the 2%-wave run-up level is given by (assuming breaking waves only):

$$\frac{R_{u2\%}}{H_{m0}} = 1.65 \cdot \gamma_b \cdot \gamma_f \cdot \gamma_\beta \cdot \xi_{m-1,0}$$

1.4

The coefficient 1.65 can be considered as a stochastic variable with a mean value of m = 1.65 and a standard deviation of $\sigma(m) = 0.10$ and gives the **mean value approach**. For a **design and assessment approach** one should use the value of 1.75 instead of 1.65.

2 Water levels and wave conditions

2.1 Introduction

This Overtopping Manual has a focus on the aspects of wave run-up and wave overtopping only. It is not a design manual, giving the whole design process of a structure. This chapter, therefore, will not provide a guide to the derivation of input conditions other than to identify the key activities in deriving water level and wave conditions, including depth-limited wave conditions. It identifies the key parameters and provides a check-list of key processes and transformations. Comprehensive references are given to appropriate sources of information. Brief descriptions of methods are sometimes given, summary details of appropriate tools and models, and cross references to other manuals.

The main manuals and guidelines, which describe the whole design and/or safety assessment process of coastal and inland structures, including water levels and wave conditions are: The Rock Manual (2007; The Coastal Engineering Manual (2006); The British Standards (2000); The German "Die Küste" (EAK, 2002);), the Dutch ENW manuals (ENW: http://kennisbank-waterbouw.nl/dicea/TAW-ENW.htm); and the DELOS Design Guidelines (2007).

2.2 Water levels, tides, surges and sea level changes

Prediction of water levels is extremely important for prediction of wave run-up levels or wave overtopping, which are often used to design the required crest level of a flood defence structure or breakwater. Moreover, in shallow areas the extreme water level often determines the water depth and thereby the upper limit for wave heights.

Extreme water levels in design or assessment of structures may have the following components: the mean sea level; the astronomical tide; surges related to (extreme) weather conditions; and high river discharges.

2.2.1 Mean sea level

For coastal waters in open communication with the sea, the mean water level can often effectively be taken as a site-specific constant, being related to the mean sea level of the oceans. For safety assessments, not looking further ahead than about 5 years, the actual mean water level can be taken as a constant. Due to expected global warming, however, predictions in sea level rise for the next hundred years range roughly from 0.2 m to more than 1.0 m.

For design of structures, which last a long time after their design and construction phase, a certain sea level rise has to be included. Sometimes countries prescribe a certain sea level rise, which has to be taken into account when designing flood defence structures. Also the return period for which to include sea level rise may differ, due to the possibility of modification in future. An earthen dike is relatively easy to increase in height and a predicted sea level rise for the next 50 years would be sufficient. A dedicated flood defence structure through a city is not easy to modify or replace. In such a situation a predicted sea level rise for the next 100 years or more could be considered.

2.2.2 Astronomical tide

The basic driving forces of tidal movements are astronomical and therefore entirely predictable, which enables accurate prediction of tidal levels (and currents). Around the UK and North Sea coast, and indeed around much of the world, the largest fluctuations in water level are caused by astronomical tides. These are caused by the relative rotation of both the sun and the moon around the earth each day. The differential gravitational effects over the surface of the oceans cause tides with well-defined periods, principally semi-diurnal and diurnal. Around the British Isles and along coasts around the North Sea the semi-diurnal tides are much larger than the diurnal components.

In addition to the tides that result from the earth's rotation, other periodicities are apparent in the fluctuation of tidal levels. The most obvious is the fortnightly spring-neap cycle, corresponding to the half period of the lunar cycle.

Further details on the generation of astronomic tides, and their dynamics, can be found in the Admiralty Manual of Tides in most countries. These give daily predictions of times of high and low waters at selected locations, such as ports. Also details of calculating the differences in level between different locations are provided. Unfortunately, in practice, the prediction of an extreme water level is made much more complicated by the effects of weather, as discussed below.

2.2.3 Surges related to extreme weather conditions

Generally speaking the difference between the level of highest astronomical tide and, say, the largest predicted tide in any year is rather small (i.e. a few centimetres). In practice, this difference is often unimportant, when compared with the differences between predicted and observed tidal levels due to weather effects.

Extreme high water levels are caused by a combination of high tidal elevations plus a positive surge, which usually comprise three main components. A barometric effect caused by a variation in atmospheric pressure from its mean value. A wind set-up; in shallow seas, such as a the English Channel or the North Sea, a strong wind can cause a noticeable rise in sea level within a few hours. A dynamic effect due to the amplification of surge-induced motions caused by the shape of the land (e.g. seiching and funnelling).

A fourth component, wave set-up causes an increase in water levels within the surf zone at a particular site due to waves breaking as they travel shoreward. Unlike the other three positive surge components, wave set-up has only a localised effect on water levels. Wave set-up is implicitly reproduced in the physical model tests on which the overtopping equations are based, but of course only over the length of foreshore reproduced in the model. There is, in general, no requirement to add on an additional water level increase for wave set-up when calculating overtopping discharges using the methods reported in this document, unless the foreshore is very long and very gently. In that case numerical models should give the wave set-up one or two wave lengths in front of the toe of the structure.

Negative surges are made up of two principal components: a barometric effect caused by high atmospheric pressures and wind set-down caused by winds blowing offshore. Large positive surges are more frequent than large negative ones. This is because a depression causing a positive surge will tend to be more intense and associated with a more severe wind condition than anticyclones.

Surges in relatively large and shallow areas, like the southern part of the North Sea, play an important role in estimating extreme water levels. The surges may become several meters for large return periods. The easiest means of predicting extreme water levels is to analyse long term water level data from the site in question. However, where no such data exists, it may be necessary to predict surge levels using theoretical or empirical methods and combine these levels with tidal elevations in order to obtain an estimation of extreme water levels.

Almost 100 years of high water level measurements in the Netherlands is shown in Figure 2.1 along with the extrapolation of the measurements to extreme low exceedance probabilities, such as 10^{-4} (once in 10,000 years).

Extreme water levels can also be determined by regarding long term wind statistics, which have been often observed for a longer duration than waves, and perform numerical modelling of the water motion with the extreme winds that have been determined.

The statistics of surge levels for hurricanes, cyclones or typhoons, is quite different from storm surge levels as described above. As a hurricane is a turning wind field, the local surge depends very much on where the event makes land fall. The maximum onshore winds at some distance away from the eye of the hurricane may generate locally very high surges, where further away from the eye and at the other side of the point of landfall (offshore winds), the surge will be much lower, as well as the wave attack. The statistics of hurricane surges should include the probability that such a hurricane makes landfall at around the location of interest. These dedicated procedures are not given in this manual.
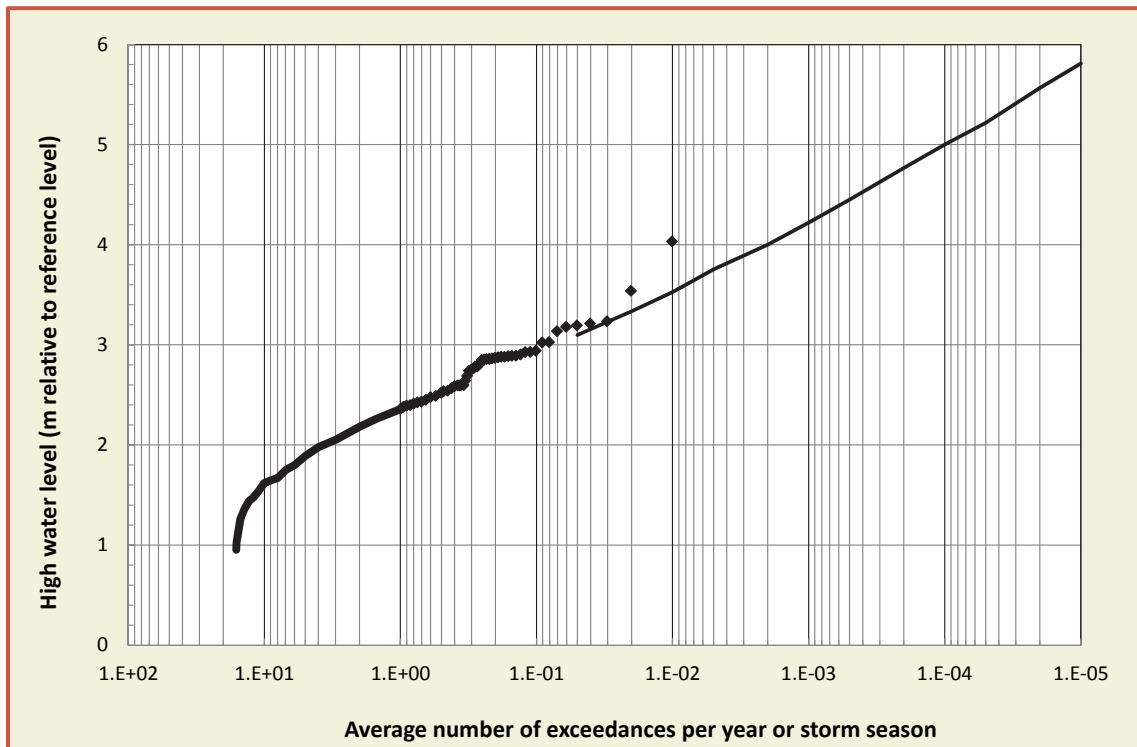
Figure 2.1: An Example of measurements of maximum water levels for almost 100 years (from 1887 to 1985) and extrapolation to extreme return periods. Hook of Holland, the Netherlands

2.2.4 High river discharges

Coastal flood defences face the sea or a (large) lake, but flood defences are also present along tidal rivers. Extreme river discharges determine the extreme water levels along river flood defences. During such an extreme water level, which may take a week or longer, a storm may generate waves on the river and cause overtopping of the flood defence. In many cases the required height of a river dike does not only depend on the extreme water level, but also on the possibility of wave overtopping. It should be noted that the occurrence of the extreme river discharge, and extreme water level, are independent of the occurrence of the storm. During high river discharges, only "normal" storms; occurring every decade; are considered, not the extreme storms.

Where rivers enter the sea both systems for extreme water levels may occur. Extreme storms may give extreme water levels, but also extreme river discharges. The effect of extreme storms and surges disappear farther upstream. Joint probabilistic calculations of both phenomena may give the right extreme water levels for design or safety assessment.

2.2.5 Effect on crest levels

During design or safety assessment of a dike, the crest height does not just depend on wave run-up or wave overtopping. Account must also be taken of a reference level, local sudden gusts and oscillations (leading to a corrected water level), settlement and an increase of the water level due to sea level rise.

The structure height of a dike in the Netherlands untill 2016 was composed of the following contributions; see Figure 2.2 and also the Guidelines for Sea and Lake Dikes (TAW, 1999):

a) the reference level with a probability of being exceeded corresponding to the legal standard (in the Netherlands this was a return period between 1,250 and 10,000 years);

b) the sea level rise or lake level increase during the design period;

c) the expected local ground subsidence during the design period;

d) an extra due to squalls, gusts, seiches and other local wind conditions;

e) the expected decrease in crest height due to settlement of the dike body and the foundation soils during the design period;

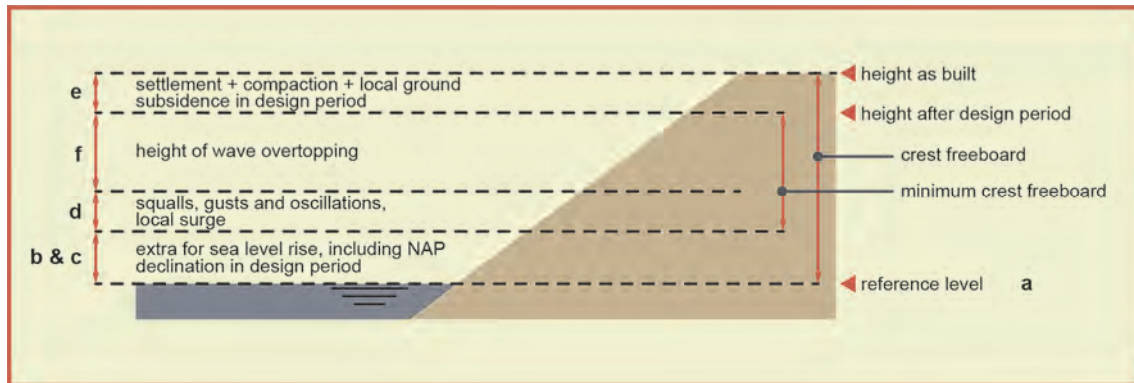f) the wave run-up height and the wave overtopping height.

Figure 2.2:   Important aspects during calculation or assessment of dike height

Contributions (a) to (d) cannot usually not be influenced, whereas contribution (e) can be influenced. Contribution (f) also depends on the outer seaward slope, which can consist of various materials, such as an asphalt layer, a cement-concrete dike cover (pitched block work) or grass on a clay layer. A combination of these types is also possible. Slopes are not always straight, and the upper and lower sections may have different slopes and also a berm may be applied. The design of a cover layer in relation to its hydraulic and geotechnical stability is not dealt with in this manual. However, the aspects related to berms, slopes and roughness elements are dealt with when they have an influence on wave run-up and wave overtopping.

Note that since 2016 the system of risk assessment for the sea defences to protect from flooding has been changed in the Netherlands. Instead of being prepared to cope with a storm event (or river discharge) with a certain return period, the whole protection system around a flood risk area should now be designed for a probability of flooding. This means a probabilistic design of all failure mechanisms for all protection systems must be included and a long dike section has a larger probability of failure than a shorter dike section, under the same conditions. Nevertheless, items a) to f) in Figure 2.2 still influence the design of the height of the flood defence.

2.3   Wave conditions

2.3.1 Offshore wave conditions

In defining the wave climate at the site, the ideal situation is to collect long term instrumentally measured data at the required location. There are very few instances in which this is even a remote possibility. The data of almost 25 years' of wave height measurements is shown in Figure 2.3. These are the Dutch part of the North Sea with an extrapolation to very extreme events, giving a once per 10,000 years wave height of $H_{m0} = 10.95$ m.

It is however more likely that data in deep water, offshore of a site will be available either through the use of a computational wave prediction model based on wind data, or on a wave model. In both of these cases the offshore data can be used in conjunction with a wave transformation model to provide information on wave climate at a coastal site. If instrumentally measured data is also available, covering a short period of time, this can be used for the calibration or verification of the wave transformation model, thus giving greater confidence in its use. A more recent option is to use data bases for a certain area that have been gathered by remote sensing (satellites).

Wind generated waves offshore of most coasts have wave periods in the range 1 s to 20 s. The height, period and direction of the waves generated will depend on the wind speed, duration, direction and the

'fetch', i.e. the unobstructed distance of sea surface over which the wind has acted. In most situations, one of either the duration or fetch become relatively unimportant. For example, in an inland reservoir or lake, even a short storm will produce large wave heights. However, any increase in the duration of the wind will then cause no extra growth because of the small fetch lengths. Thus such waves are described as 'fetch limited". In contrast, on an open coast where the fetch is very large but the wind blows for only a short period, the waves are limited by the duration of the storm. Beyond a certain limit, the exact fetch length becomes unimportant. These waves are described as 'duration limited'.
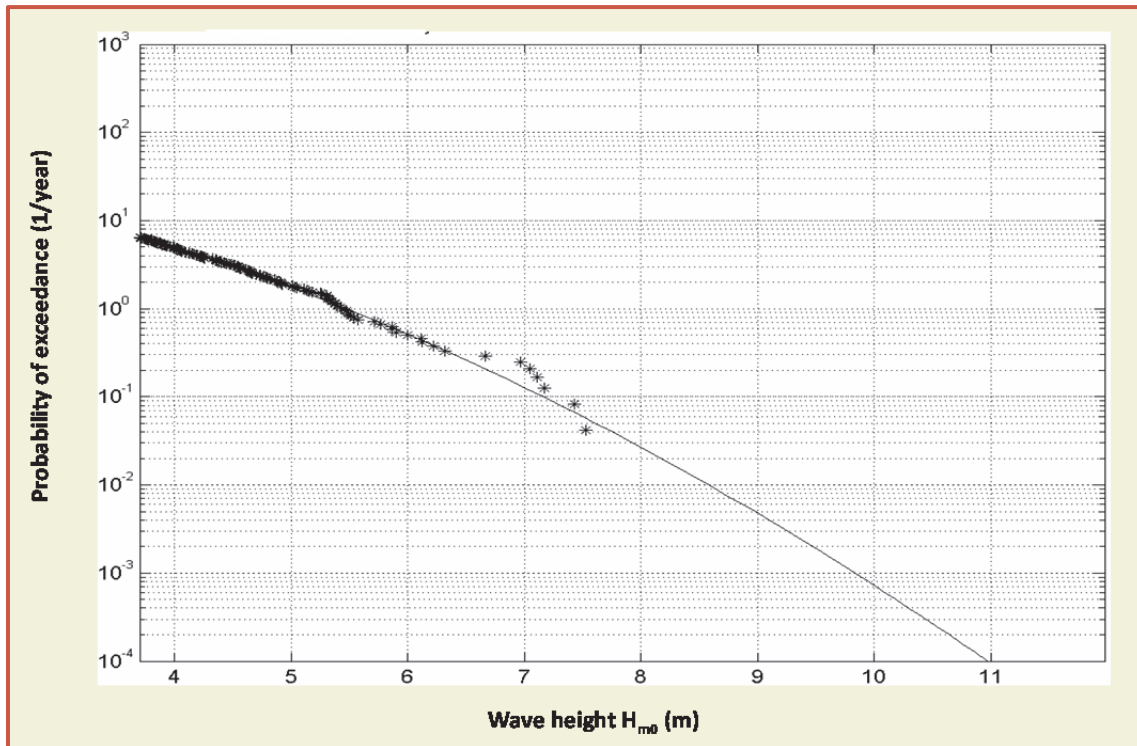

Figure 2.3:   Wave measurements at the North Sea (1979-2002) and extrapolation to very small probabilities of exceedance. SON-platform north of the Wadden islands at a depth of 19 m. Source Weerts and Diermanse (2004)

On oceanic shorelines the situation is usually more complicated. Both the fetch and duration may be extremely large, waves then become "fully developed" and their height depends solely on the wind speed. In such situations the wave period usually becomes quite large, and long period waves are able to travel great distances without suffering serious diminution. The arrival of 'swell' waves, defined as waves not generated by local and/or recent wind conditions, presents a more challenging situation from the viewpoint of wave predictions. In some situations swell waves may become the design condition. They may arrive quite unpredicted at the coast and without wind, as the waves were generated days before and far away from the considered location. Examples are parts of the Brazilian coast as well as parts of the West African coast.

2.3.2 Wave conditions at depth-limited situations

Wave breaking remains one phenomenon that is difficult to describe mathematically. One reason for this is that the physics of the process is not yet completely understood. However, as breaking has a significant effect on the behaviour of waves, the transport of sediments, the magnitude of forces on coastal structures and the overtopping response, it is represented in computational models. The most frequent method for doing this is to define an energy dissipation term which is used in the model when waves reach a limiting depth compared to their height.

There are also relatively simple empirical methods for a first estimate of the incident wave conditions in the surf zone. The methods by Goda (2000); Owen (1980) and Rock Manual (2007 – Figure 4.40) are regularly used. Goda (2000) states that inshore wave conditions are influenced by shoaling and wave

breaking. These processes are influenced by a number of parameters such as the sea steepness and the slope of the bathymetry. To take all the important parameters into account Goda (2000) provided a series of graphs to determine the largest and the significant wave heights (H_{max} and H_s) for 1:10, 1:20, 1:30 and 1:100 sloping bathymetries.

Results obtained from a simple 1D energy decay numerical model Rock Manual (2007 – Figure 4.40) in which the influence of wave breaking is included, are presented in Figure 2.4. This method has also been described in the CIRIA/CUR Manual (1991). Tests have shown that wave height predictions using the design graphs from this model are accurate for slopes ranging from 1:10 to 1:100. For slopes flatter than 1:100, the predictions for the 1:100 slopes should be used. The method does not include the influence of long waves generated by wave breaking, nor a change of the wave period.

24
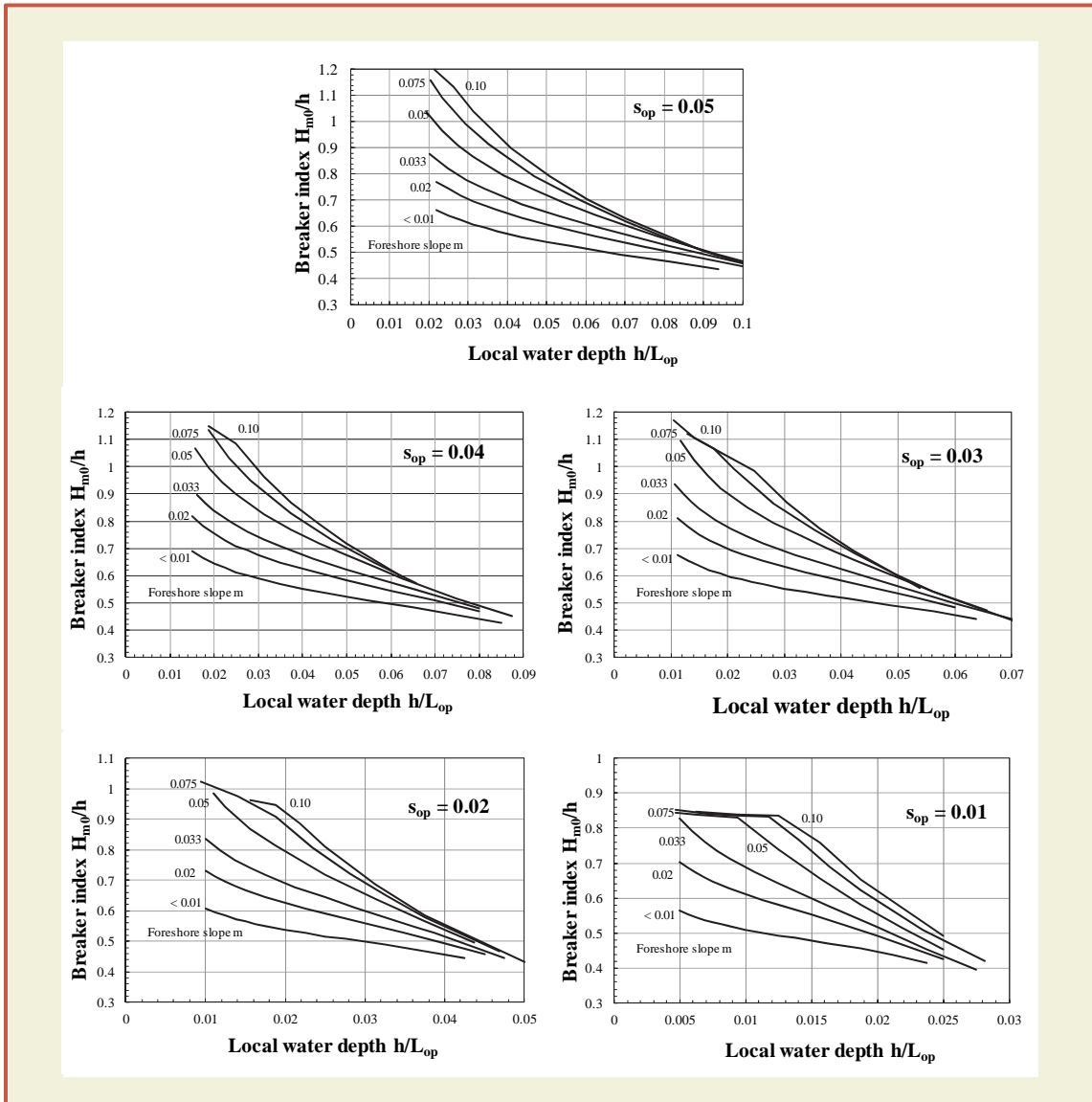
Figure 2.4:   Depth-limited significant wave heights for uniform foreshore slopes

The method for using these graphs is:

1) Determine the deep-water wave steepness, $s_{op} = H_{so}/L_{op}$ (where $L_{op} = gT_p^2/(2\pi)$). This value determines which graphs should be used. Suppose here for convenience that $s_{op} = 0.043$, then the graphs of Figure 2.4 for $s_{op} = 0.04$ and 0.05 have to be used, interpolating between the results from each.

2) Determine the local relative water depth, h/L_{op}. The range of the curves in the graphs covers a decrease in wave height by 10 per cent to about 70 per cent. Limited breaking occurs at the

right-hand side of the graphs and severe breaking on the left-hand side. If h/L_{op} is larger than the maximum value in the graph this means that there is no or only limited wave breaking and one can then assume no wave breaking (deep-water wave height = shallow-water wave height).

3) Determine the slope of the foreshore (m = tan α). Curves are given for range m = 0.075 to 0.01 (1:13 to 1:100). For gentler slopes the 1:100 slope should be used.
4) Enter the two selected graphs with calculated h/L_{op} and read the breaker index H_{m0}/h from the curve of the calculated foreshore slope.
5) Interpolate linearly between the two values of H_{m0}/h to find H_{m0}/h for the correct wave steepness.

Example: Suppose H_{so} = 6 m, T_p = 9.4 s, foreshore slope is 1:40 (m = 0.025). Calculate the maximum significant wave height H_{m0} at a water depth of h = 7 m.

1) The wave conditions in deep water give s_{op} = 0.043. Graphs with s_{op} = 0.04 and 0.05 should to be used.
2) The local relative water depth h/L_{op} = 0.051.
3) The slope of the foreshore (m = 0.025) is in between the curves for m = 0.02 and 0.033.
4) From the graphs, H_{m0}/h = 0.64 is found for s_{op} = 0.04 and 0.68 is found for s_{op} = 0.05.
5) Interpolation for s_{op} = 0.043 gives H_{m0}/h = 0.65 and finally a depth-limited spectral significant wave height of H_{m0} = 3.9 m.

Wave breaking in shallow water does not only affect the significant wave height H_{m0}, but also the distribution of wave heights will change. In deep water, wave heights have a Rayleigh distribution and the spectral wave height H_{m0} will be close to the statistical wave height $H_{1/3}$. In shallow water, these wave heights become different due to the breaking process. Moreover, the highest waves break first when they feel the bottom, where the small waves stay unchanged. This results in a non-homogeneous set of wave heights: broken waves and non-broken waves. For this reason Battjes and Groenendijk (2000) developed the composite Weibull distribution for wave heights in shallow water. For horizontal sea beds this distribution should not be used with a zero slope, as there is evidence that the distribution will again tend to develop into a Rayleigh distribution (Caires and Van Gent, 2012).

Although prediction methods in this manual are mainly based on the spectral significant wave height, it might be useful in some cases to consider other definitions, like the 2%-wave height $H_{2\%}$ or $H_{1/10}$, the average of the highest 1/10-the of the waves. For this reason a summary of the method of Battjes and Groenendijk (2000) is given here. The example given above with a calculated H_{m0} = 3.9 m at a depth of 7 m on a 1:40 slope foreshore has been explored further in Figure 2.5. The distribution requires the root mean square wave height H_{rms}, which is calculated as:

$$H_{m0} = 4\sqrt{m_0}$$
$$H_{rms} = \left(2.69 + 3.24\sqrt{m_0}/h\right)\sqrt{m_0}$$

<div align="right">2.1</div>

where H_{rms} = root mean square wave height. The transition wave height, H_{tr}, between the lower Rayleigh distribution and the higher Weibull distribution (see Figure 2.5) is then given by:

$$H_{tr} = (0.35 + 5.8\tan\alpha)h$$

<div align="right">2.2</div>

One then has then to compute the non-dimensional wave height H_{tr}/H_{rms}, which is used as input to Table 2.1 of Battjes and Groenendijk (2000) to find the (non-dimensional) characteristic heights: $H_{1/3}/H_{rms}$, $H_{1/10}/H_{rms}$, $H_{2\%}/H_{rms}$, $H_{1\%}/H_{rms}$ and $H_{0.1\%}/H_{rms}$. Some particular values have been extracted from this table and are included in Table 2.1, only for the ratios $H_{1/3}/H_{rms}$, $H_{1/10}/H_{rms}$, and $H_{2\%}/H_{rms}$.

The final step is the computation of the dimensional wave heights from the ratios read in the table and the value of H_{rms}. For the given example one finds: $H_{1/3}$ = 4.16 m; $H_{1/10}$ = 4.77 m and $H_{2\%}$ = 5.4 m. Note that the value $H_{2\%}/H_{1/3}$ changed from 1.4 for a Rayleigh distribution (see Figure 2.5) to a value of 1.21.

Table 2.1: Values of dimensionless wave heights for some values of H_{tr}/H_{rms}. From Battjes and Groenendijk (2000)

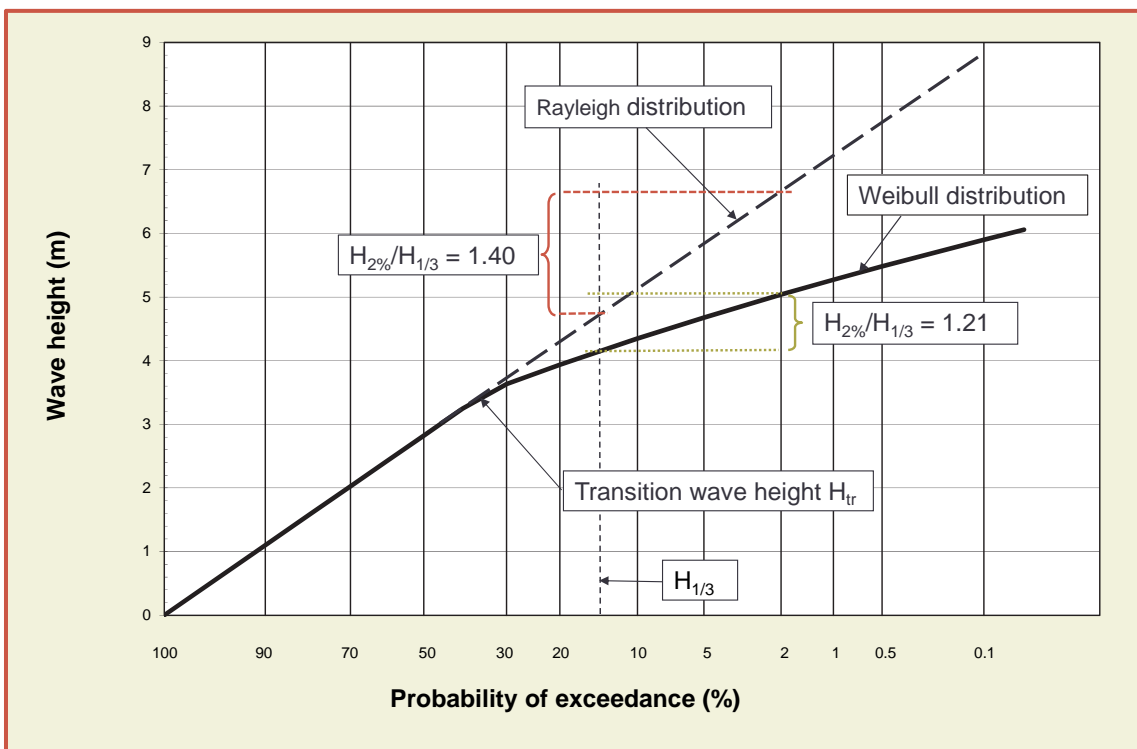| Characteristic height	Non-dimensional transitional wave H_{tr}/H_{rms}									
	0.05	0.50	1.00	1.20	1.35	1.50	1.75	2.00	2.50	3.00
$H_{1/3}/H_{rms}$	1.279	1.280	1.324	1.371	1.395	1.406	1.413	1.415	1.416	1.416
$H_{1/10}/H_{rms}$	1.466	1.467	1.518	1.573	1.626	1.683	1.759	1.786	1.799	1.800
$H_{2\%}/H_{rms}$	1.548	1.549	1.603	1.662	1.717	1.778	1.884	1.985	1.978	1.978

Figure 2.5: Computed composite Weibull distribution. H_{m0} = 3.9 m; foreshore slope 1:40 and water depth h = 7 m

2.3.3 Joint probability of waves and water levels

If both water level and wave height are determined for a certain return period (based on their marginal distribution), then the overtopping discharge for the combination of these extreme conditions will be larger than the actual overtopping occurring with that return period. This is caused by the fact that the combination of these two extreme values will have a lower probability of occurrence if the two are not fully correlated. Therefore, if the joint probability of occurrence is taken into account, a lower (or at maximum equal) overtopping will be calculated. Assuming the occurrence of the high water level together with high wave height (with the same return period), is therefore conservative.

In the design or assessment of coastal structures with respect to overtopping, the primary hydraulic may be derived from a Joint Probability Analysis of the variables that have the most significant impact on wave overtopping. For the overtopping of typical coastal structures, the primary metocean variables of interest may be wave height, wave period (here wind-sea and swell could be considered separately), sea level

(tidal plus surge). These primary variables are often assessed in an analytical way as independent variables (or completely dependent, with some scatter). Other secondary metocean variables of potential interest are wind speed, surge, wave direction, and wind direction.

In the UK and the Netherlands, multi-variable assessment were beginning to become routine 20-30 years ago in coastal flood studies (and to a lesser extent river flood studies). In the sea defence assessments in the Netherlands the so-called illustration point is calculated for each coastal location. This is a combination of stochastic values of wind speed and direction, and corresponding water level and wave height, period, and direction, that is most likely to lead to the maximum overtopping for the designated return period. This combination thereby determines the minimum required crest level. Many methods exist to determine the joint probability conditions (e.g. crude Monte Carlo simulation, FORM, etc.).

2.3.4 Currents

Where waves are propagating towards an oncoming current, for example at the mouth of a river, the current will tend to increase the steepness of the waves by increasing their height and decreasing their wave length. Refraction of the waves by the current will tend to focus the energy of the waves towards the river mouth. In reality both current and depth refraction are likely to take place producing a complex wave current field. It is clearly more complicated to include current and depth refraction effects, but at sites where currents are large they will have a significant influence on wave propagation. Computational models are available to allow both these effects to be represented. The effect of currents on wave overtopping is described in Section 5.4.5.

2.3.5 Return periods and probability of events

The selection of a given return period for a particular site will depend on several factors. These will include the expected lifetime of the structure, expected maximum wave and water level conditions and the intended use of the structure, as well as the consequences if failure occurs. If, for instance, the public are to have access to the site then a higher standard of defence will be required than that to protect farm land. Further examples are given in Chapter 3.
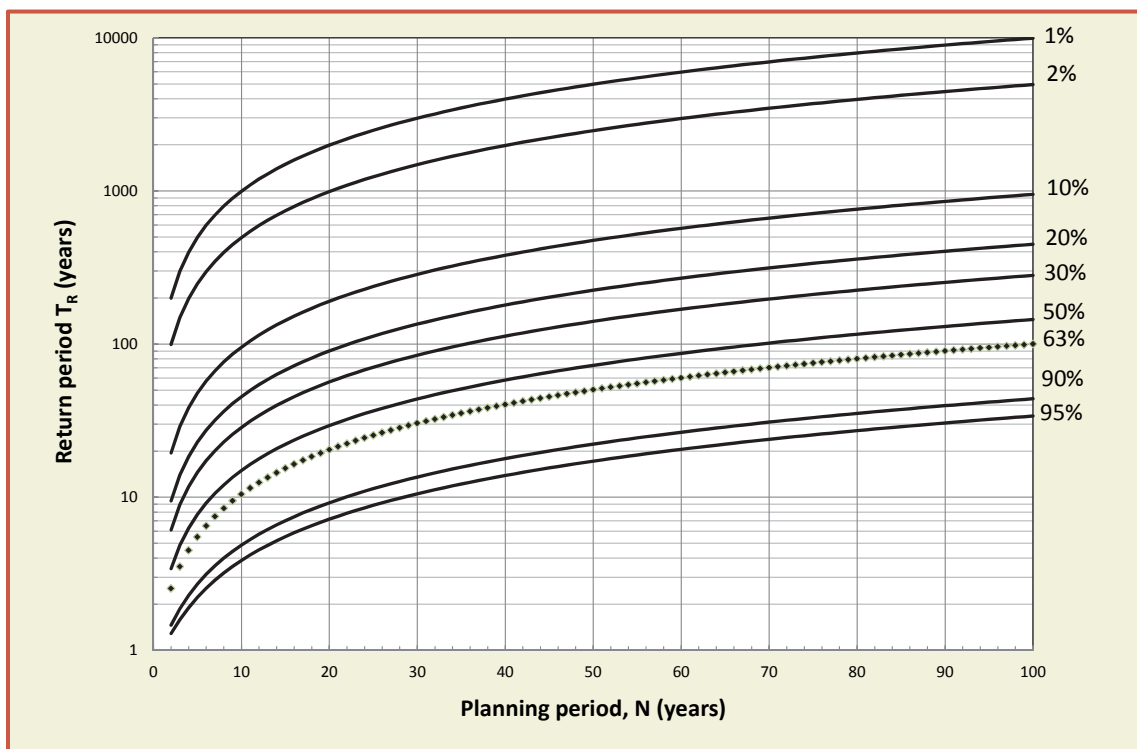

Figure 2.6:   Encounter probability

A way of considering an event with a given return period, T_R, is to consider that (for $T_R \geq 5$ years) the probability of its occurrence in any one year is approximately equal to $1/T_R$. For example, a 10,000 year return period event is equivalent to one with a probability of occurrence of 10^{-4} in any one year.

Over a planned lifetime of N years for a structure (not necessarily the same as the design return period) the probability of encountering the wave condition with return period T_R, at least once, is given by Poisson distribution:

$$P\left(\underline{T}_R \geq T_R\right) = 1 - \left(1 - 1/T_R\right)^N \qquad\qquad 2.3$$

Figure 2.6 presents curves for this encounter probability with values between 1 per cent and 95 per cent shown as a function of T_R and N. It follows that there will not be exactly T_R years between events with a given return period of T_R years. It can be seen (dotted line) that for a time interval equal to the return period, there is a 63% chance of occurrence within the return period. A 100-year event has a probability of 63% of occurring in a period of 100 years; a 1000-year event gives a probability of 10% of occurring in a planned period of 100 years. Further information on design events and return periods can be found in the British Standard Code of practice for Maritime Structures BS6349 Part 1 2000 and Part 7 1991, the PIANC working group 12 report (PIANC 1992) and in the Rock Manual (2007).

2.3.6 Uncertainties in inputs

The principal input parameters discussed in this section comprised water levels, including tides, surges, and sea level changes. Sea state parameters at the toe of the structure have been discussed and river discharges and currents have been considered.

It is assumed here that all input parameters can be defined at the toe of the structure. Depending on different foreshore conditions and physical processes such as refraction, shoaling and wave breaking the statistical distributions of those parameters will have changed over the foreshore. Methods to account for this change are given in the previous sections and elsewhere.

If no information on statistical distributions, or error levels, is available for water levels or sea state parameters, the following assumptions could be taken: all parameters are normally distributed; significant wave height H_s or spectral wave height H_{m0} have a coefficient of variation $\sigma(x)' = 5.0\%$; peak wave period T_p or spectral wave period $T_{m-1.0}$ have a coefficient of variation $\sigma(x)' = 5.0\%$;and design water level at the toe $\sigma(x)' = 3.0\%$, see Schüttrumpf *et al.* (2006). Note that for design sometimes a range is taken, for instance a design wave height with a certain return period may occur with wave period in a certain range of 8-12 s. In such a case a coefficient of variation on the wave period becomes meaningless.

The aforementioned values were derived from expert opinions on these uncertainties. About 100 international experts and professionals working in coastal engineering have been interviewed for this purpose. Although these parameters may be regarded rather small in relation to what Goda (2000) has suggested, results have been tested against real cases and found to give a reasonable range of variations. It should be noted that these uncertainties are applied to significant values rather than mean sea state parameters. This will both change the type of the statistical distribution and the magnitude of the standard deviation or the coefficient of variation.

3 Tolerable wave overtopping

3.1 Introduction

Most sea defence structures are constructed primarily to limit overtopping volumes that might otherwise cause flooding. Over a storm or tide, the overtopping volumes that can be tolerated will be site specific as the volume of water that can be permitted will depend on the size and use of the receiving area, extent and magnitude of drainage ditches, damage versus inundation curves, and return period. Guidance on modelling inundation flows has previously been given in the FLOODSITE project, but flooding volumes and flows away from the defence, *per se*, are not distinguished further in this chapter.

For sea defences that protect people living, working or enjoying themselves, designers and owners of these defences must, however, also deal with potential direct hazards from overtopping. This requires that the level of hazard and its probability of occurrence be assessed, allowing appropriate action plans to be devised to ameliorate risks arising from overtopping. Such plans can be to limit wave overtopping during severe storm events, but plans can and sometimes also have be to made to exclude people and/or vehicles during severe storm events when overtopping may occur. The latter is specially applicable for structures that allow access for people during normal conditions.

Breakwaters also limit wave transmission into harbour or marina areas, so the prime concern may then be the degree of wave transmission, often given by a coefficient of transmission K_t, or may be assessed by the contribution to total wave disturbance given by the transmitted wave.

Major hazards on or close to sea defence structures may be of death, injury, property damage or transport disruption from direct wave impact, or drowning. On average, approximately 2-5 people are killed each year in each of UK and Italy through wave action, chiefly on seawalls and similar structures (although this rose to 11 in UK during 2005). It is often helpful to analyse direct wave and overtopping effects, and their consequences under four general categories:

- Damage to defence structure(s), either short-term or longer-term, with the possibility of breaching and flooding.

- Direct hazard of injury or death to people immediately behind the defence, whether they are pedestrians, cyclists or travelling in a vehicle;

- Damage to property, operation and / or infrastructure in the area defended, including loss of economic, environmental or other resource, or disruption to an economic activity or process;

- Low depth flooding (inconvenient but not dangerous)

The character of overtopping flows or jets, and the hazards they cause, also depend upon the geometry of the structure, of upon the nature of the immediate hinterland behind the seawall crest, and the form and trajectory of overtopping. For instance, rising ground behind the seawall may permit visibility of incoming waves, and will slow overtopping flows, perhaps at the crest of a dike or at promenades or boulevards behind a seawall. Conversely, a defence that is elevated significantly above the land defended may obscure visibility of incoming waves, and post-overtopping flows may increase in speed down the rear slope. The particular hazards caused by overtopping therefore depend upon both the local topography and structures as well as on the direct overtopping characteristics.

It is not possible to give unambiguous or precise limits to tolerable overtopping for all conditions. Some guidance is offered here on tolerable mean discharges and maximum overtopping volumes for a range of circumstances or uses. These limits may be adopted or modified depending on the circumstances and uses of the site.

One of the main insights since the first EurOtop Manual (2007) is that the wave height that causes overtopping is strongly related to tolerable overtopping, as tolerable overtopping depends very strongly on individual volumes. For a given mean discharge, small waves only give small overtopping volumes,

perhaps many of them. But large waves against a high defence crest (large freeboard) may give many cubic metres of overtopping water in one wave, even though far fewer waves may overtop. In that sense a mean tolerable overtopping discharge should be coupled to a wave height causing that discharge. This was not yet the case in EurOtop (2007).

3.2   Wave overtopping behaviour

3.2.1   Wave overtopping processes and hazards

Hazards driven by overtopping can be linked to a large number of flow parameters, but there are a few simple direct flow parameters:

- mean overtopping discharge, q;

- individual maximum overtopping volume V_{max}.

These simple direct flow parameters (q and V_{max}) will primarily be used in this chapter to give advice on tolerable wave overtopping. The maximum volume V_{max} follows from the distribution of overtopping wave volumes, which will also be described in this chapter.

Less direct responses (or similar responses, but farther back from the defence) may be used to assess the effects of overtopping, perhaps categorised by:

- overtopping velocities over the crest or promenade, horizontally and vertically;

- overtopping flow thickness, measured or calculated on the crest or promenade;

- overtopping falling distances;

- post-overtopping flow thicknesses and horizontal velocities or velocities down a rear slope;

- post-overtopping wave pressures / forces (non-impulsive or impulsive).

Most of these responses, except for wave pressures / forces, are described for sloping seawall and embankments, rubble mound breakwaters in Chapters 5, 6 and to a lesser degree on vertical structures in Chapter 7. The main response to these hazards has most commonly been the construction of new defences, or the extension or improvement of existing defences. Responses should now always consider three options, in increasing order of intervention:

- Move human activities away from the area subject to overtopping and/or flooding hazard, thus modifying the land use category and/or habitat status;

- Accept hazard at a given probability (acceptable risk) by providing for temporary use and/or short-term evacuation with reliable forecast, warning and evacuation systems, and/or use of temporary / demountable defence systems;

- Increase defence standard to reduce risk to acceptable levels probably by enhancing the defence and / or reducing loadings.

For any structure expected to reduce wave overtopping, the crest level and/or the front face configuration will be dimensioned to give acceptable levels of wave overtopping under specified extreme conditions or combined conditions (e.g. water level and waves). Setting acceptable levels of overtopping depends on:

- the use of the defence structure itself, including access to defence for public and/or staff;

- use of the land (or water) behind;

- national and/or local standards and administrative practice;

- economic and social basis for funding the defence.

Under most forms of wave attack, waves tend to break before or onto sloping embankments with the overtopping process being relatively gentle. Relatively few water levels and wave conditions may cause "impulsive" breaking where the overtopping flows are sudden and violent. Conversely, steeper, vertical or compound structures are more likely to experience impulsive breaking, and may overtop violently and with greater velocities. The form of breaking will therefore influence the hazards that overtopping will cause.

Additional hazards that are not dealt with here are those that arise from wave reflections, often associated with steep faced defences. Reflected waves increase wave disturbance, which may cause hazards to navigating or moored vessels; may increase waves along neighbouring frontages, and/or may initiate or accelerate local bed erosion thus increasing depth-limited wave heights (Section 2.3.2).

3.2.2 Types of overtopping

Wave overtopping which runs up the face of the seawall and over the crest in (relatively) coherent water mass is often termed 'green water', see Figure 3.1. In contrast, 'white water' or spray overtopping tends to occur when waves break seaward of the defence structure or break onto its seaward face, producing non-continuous overtopping, and/or significant volumes of spray, see Figure 3.2. Overtopping spray may be carried over the wall either under its own momentum, or driven / assisted by an onshore wind. Additional spray may also be generated by wind acting directly on wave crests, particularly when reflected waves interact with incoming waves to give severe local 'clapotii'. This type of spray is not classed as wave overtopping, nor is it predicted by the methods described in this manual.

Figure 3.1:   Green water overtopping Howth, UK

Figure 3.2:   Spray overtopping at the breakwater at Margate, UK

Without a strong onshore wind, spray will seldom contribute significantly to overtopping volumes, but may cause local hazards. Light spray may reduce visibility for driving (important on coastal highways), and will extend the spatial extent of salt spray effects such as damage to crops / vegetation, or deterioration of building fabric. The effect of spray in reducing visibility on coastal highways (particularly when intermittent) can cause sudden loss of visibility, in turn leading drivers to veer suddenly. Strong wind and significant spray may conceal debris (wooden pieces, bottles, plastics, etc.) and sand or shingle carried over the crest of a sea defence. It is for this reason that highways very close to a sea defence may be closed for traffic well before significant wave overtopping discharges / volumes are experienced.

The effects of wind and generation of spray have not often been fully modelled. Some research studies have suggested that the effects of onshore winds on green water overtopping discharges are small, but that overtopping well below $q = 1$ l/s per m might increase by up to 4 times under strong winds.

3.2.3 Return periods

Return periods at which overtopping hazards are analysed, and against which a sea defence scheme or structure might be designed, may be set by national regulation or guidelines. For harbour / marina breakwaters, flooding is not a major concern, but wave disturbance and vessel motions are often of greater concern. As with any area of risk management, different levels of hazard are likely to be tolerated at inverse levels of probability or return period. Risk levels that can be tolerated (probability multiplied by consequence of the event) will depend on local circumstances, local and national guidelines, the balance between risk and benefits, and the level of overall exposure. If normalising risk, heavily used areas might be designed to experience lower levels of hazard applied to more people than lightly used areas, or perhaps the same hazard level at longer return periods. Guidance on return periods used in evaluating levels of protection suggest example protection levels versus return periods as shown in Section 2.3.5.

In practice, some of these return periods may be regarded as too short. National guidelines have recommended lower risk, e.g. a low probability of flooding in UK is now taken as < 0.1% probability in any given year (1:1000 year return) and medium probability of sea flooding as between 0.5% and 0.1% (1:200 to 1:1000 year return). Many existing sea defences in the UK however offer levels of protection far lower than these. In describing flood risk to UK residents, the Environment Agency uses the following flooding probabilities:

	high	→	more than 1 in 30 (3.3%) in any given year
.	medium	→	between 1 in 30 (3.3%) and 1 in 100 (1%) in any given year
.	low	→	between 1 in 100 (1%) and 1 in 1000 (0.1%) in any given year
.	very low	→	less than 1 in 1000 (0.1%) in any given year.

In the Netherlands, two-thirds of the country's land area lies below design storm surge level. Levels of protection were increased after 1953 when almost 2000 people drowned. A level of protection means that the defence structure should be designed to withstand the event with the given return period. Large urban areas have a level of protection of 10,000 years; less densely populated areas 4,000 years; and protection for high river discharge (without threat of storm surge) of 1,250 years.

The safety system in the Netherlands, however, changed in 2016. Now each area should have a maximum probability of being flooded. The flood probability is given by a return period and is 100,000 years for large urban areas. Now the risk analysis process must also consider the possibility of a breach in the defences.

The design life in the Netherlands for flood defences like dikes, which are fairly easy to upgrade, is taken as 50 years. In urban areas, where it is more difficult to upgrade a flood defence, the design life is taken as 100 years. This design life increases for very special structures with high capital costs, like the Eastern Scheldt storm surge barrier, Thames barrier, or the Maeslandtkering in the entrance to Rotterdam. A design life of around 200 years is then usual. Breakwaters are often designed for a design life of 50 or 100 years, although for successful ports some have already exceeded 120 years.

Variations from simple "acceptable risk" approach may be required for publicly-funded defences based on benefit / cost assessments, or where public aversion to hazards causing death require greater efforts to reduce the risk, either by reducing the probability of the hazard or by reducing its consequence.

3.3 Tolerable mean discharges and maximum volumes

The main recommendations of tolerable overtopping limits are given in the Tables within the following sections. Considerable effort has however been made in the text to describe the situations for which these limits might apply. Use of the values suggested in the Tables is NOT therefore a substitute for careful study of the reasons that have led the Author Team to these suggestions.

3.3.1 Influence of wave height on tolerable overtopping

The first EurOtop Manual (2007) gave four tables with estimated tolerable overtopping for specific hazards, like limits for pedestrians, vehicles, property behind the defence and structural damage to the crest and rear slope. These tables have been used many times in assessing the crest level for design purposes. One of the main insights developed since EurOtop (2007) is that tolerable overtopping depends very strongly on the peak volume, and hence on the wave height that causes the overtopping. For a given mean overtopping discharge, small waves only give small overtopping volumes, whereas large waves may give many cubic metres of overtopping water in one wave. In that sense a mean tolerable overtopping discharge should be coupled to a wave height causing that discharge (simpler than assessing the maximum volume itself, but see below). This important insight changes the limits for tolerable overtopping.

Research in recent years has focussed on the description of distributions of overtopping wave volumes over the crest, see Chapters 5, 6 and 7. In this way the maximum overtopping volume V_{max} may now be calculated for some structures of simple geometry with reasonable accuracy. Of course it will not only be the maximum volume that may cause damage, but all overtopping volumes that are close to this maximum overtopping volume. Nevertheless, V_{max} is a good parameter to describe how severe the wave overtopping is or can be.

The statistical distribution of overtopping wave volumes depends on structure type, incident wave conditions (wave height and wave period), freeboard, duration of wave overtopping and the mean overtopping discharge. If wave conditions and resulting mean overtopping discharges are similar for various structures like sloping seawalls and embankments, rubble mound breakwaters and vertical structures, the distribution of overtopping wave volumes will also be of the same order. The main influence of the wave height can be illustrated by just choosing one structure type, one wave steepness and one duration of the sea state. A sloping smooth structure was chosen with a wave steepness of $s_{op} = 0.04$ (fairly steep wind waves) and a storm duration of one hour. Choosing a lower wave steepness will result in fewer but larger overtopping volumes. A longer storm duration will just increase the maximum overtopping volume a little.

Examples of statistical distributions of overtopping wave volumes will be given here, based on equations given in Chapters 5, 6 and 7. Calculations were made for wave heights of $H_{m0} = 1$ m; 3 m and 5 m and for mean wave overtopping discharges of 0.1 l/s per m up to 75 l/s per m. It should be noted that if distributions of overtopping wave volumes are based on less than 5-10 waves, the distribution will be quite uncertain and calculated overtopping volumes will not be accurate.

The three wave heights above distinguish "roughly" between three situations that might occur in practice:

$H_{m0} \leq 1$ m   Rivers, wide canals and small lakes. Often embankments covered with grass.

$H_{m0} = 1 - 3$ m   Sheltered seashores and large lakes. Embankments, seawalls with the wave attack zone protected by rock, concrete units or block revetments. Grass covered crest or protected promenades / boulevard.

$H_{m0} \geq 3 - 5$ m   High waves and large water depths (> 10 m) near the structure. Breakwaters, seawalls at land reclamations.

Figure 3.3 to Figure 3.5 show the distributions of overtopping wave volumes for H_{m0} = 1 m; 3 m and 5 m, respectively. The graphs give the maximum overtopping wave volume, V_{max}, as well as the number of overtopping waves. Each graph illustrates how, if the mean overtopping discharge increases, then the number of overtopping waves increases, as well as the maximum volume, V_{max}. The graphs also show one of the main characteristics of wave overtopping: there are many overtopping wave volumes that are relatively small and a small number with much larger overtopping wave volumes.

The smallest mean overtopping discharge of q = 0.1 l/s per m is only present in Figure 3.3. For H_{m0} = 1 m, this discharge is the result reached by only six overtopping waves. If the wave height is H_{m0} = 2 m, one overtopping wave will be enough to cause this discharge; a single volume of 360 l per m will give 0.1 l/s per m over 3600 s, or one hour. The same is found for a wave height of H_{m0} = 5 m and a mean overtopping discharge of 1 l/s per m: only two waves may cause this discharge. This shows that very small mean discharges of q = 0.1 l/s per m or 1 l/s per m may only happen if the wave height itself is quite small. Again we should note that the results with respect to very small overtopping discharges can now be rather variable as the storm duration of 1 hour might coincide with some waves overtopping, or not.
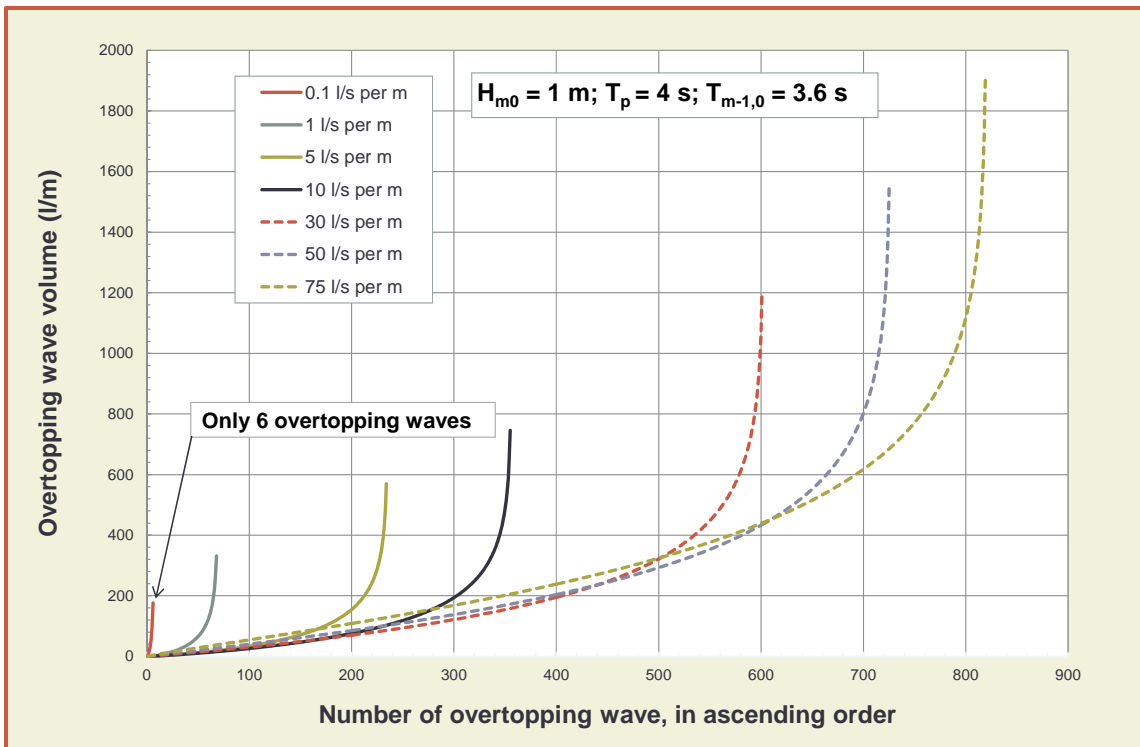
Figure 3.3: Distribution of overtopping wave volumes for a wave height of H_{m0} = 1 m; wave steepness s_{op} = 0.04 and duration of sea state is one hour. The lines represent different mean overtopping discharges from 0.1 to 75 l/s per m

The main difference between Figure 3.3 to Figure 3.5 is the difference in vertical scale in overtopping volumes. For a wave height of H_{m0} = 1 m the maximum overtopping wave volume is smaller than V_{max} < 2000 l per m or 2 m^3 per m, even for a mean discharge of 75 l/s per m (Figure 3.3). This volume is reached for almost the entire range of q = 1 to 75 l/s per m if the wave height rises to H_{m0} = 3 m. Maximum overtopping wave volumes may now be up to 7000 l per m or 7 m^3 per m (Figure 3.4). Figure 3.5 shows the same picture, but now for an increase of the wave height to H_{m0} = 5 m. Many mean overtopping discharges exceed a V_{max} of 7 m^3 per m and for q = 75 l/s per m the maximum overtopping wave volume becomes even higher, V_{max} = 13.5 m^3 per m. This is comparable to the contents of a small private swimming pool per m width. This volume of 13.5 m^3 per m can never be reached by a small wave height of 1 m, even if the crest is at the water level, since small waves simply do not carry enough water to give an overtopping volume of 13.5 m^3 per m.
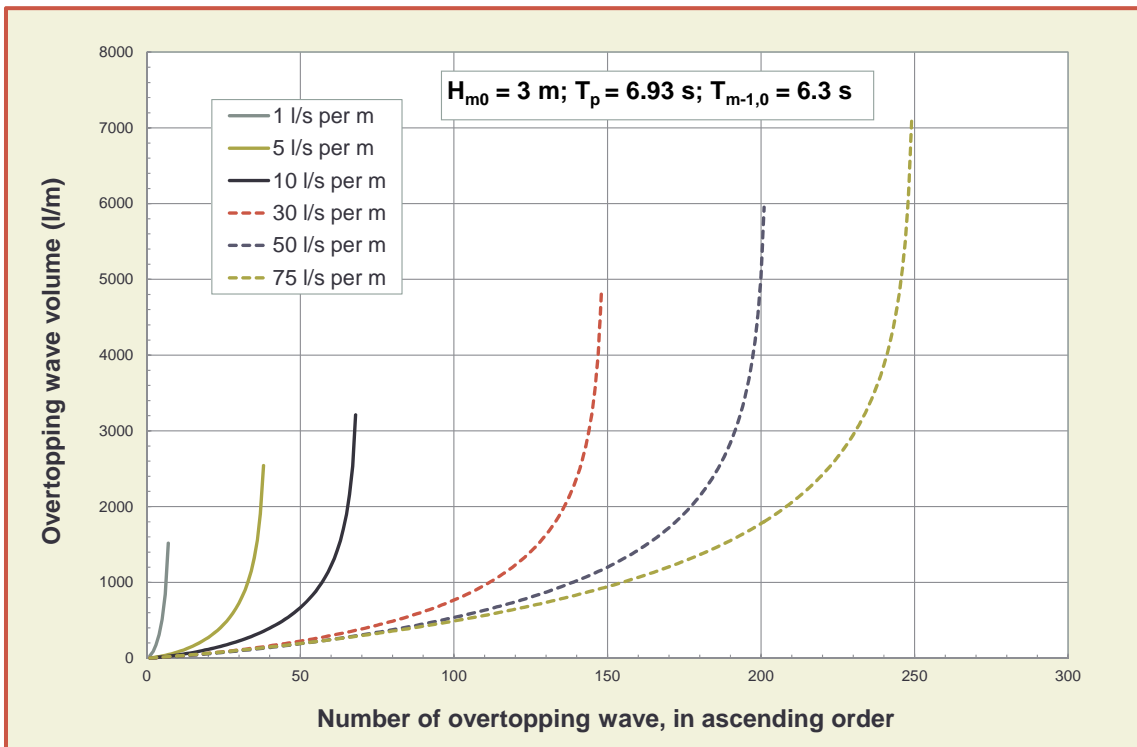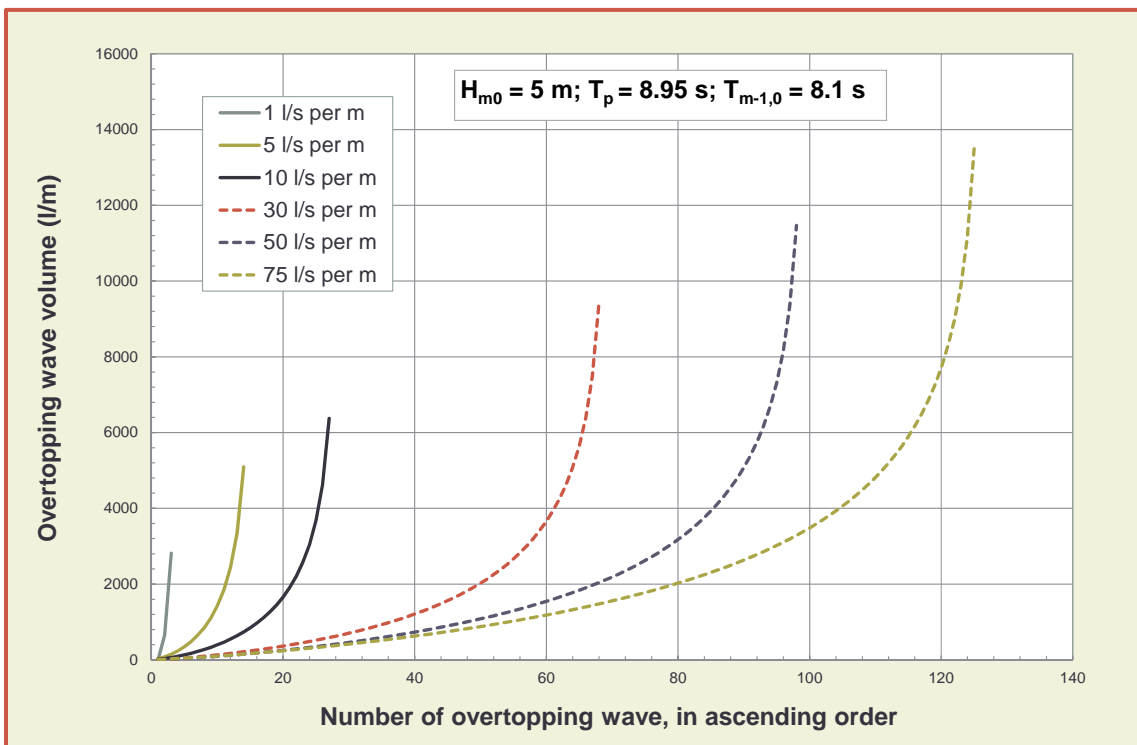
Figure 3.4:   Distribution of overtopping wave volumes for a wave height of H_{m0} = 3 m; wave steepness s_{op} = 0.04 and duration of sea state is one hour. The lines represent different mean overtopping discharges from 0.1 to 75 l/s per m

Figure 3.5:   Distribution of overtopping wave volumes for a wave height of H_{m0} = 5 m; wave steepness s_{op} = 0.04 and duration of sea state is one hour. The lines represent different mean overtopping discharges from 0.1 to 75 l/s per m

It is very clear from Figure 3.3 to Figure 3.5 that it is mainly the wave height that has a large influence on the maximum overtopping volume. Figure 3.6 gives a similar conclusion, in this graph the mean overtopping discharge is equal to q = 5 l/s per m for all four wave conditions considered. The wave height of H_{m0} = 1 m gives almost 250 overtopping waves, but the maximum overtopping volume is just 500 l per m. For a wave height of H_{m0} = 5 m, only 14 waves overtop during one hour, but the maximum overtopping volumes exceeds 5000 l per m. This is about ten times more than for a wave height of 1 m.

It is likely that most (perhaps all) damage close to the defence is caused by the largest overtopping volumes, so tolerable limits should be based on these volumes and not only on tolerable mean discharges. A maximum tolerable overtopping volume, however, may be given by different wave heights combined with different mean discharges. If for example V_{max} were to be limited to 2000-3000 l per m, then H_{m0} = 1 m may exceed a mean discharge of q = 75 l/s per m (Figure 3.3). A wave condition of H_{m0} = 3 m may then not exceed q = 10 l/s per m (Figure 3.4); and a wave height of H_{m0} = 5 m not exceed q = 1 l/s per m.
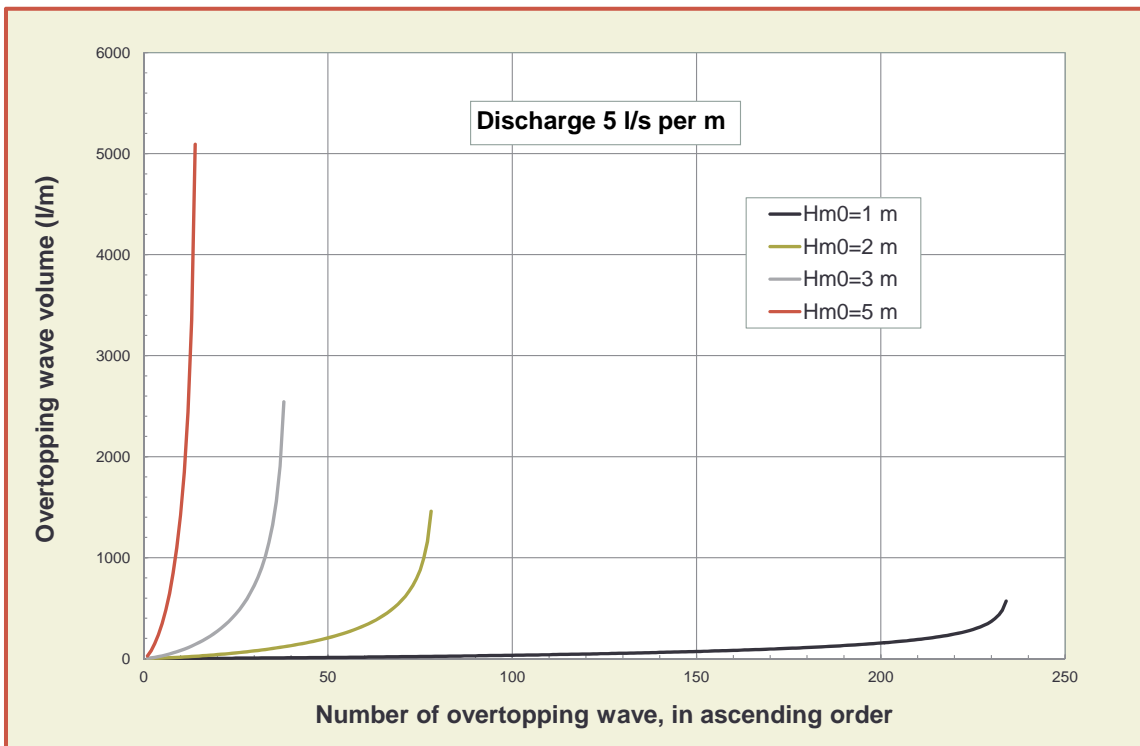

Figure 3.6: Distribution of overtopping wave volumes for a discharge of 5 l/s per m and for various wave heights; wave steepness s_{op} = 0.04 and duration of sea state is one hour

3.3.2 Simulated wave overtopping on videos

For many people an overtopping discharge is simply a figure without any physical feeling. This is logic as real overtopping is random in time and with different overtopping wave volumes. Since the testing with the wave overtopping simulator at real dikes (see Section 4.8) it is possible to simulate mean overtopping discharges for all kind of wave conditions. And every year since 2007 dikes in the Netherlands or Belgium, US and Vietnam have been tested for a variety of wave and overtopping conditions. The main objective was to test the strength of grass cover, under laying soil and transitions against wave overtopping and to come to improved guidelines.

But such a wave overtopping simulator can also be used to demonstrate how wave overtopping looks like for a certain condition. Infram in the Netherlands performed the logistic operation of testing with the wave overtopping simulator. After completion of the testing in 2014 Infram has installed the wave overtopping simulator on the crest of a dike and simulated a large number of overtopping discharges, which were taken on video. Elaborated videos have been placed on the overtopping website, www.overtopping-manual.com.

The videos have been prepared in the following way. In total 18 conditions were prepared, being for mean overtopping discharges of 1; 5; 10; 30; 50; and 75 l/s per m and for wave heights of H_{m0} = 1; 2; and 3 m. Each distribution of overtopping wave volumes was calculated for a smooth gentle 1:3 slope, a wave steepness of s_{op} = 0.04 and a duration of one hour. Example distributions for wave heights of 1 and 3 m were discussed in the previous Section. The simulation of the overtopping events by the wave overtopping simulator occurred by choosing randomly volumes from the distribution. Then the first three minutes of the steering file of one hour was taken, simulated and the test was recorded on video. It was judged that a video of three minutes would be long enough to give a good impression of a certain overtopping discharge, coupled to a certain wave height.

The mean overtopping discharge for a wave height of H_{m0} = 5 m could not be simulated as for a discharge of 5 l/s per m the maximum capacity of the wave overtopping simulator of 3000 l per m was already exceeded. Therefore, simulations and videos were limited to a wave height of H_{m0} = 3 m.

Videos were recorded from two locations, one at the down-slope looking upwards and one next to the wave overtopping simulator and looking downwards. Videos were processed in a way that they also show the distribution of overtopping wave volumes and the volume illustrated on the video. Figure 3.7 gives a snapshot of a video taken from the downslope. The video shows a mean discharge of 50 l/s per m for a wave height of 2 m. The actual overtopping wave volume shown on the video is marked by a yellow square and amounts about 700 l per m. The video gives an impression of how many waves overtop in three minutes, what overtopping wave volumes they reach and what the velocity and flow thickness is over the slope. Figure 3.8 shows a snapshot from above at the crest of the dike.
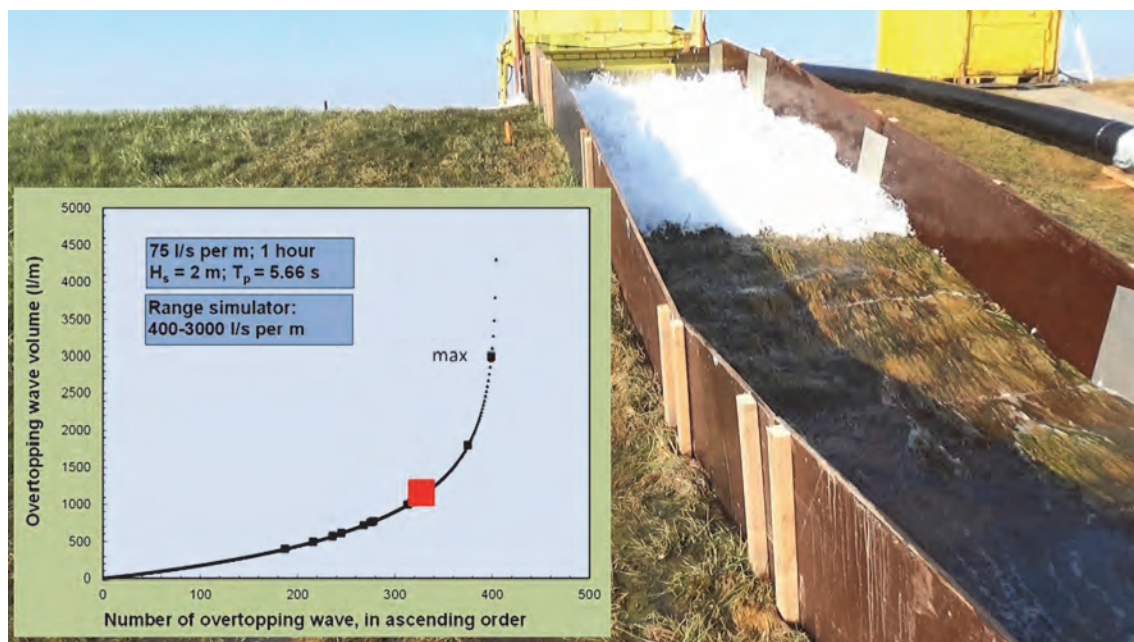

Figure 3.7   Snapshot of a three-minute video showing the overtopping wave volume from the wave overtopping simulator as well the size in the graph (red square)

Besides taking three-minute videos also specific overtopping wave volumes were captured, from 100 l per m up to 3000 l per m. In summary the following videos were prepared for the website:

- Three-minute videos looking up-slope, with the distribution of overtopping wave volumes
- Three-minute videos from the crest of the dike looking downwards

For conditions: H_{m0} = 1 m; 2 m and 3 m
and: q = 1; 5; 10; 30; 50 and 75 l/s per m

- Individual overtopping wave volumes of 100; 150; 200; 250; 300; 400; 500; 600; 700; 800; 1000; 1200; 1400; 1600; 1800; 2000; 2250; 2500; 2750 and 3000 l per m.

Figure 3.8   Snapshot of a three-minute video showing the overtopping wave volume from the wave overtopping simulator from above

The objective of making the videos available is that people interested in wave overtopping may get a clear view of a given mean overtopping discharge. Moreover, the videos can be used to make a judgement on whether these overtopping discharges can be tolerated, depending on the actual situation. It should be noted that wave heights larger than 3 m always give large overtopping wave volumes if the mean discharge exceeds 1-5 l/s per m. These volumes exceed the capacity of the wave overtopping simulator and videos for these circumstances could not be made.

3.3.3 Tolerable overtopping for structural design

Sea defences and breakwaters should withstand severe wave attack and are often armoured on the seaward side with rock, concrete units, or block revetments. River dikes and small reservoir dams are often only protected by a grass cover, but wave heights in these situations are limited. Waves that overtop the structure may attack the crest and rear side of the structure. Such a rear side could be a grass covered slope (dike), but might also be a promenade or other higher ground. A breakwater with limited wave overtopping may have a rear face protected by smaller material than on the seaward side. In all such cases, however, the tolerable wave overtopping should not significantly damage the crest or rear side, regardless of structure type.

Breakwaters For low-crested breakwaters, the crest and rear side will be protected similarly to the seaward side. Heavy overtopping may generate significant wave transmission, but if such transmission is allowed, there is little utility in assessing overtopping discharges and overtopping volumes. The transition from wave overtopping to wave transmission is described in Section 4.2.5. The transition from wave overtopping to overflow (crest below water level) has been given in Section 5.3.4.

Caisson breakwaters or vertical quays or seawalls are often capped by solid concrete which can withstand heavy overtopping. Tolerable overtopping for these types of structure is therefore often not related to structural design, but more to restrictions from port operations or vulnerable equipment on the breakwater crest (pipelines, containers), or behind the structure (moored ships).

Wave overtopping for rubble mound breakwaters may, however, be very important for structural design and can lead to disastrous failures, where the whole breakwater may collapse and disappear under water. Even if the seaward side has been fully protected against wave attack, overtopping may hit the rear side and displace the rear face armour downwards. This may lead to reduced support of the crown wall element which may then start to slide. Two examples are given here.

In the first example a rubble mound breakwater was designed with a crown wall for q= 1 l/s per m for the 100 year design condition at H_{m0} = 4.5 m. The rear side was protected by 0.5-2 t rock. Model tests showed that q ~ 1 l/s per m and the structure was stable without any damage to the rear side. It was then tested for a 20% overload to determine the resiliency of the structure at H_{m0} = 5.4 m. Overtopping increased to q = 24 l/s per m with three overtopping wave volumes between 20-30 m^3 per m in the first hour of testing (prototype). The rear side 0.5-2 t rock was heavily damaged, then two crest elements slid backwards down the rear slope. The structure was now close to a complete failure and the test was terminated. Figure 3.9 shows the damage development at the 0.5-2 t rock and Figure 3.10 shows the situation close to termination of the test with one crest element displaced below water (right side of picture).

The lesson learnt is that overtopping of ~ 10 to 30 l/s per m, with maximum volumes over 20 m^3 per m needs a strong rear side design. It also shows that relatively limited overtopping between 5 to 20 l/s per m with wave heights larger than $H_{m0} \approx 5$ m may result in significant damage to the crest or rear side, which may fail if not designed for heavy overtopping. In general, if $H_{m0} \geq 5$ m and q > 5 l/s per m, significant attention should be paid to the rear side and crest design, perhaps including physical model tests.

Figure 3.9: Damage to the 0.5-2 t rear side rock of a breakwater by wave overtopping.

Figure 3.10: Breakwater design under overload conditions and near to complete failure

A further example of a rubble mound breakwater failure by overtopping is shown in Figure 3.11. Cyclone waves gave more or less design conditions, but overtopping damaged the rear side that was (probably) not designed to resist overtopping. As with the model tests shown in Figure 3.10, the crown wall slid backwards and the crest level was eroded down by about 7 m, leaving a few Tetrapods visible above the water.

Figure 3.11: Remains (tetrapods) of a breakwater failed by wave overtopping, destroying the rear side of the structure and then a full collapse of the crest. Porbandar, India

Dikes, embankments and seawalls Many sea dikes and embankments may be subject to design wave heights in H_{m0} = 1 to 3 m, significantly less than for the breakwaters described above. The crest is often covered by grass, as well as the landward side down slope. Extensive research has been performed on the resistance of grass covered slopes since the Overtopping Simulator was developed, see Section 4.8. A good closed grass cover without open holes is very resilient to wave overtopping for wave heights H_{m0} < 3 m. Sometimes mean discharges of q ~ 100 l/s per m could not damage the slope, but a badly maintained grass cover with open holes and a lot of moss may fail well below q < 5 l/s per m. Moreover, transitions and obstacles (such as staircases, transitions to paths or roads, trees, etc.) on the slope may well cause failure before the grass slope itself.

Whist the simulator tests have shown when damage or failure may occur, safety factors should be included for design as breaching of the sea dike or embankment must be avoided. Lower tolerable limits are therefore used for design than those that caused failure. A well-maintained grass cover leading to a closed grass cover may be designed for a mean discharge of 5 l/s per m. But if the rear side is not maintained at all, giving open bare patches (as if for a vegetable garden), the tolerable overtopping should be limited to 0.1 l/s per m only, which effectively means no overtopping at all. These limits are summarised in Table 3.1.

River dikes and small (reservoir) lake dams may be subject to design wave heights that do not exceed H_{m0} = 1 m. In these situations, larger mean discharges may be allowed than for sea dikes and embankments. For wave heights smaller than H_{m0} = 0.3 m, good grass cover will always resist any overtopping volumes that can be generated by such small waves.

Besides this overall guidance on grass covered slopes, a more refined method has been developed in the Netherlands, called the cumulative overload method. This method considers the front velocity of overtopping wave volumes and the strength of grass and has been described by a critical velocity. Each large overtopping wave exceeding the critical velocity adds to the overload. Start of damage to grass covers, intermediate damage (several damaged areas) and failure (large deep holes, ongoing damage) have specific values of cumulative overload. More information on this is given in Section 4.8.

It should be noted, however, that grass cover strength depends largely on the local situation. Type and behaviour of grass cover in tropical or sub-tropical countries may differ substantially from situations in

western Europe. Even grass types on sea, lake, reservoir or river dikes in the countries around the North Sea may differ significantly. It is probable that the generally tolerable discharges for grass cover given here (0.1 to 5 l/s per m) are quite safe and may be applied all around the world. But the discharges that lead to failure may differ substantially. Overall the cumulative overload method might be applicable in every situation, but should be validated / calibrated to the circumstances in the specific country of interest.

Table 3.1 Limits for wave overtopping for structural design of breakwaters, seawalls, dikes and dams

Hazard type and reason	Mean discharge q (l/s per m)	Max volume V_{max} (l per m)
Rubble mound breakwaters; $H_{m0} > 5$ m; no damage	1	2,000-3,000
Rubble mound breakwaters; $H_{m0} > 5$ m; rear side designed for wave overtopping	5-10	10,000-20,000
Grass covered crest and landward slope; maintained and closed grass cover; $H_{m0} = 1 - 3$ m	5	2,000-3,000
Grass covered crest and landward slope; not maintained grass cover, open spots, moss, bare patches; $H_{m0} = 0.5 - 3$ m	0.1	500
Grass covered crest and landward slope; $H_{m0} < 1$ m	5-10	500
Grass covered crest and landward slope; $H_{m0} < 0.3$ m	No limit	No limit

3.3.4 Tolerable overtopping for property and operation

Wave overtopping over a breakwater or sea defence structure may hit anything behind the structure crest. The level of tolerable overtopping will be very site and structure specific. A few general examples will be given in this section, for promenades / boulevards, (temporary) storm walls, buildings and property and ships / yachts moored behind a breakwater. It is useful to recall that large incident wave heights may lead to large overtopping volumes, even if the mean overtopping discharge is quite small. And if a given overtopping limit is exceeded, it may lead to significantly larger overtopping volumes, perhaps destroying the property.

Property / equipment In some ports, property or equipment may be located on the breakwater crown wall (rubble mound or caisson), like pipelines, conveyer belts, etc. Such equipment is seldom designed to resist significant overtopping, which leads to two possible solutions for design: limit the overtopping to an acceptable limit by revising the structure design; or, protect the property / equipment to resist projected overtopping. For the latter case, it may be better to protect or cover the equipment with a structure that can withstand wave overtopping. In case the property is not protected, the mean overtopping discharge should be limited to say ≤ 1 l/s per m, if the incident wave height exceeds $H_{m0} \sim 4$ to 5 m. As the failure may be sudden, this limit should probably be applied to the overload condition, not only just to the design condition, where the overload condition is assumed to be 10%-20% larger than the design condition.

Large overtopping wave volumes may take an airborne trajectory over the breakwater crest and hit boats or yachts that are moored within a relatively short distance from the rear side of the breakwater. The overtopping shown in Figure 3.12 at a marina where boats are moored directly behind the breakwater may damage and sink yachts and smaller boats. For large wave heights, say $H_{m0} > 5$ m, overtopping volumes larger than 5 to 30 m^3 per m may severely damage or sink larger yachts. A safe approach will limit overtopping for these wave heights to q < 5 l/s per m. For smaller wave heights, overtopping might be increased to q < 10 l/s per m. Small boats, as in Figure 3.12, set 5 to 10 m away from the crest wall, may sink if wave heights are between 3 & 5 m and overtopping volumes exceed 3 to 5 m^3 per m. Safe mean overtopping discharges for such wave heights would be around q < 1 l/s per m.

Figure 3.12:   Wave overtopping at the marina of San Remo, Italy, damaging small boats

Urban defences In many coastal towns, buildings or apartments may be built immediately shoreward of the coastal boulevard or promenade. The promenade itself may be well protected, but overtopping volumes may travel across it and hit buildings. Few windows or doors, are designed to resist such forces.

An example is shown in Figure 3.13 for the sea coast of Belgium. Waves may overtop the seawall and run along the promenade to the apartments. Potentially weak elements like doors and windows are clearly seen on Figure 3.13. Without further research, mean wave overtopping discharges should be limited to q = 1 l/s per m. For this case, predictions showed that overtopping under design conditions exceeded q ≤ 1 l/s per m and the solution chosen was a demountable storm wall to be installed when overtopping onto the boulevard / promenade is forecast. The storm wall is designed to reduce overtopping at the buildings to q ≤ 1 l/s per m. General (tolerable) overtopping discharges and overtopping wave volumes described in this section have been summarised in Table 3.2.

Figure 3.13:   Apartments on the boulevard at Oostende, Belgium, protected by a movable storm wall to reduce impacts by overtopping waves

Table 3.2:   General limits for overtopping for property behind the defence

Hazard type and reason	Mean discharge q (l/s per m)	Max volume V_{max} (l per m)
Significant damage or sinking of larger yachts; $H_{m0} > 5$ m	>10	>5,000 – 30,000
Significant damage or sinking of larger yachts; $H_{m0} = 3$-5 m	>20	>5,000 – 30,000
Sinking small boats set 5-10 m from wall; $H_{m0} = 3$-5 m Damage to larger yachts	>5	>3,000-5,000
Safe for larger yachts; $H_{m0} > 5$ m	<5	<5,000
Safe for smaller boats set 5-10 m from wall; $H_{m0} = 3$-5 m	<1	<2,000
Building structure elements; $H_{m0} = 1$-3 m	≤1	<1,000
Damage to equipment set back 5-10m	≤1	<1,000

43

3.3.5 Tolerable overtopping for people and vehicles

It is in people's nature to watch violent wave action and overtopping. Some people may take risks, perhaps of injury or even of being drowned. To some extent owners / operators of coastal facilities can never avoid this. At some sites, public access may however be restricted when severe storms are forecast, but in others this may not be possible. For those sites, people should be warned of potential hazards from wave overtopping. A more focussed 'duty of care' will apply to staff who have a task to inspect and monitor the condition of sea defences during a storm surge.

Breakwaters may be particularly dangerous in storms where people can be washed off. In some instances an operating authority may be able to exclude access, but at others the public may still be able to access under severe wave conditions, even when such overtopping could be dangerous for people. Such an example is given in Figure 3.14 for Alderney breakwater in the UK. A large wave wall blocks the sea view for pedestrians on the harbour side walkway. The large mound in front of the wall often shoals up long period waves, so that impulsive breaking and overtopping may occur onto the (near) vertical wall under either storm or swell conditions.
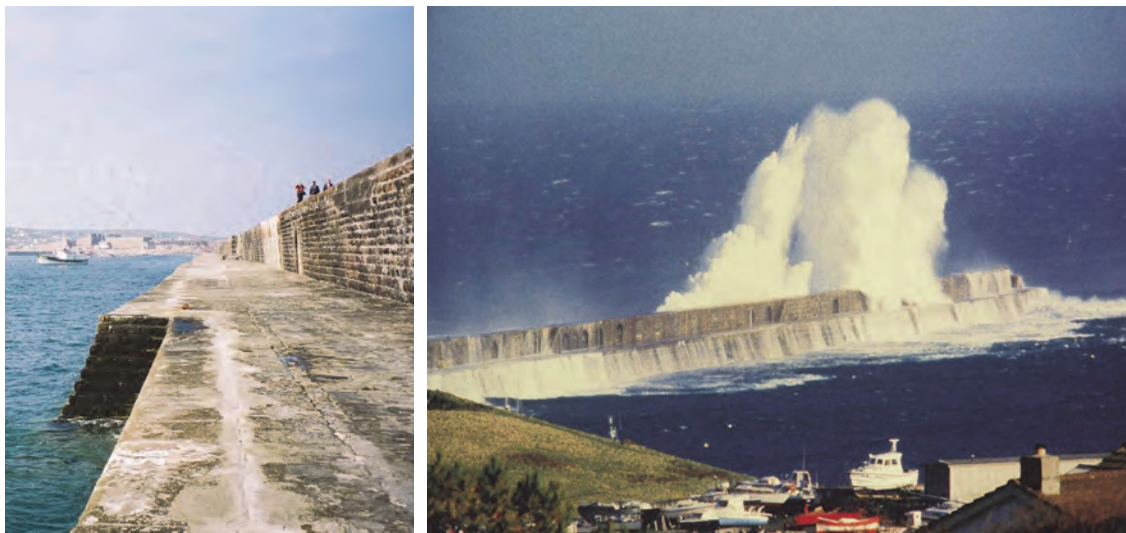
Figure 3.14:   Alderney breakwater, UK during violent wave overtopping

There are also rubble mound breakwaters that are not overtopped under daily (summer) conditions, but that might be severely overtopped during normal winter conditions. One example is given in Figure 3.15 for the breakwater of IJmuiden, the Netherlands, where access during winter is prohibited. It is hoped that it is obvious that people should not access the breakwater under the conditions shown.

Figure 3.15   Severe wave overtopping and wave transmission at the breakwater of IJmuiden, the Netherlands

Figure 3.16   New breakwater at Oostende, Belgium, with a main function of access for people

Some coastal locations use seawalls and breakwaters for recreation such as the breakwater at Oostende, Belgium, Figure 3.16. Both in summer and winter, the breakwater allows access to people, indeed that is one of its functions. The crest is wide, has many places to sit, and is illuminated at night.

Still the breakwater is not high, and with normal winter storms, overtopping may be expected at high tides. This overtopping will start for wave heights of H_{m0} ~ 2 to 3 m at or near high tide. Following analysis of the videos described in Section 3.3.2, a maximum of ~ 600 l per m was taken for the maximum tolerable overtopping volume for people on the breakwater. The weather forecast system was used to calculate mean overtopping discharge and maximum overtopping wave volumes for predicted wave conditions and water levels. As soon as a condition is predicted to exceed the maximum overtopping volume of 600 l per m, the breakwater is closed at low water preceding the expected high tide overtopping. For wave heights exceeding H_{m0} = 2 m, the maximum overtopping volume, V_{max} = 600 l per m, at Oostende was

calculated for overtopping discharges well below 1 l/s per m. For H_{m0} = 3 m the tolerable mean discharge was calculated at q < 0.3 l/s per m.

A similar operation to warn or exclude visitors has been used for approximately 20 years at the Samphire Hoe reclamation, near Dover UK where a warning system was calibrated against observations of hazardous conditions at the reclamation. Here wave overtopping over the vertical wall can be sudden and rather violent, see Figure 3.17, as discussed in Chapter 7, so warning / exclusion levels were set on a precautionary basis.

Figure 3.17   Severe wave overtopping at Samphire Hoe, UK.

During the CLASH research project, overtopping was measured at Ostia, Italy, and Figure 3.18 shows an overtopping volume being caught by the overtopping tank, used for overtopping collection and measurement. It was judged that the conditions in Figure 3.18 with q ~ 0.3 - 0.6 l/s per m and maximum volumes between 300 and 600 l per m could not be tolerated by harbour users. Wave heights were between H_{m0} = 2.2 and 2.4 m. Those observations match quite well with the estimations for Oostende, described above.
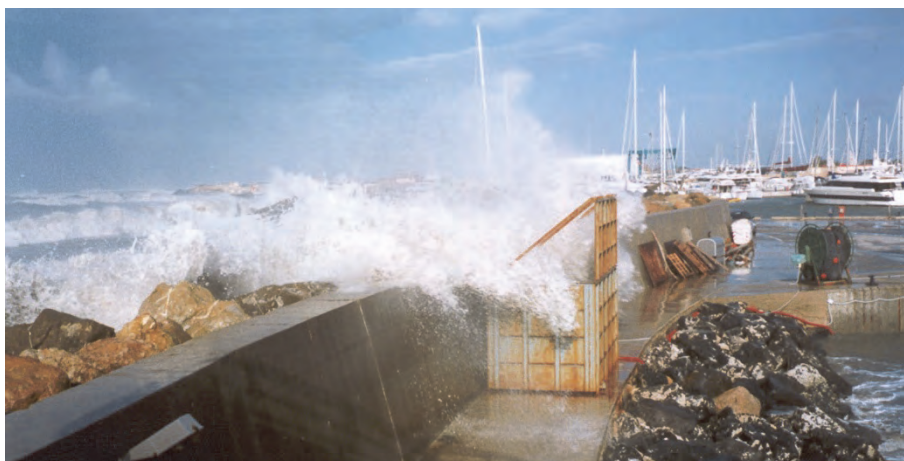
Figure 3.18   Measuring real wave overtopping during CLASH at Ostia, Italy.

Situations at a dike or embankment crest differ from those at a rubble mound breakwater in that overtopping waves run relatively smoothly over the crest and down the rear face. Overtopping waves are not projected upwards, nor do they fall from elevated crest walls. Figure 3.19 shows an example of such an event, although it is not clear whether the person on the crest was in danger, or not. Even if overtopping waves would make him/her fall, he/she would simply slide down the landward slope and would not fall into deep and cold water, which would be the case at a breakwater.

Figure 3.19   Wave overtopping over a sea dike (photo Zitscher)

Tests in the Delta flume for $H_{m0} \sim 1.5$ m showed that a person with a life line on the crest of a dike was swept off several times for overtopping discharges around 10 to 20 l/s per m and maximum volumes of around 1000 l per m; without wind. It is suggested, therefore, that for persons on a dike crest or similar, a safe limit, for $H_{m0} < 2$ m, would be a maximum volume of ~ 500 l per m, reached for q ~ 5 l/s per m. Only if $H_{m0} < 1$ m, overtopping volumes become so small that the 500 l per m limit will hardly be reached. In that sense a river dike is much safer than a sea dike, even with similar mean overtopping discharges.

In many situations it might be clear for persons whether they should access a structure during overtopping or not, and Figure 3.20 gives an example where a wave height between 1 and 1.5 m creates wave overtopping over a smooth low-crested structure. It is quite clear that access would be dangerous, or potentially fatal.

Figure 3.20   Dangerous overtopping over a smooth low-crested structure. Near locks at Afsluitdijk, NL

Figure 3.21 gives an example of a seawall with a wide boulevard behind. Here people can approach the defence without being in significant danger. In such a situation with a boulevard it is very difficult or even impossible to forbid people access, in contrast to a breakwater where the access may be blocked at the root of the breakwater. Here the common sense of people must prevail. This is different to the situation in Figure 3.17 at Samphire Hoe, UK. There the overtopping is very violent, but the site is managed and access can be blocked for people when stormy weather is forecast.

Figure 3.21   Wave overtopping at a seawall with a wide boulevard

A few general conclusions can be made on tolerable overtopping with respect to people. If the wave height exceeds about 3 m it may be dangerous to allow people on any structure during wave overtopping. If the wave height is smaller than 3 m and wave overtopping flows are generally horizontal, as over a dike crest or boulevard, then tolerable overtopping volumes will be close to 500 l per m. For wave heights just above 2 m this results in tolerable mean discharges smaller than 1 l/s per m. For smaller wave heights the mean overtopping might increase to 5 l/s per m. For very small wave heights, say < 0.5 m, no limits are needed.

Use of vehicles may also be dangerous under wave overtopping, particularly if flood depths can 'float' the vehicle away. If it is too dangerous for a dike watch to be on foot during storm conditions, it may be safer to drive along the crest in a vehicle, perhaps four-wheel drive. If overtopping volume or velocities that hit the vehicle become too large, it may slide. Such an event i estimated at wave overtopping volumes of around 1000 to 2000 l per m, perhaps given by wave heights around 3 m and a mean discharge of 5 l/s per m. For a wave height around 2 m this becomes a tolerable mean discharge of 10 to 20 l/s per m; and for a wave height around 1 m this is about 75 l/s per m, provided that flood depths are less than 0.3m.

For vehicles driven at speed on an exposed causeway, almost any overtopping will endanger the traffic. Experience with the Afsluitdijk in the Netherlands, a 32 km long dike and road between the Wadden Sea and the IJsselmeer (Figure 3.22), is that the road is closed for traffic well before actual wave overtopping occurs. Very strong winds (say Beaufort 10 or more) create spray, which may carry beach material or debris like wood, (plastic) bottles, etc. These can be very dangerous for traffic, much more than the actual spray. Such highways should probably be closed or severely restricted before real overtopping starts.

Figure 3.22:   The highway on the Afsluitdijk, the Netherlands, with the Wadden Sea and the sea defence on the left side and the fresh water lake, the IJsselmeer, on the right side

Railways may also have tracks close to the sea, see Figure 3.23. Trains will be more stable than road vehicles, heavier and less likely to float, but they will need to travel slowly, certainly if beach material or debris may be in the water. The wave overtopping in the picture flies through the air and solid water may hit the train windows. Tolerable overtopping volumes should probably be less than 2000 l per m, depending on violence of the overtopping and the distance of the railway from the seawall.

Figure 3.23: Wave overtopping onto a moving train, UK

Finally, the (tolerable) overtopping discharges and overtopping wave volumes described in this section are summarised in Table 3.3.

Table 3.3: Limits for overtopping for people and vehicles

Hazard type and reason	Mean discharge q (l/s per m)	Max volume V_{max} (l per m)
People at structures with possible violent overtopping, mostly vertical structures	No access for any predicted overtopping	No access for any predicted overtopping
People at seawall / dike crest. Clear view of the sea. $\quad$ $H_{m0} = 3$ m $\quad$ $H_{m0} = 2$ m $\quad$ $H_{m0} = 1$ m $\quad$ $H_{m0} < 0.5$ m	0.3 1 10-20 No limit	600 600 600 No limit
Cars on seawall / dike crest, or railway close behind crest $\quad$ $H_{m0} = 3$ m $\quad$ $H_{m0} = 2$ m $\quad$ $H_{m0} = 1$ m	<5 10-20 <75	2000 2000 2000
Highways and roads, fast traffic	Close before debris in spray becomes dangerous	Close before debris in spray becomes dangerous

3.3.6 Effects of debris and sediment in overtopping flows

There are hardly any data on the effect of debris on hazards caused by wave overtopping, although anecdotal comments suggest that damage can be substantially increased for a given overtopping discharge or volume if "hard" objects such as rocks, shingle or timber are included in overtopping. It is known that impact damage can be particularly noticeable for seawalls and promenades where shingle may form the "debris" in heavy or frequent overtopping flows.

Another example is given in Figure 3.24 and Figure 3.25, where a hurricane by a large surge lifted large debris like logs that was accumulated over years on marsh land. A lot of the debris was locked by a bend in the flood protection (corner), see Figure 3.29. Another part of the flood protection was fully attacked by waves, including the logs and other large debris. It broke a pvc sheetpile, which was placed to limit wave overtopping. A lot of debris was transported over the crest, see Figure 3.30. and the wave overtopping at this location was much higher than expected

Figure 3.24:   Debris gathered in a corner by a hurricane. Gulf coast, USA

Figure 3.25:   Debris such as logs in the water broke a pvc sheetpile during a hurricane and the material was transported over the crest to the landward slope. Picture taken from inside, looking at the landward slope. Gulf coast, USA

3.3.7 Zero overtopping

Experience has shown that some clients and designers may want to design for "zero overtopping". It is, however not easy to define what 'zero overtopping' is, particularly as the prediction equations are exponential, so never actually predict zero! When there is no strong wind, and waves are low, it is clear that a structure will effectively have zero overtopping, even if the prediction equations might predict some (vanishingly small) discharge. A critical question may be "When does overtopping start?" if there is a storm, waves may be large, and water levels are increased by a surge. One logical limit for overtopping discharge that has been used is to set a lower limit for wave overtopping at that predicted for heavy

rainfall, of (say) 50 mm per hour onto a 10 m wide promenade. This gives a lower limit for mean discharge of 0.1 l/s per m. This may not however be small enough when considering individual overtopping volumes.

The elaborations in Section 3.3 have shown that the accuracy of small overtopping discharges depend strongly on the incident wave height. For example, a discharge of q = 0.1 l/s per m gives only 360 l per m overtopping water in one hour. If the wave height is small, say around 1 m or smaller, around five to ten waves in one hour will overtop the structure to give the mean discharge of 0.1 l/s per m. This is still quite well defined and cannot be seen as 'zero overtopping', although it is very limited overtopping.

If the wave height is much larger, say 5 m, then ten to fifteen overtopping waves will give a mean discharge of around q = 5 l/s per m. Only one or two overtopping waves may give 1 l/s per m and the calculation procedures suggests that less than one wave can produce a mean discharge of q = 0.1 l/s per m. This simply means that some samples of 1 hour may see no overtopping, others will see one or two overtopping events, but averaging less than one event per hour. For mean overtopping between 0.1 and 1 l/s per m, very few largest waves may give an overtopping volume or not. The estimation of overtopping for these wave heights with mean overtopping smaller than 0.1 l/s per m is highly uncertain. However, if for large wave heights only one or two waves overtop in one hour, the overtopping wave volumes may be large enough to damage property, equipment at the crest or injure people.

Limits in measuring mean overtopping discharges in laboratory tests can be found in Chapters 5, 6 and 7. Such overtopping discharges are given in a dimensionless way: $q/(gH_{m0}^3)^{0.5}$ and are given versus a dimensionless freeboard. In the graphs in Chapters 5 and 6, the (dimensionless) limit of $q/(gH_{m0}^3)^{0.5} = 10^{-5}$ is hardly exceeded so this limit might be used as a "zero overtopping" in the laboratory. Depending on the wave height in reality, 'calculated zero mean overtopping discharges' then becomes:

H_{m0} = 1 m: q = 0.03 l/s per m

H_{m0} = 3 m: q = 0.16 l/s per m

H_{m0} = 5 m: q = 0.4 l/s per m

H_{m0} = 7 m: q = 0.6 l/s per m

In reality the overtopping may be really zero or it may be ten times larger than calculated above, as all depends on whether one or two waves do overtop or not. At real structures one may be able to measure overtopping that is smaller than the values given above, but it is hardly possible to measure them in small scale. Above values, depending on the wave height, can be seen as zero overtopping in reality.

4 Overtopping tools in perspective

4.1   Introduction

A number of different methods are available to predict overtopping of particular structures (usually simplified sections) under given wave conditions and water levels. Each method will have strengths or weaknesses in different circumstances. In theory, an analytical method can be used to relate the driving process (waves) and the structure to the response through equations based directly on a knowledge of the physics of the process. It is however extremely rare for the structure, the waves and the overtopping process to all be so simple and well-controlled that an analytical method on its own can give reliable predictions. Analytical methods are not therefore discussed further in this manual.

The primary prediction methods are therefore based on empirical methods, mainly formulae, (Section 4.2) that relate the overtopping response (usually mean overtopping discharge, q) to the main wave and structure parameters. Another method has been derived during the CLASH European project based on the use of measured overtopping from model tests and field measurements and this method became a calculation tool described in the first edition of EurOtop (2007). In CLASH a large database was constructed of structures, waves and overtopping discharges, with each cross-section of the tested structure described by 13 parameters. Then a Neural Network tool was trained using the test results in the database, which became available as calculation tool in EurOtop (2007). The Neural Network tool can be run automatically on a computer as a stand-alone device, or embedded within other simulation methods.

For the present manual the database has largely been extended and optimised and improved Neural Networks have been made, see Sections 4.4 and 4.5. The database is available on the website as the EurOtop database, as are the EurOtop Neural Networks. Using data directly from the database is possible, but potentially complicated, requiring some familiarity with these type of data and filtering in Excel. Nonetheless, a situation may be found in the database that will be similar to the one being examined, but for most of these cases the EurOtop Neural Networks will give a good prediction and are simpler to use.

For situations for which empirical test data do not already exist, or where the methods above do not give reliable enough results, then two alternative methods may be used, but both are more complicated than the three methods described in Sections 4.2 to 4.5. A range of numerical models can be used to simulate the process of overtopping (Section 4.6). All such models involve some simplification of the overtopping process and are therefore limited to particular types of structure or types of wave exposure. They may however run sequences of waves giving overtopping (or not) on a wave-by-wave basis. Generally, numerical models require more skill and familiarity to run successfully.

Another method discussed here is physical modelling in which a scale model is tested with correctly scaled wave conditions (Section 4.7). Typically such models may be built to a geometric scale typically in the range 1:20 to 1:60, see discussion on model and scale effects in Section 4.9. Waves will be generated as random wave trains each conforming to a particular energy spectrum. The model may represent a structure cross-section in a 2-dimensional model tested in a wave flume. Structures with more complex plan shapes, junctions, transitions etc., may be tested in a 3-dimensional model in a wave basin. Physical models can be used to measure many different aspects of overtopping, such as individual overtopping wave volumes, overtopping velocities and depths, as well as other responses.

A final method described in this chapter is not on prediction or calculation of wave overtopping, but on simulating wave overtopping in reality: the hydraulic simulators (Section 4.8). Hydraulic simulators may "bring the laboratory to the dike". By simulating wave overtopping at real structures it is possible to observe and measure the effect of wave overtopping. This may be the strength of grass covered dikes, including obstacles and transitions, but also wave pressures or forces on vertical (storm) walls. At this moment there are three simulators that are able to simulate or reproduce a specific aspect of the wave-structure-interaction: wave run-up, impact and overtopping simulators. This chapter describes the processes they can simulate. Results of many years of testing will not be described, as that is not the subject of this manual, but a quick overall view will be given.

4.2 Empirical models, including comparison of structures

4.2.1 Mean overtopping discharge, introduction

Empirical methods use a simplified representation of the physics of the process presented in (usually dimensionless) equations to relate the main response parameters (overtopping discharge etc.) to key wave and structure parameters. The form and coefficients of the equations are adjusted to reproduce results from physical model (or field) measurements of waves and overtopping. Empirical equations may be solved explicitly, or may occasionally require iterative methods to solve. Historically some empirical methods have been presented graphically, although this is now very rare.

The mean overtopping discharge, q, is the main parameter in the overtopping process. It is of course not the only parameter, but it is easy to measure in a laboratory wave flume or basin, and most other parameters are related in some way to this overtopping discharge. The overtopping discharge is given in m^3/s per m width and in practical applications often in litres/s per m width (l/s per m). Although it is given as a discharge, the actual process of wave overtopping is much more dynamic, see also Section 1.4.13. Only large waves will reach the crest of the structure and will overtop with a lot of water in a few seconds. This wave by wave overtopping is more difficult to measure in a laboratory than the mean overtopping discharge.

As the mean overtopping discharge is quite easy to measure many physical model tests have been performed all over the world, both for scientific (idealised) structures and real applications or designs. The new EurOtop database is an extension of the CLASH database and resulted in more than 13,000 wave overtopping tests on all kinds of structures (see Section 4.4). Some test series have been used to develop empirical methods for prediction of overtopping. Very often the empirical methods or formulae are applicable for typical structures only, like smooth slopes (dikes, sloping seawalls), rubble mound structures or vertical structures (caissons or walls).

Chapters 5, 6 and 7 will describe in detail formulae for the different kinds of structure. In this section, *an overall view* will be given in order to *compare different structures* and to give more insight into how wave overtopping behaves for different kinds of structure. The structures considered here with governing overtopping equations (more details in Chapters 5, 6 and 7) are: smooth sloping structures (dikes, seawalls); rubble mound structures (breakwaters, rock slopes); and vertical structures (caissons, sheet pile walls), including very steep slopes. But first a comparison will be given between the main wave overtopping formulae in EurOtop (2007) and the present manual.

4.2.2 Mean overtopping discharge – old and new formulae in EurOtop

The main equations for wave overtopping over sloping structures in this manual have been changed compared to EurOtop (2007). The improvement is specially in the area for very low freeboards including a zero freeboard (crest level equal to the water level). For sloping structures, where the freeboard is at least half the wave height ($R_c/H_{m0} > 0.5$), the differences between the "old" EurOtop (2007) formulae and the new ones is quite small. For that reason one may also continue to use the EurOtop (2007) formulae if that would have preference, as long as the crest freeboard is large enough. Chapters 5, 6 and 7 only describe the new formulae. Therefore, the old and new formulae are compared here first.

The principal formula used for wave overtopping is:

$$\frac{q}{\sqrt{gH_{m0}^3}} = a \exp\left[-\left(b\frac{R_c}{H_{m0}}\right)^c\right] \qquad \text{for } R_c \geq 0 \qquad\qquad 4.1$$

It is a Weibull-shaped function with the dimensionless overtopping discharge $q/(gH_{m0}^3)^{1/2}$ and the relative crest freeboard R_c/H_{m0}. The EurOtop (2007) formulae for sloping structures use for the exponent c in Equation 4.1 a value of c = 1, which then becomes an exponential function. The EurOtop (2007) formulae are given by:

$$\frac{q}{\sqrt{g \cdot H_{m0}^3}} = \frac{0.067}{\sqrt{\tan \alpha}} \gamma_b \cdot \xi_{m-1,0} \cdot \exp\left(-4.75 \frac{R_C}{\xi_{m-1,0} \cdot H_{m0} \cdot \gamma_b \cdot \gamma_f \cdot \gamma_\beta \cdot \gamma_v}\right)$$

with a maximum of: $\frac{q}{\sqrt{g \cdot H_{m0}^3}} = 0.2 \cdot \exp\left(-2.6 \frac{R_C}{H_{m0} \cdot \gamma_f \cdot \gamma_\beta \cdot \gamma_v}\right)$

4.2

For detailed explanation of the parameters, see Chapters 5 and 6. In the present manual the formulae are given as:

$$\frac{q}{\sqrt{g \cdot H_{m0}^3}} = \frac{0.023}{\sqrt{\tan \alpha}} \gamma_b \cdot \xi_{m-1,0} \cdot \exp\left[-\left(2.7 \frac{R_c}{\xi_{m-1,0} \cdot H_{m0} \cdot \gamma_b \cdot \gamma_f \cdot \gamma_\beta \cdot \gamma_v}\right)^{1.3}\right]$$

4.3

with a maximum of: $\frac{q}{\sqrt{g \cdot H_{m0}^3}} = 0.09 \cdot \exp\left[-\left(1.5 \frac{R_c}{H_{m0} \cdot \gamma_f \cdot \gamma_\beta \cdot \gamma_v}\right)^{1.3}\right]$

4.4

The main differences in Equations 4.2 and 4.3 or 4.4 are the values of the coefficients and the different value of c. The value of c=1.3 gives a slightly curved line on a log-linear graph, where the exponential distribution gives a straight line. Figure 4.1 shows a comparison between new formula in this manual and the EurOtop (2007) formula for breaking waves. The graph is almost identical for non-breaking waves. The differences are small and indeed largest for the area $R_c/H_{m0} < 0.5$, where the EurOtop (2007) formulae are not valid anymore.
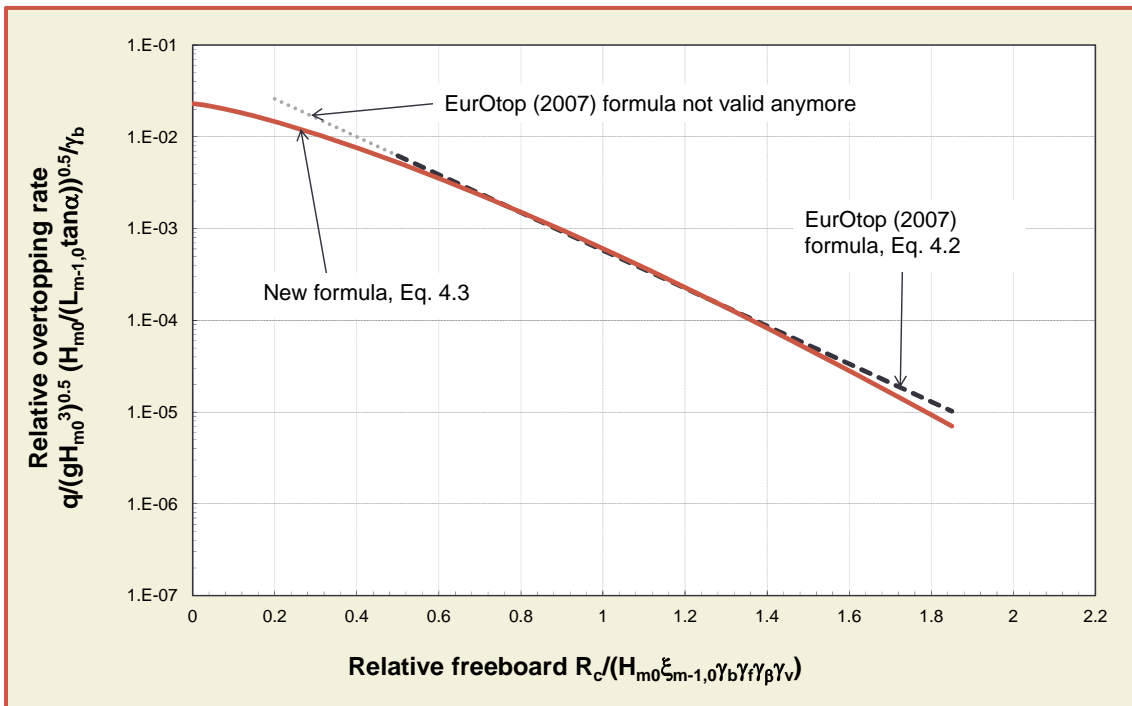
Figure 4.1. Comparison of EurOtop (2007) formula with the new one in this manual

Although the differences between the old and new formulae may be small, it is good to give a more precise description of the differences, as these are the basic formulae for wave overtopping. The reliability of overtopping can be given by the 5% exceedance and 5% non-exceedance values, giving the band where 90% of the data will be present. The uncertainty increases if the overtopping discharge decreases, see also Chapter 5 and for example Figure 5.12. The difference between the upper and lower 5% boundary is

about a factor 2.5 for small values of the relative freeboard R_c/H_{m0}. For example the discharge may range between 100 l/s per m and 250 l/s per m. The difference increases up to factors of 20 and more for very small overtopping discharges. For example the discharge may range between 0.1 l/s per m and 2 l/s per m.

Figure 4.2 shows the difference between calculated overtopping discharges by the new and EurOtop (2007) formulae. On the left side of the graph the new formulae give up to 20% lower values. In the middle of the range of relative freeboards, the new formulae may give up to 4% (breaking waves) or 27% (non-breaking waves) more overtopping than the old formulae. For very low overtopping discharges, the right part of the curves, the new formulae may give up to 30% less overtopping than the old ones. Compared to the reliability of overtopping predictions (a factor 2.5 to 20, see above), differences of 30% or less are of course much smaller. It can be concluded that the differences in wave overtopping discharge between the new and EurOtop (2007) is insignificant for relative freeboards $R_c/H_{m0} > 0.5$.
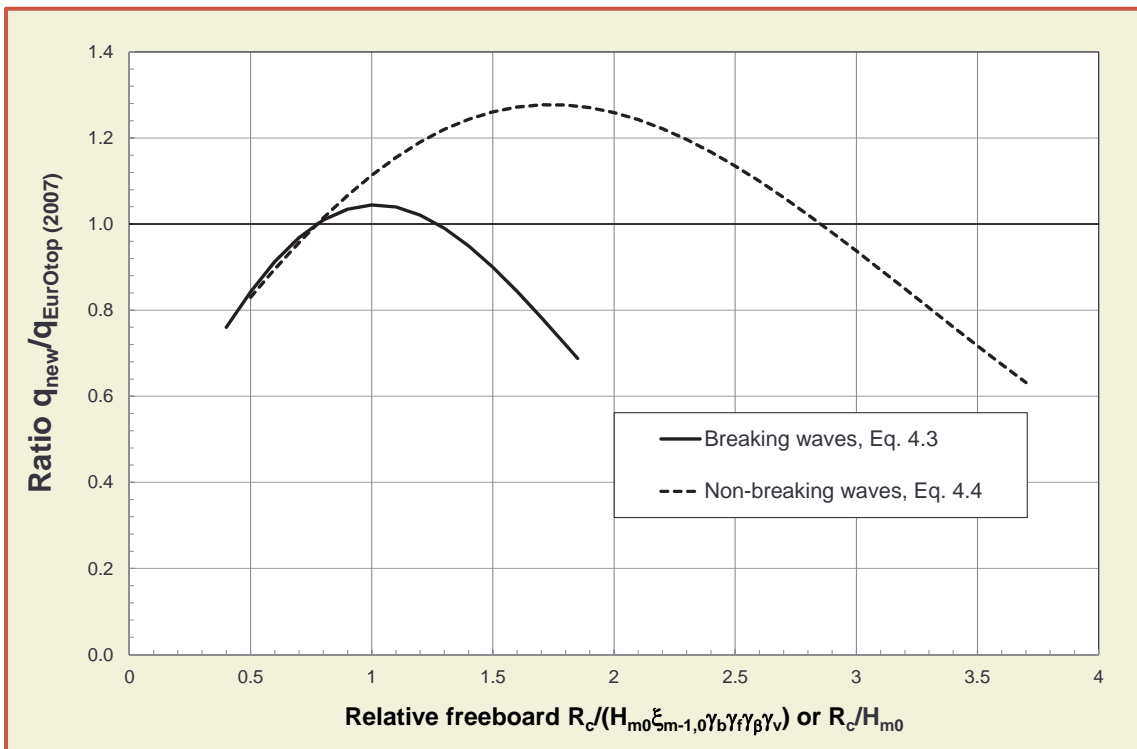
Figure 4.2.   Difference in calculated overtopping discharges by the new and EurOtop (2007) formulae

4.2.3 Mean overtopping discharge – comparison of types of structure

The new equation for wave overtopping discharge, as in Equations 4.3 and 4.4, is a Weibull-shaped function with the dimensionless overtopping discharge $q/(gH_{m0}^3)^{0.5}$ and the relative crest freeboard R_c/H_{m0}. This type of equation shown in a log-linear graph gives a slightly curved line and it is possible to compare the formulae for various structures. Specific equations are given in Chapters 5 and 6 for smooth and rubble mound structures and sometimes include a berm, oblique wave attack, wave walls and the slope angle and wave period or wave steepness.

Chapter 7 describes wave overtopping at vertical structures. A distinction should be made for structures without an influencing foreshore (caissons, quay walls, locks, see also Section 1.4.6) and those with an influencing foreshore. If an influencing foreshore is present, waves may become impulsive, break onto the structure and give overtopping for very large relative freeboard. This will not be the case for non-impulsive waves, which give overtopping more in line with a structure without an influencing foreshore.

To put wave overtopping in perspective, various kinds of structures will be compared here. For easy comparison of different structures, like smooth and rubble mound sloping structures and vertical structures for non-impulsive and impulsive waves, some simplifications will be assumed. In order to simplify the **smooth structure** no berm is considered ($\gamma_b = 1$), only perpendicular wave attack is present ($\gamma_\beta = 1$), no

vertical wall on top of the structure is present ($\gamma_v = 1$), and a smooth / impermeable structure is considered ($\gamma_f = 1$). The slope angles considered for smooth slopes are $\cot\alpha = 1.5$ to 8, which means from very steep to very gentle. If relevant a wave steepness of $s_{m-1,0} = 0.04$ (steep storm waves) and 0.01 (long waves due to swell or wave breaking) will be considered. Smooth slopes can become very steep, almost vertical, therefore slope angles of 1:4 (gentle); 1:2 (steep) and 2:1 (very steep) are included.

The same equation as for smooth sloping structures is applicable for **rubble mound slopes**, but now a roughness factor of $\gamma_f = 0.5$ will be assumed, simulating a rock armoured structure. Rubble mound structures are often steep, but rock slopes may also be gentle, and so slope angles with $\cot\alpha = 1.5$ and 3.0 are considered.

Vertical structures under non-impulsive waves are divided in those having an influencing foreshore and those without that influence. The overtopping for impulsive, breaking waves, on vertical structures on a foreshore depends on the breaker index H_{m0}/h and the wave steepness, $s_{m-1,0}$. Three combinations will be considered: $H_{m0}/h = 0.3$ with $s_{m-1,0} = 0.04$ (non-depth limited waves with steep wind waves); $H_{m0}/h = 0.6$ with $s_{m-1,0} = 0.02$ (depth limited waves with relatively long waves); and $H_{m0}/h = 0.9$ with $s_{m-1,0} = 0.01$ (severe breaking on a steep foreshore with very long waves).
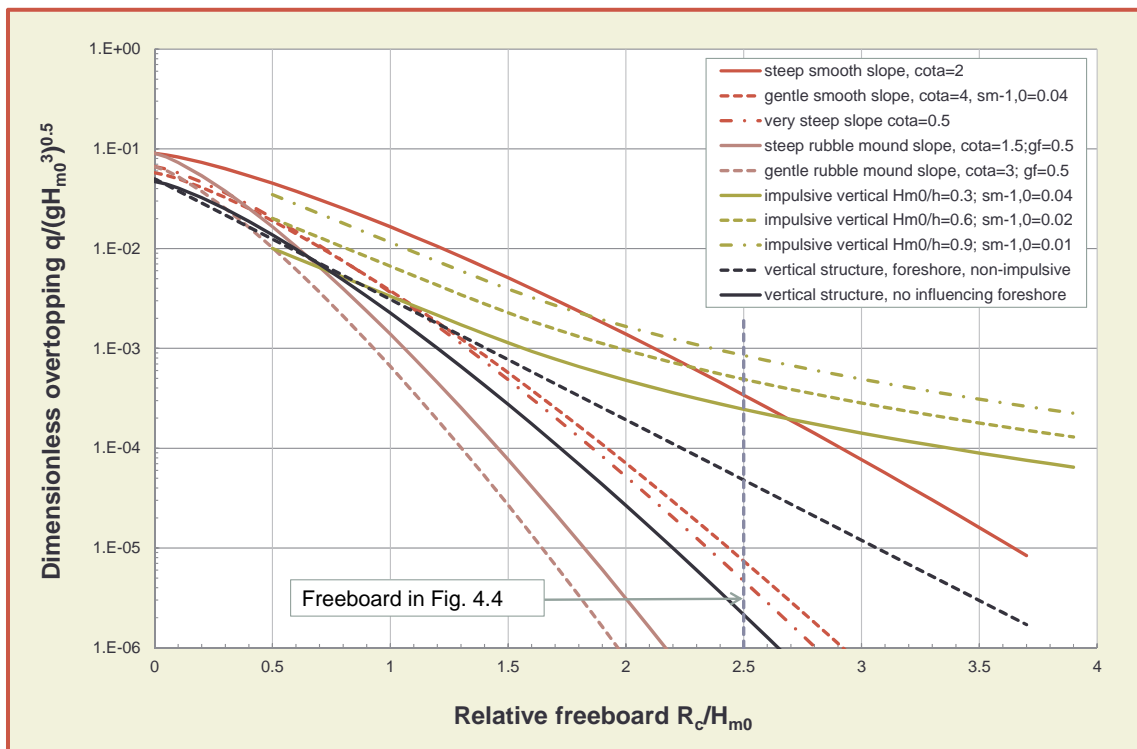
Figure 4.3:   Comparison of wave overtopping formulae for various kind of structures

Smooth slopes can be compared with rubble mound slopes and with vertical structures under pulsating or impulsive conditions. First the traditional graph is given in Figure 4.3 with the relative freeboard R_c/H_{m0} versus the logarithmic dimensionless overtopping $q/(gH_{m0}^3)^{0.5}$. Each structure type has the same colour.

A number of observations can be made. The curves that deviate most from the general trend are the impulsive waves on vertical structures, given by the green/yellow lines. The influence of the breaker index and wave steepness is fairly small as all three curves are quite close. The difference with the other structures becomes very significant for higher structures with large relative freeboards, say $R_c/H_{m0} > 3$. With impulsive conditions water is thrown high into the air, which means that overtopping occurs even for very high structures. The vertical distance that the overtopping wave travels is more or less independent of the actual height of the structure. For $R_c/H_{m0} > 3$ the curves are almost horizontal.

In all other cases the steep smooth slope (solid red line) gives the largest overtopping. Steep means cotα ~ 2, but also if longer (small steepness) waves are considered, waves may surge up the steep slope. For gentler slopes, waves break as plunging waves and this reduces wave overtopping significantly. The gentle slope with cotα = 4 gives much lower overtopping than the steep smooth slope with cotα = 2. Both slope angle and wave period have influence on overtopping for gentle slopes. The very steep smooth slope of cotα = 0.5 (or a slope 2:1), is quite close to the gentle smooth slope of 1:4 (both dashed red lines).

The large roughness and high permeability of a rubble mound structures (brown lines) reduces wave overtopping to a great extent. A roughness factor of $\gamma_f = 0.5$ was used for the examples shown, but $\gamma_f = 0.4$ (two layers of rock on a permeable under layer) would have reduced the overtopping still further. The gentle rubble mound slope with cotα = 3 gives the lowest overtopping of all structures considered in Figure 4.3.

Vertical structures under pulsating waves, with and without an influencing foreshore (black lines), deviate mainly for larger freeboards, where the structure on a foreshore gives the largest overtopping. On average these type of structures show similar overtopping behaviour to the gentle smooth 1:4 slope, but give more overtopping than a rubble mound slope. The very steep smooth slope of cotα = 0.5 gives overtopping close to the vertical wall without an influencing foreshore.

Another way of comparing various structures is to show the influence of the slope angle on wave overtopping, and this is shown in Figure 4.4. Note that the vertical axes in Figure 4.3 and Figure 4.4 are the same. A vertical structure has cotα = 0, very steep smooth slopes (also called battered walls) have 0 < cotα < 1, and steep smooth structures can roughly be described by 1 ≤ cotα ≤ 3, whereas gentle slopes start from around cotα ≥ 3. Figure 4.4 shows the full trend for cotα = 0 - 8, which is from vertical walls (without an influencing foreshore) to gentle smooth slopes for $\gamma_f = 1$. A distinction has been made for the wave steepness, which is important for gentle slopes. Wave steepnesses of $s_{m-1,0} = 0.01$ (long waves) and 0.04 (short wind waves) have been taken. A fixed relative freeboard of $R_c/H_{m0} = 2.5$ has been taken and this level has also been given in Figure 4.3 with the vertical dashed line.
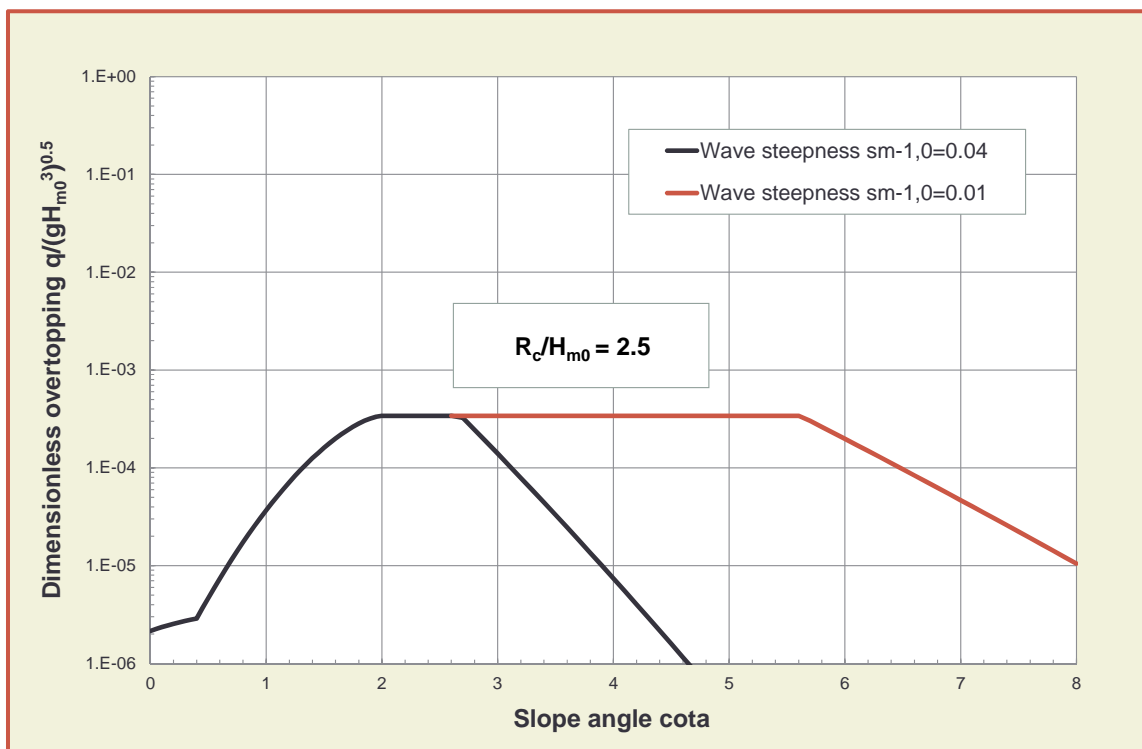
Figure 4.4: Comparison of wave overtopping as function of slope angle

There is a clear trend in Figure 4.4. Steep slopes around 1:2 to 1:3 give the largest overtopping, but for gentler slopes with much longer waves large overtopping is still observed, due to the fact that waves are

still surging (non-breaking). Vertical structures with $\cot\alpha = 0$, but without an influencing foreshore, give quite low overtopping and this increases only slightly for battered walls, say up to $\cot\alpha = 0.5$. With increasing slope angle the overtopping then increases rapidly to the maximum that is reached for $\cot\alpha = 2$. As soon as waves start to break on a gentle foreshore, the overtopping decreases fast, which is given by the decreasing lines on the right side of the graph. Details of all equations used here are described in Chapter 5 (sloping smooth structures), Chapter 6 (rubble mound structures) and Chapter 7 (vertical structures).

4.2.4 Overtopping volumes and V_{max}

Wave overtopping is a dynamic and irregular process and the mean overtopping discharge, q, does not fully describe the process. By knowing the storm duration, t, and the number of overtopping waves during that time, N_{ow}, it is possible to describe this irregular and dynamic overtopping, if the overtopping discharge, q, is known. Each overtopping wave gives a certain overtopping volume of water, V, and this can be given as a distribution.

As with many equations in this manual, the two-parameter Weibull distribution describes the behaviour quite well, see Equation 4.5. This equation has a shape parameter, b, and a scale parameter, a. The shape parameter gives a lot of information on the type of distribution.

$$P_{V\%} = P(V_i \geq V) = \exp\left[-\left(\frac{V}{a}\right)^b\right] \cdot (100\%)$$
4.5

where $P_{V\%}$ is the percentage of all overtopping wave volumes that an individual wave volume (V_i) will exceed a specified volume (V). P_V, which is not in the equation, is the portion of wave volumes that will exceed the specified volume (V), so $P_{V\%} = P_v \cdot 100\%$. More information on the Weibull distribution is given in Section 5.5.2.
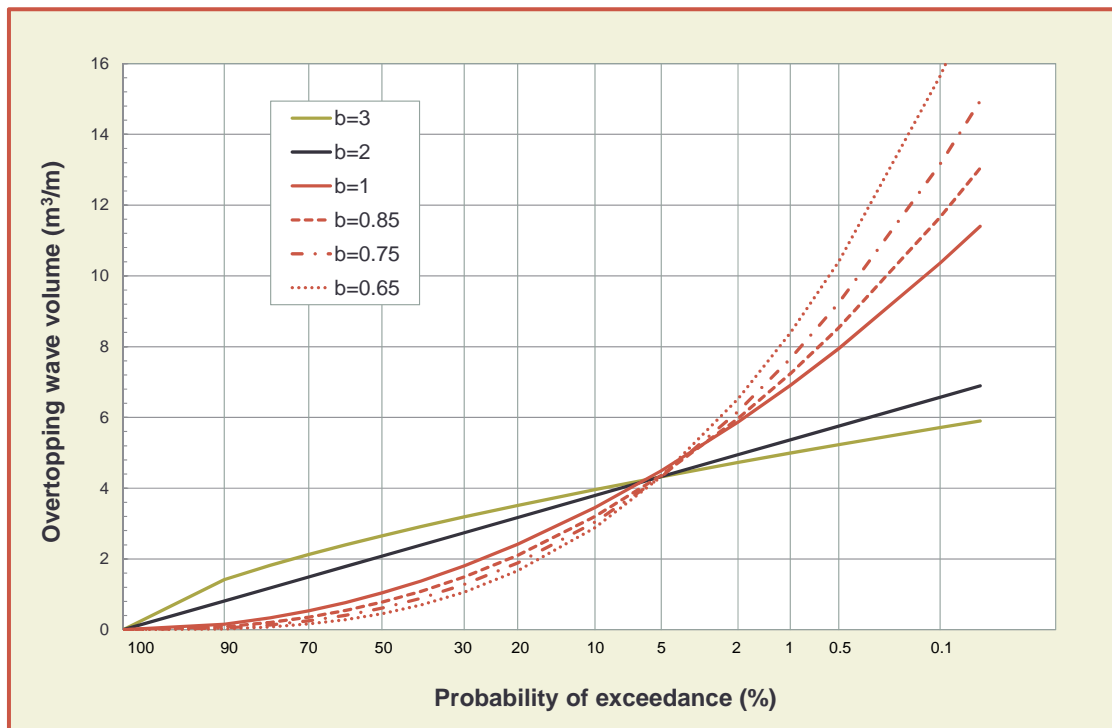
Figure 4.5:   Various distributions on a Rayleigh scale graph. A straight line (b = 2) is a Rayleigh distribution

Figure 4.5 gives an overall view of some well-known distributions. The horizontal axis gives the probability of exceedance (portion) and has been plotted according to the Rayleigh distribution. The reason for this is that waves in deep water have a Rayleigh distribution and every parameter related to the deep water wave conditions, like shallow water waves or wave overtopping, directly show the deviation from such a Rayleigh distribution in the graph. A Rayleigh distribution should be a straight line in Figure 4.5 and a deviation from a straight line is a deviation from a Rayleigh distribution.

When waves approach shallow water and the highest waves break, the wave height distribution that first could be described by a Rayleigh-distribution (b = 2), turns into a Weibull distribution with b > 2; also refer to Figure 2.5. An example with b = 3 is shown in Figure 4.5 and this indicates that there are more large waves of similar height. Battjes and Groenendijk (2000) give a composite Weibull-distribution for wave heights on shallow water, which are quite close to Weibull-distributions with b > 2. The exponential distribution (often found for extreme wave climates) has b = 1 and shows that extremes become larger compared to most of the data. Such an exponential distribution would give a straight line in a log-linear graph.

The distribution of overtopping wave volumes for all kinds of structures may have average values even smaller than b = 1. Such a distribution is even steeper than an exponential distribution, which means that the wave overtopping process can be described by a lot of fairly small or limited overtopping wave volumes and a few very large volumes. For comparison curves with b = 0.65, 0.75 and 0.85 are given in Figure 4.5. The curves are very similar, except that the extremes differ a little. It is for this reason that in EurOtop (2007) for smooth slopes an *average* b-value of 0.75 was chosen and not different values for various subsets of data. Recent investigations (see Chapter 5) have shown that the shape factor b may increase with increasing overtopping discharge and that b should not be kept at 0.75 if overtopping really becomes significant. For emerged structures, however, b will always be smaller than 1.5, which still is quite a steep distribution.

The scale parameter, a, depends on the overtopping discharge, q, but also on the mean period, T_m, and probability of overtopping, N_{ow} / N_w, or alternatively, on the storm duration, t, and the actual number of overtopping waves N_w. See Section 5.5.2 for a further explanation on this scale parameter.

Equations for calculating the overtopping wave volume for a given probability of exceedance, is given by Equation 4.5. The maximum overtopping during a certain event is fairly uncertain, as with most maxima, as it depends on the duration of the event. In a 6 hours period one may expect a larger maximum than during a shorter 15 minute period. The expected maximum overtopping volume by only one wave during an event depends on the actual number of overtopping waves, N_{ow}, and can be calculated by:

$$V_{max} = a \cdot \left[\ln(N_{ow}) \right]^{1/b} \qquad\qquad 4.6$$

Chapters 5, 6 and 7 give formulae for smooth slopes, rubble mound slopes and vertical walls, respectively. In this section and example is given between the mean overtopping discharge, q, and the maximum overtopping wave volume in the largest wave. Note that the mean overtopping discharge is given in l/s per m width and that the maximum overtopping volume is given in l per m width.

As example a smooth slope with angle 1:4 is taken, a rubble mound slope with a steeper slope of 1:1.5 and a vertical wall without influencing foreshore. The storm duration has been assumed as 2 hours (the peak of the tide) and a fixed wave steepness of $s_{om-1,0} = 0.04$ has been taken. Figure 4.6 gives the q - V_{max} lines for the three structures and for relatively small waves of $H_{m0} = 1$ m (red lines) and fairly large waves of $H_{m0} = 2.5$ m (black lines).

A few conclusions can be drawn from Figure 4.6. Firstly, the ratio q / V_{max} is about 1000 (s[-1]) for small q (roughly around 1 l/s per m) and about 100 (s[-1]) for large q (roughly around 100 l/s per m). So, the maximum overtopping wave volume in the largest wave is about 100 - 1000 times larger than the mean overtopping discharge. Secondly, the red lines are lower than the black lines, which means that for lower wave heights, but similar mean discharge, the maximum overtopping volume is also smaller. For example, a vertical structure with a mean discharge of 10 l/s per m gives a maximum volume of 1000 l per m for a

1 m wave height and a volume of 4000 l per m for a 2.5 m wave height. This has an effect on the allowable discharge as it is the overtopping wave volumes that are important, see Chapter 3.

Finally, the three different structures give different relationships, depending on the equations to calculate q and the equations to calculate the number of overtopping waves. More discussion can be found in Chapters 5, 6 and 7.
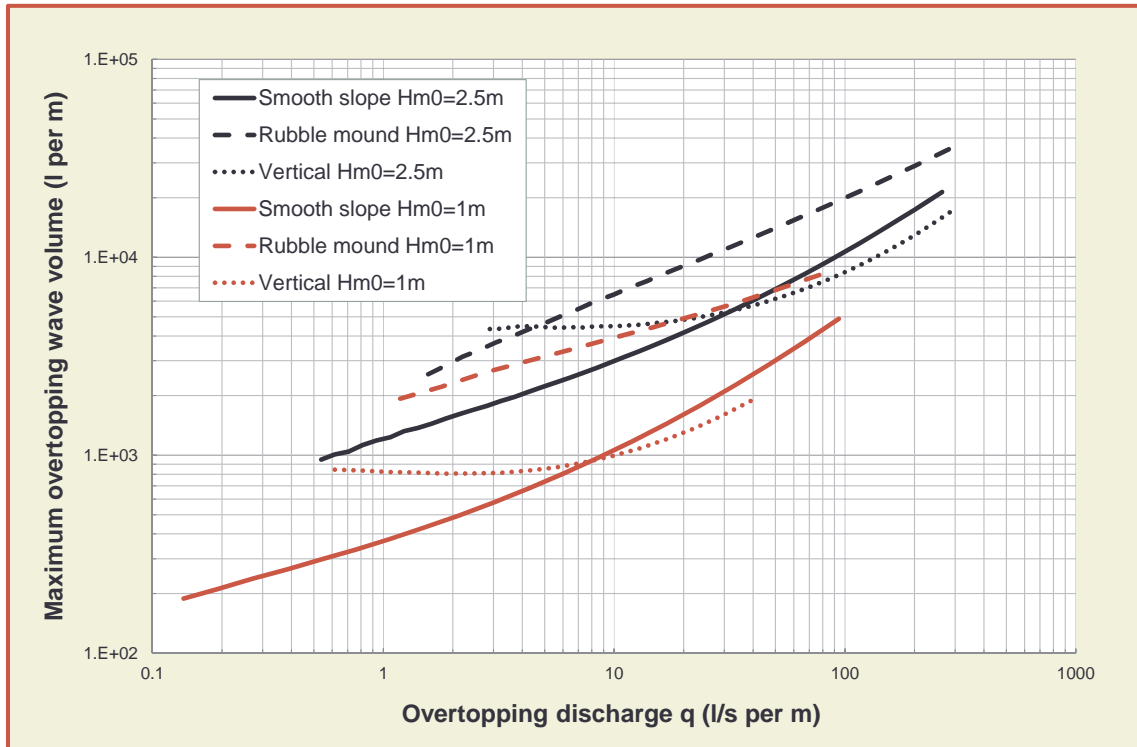
Figure 4.6:   Relationship between mean discharge and maximum overtopping wave volume for smooth, rubble mound and vertical structures for wave heights of 1 m and 2.5 m

4.2.5 Wave transmission by wave overtopping

Admissible overtopping depends on the consequences of this overtopping. If water is behind a structure, in the lea of a breakwater or low-crested structure, large overtopping can be allowed as this overtopping will plunge into that water again. What happens is that the overtopping waves cause new waves behind the structure to be formed. This is called wave transmission and is defined by the wave transmission coefficient $K_t = H_{m0,t}/H_{m0,i}$, with $H_{m0,t}$ = transmitted significant wave height and $H_{m0,i}$ = incident significant wave height. The limits of wave transmission are $K_t = 0$ (no transmission) and 1 (no reduction in wave height). If a structure that blocks the entire water depth has its crest above water, the transmission coefficient will never be larger than about 0.4 - 0.5. Note that also the wave energy density spectrum may be quite different behind the low-crested structure than the incident spectrum.

Wave transmission has been investigated in the European DELOS project. For smooth sloping structures the following prediction formula was derived:

$$K_t = \left[-0.3 \cdot \frac{R_c}{H_{m0,i}} + 0.75 \cdot \left(1 - \exp\left(-0.5 \cdot \xi_{op} \right) \right) \right] \cdot \left(\cos \beta \right)^{2/3} \qquad 4.7$$

with as a minimum $K_t = 0.075$ and maximum $K_t = 0.8$, and limitations $1 < \xi_{op} < 3$, $0° \leq \beta \leq 70$. and $1 < B/H_{m0,i} < 4$, where β is the angle of wave attack. Note that for wave transmission the peak period, T_p, is used in the breaker parameter and not the spectral period, $T_{m-1,0}$.
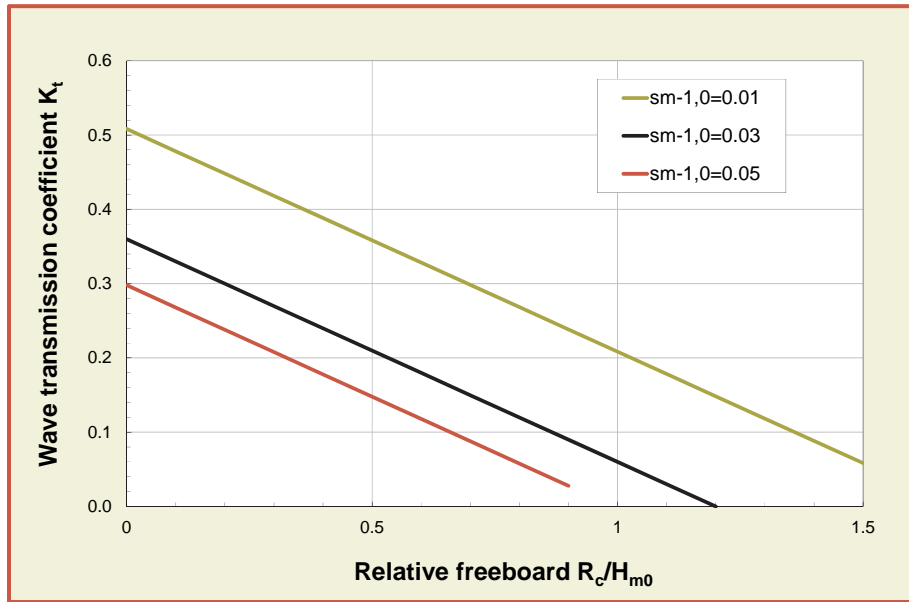
Figure 4.7:   Wave transmission for a gentle smooth structure of 1:4 and for different wave steepness

Figure 4.7 shows the transmission coefficient K_t as a function of the relative freeboard R_c/H_{m0} and for a smooth structure with slope angle $\cot\alpha = 4$ (a gentle smooth low-crested structure) and with an emerged crest. For a sub-merged crest wave transmission is still very important, but for wave overtopping it would mean that direct overflow would govern the process, not wave overtopping. For reasons of comparison, the crest freeboard is taken positive here for the example.

Three wave steepnesses have been used: $s_{m-1,0} = 0.01$ (long waves); 0.03; and 0.05 (short wind waves). A relationship of $T_p = 1.1\ T_{m-1,0}$ has been used to calculate the correct wave steepness, and perpendicular wave attack has been assumed. Wave transmission decreases for increasing crest height and a longer wave gives more transmission. Wave overtopping can be calculated for the same structure and wave conditions, see Chapter 5 for equations, and is given in Figure 4.8 where it can be seen that a longer wave gives also more wave overtopping.
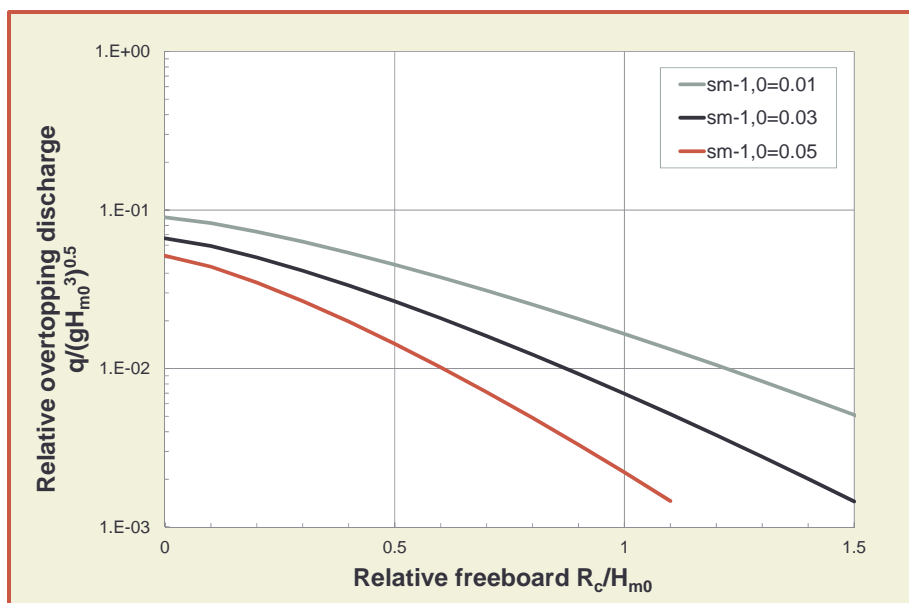
Figure 4.8:   Wave overtopping for a gentle smooth structure of 1:4 and for different wave steepness

The relationship between wave overtopping and transmission is found if both figures are combined as shown in Figure 4.9, where for convenience the graphs are not made in a dimensionless way, but for a wave height of 3 m. A very small transmitted wave height of 0.1 m is only found if the wave overtopping is at least 50 - 100 l/s per m. In order to reach a transmitted wave height of about 1 m (one-third of the incident wave height) the wave overtopping should at least be 600 - 1000 l/s per m or about 1 m³/s per m or less. Then the crest freeboard will be about zero. One may conclude that wave transmission is always associated with (very) large wave overtopping.
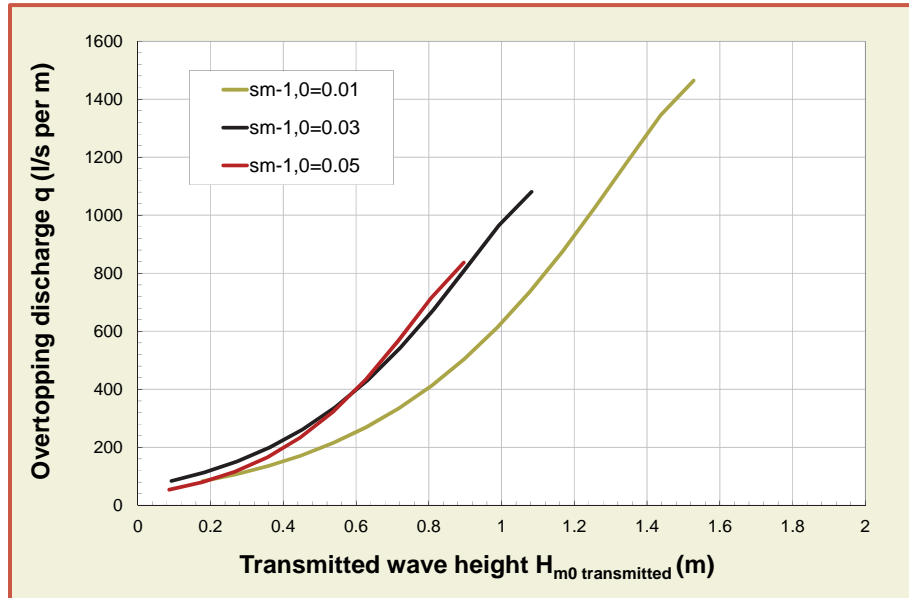
Figure 4.9: Wave transmission versus wave overtopping for a smooth 1:4 slope and a wave height of H_{m0} = 3 m

Wave transmission for rubble mound structures has also been investigated in the European DELOS project and the following prediction formulae were derived for wave transmission:

$$K_t = -0.4\frac{R_c}{H_{m0}} + 0.64\left(\frac{B}{H_{m0}}\right)^{-0.31} * \left(1 - \exp\left(-0.5\xi_{op}\right)\right) \text{ for } 0.075 \le K_t \le 0.8 \qquad 4.8$$

Wave overtopping for a rubble mound structure with simple slope can be calculated by the Equations in Chapter 6. A typical rubble mound structure has been used as example, with cotα = 1.5; 6 - 10 ton rock (D_{n50} = 1.5 m) as armour and a crest width of 4.5 m (3 D_{n50}). This gives an influence factor of the roughness of γ_f = 0.4. A wave height of 3 m has been assumed with the following wave steepnesses: $s_{m-1,0}$ = 0.01 (long waves), 0.03 and 0.05 (short wind waves). In the calculations the crest height has been changed to calculate wave transmission as well as wave overtopping. Figure 4.10 shows the comparison, where a longer wave ($s_{m-1,0}$ = 0.01) gives more wave transmission for the same overtopping discharge. The reason could be that wave overtopping is defined at the rear of the crest, where (without superstructure or capping wall), waves can penetrate through the armour layer at the crest and generate waves behind the structure. This is easier for longer period waves.

In contrast to smooth structures, one may conclude that even without considerable wave overtopping discharge at the rear of the crest, there still might be considerable wave transmission through the structure. In this example transmitted wave heights between 0.5 m and 1 m are found for overtopping discharges smaller than 100 – 200 l/s per m. Only larger transmitted wave heights are associated with extreme large overtopping discharges of more than 500 – 1000 l/s per m.
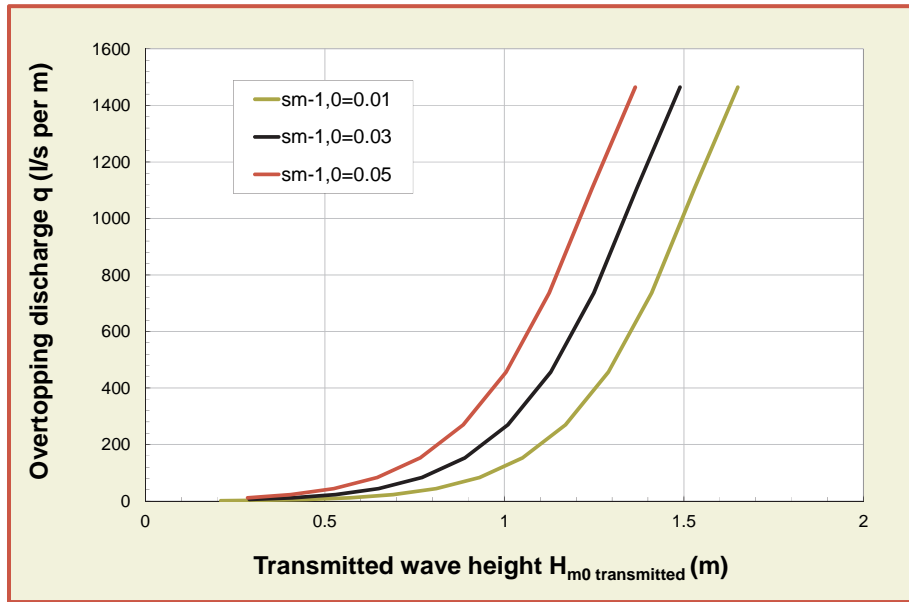
Figure 4.10:   Wave transmission versus wave overtopping discharge for a rubble mound structure, cotα = 1.5; 6-10 ton rock, B = 4.5 m and H_{m0} = 3 m

A simple equation for wave transmission at vertical structures has been given by Goda (2000):

$$K_t = 0.45 - 0.3 R_c/H_{m0} \text{ for } 0 < R_c/H_{m0} < 1.25 \qquad 4.9$$

Wave overtopping for a vertical structure without influencing foreshore can be calculated by equations in Chapter 7. In the formula only the relative crest height plays a role and no wave period, steepness or slope angle. A simple vertical structure has been used as example with a fixed incident wave height of H_{m0} = 3 m. Figure 4.11 gives the comparison of wave overtopping and wave transmission, where in the calculations the crest height has been changed to calculate wave transmission as well as wave overtopping.
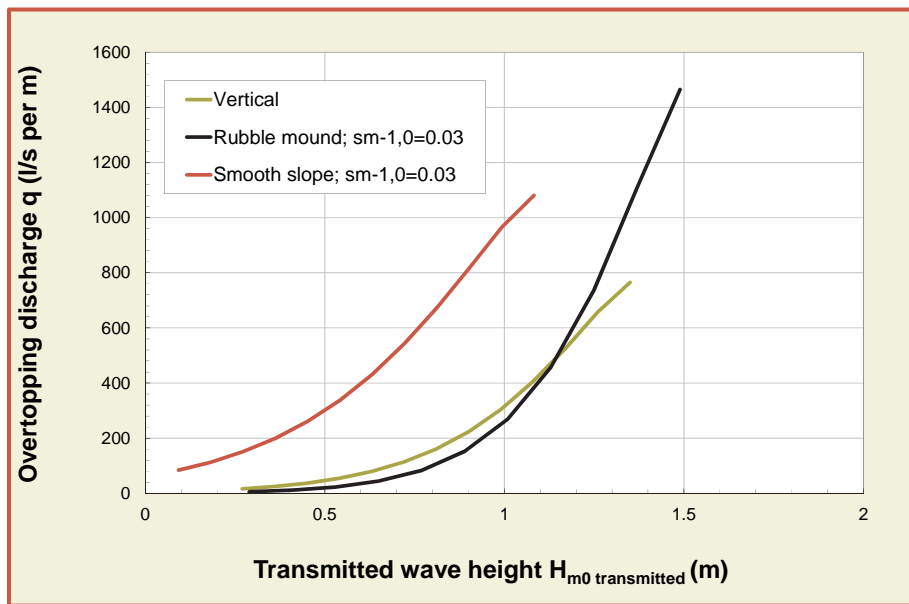
Figure 4.11:   Comparison of wave overtopping and transmission for a vertical, rubble mound and smooth structure

For comparison the same rubble mound structure has been used as the example in Figure 4.10, with $\cot\alpha = 1.5$; $6 - 10$ ton rock ($D_{n50} = 1.5$ m) as armour, a crest width of 4.5 m (3 D_{n50}) and a wave steepness $s_{m-1,0} = 0.03$. The curve for a smooth structure (Figure 4.9) and for $s_{m-1,0} = 0.03$ is also given Figure 4.11.

A rubble mound structure gives more wave transmission than a smooth structure, under the condition that the overtopping discharge is similar, but a vertical structure gives even more transmission. The reason may be that overtopping water over the crest of a vertical breakwater always falls directly onto the water, where at a sloping structure water flows over and/or through the structure. It seems that even without considerable wave overtopping discharge at the crest of a vertical structure, there still might be considerable wave transmission. In this example of a vertical structure, transmitted wave heights between 0.5 m and 1 m are found for overtopping discharges smaller than $100 - 200$ l/s per m. An example of wave overtopping as well as wave transmission in reality is shown in Figure 4.12.

Figure 4.12:   Wave overtopping and transmission at breakwater IJmuiden, the Netherlands

4.3   PC-OVERTOPPING

The programme PC-Overtopping was made on the results of TAW (2002), the Technical TAW Report "Wave run-up and wave overtopping at dikes" and is used for the safety assessment of all water defences in the Netherlands. The TAW Report was replaced by Chapter 5 (dikes and embankments) of EurOtop (2007) which was extended to include rubble mound and vertical structures in Chapters 6 and 7. The programme was mainly based on a *dike type structure,* such as in Figure 4.13. It means that the structure should be sloping, although a small vertical wall on top of the dike may be taken into account. Also roughness/permeability can be taken into account, but not a crest with permeable and rough rock or armour units. In such a case the structure should be modelled up to the transition to the crest and other formulae should be used to take into account the effect of the crest (see Chapter 6).
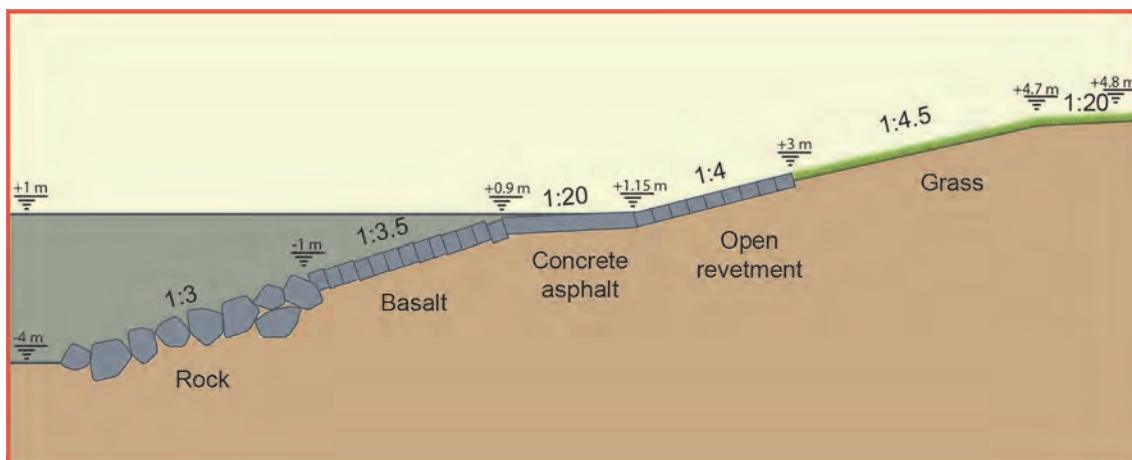
Figure 4.13:   Example cross-section of a dike-type structure for calculation by PC-Overtopping

The core of pc-overtopping has been used in the Calculation Tool on the Manual's website (www.overtopping-manual.com) and a web-based application has been made, and this section describes the tool. *PC-Overtopping has not been updated to reflect the changes to the new formulae in this manual and will continue to use the original formulae in EurOtop (2007) indefinitely.* It should be noted, however, that the output will remain fairly close to the new predictions for cases where $R_c/H_{m0} > 0.5$, see also Section 4.2.1.

The programme was set-up in such a way that almost *every sloping structure* can be modelled by an unlimited number of sections. Each section is given by x-y coordinates and each section can have its own roughness factor. The programme calculates almost all relevant overtopping parameters (except flow velocities and flow depths), such as: 2% run-up level; mean overtopping discharge; percentage of overtopping waves; overtopping volumes per wave; and the required crest heights for given list of mean overtopping discharges.

Section	X begin	Y begin	X end	Y end	Slope (tan)	Material	Roughness factor		
1	0.000	-4.000	9.000	-1.000	0.333	Natural rubble mound of rock	0.550	✏	✖
2	9.000	-1.000	15.650	0.900	0.286	Basalt, set	0.900	✏	✖
3	15.650	0.900	20.650	1.150	0.050	Mastic (asphalt)	1.000	✏	✖
4	20.650	1.150	28.050	3.000	0.250	Growth enabling stone, concrete	0.950	✏	✖
5	28.050	3.000	36.060	4.800	0.225	Grass, sown	1.000	✏	✖

parameter	symbol	value	unit
Significant wave height	Hm0	2.500	[m]
Wave direction	β	12.000	°
Storm duration	tsm	7200.00(	[s]
Water level	SWL	1.000	[m]
Average period	Tm	6.000	[s]
Spectral wave period	○ Tm-1,0	6.364	[s]
Spectral peak period	◉ Tp	7.000	[s]

calculate...

Figure 4.14: Input of geometry by x-y coordinates, choice of material and hydraulic parameters

The main advantages of pc-overtopping are: modelling of each sloping structure, including different roughness along the slope; and, calculation of most overtopping parameters in addition to the mean discharge. Its main disadvantages are that it is unable to calculate overtopping discharges for vertical structures and cannot reduce the discharge over rough / permeable crests.

In order to show the capabilities of the programme an example will be given. Figure 4.13 shows the cross-section of a dike with the design water level 1 m above CD. Different materials are used on the slope: rock, basalt, concrete asphalt, open concrete system and grass on the upper part of the structure. The structure has been schematised in Figure 4.14 by x-y coordinates and a selection of the material of the top layer. The programme selects the right roughness factor, although the user can select a specific roughness factor. The input parameters are the wave height, wave period (choice between the spectral parameter $T_{m-1,0}$ and the peak period T_p), the wave angle, water level (with respect to CD, the same level as used for the structure geometry) and finally the storm duration and mean period (for calculation of overtopping volumes, etc.). gives the input file.

The ratio of T_p/T_{m-10} is standard taken as 1.1. On a shallow foreshore this ratio can differ very much from 1.1 and can even be as low as 0.3. The overtopping formula is based on $T_{m-1,0}$, and the correct value should be used in the case of a shallow foreshore, not the T_p at deeper water.

The output is given in three tables shown in Figure 4.15. The upper table gives the 2%-run-up level, the mean overtopping discharge and the percentage of overtopping waves. If the 2%-run-up level is higher than the actual dike crest, this level is calculated by extending the highest section in the cross-section. The middle table gives the required dike height for given mean overtopping discharges. Also here the highest section is extended, if required. Finally, in the lowest table the number of overtopping waves in the given storm duration are given, together with the maximum overtopping volume and other volumes, belonging to specified overtopping percentages (percentage of the number of overtopping waves).

Calculated parameters	Average value
2% wave runup	4.486
2% wave runup	2.768
Percentage of overtopping	6.039

Overtopping[l/s/m]	Crest height[m]
0.100	2.728
1.000	1.274
10.000	0.999

Percentage[%]	Amount[l/m]
Number of waves	72
Vmax	1606.8
1.000%	0.000
10.000%	0.000
50.000%	0.000

Figure 4.15: Output of PC-Overtopping as in the Calculation Tool

4.4 The new EurOtop database

4.4.1 Relation to the CLASH-work in EurOtop (2007)

The previous Sections 4.4 and 4.5 in EurOtop (2007) were completely based on the work carried out in the European research programme CLASH. That project was just finished at that time and reference to the website of that project gave all the background, reports, database and artificial neural network for predicting wave overtopping discharge. Due to the availability of these results and tools, the sections in the previous EurOtop (2007) were mainly dedicated to application in design and assessment work: how to use to artificial neural network or database in receiving valuable design information.

The objective of CLASH (www.clash-eu.org) was two-fold:

- measure wave overtopping in reality and define scale effects;

- make a large homogeneous database and train an artificial neural network for prediction of wave overtopping for all kind of structure geometries.

The sections on scale effects in this Manual are based on the first point mentioned above and are still valid, although due to increasing insight, have changed slightly. However, since the issue of EurOtop (2007), a lot of work has been performed on enlarging the database and on improving the predicting artificial neural network. The work was carried out by the University of Bologna, partially funded by the THESEUS project, and by Dr. Van der Meer (voluntary cooperation). Sections 4.4 and 4.5 describe the extension of the database and the improvements on the neural network, respectively.

The CLASH database is of course still valid and is part of the new EurOtop database. Some errors in the CLASH database have been repaired. The new EurOtop ANN is an improvement of the existing prediction tool, as it is based on a larger dataset with significant new contributions, but it is also better prepared for small overtopping discharges. Both ANN's can still be used, but if significant changes appear between the two methods, it is likely that the new EurOtop ANN gives a better prediction.

The new neural network is available at the overtopping website (www.overtopping-manual.com) and the database is available upon registration at www.unibo.it/overtopping-neuralnetwork. The main references to this work are Formentin *et al.* (2016) and Zanuttigh *et al.* (2016).

4.4.2 Structure of the new database

The new extended database is now composed by more than 17,000 tests with nearly 13,500 for wave overtopping only. The original CLASH database (Van der Meer *et al.*, 2009) consisted of about 10,000 schematised tests on wave overtopping discharge q, gathered from all over the world. The tests include dikes, rubble mound breakwaters, berm breakwaters, caissons and combinations of these structures resulting in complicated geometries.

All the tests were thoroughly screened, whereby a reliability factor, RF, was given to each test (depending on the amount and reliability of the data), as well as a complexity factor, CF. This complexity factor depends on how easy it is to schematise the structure geometry by a number of geometrical parameters. Reliable data or easy geometries were given a value of 1, less reliable data or difficult geometries a value of 3. A value of 4 means that the data were not reliable enough to be used, or the geometry was too complex to be schematised.

The first extension of the database was by including existing databases on wave transmission and wave reflection. The assemblage of the data has been carried out by maintaining the same geometrical parameters, as well as the relevant climate parameters, already identified within the CLASH project. The tests including the wave transmission coefficient, K_t, were based on the DELOS database (www.delos.unibo.it), Panizzo and Briganti (2007) and the tests on reflection coefficient, K_r, were based on the database by Zanuttigh and Van der Meer (2008). All the original data were searched again for possible missing values of the reflection coefficient: if wave overtopping or transmission was given, then the reflection coefficient was taken too.

The main geometrical parameters required to schematise each structure are given in Figure 4.16. These parameters have also been used to train the neural network (next Section 4.5) and are needed to make a calculation with the neural network.
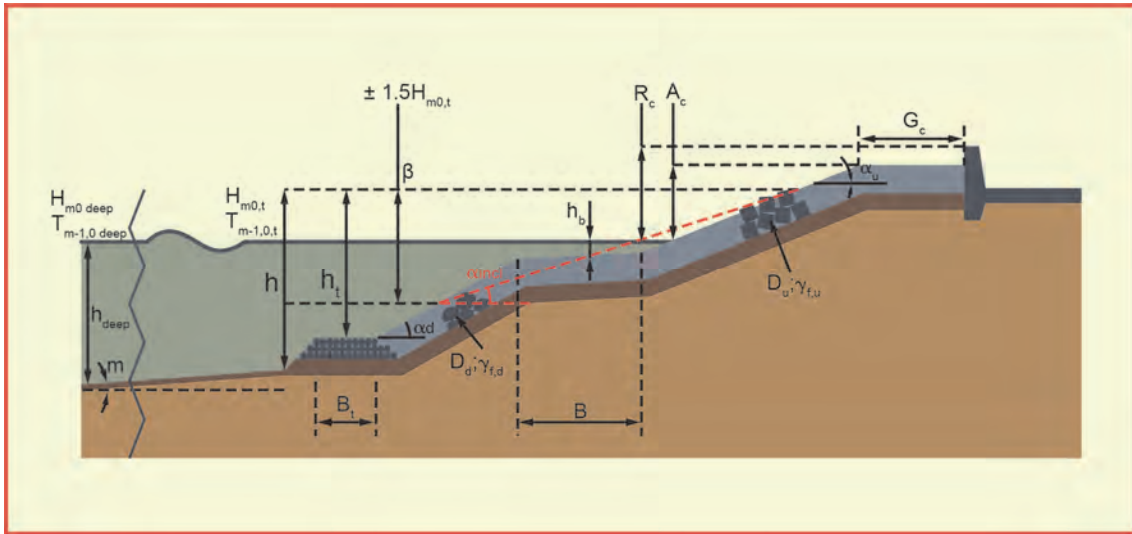
Figure 4.16: Schematization of the structure based on CLASH, including some of the geometrical and hydraulic parameters
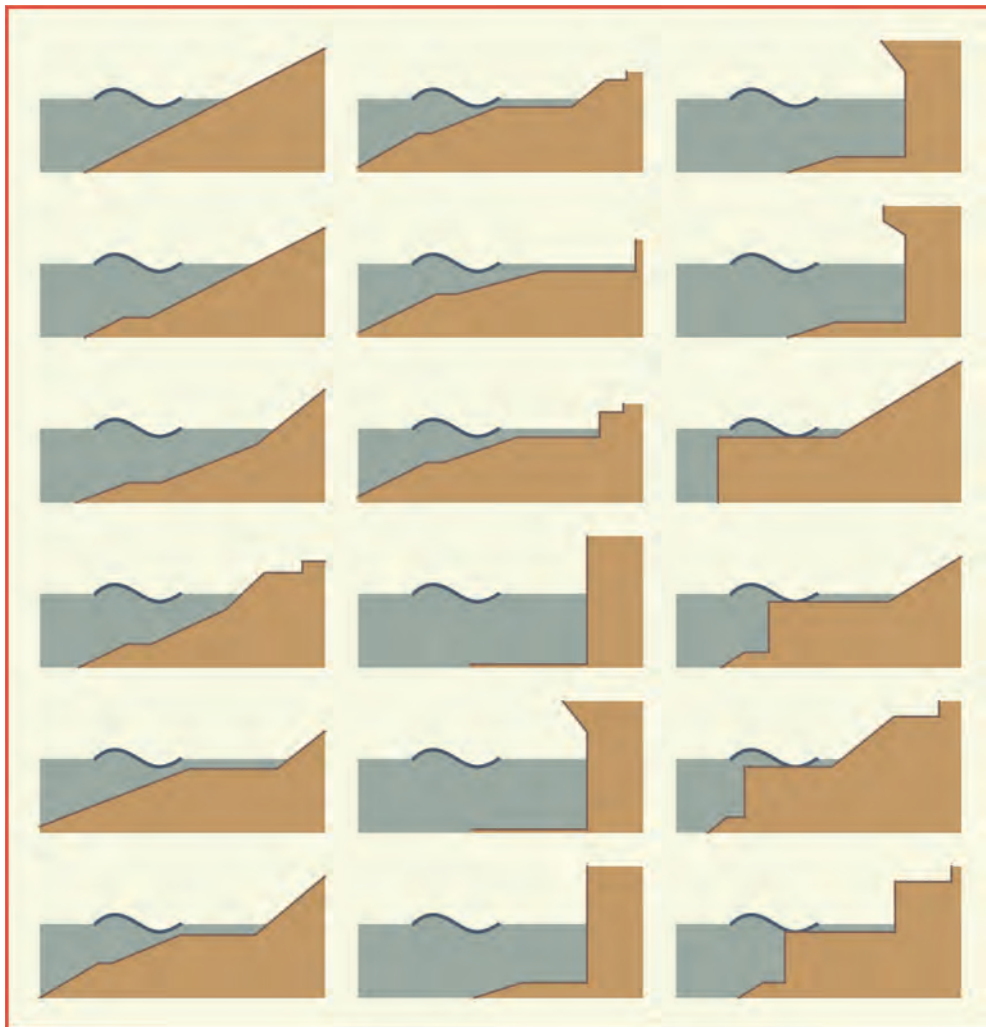
Figure 4.17: Overall view of possible structure configurations for the neural network

Figure 4.17 shows what kind of geometries can be schematised. Besides the geometrical parameters a number of hydraulic parameters were gathered for each test. Wave conditions at deep water and in front of the structure toe are given, where the conditions at the toe of the structure have been used as input for the training of the neural network. Also for application of the neural network one needs the conditions at the toe of the structure, see also Figure 4.16.

The new extended EurOtop database was enlarged with the transmission and reflection coefficients (as described above). Another new parameter was included, starting from the wave transmission database: the average unit size D representative of the structure elements around the water level. It could be the D_{n50} for rock armour, D_n for concrete armour, but it could also be the height of a step of a staircase geometry. A smooth slope has D =0.

In CLASH it was sometimes difficult and not always objective to conclude on an average roughness factor, γ_f, for the whole structure, if parts of the structure had different roughness: for example a smooth slope confronted with a large rock berm. In order to be more consistent, the roughness factors for both the upper and down slope have now been gathered in the database. The downslope of a rock berm has now a different roughness, as well as unit size, than a smooth upper slope.

An original procedure has been developed to evaluate, for the whole structure, a few parameters (D, γ_f, $cot\alpha_{incl}$) in such a way to be consistent through the database. The user only has to give the correct roughness factor, average element size and slopes of the parts of the structure, the tool will then calculate the average values. D is calculated as the weighted average of the characteristic downslope D_d and upslope D_u sizes of the elements in the run-up/down area, i.e. within ±1.5 $H_{m0,t}$ above and below the still water level, following the formula:

$$D=\frac{D_d\cdot(h_{sub}-h_b)+D_u\cdot(h_b+h_{em})}{h_{sub}+h_{em}}$$

(4.10)

where $h_{sub}=\min(1.5\cdot H_{m0,t};h)$; $h_{em}=\min(1.5\cdot H_{m0,t};A_c)$.

Consistently, also the roughness factor γ_f and the average slope $cot\alpha_{incl}$, that is the average slope in the run-up/down area, are now respectively evaluated as:

$$\gamma_f=\frac{\gamma_{fd}\cdot(h_{sub}-h_b)+\gamma_{fu}\cdot(h_b+h_{em})}{h_{sub}+h_{em}}$$

(4.11)

$$cot\alpha_{incl}=\frac{cot\alpha_d\cdot(h_{sub}-h_b)+B+cot\alpha_u\cdot(h_b+h_{em})}{h_{sub}+h_{em}}$$

(4.12)

Equation 4.12 is valid for $|h_b| < 1.5\cdot H_{m0t}$; otherwise $cot\alpha_{incl} = cot\alpha_d$ ($h_b > 0$) or $cot\alpha_{incl} = cot\alpha_u$ ($h_b < 0$).

As for the EurOtop neural network, see Section 4.5, the user only has to enter the correct values of D_d and D_u, of γ_{fd}, γ_{fu}, as well as he/she already provides the values of $cot\alpha_d$, $cot\alpha_u$ following CLASH. The tool will then calculate the average values according to Equations 4.10 - 4.12.

Sometimes interesting data were found during the CLASH-project that could not be used for training the neural network. For example, tests with a wind simulator might be interesting, but wind was not an input for training. In the CLASH database these tests were present, but were given a reliability factor RF = 4, indicating that the data should not be used. But in reality the data could be quite reliable. To overcome this problem an extra column has been created in the new database. This column notes whether the test belongs to the "core" data, which means that it can be considered as a case to be used for training of the neural network, or that it is outside this core data, but with a peculiar feature indicated by a letter, for instance: w=wind, p=prototype, c=current, b=bullnose, pc=perforated caisson.

Table 4.1:   Parameters included in the new extended database compared with the ones included in the original CLASH (2004) database

#	Parameter	Unit	Type	CLASH	New	Definition of the parameter
1	Name	[-]	general	√	√	
2	$H_{m,0,deep}$	[m]	hydraulic	√	√	Off-shore significant wave height
3	$T_{p,deep}$	[s]	hydraulic	√	√	Off-shore peak wave period
4	$T_{m,deep}$	[s]	hydraulic	√	√	Off-shore average wave period
5	$T_{m-1,deep}$	[s]	hydraulic	√	√	Off-shore spectral wave period
6	h_{deep}	[m]	structural	√	√	Off-shore water depth
7	m	[-]	structural	√	√	Foreshore slope, 1 : m
8	β	[°]	hydraulic	√	√	Angle of wave attack
9	Spreading	[-]	hydraulic		√	Spreading s
10	h	[m]	structural	√	√	Water depth at the structure toe
11	$H_{m,0,t}$	[m]	hydraulic	√	√	Significant wave height at the structure toe
12	$T_{p,t}$	[s]	hydraulic	√	√	Peak wave period at the structure toe
13	$T_{m,t}$	[s]	hydraulic	√	√	Average wave period at the structure toe
14	$T_{m-1,0t}$	[s]	hydraulic	√	√	Spectral wave period at the structure toe
15	h_t	[m]	structural	√	√	Toe submergence
16	B_t	[m]	structural	√	√	Toe width
17	Type	[-]	structural		√	Type of structure and armour unit
18	$cot\alpha_d$	[-]	structural	√	√	Cotangent of the angle that the structure part below/above the berm makes with a horizontal
19	$cot\alpha_u$	[-]	structural	√	√	
20	$cot\alpha_{excl}$	[-]	structural	√	√	Cotangent of the mean angle that the structure makes with a horizontal, excluding/including the berm, in the run-up/run-down zone (Equation 4.12)
21	$cot\alpha_{incl}$	[-]	structural	√	√	
22	γ_{fd}	[-]	structural		√	Roughness factor for $cot\alpha_d$
23	γ_{fu}	[-]	structural		√	Roughness factor for $cot\alpha_u$
24	γ_f	[-]	structural	√	√	Roughness factor (average in the run-up/down area in the new database, Equation 4.11)
25	D_d	[-]	structural		√	Size of the structure elements along $cot\alpha_d$
26	D_u	[-]	structural		√	Size of the structure elements along $cot\alpha_u$
27	D	[m]	structural		√	Average size of the structure elements in the run-up/down area (Equation 4.10)
28	B	[m]	structural	√	√	Berm width
29	d_b	[m]	structural	√	√	Berm submergence
30	$tan\alpha_b$	[-]	structural	√	√	Berm slope
31	B_h	[m]	structural	√	√	Horizontal berm width
32	R_c	[m]	structural	√	√	Crest height with respect to SWL
33	A_c	[m]	structural	√	√	(Armour) crest freeboard without crown wall
34	G_c	[m]	structural	√	√	Crest width or promenade width
35	RF	[-]	general	√	√	Reliability Factor
36	CF	[-]	general	√	√	Complexity Factor
37	Label ANN	[-]	general		√	Core/no core data for neural network training
38	Pow	[-]	hydraulic	√	√	Overtopping probability
39	q	[m³/s per m]	output	√	√	Wave overtopping discharge
40	K_r	[-]	output		√	Wave reflection coefficient
41	K_t	[-]	output		√	Wave transmission coefficient
42	Reference	[-]	general		√	Full reference of publication/report

The original CLASH database consisted of 33 columns with parameters, remarks or references, where 13 of them where used to train the predicting neural network. The new database includes 9 parameters more than the CLASH database, consisting of:

- 11 hydraulic parameters, characterizing the wave conditions (extension with the spreading parameter, as all the available laboratory reports include this value in the case of short-crested waves; long-crested waves will get the spreading=0);

- 23 structural parameters (extension with the structure type, the average element size D, and with the element sizes and roughness factors along the down and up slope, D_d, D_u, γ_{fd}, γ_{fu});

- 5 general parameters (extension with the indication of core data for the neural network training and with the reference to publications where available);

- 3 output parameters (extension with K_r and K_t).

Table 4.1 gives the type and the number of all the parameters included in the extended database, in comparison with the original CLASH database.

4.4.3 Characterisation of the new database

The extended database is categorized into 7 sections (since Zanuttigh and Van der Meer, 2008), labelled progressively from A to G, in order to distinguish different types of structures and/or wave conditions. These sections are: straight permeable rock slopes ("A"), straight impermeable rock slopes ("B"), straight slopes with armour units ("C"), straight smooth slopes ("D"), structures with combined slopes and berms ("E"), vertical walls ("F") and oblique wave attack or 3D wave basin tests ("G").

As for the average wave overtopping discharge q, a total amount of about 13,500 tests are available. These data have been collected mainly from the CLASH database (10,000 data), by adding datasets on vertical walls, rubble mound structures, smooth structures with berms and harbour walls and caissons. Extra data covering a range of parameters not included before in the database are berm breakwaters (now described by means of the initial profile), see Section 6.3.4; very steep smooth slopes, see Section 5.3.3; smooth slopes and promenades in combination with storm walls, see Section 5.4.7.

As for the wave reflection coefficient K_r, 7,600 data are available, mainly derived from the wave reflection database (Zanuttigh and Van der Meer, 2008), which collects more than 5,700 data. The extension was reached by including the available wave reflection data in the background reports of the CLASH database, and additional data on vertical structures, steep slopes and berm breakwaters.

As for the wave transmission coefficient K_t, nearly 3,400 tests are now available. Most of the data were derived from the DELOS database (www.delos.unibo.it) on low crested breakwaters (Van der Meer *et al.*, 2005), including rubble mound structures, aquareefs, rubble mounds with different kind of armour units and smooth slopes.

The assortment of the overtopping data is described by Figure 4.18 and Figure 4.19. Figure 4.18 shows that the tests are nicely distributed throughout the 7 sections from A to G, with a slightly greater number of data for vertical walls.

Figure 4.19 characterizes the numerical values of q, by grouping the data according to the order of magnitude. The available q values range from 10^{-9} to 1 m^3/s per m and a non-negligible portion of data (more than the 11% of the total) equals zero. The given values of q are the *measured* values, in small scale or large scale tests, or in prototype; they are not up-scaled to prototype. Most of the data (around 70%) is well distributed within the area of interest, i.e. from 10^{-6} to 10^{-3} m^3/s per m, while a few data are available as for extreme conditions, i.e. q>10^{-3} m^3/s per m and q<10^{-6} m^3/s per m, corresponding to nearly overflow conditions and almost zero overtopping respectively.
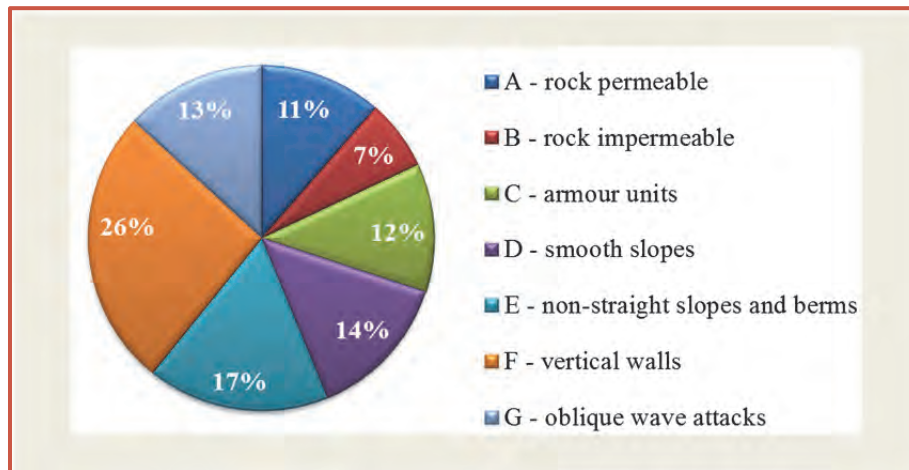
Figure 4.18: Distribution of the wave overtopping data depending on the structure type within the overtopping dataset
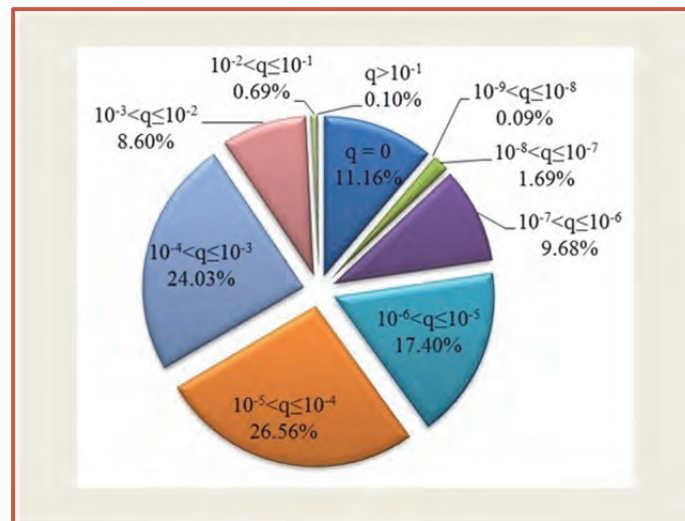
Figure 4.19: Distribution of the experimental values of q, divided into different classes according to the order of magnitude, within the overtopping dataset

4.5   The EurOtop Neural Network prediction tool

4.5.1 Introduction to Artificial Neural Networks

Artificial Neural Networks (ANNs) fall in the field of artificial intelligence and can in this context be defined as systems that simulate intelligence by attempting to reproduce the structure of human brains. ANNs are organised in the form of layers and within each layer there are one or more processing elements called 'neurons'. The first layer is the input layer and the number of neurons in this layer is equal to the number of input parameters. The last layer is the output layer and the number of neurons in this layer is equal to the number of output parameters to be predicted. The layers in between the input and output layers are the hidden layers and consist of a number of neurons to be defined in the configuration of the ANN. Each neuron in each layer receives information from the preceding layer through the connections, carries out some standard operations and produces an output. Each connectivity has a weight factor assigned, as a result of the calibration of the neural network: this is a learning process that is carried out by training the ANN on a database including input and output parameters. The input of a neuron consists of a weighted sum of the outputs of the preceding layer; the output of a neuron is generated using a linear activation

function. This procedure is followed for each neuron; the output neuron/s generates/e the final prediction/s of the neural network.

The development and/or use of an ANN is particularly recommended in case of complicated structure geometries and variable wave conditions. This kind of predictive method requires however a homogeneous and "wide-enough" database: the number of data should be sufficient for training the ANN based on the number of the ANN input parameters and should be at the same time sufficiently high and well distributed to cover the whole range of possible output values.

ANNs have applications in many fields and also in the field of coastal engineering for the prediction of rock stability, forces on walls, wave transmission, wave reflection and wave overtopping (see the short review in Zanuttigh *et al.*, 2013).

4.5.2 Developments in ANN's

During and after CLASH the following ANNs were developed to predict the main parameters of wave structure interaction, and specifically:

- the average wave overtopping discharge q (Van Gent *et al.*, 2007; Verhaeghe *et al.*, 2008);

- the wave transmission coefficient K_t (Van Oosten and Peixó Marco, 2005; Panizzo and Briganti, 2007);

- the wave reflection coefficient K_r (Zanuttigh *et al.*, 2013). This latter ANN was tested to predict also K_t (Formentin and Zanuttigh, 2013) and was then further modified to predict q (Formentin *et al.*, 2016; Zanuttigh *et al.*, 2016).

Each of these ANNs actually overcomes most of the limits imposed by the traditional empirical formulae, but is still restricted to reproduce only one of the processes involved in the wave-structure interaction. As all the processes are physically correlated, it should be possible to represent them by means of one ANN tool. This observation was the motivation leading to the new EurOtop ANN. This new ANN tool allows to accurately estimate q, K_r and K_t by using consistently the same input parameters and ANN-architecture. The designer can therefore get the predictions of the three outputs q, K_r and K_t from the three trained ANNs by introducing the same input parameters once.

4.5.3 Characterisation of the new ANN

The new ANN tool is composed of three similar ANNs with the same architecture and main characteristics, but each trained on the dataset including K_r or K_t or q. The input layer is composed by 15 input parameters, while the output layer consists of one of the three possible outputs (K_r or K_t or q), see Figure 4.20. The full list of the ANN input parameters is given in Table 4.2.
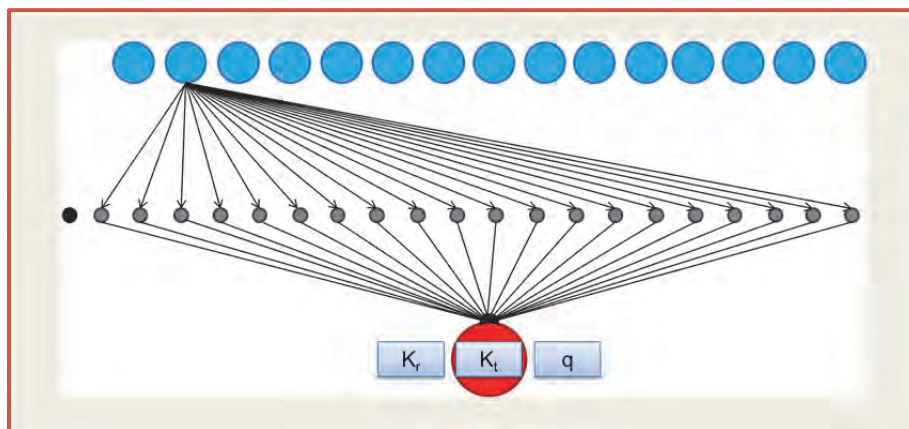
Figure 4.20:   Schematization of the ANN layout. The input layer consists of 15 dimensionless input parameters, the hidden layer of 20 hidden neurons and 1 bias. The output layer consists of 1 output neuron that can be *q*, *K$_r$* or *K$_t$*

Table 4.2:   Synthesis of the 15 selected dimensionless input parameters of the new ANN

#	Parameter	Type	Representation of
1	$H_{m0,t}/L_{m-1,0,t}$	Wave conditions	Wave steepness (breaking)
2	β [rad]	Wave conditions	Wave obliquity
3	$h/L_{m-1,0,t}$	Wave conditions	Shoaling parameter
4	$h_t/H_{m0,t}$	Geometry	Effect of the toe submergence
5	$B_t/L_{m-1,0,t}$	Geometry	Effect of the toe width
6	$d_b/H_{m0,t}$	Geometry	Effect of the berm level
7	$B/L_{m-1,0,t}$	Geometry	Effect of the berm width
8	$R_c/H_{m0,t}$	Geometry	Effect of the relative crest height (including the crown wall if present)
9	$A_c/H_{m0,t}$	Geometry	Effect of the relative crest height
10	$G_c/L_{m-1,0,t}$	Geometry	Effect of the crest width
11	m	Geometry	Effects of the foreshore slope
12	$cot\alpha_d$	Geometry	Downstream slope
13	$cot\alpha_{incl}$	Geometry	Average slope in the run-up/down area
14	$D/H_{m0,t}$	Structure characteristics	Indication of structure permeability and/or roughness
15	γ_f	Structure characteristics	Dissipation induced by structure roughness and permeability

The basic parameters are essentially the same as in the CLASH ANN (Van Gent *et al.*, 2007), with the exception of the additional input parameters D and the foreshore slope m. Characteristic structure slopes include the downstream slope, as it is important in the wave reflection process, and the average slope in the run-up/down area, as it proved to be most relevant for estimating wave overtopping in case of complex structures. Note that the parameters in Table 4.2 are not the same as those that have to be given by the user of the neural network. Here the dimensionless parameters are calculated by the neural network and where the training of the neural network was based on. The user has to provide parameters with dimension, in small scale or prototype, see the next section, Table 4.3.

The input parameters of the ANN tool are made dimensionless, to reproduce the relevance of specific key geometrical and physically based parameters. Parameters related to the wave conditions represent wave breaking due to wave steepness and water depth, shoaling and effects induced by wave obliquity. The structure heights (of toe, berm, crest) are all made dimensionless with the significant wave height, to represent the effects induced by local breaking and by wave run-up. The structure widths (of toe, berm, crest) are all made dimensionless with the wave length, to account for the induced local reflection that might be in phase or not with the wave reflection from other parts of the structure slope. The use of dimensionless parameters adopted here differs therefore substantially from the one developed in the previous CLASH ANN, whose parameters are in principle dimensional and the experimental data are re-scaled according to the Froude Law to the same prototype condition by using the "scaling factor" $H_{m0,t} = 1$ m. The present method with dimensionless physically based scaling of the input parameters proved to give a more accurate ANN than the previous methods.

The new ANN was trained against the database presented in Section 4.4. Special structures such as perforated caissons and structures with crown walls including bullnoses were excluded from training, as well as test conditions including wind (all these data are identified with an appropriate label by adding a specific column in the database, see Table 4.1).

4.5.4 An example application of the ANN

The application of the ANN is providing an Excel or ASCII input file with parameters, run the programme (push a button) and get a result file with mean overtopping discharge(s), wave reflection and transmission coefficients. Such an application is as easy as getting an answer from a formula programmed in Excel or Matlab and does not need knowledge about ANNs. The advantages of the ANN are:

- it works for almost every structure configuration (see Figure 4.17);

- it is easy to calculate trends instead of just one calculation with one answer.

An example application of the ANN tool to a rubble mound embankment with a wave wall, see Figure 4.21, is shown here. The neural network predicts an overtopping discharge of 37 l/s per m, which in this example is considered as too much. In order to reduce wave overtopping, the following measures may be considered:

- an increase of the crest height (R_c and A_c);

- an increase of the crest width (G_c);

- the introduction of a berm (B);

- the heightening of the crest wall (R_c only, while A_c is kept constant).
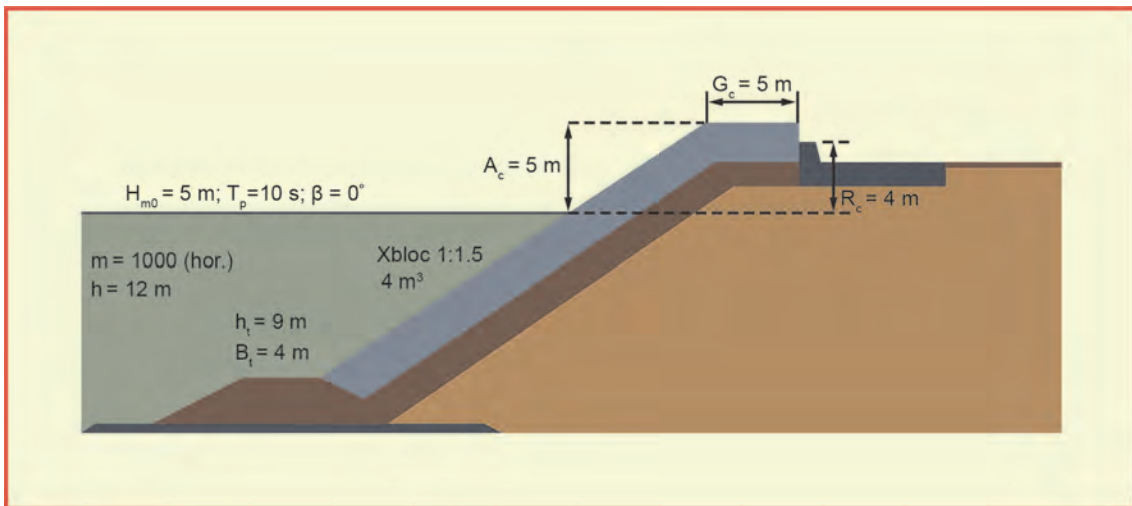
Figure 4.21:   Example cross-section with parameters for application of the neural network

Table 4.3:   Example input file for the ANN with 18 input parameters per calculation

Nr	m	h [m]	$H_{m0,t}$ [m]	$T_{m-1,0,t}$ [s]	β [°]	h_t [m]	B_t [m]	d_b [m]	B [m]	$\cot(\alpha_d)$	$\cot(\alpha_u)$	γ_{fd}	γ_{fu}	D_d [m]	D_u [m]	A_c [m]	R_c [m]	G_c [m]
1	1000	12	5	9.1	0	9	4	0	0	1.5	1.5	0.49	0.49	1.58	1.58	5	4	5
2	1000	12	5	9.1	0	9	4	0	0	1.5	1.5	0.49	0.49	1.58	1.58	5.1	4.1	5
3	1000	12	5	9.1	0	9	4	0	0	1.5	1.5	0.49	0.49	1.58	1.58	5.2	4.2	5
4	1000	12	5	9.1	0	9	4	0	0	1.5	1.5	0.49	0.49	1.58	1.58	5.3	4.3	5
5	1000	12	5	9.1	0	9	4	0	0	1.5	1.5	0.49	0.49	1.58	1.58	5.4	4.4	5
6	1000	12	5	9.1	0	9	4	0	0	1.5	1.5	0.49	0.49	1.58	1.58	5.5	4.5	5

Table 4.3 shows the input file with the first 6 calculations out of 200, where the incremental increase of the structure height (R_c and A_c) shows the heightening of both the crest and the wall. Calculations give an

output file (Table 4.4 – again the first 6 rows) with the mean overtopping discharge q (m³/s per m width), both without and with scale effect rules, i.e. by applying the scale effect method proposed in this manual. The 90% confidence band by the 5% and 95% exceedance values are also provided for the ANN output (i.e. without scale effects for q).

Table 4.4:   Corresponding example output file of the ANN for q, with confidence limits and values at prototype scale, following the correction method for scale effects given in this manual. In the given example, no correction should be applied as the values are above 1 l/s per m

Nr	average q [m³/s per m]	prototype q [m³/s per m]	Confidence bands	
			5% [m³/s per m]	95% [m³/s per m]
1	3.67E-02	3.67E-02	1.72E-02	7.24E-02
2	3.35E-02	3.35E-02	1.58E-02	6.60E-02
3	3.06E-02	3.06E-02	1.44E-02	5.98E-02
4	2.79E-02	2.79E-02	1.31E-02	5.54E-02
5	2.55E-02	2.55E-02	1.22E-02	5.01E-02
6	2.33E-02	2.33E-02	1.11E-02	4.61E-02

To make the input text file for this example with 200 calculations took about 15 mins (by using a text editor) and the calculation of the ANN took less than 1 min. The results were copied to an Excel file and the resulting graph, Figures 4.5.3, took other 10 minutes. The figure shows the four trends for the measures to reduce overtopping as listed above. The increase of the structure height or of the crest wall, i.e. the increase of A_c and/or R_c, is more effective than the widening of the crest or the introduction of a berm in reducing q. It is worth to remark that the values of the confidence bands will help the user identifying when the ANN tool has been applied to predict cases that are far from the training data. In this case the 90%-confidence band is relatively small: for the first calculation it is q = 17 – 72 l/s per m, where the average prediction was q = 37 l/s per m.
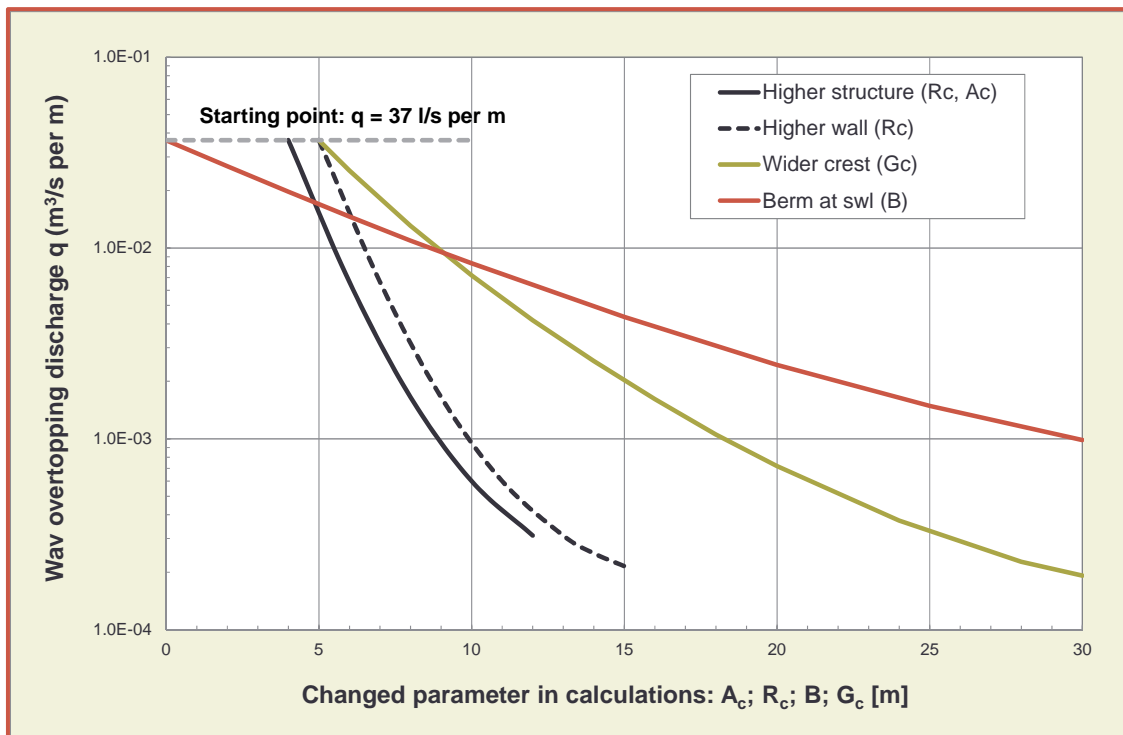
Figure 4.22:   Results of a trend calculation for the wave overtopping discharge

4.6 Numerical modelling of wave overtopping

4.6.1 Introduction

Empirical models, usually referred to as overtopping prediction formulae, are most frequently applied for structure design. These models use relatively simple analytical equations to calculate average wave overtopping rates as a function of pre-defined wave and structure parameters. The equation form is based on physical insight in the governing parameters, but additional empirical constants are required, which have been determined by fitting to experimental data from physical model tests. This semi-empirical approach provides a fast calculation tool but limits the application to the tested ranges of input parameter values for a rather limited number of simplified structure configurations. Extrapolation towards out-of-range parameter values or other structure types than those used for the fitting, may result in inaccurate and even invalid overtopping predictions.

Numerical models simulate wave overtopping as part of the numerical modelling of wave interaction with the structure, by solving complex flow equations in a numerical domain using a numerical solution technique. Numerical models, once validated, are less restrictive in structure configurations and provide much more detailed information on the overtopping flow (both instantaneous parameters like velocities, pressures and free surface configuration and integrated parameters like forces or individual and average overtopping volumes), but at a much higher computational effort and cost. During the last decade, an impressive research progress has been made in the capabilities of the numerical models, making these suitable for more detailed structure design purposes.

An accurate numerical simulation of wave overtopping over the structure crest requires the adequate numerical treatment of all the relevant physical processes:

- the wave generation from the offshore boundary, requiring stable numerical methods for generating and absorbing waves, in order to reproduce statistically meaningful sea states;
- the wave transformation from offshore to nearshore, such as shoaling, refraction, diffraction and, reflection, for irregular short-crested waves;
- wave breaking and wave run-up on or over the structure, resulting in very complex free surface configurations such as possible overturning of waves or thin layers of water flowing over the crest;
- violent wave breaking with air entrainment or impulsive wave breaking onto the structure, resulting in 3D turbulent flow and requiring flow compressibility and the ability to continue the simulation beyond this point;
- porous flow in permeable parts of the structure, such as in the coarse granular material or the armour layer, governing the infiltration and seepage of water in and out the permeable structure and the phreatic set-up in the core
- dynamic response of sea defences including structure motion and scour in foundations, slopes and rubble mounds

All of those processes may affect the overtopping characteristics and therefore need to be modelled. None of the existing numerical models is capable of including all of the above processes in a computationally efficient way, despite the recent progress made. Additionally, analysis of physical model tests suggests that between 500 and 1000 random waves are required to avoid significant variations in extreme statistics. This large number of waves is still a significant problem for the numerical models, see Section 4.6.4.

There are, however, various model types each capable of (and optimized for) simulating a particular selection of those processes. They essentially fall into two principal categories: the nonlinear shallow water equations models (NLSW), and the Navier Stokes equations models (NS). Each of those two types are discussed below, with the emphasis on the range of applicability and performance for wave overtopping, rather than the underlying mathematical principles.

Recently, coupling of the NLSW and NS numerical models with other types of wave propagation models, or coupling 2D and 3D NS models, have provided improved computational efficiency increasing both the

spatial and temporal resolution. This results in improved wave characteristics near the structure toe for the overtopping model at a lower computational cost. That is, the models are able to increase the number of waves and geometric resolution only where they are needed increasing the overall computational efficiently significantly. These innovative developments in coupling methodologies are very promising, but still need some more time before they will become standard design tools.

4.6.2 Nonlinear shallow water equation models

The nonlinear shallow water (NLSW) equations are a simplified form of the Navier-Stokes equations and describe one-dimensional, near horizontal, depth-integrated free surface flow, by solving for water depth and horizontal flow velocity in time and space, i.e. vertical velocities are neglected and the pressure is assumed hydrostatic. Further restrictions of the model are that it is only valid for shallow water (h/L < 0.05), waves travel in the domain as bores, thus simplifying considerably the breaking behaviour, offshore boundaries need to be prescribed at the structure toe, and the applied bottom slopes are mild indicating that the vertical component of the flow remains small. On the other hand, the model is popular due to its simplicity and low computational requirements, which makes it possible to extend towards a realistic large number (up to 1000) of incident waves and 2D (horizontal) domains in a reasonable computational time.

A number of NLSW models have been developed and validated for wave overtopping prediction over coastal structures, such as RBREAK, ODIFLOCS, AMAZON, the ANEMONE suite (OTT-1D and OTT-2D) and Tuan and Oumeraci (2010). At the crest of the sloping sea defence structure, the NLSW models are typically able to continue computing as the flows separate either side of the crest, overtop or return. Structure slopes, both mild and steep (10:1, well beyond the maximum slope of underlying assumptions) are possible, and regular and irregular wave conditions have been applied, including the option to absorb reflected waves at the seaward boundary. Structures are mainly impermeable, but also permeable structures can be modelled. The model runs are typically robust and stable. An example output of the NLSW WAF-TVD solver is given in Figure 4.23 (Briganti et al., 2011).
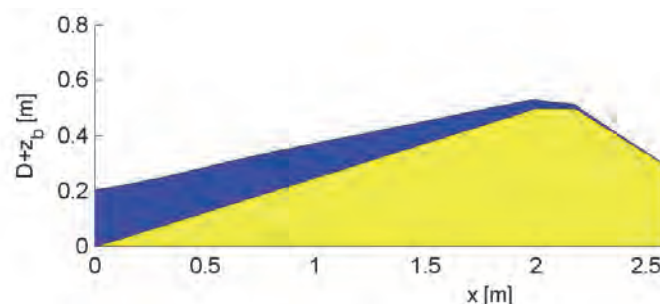
Figure 4.23: Numerical modelling results using the hydrostatic NLSW WAF-TVD solver for wave overtopping over a simple dike geometry with uniform slope. *Courtesy of R. Briganti*

Typically, these NLSW models require, as boundary condition, wave information from a wave propagation model or another tool, which brings the waves as close as possible to the structure. The achieved accuracy in overtopping prediction is reported in the literature as reasonable, but due to the intrinsic drawbacks of the NLSW equations, the characteristics of individual overtopping events are much less accurate. These models can be used to examine the difference in overtopping performance when modifications to a scheme design are to be investigated. Long duration runs for a variety of sea states, for say, a range of crest levels, is a problem well suited to these models. Nevertheless, use of the NLSW models and interpretation of results requires specific modelling expertise.

Recently, Boussinesq type models have been used extensively for wave overtopping research. Their advantage with respect to NLSW models is to model waves also in intermediate water depth conditions. This makes it possible to locate the offshore boundary further from the structure than NLSW models allow and to control the onset of wave breaking. In this way the propagation of the waves on the foreshore and the breaking process are better described. Examples of this class of models are given by Stansby (2003), Lynett et al. (2010), McCabe et al. (2013) and Tonelli and Petti (2013) among others.

Another recent trend is the application of SWASH to wave overtopping modelling. SWASH is based on the dispersive NLSW equations and allows a resolution of the vertical structure of the flow and non-hydrostatic pressure, thereby increasing even more the accuracy of wave propagation in shallow water. An example is given by Suzuki *et al.* (2014) for wave overtopping over a dike in shallow foreshores, see Figure 4.24.
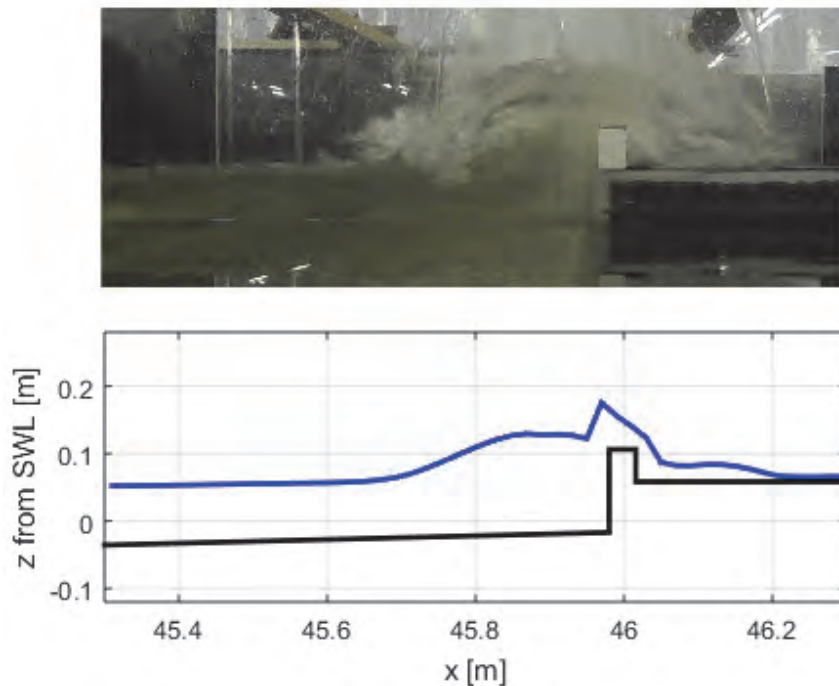
Figure 4.24: A snapshot of a 1/25 scale physical model (top panel) and simulated free surface by SWASH (bottom panel) at a moment of large wave overtopping over a sea wall on top of a vertical dike in a shallow foreshore. C*ourtesy of T. Suzuki*

4.6.3 Navier-Stokes models

The full Navier-Stokes (NS) equations present the most complete flow description in three dimensions, by solving for pressure, the three flow velocity components and turbulence in time and space. A NS model, usually extended with a turbulence model to represent the turbulent flow characteristics, yields in principle the most accurate flow simulation results, however at a much higher computational cost than the NLSW model type. There are two predominant approaches to formulate and solve numerically the Navier-Stokes equations: i) The Eulerian and ii) the Lagrangian approach. Typically, in the Eulerian approach, the fluid is considered as a continuum and the flow domain is discretized in control volumes. The solution algorithm ensures that conservation of flow variables are satisfied within each control volume of the domain. On the other hand, in the Lagrangian frame, the discretisation unit is a particle and the flow evolution is calculated by solving numerically for the kinematics and the interaction of a cloud of particles in time.

Using the Eulerian approach for free-surface flows typically requires special treatment of the free surface motion, and there are various techniques of which the Volume Of Fluid (VOF) method (Hirt and Nichols, 1981), and the level-set method (Osher and Sethian 1988) are most widely used for water waves.

Based on the pioneering work by Hirt and Nichols, on modelling free surface flows using the VOF method, various researchers have used and extended their original NASA-VOF2D/RIPPLE code into NS models applicable for the field of coastal engineering, e.g. by adding boundary conditions for generation and absorption of water waves, and by adding additional terms in the NS equations representing the flow resistance induced by porous media flow in the permeable parts of the structure, or by adding (limited) compressibility of the fluid for cases with impulsive wave breaking. Such pioneering codes in the validation and application of wave interaction with permeable coastal structures are SKYLLA, COBRAS, VOFbreak², IH-2VOF, IH-3VOF, ComFLOW and LVOF. More recent developments (both in academia and consulting) are frequently based on specific extensions of the OpenFOAM CFD code which is freely available under

open source license. Also commercial solvers, such as FLOW-3D, have been applied successfully for modelling wave-structure interaction.

NS models are applicable to a wide range of impermeable and permeable structures with complex geometries (for both low mound or high mound, with sloping or vertical faces), yielding an accurate and detailed temporal and spatial flow field and pressure field description. Wave nonlinearity (e.g. for shallow water wave propagation cases) is inherent to the equations, and overturning waves or other complex flow configurations at the structures are easily treated by the VOF method. NS models overcome the inherent limitations presented by the NLSW and Boussinesq equations models related mainly with wave dispersion and breaking, vertical flow characterization, non-hydrostatic pressure field and flow inside porous coastal structures. The porous flow resistance is expressed using the Forchheimer extension of Darcy flow.

Regular and irregular waves can be generated, with active absorption functionality. For wave overtopping applications, average and individual overtopping events can be simulated easily, providing very detailed flow information. In 2D (wave flume) cases, simulating 100 waves is feasible in a reasonable time (say 12 hours, but obviously depending on the availability of computational resources and on grid resolution), for 3D (wave basin) cases the computational effort is still beyond practical design requirements. Some of the models use two-phase flow by calculating both the water and air phases, however, the added value of obtaining the air phase is limited and computationally expensive, if compressibility and / or aeration effects are not considered important. The incompressible flow treatment is usually sufficient for overtopping applications, however, for cases with severe wave breaking or impulsive loading of vertical parts of the structure (with significant air entrainment) a treatment of the compressibility of the flow is recommended. In addition to this, 2DV Navier Stokes models may result in air non-physical entrapment and pressurisation, as the air does not have the opportunity of escaping sideways. Use of the NS models and interpretation of results requires specific modelling expertise, in particular to the interpretation of "unusual" variables for design engineers, such as e.g. the volume fraction and the turbulent kinetic energy, among others.

Figure 4.25: Numerical modelling results using the NS solver IHFOAM for the harbour of Laredo (Spain). The geometries of the bed, the rubble mound breakwater and the harbour quay walls are shown. At several sections along the breakwater, the simulated wave overtopping (i.e. the free surface configuration of the overtopping waves) has been visualised in 2D slices, to illustrate the complex and highly 3D wave interaction with the breakwater. Courtesy of J.L. Lara

Recently, new VARANS (Volume Averaged Reynolds Averaged Navier Stokes) equations based models have been presented, increasing the accuracy of porous media flow treatments and correcting discrepancies in the original OpenFOAM code (del Jesus *et al.*, 2012; Jensen *et al.* 2014).

Validation and application of NS models for simulating wave overtopping over various types of coastal structures, pore pressure propagation inside the permeable layers and core of structures, wave-induced impact loads and forces on caisson breakwaters, wave forces on crown walls and storm return walls, have been reported extensively in the literature. This is especially so for the 2D cases, by using data obtained from both small scale and large scale physical model tests. Validation has been reported also for very few 3D cases (a high mound vertical breakwater, and a porous caisson structure), however 3D is still not generalized, is posing a much higher computational demand, and requires an experienced user of this type of models. Examples of such state-of-the-art codes are IHFOAM and waves2Foam. An example output of IHFOAM is given in Figure 4.25.

4.6.4 Smooth Particle Hydrodynamics

Recent advances have been made in applying the Lagrangian approach in free-surface flows. Particle models and in particular SPH (Smoothed Particle Hydrodynamics) models have recently been applied to coastal engineering. SPH models do not require complex meshes, nor a special treatment for the free-surface flows, however, they are very expensive from the computational point of view and they cannot (yet) be applied to solve the large domains and long duration wave trains required for wave-structure interaction. A detailed explanation of the SPH theories and formulations can be found in Monaghan (1992), although the method was first applied to coastal engineering by Dalrymple *et al.* (2001). Recent literature is showing large progress on the definition of the boundary conditions and the improvement of the numerical prediction, see for example Narayanaswamy *et al.*, 2010 and Altomare *et al.*, 2016. More recently, Shao (2010) has published the first work describing wave interaction with a porous coastal structure. Validation simulations have been proved to describe the wave induced hydrodynamics and forces, illustrated by the DualSPHysics validations, e.g. for wave induced forces on storm return walls (Altomare *et al.*, 2015), see for example Figure 4.26. Due to the high computational cost, however, the model cannot be used at this stage as a predictive tool for overtopping outside research practice.
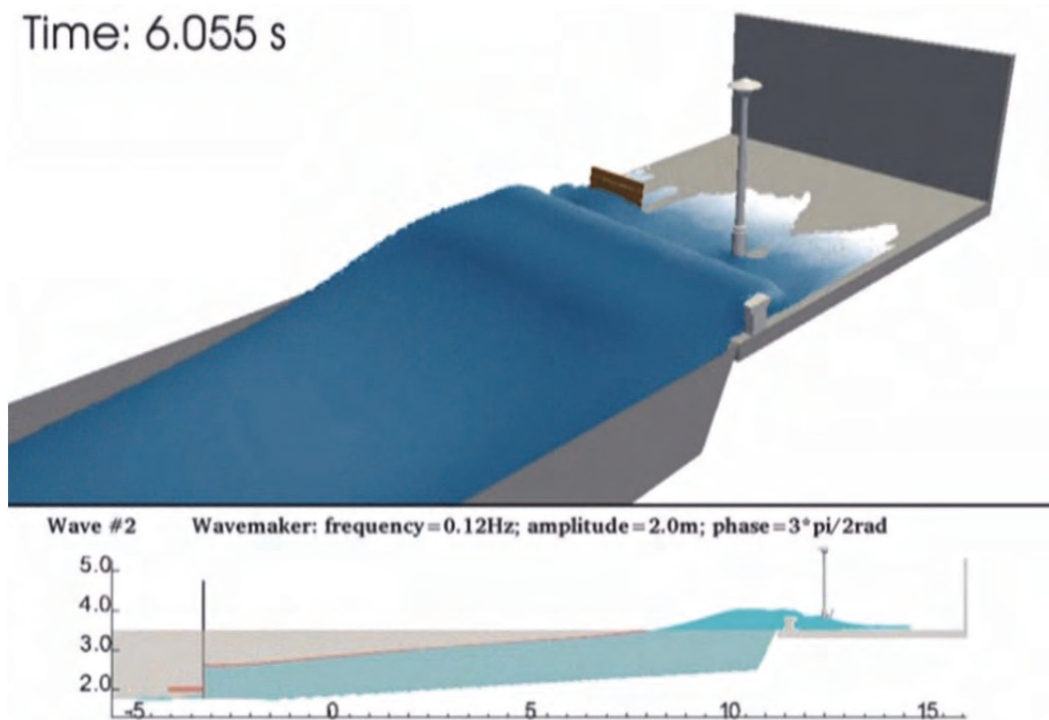
Figure 4.26:   Numerical modelling results using the SPH solver DualSPHysics for a dike with a storm wall. The geometries of the bed, the dike and the road with storm wall are shown. At a particular time instant, the simulated wave overtopping has been visualised in a 2D slice and in a 3D picture, to illustrate the 3D flow processes. Courtesy of A. Crespo

4.7   Physical modelling

Physical model tests are an established and reliable method for determining mean wave overtopping discharges for arbitrary coastal structural geometries; additional levels of sophistication allow individual overtopping volumes to be measured. Typically at geometrical scales of 1:5 to 1:50, physical models represent the prototype structure in 2D (wave flumes) or 3D (wave basins), and frequently occurring and extreme storm events can be modelled. Wave flumes are usually of 0.3 m to 1.5 m wide with a depth of 0.5 to 2.0 m and often fitted with a piston based wave paddle. Some form of wave absorbing system to compensate for waves reflected from the model structure is essential for overtopping studies in wave flumes, as the omission of such a system may lead to unwanted long waves in the flume, giving excessive and uncontrollable wave energy in side of the flume. Wave basin models vary in size and complexity, and overtopping may often be measured at several locations on the model in a 3D physical model. This sections gives only a summary on physical modelling. More information on physical modelling can be found in Hughes (1993) and Hydralab III Guidelines (Frostick, 2011).

Examples of testing wave overtopping in wave flumes are given in Figure 4.27 and Figure 4.28, both for vertical structures. Testing wave overtopping with oblique wave attack as well as with currents (along the wave direction as well as against) is shown in Figure 4.29 for a 1:3 smooth dike-type slope.

Figure 4.27:   Massive wave overtopping simulated in a wave flume on scale 1:50. Wave flume at Deltares, NL

Physical model tests are particularly useful when assessing wave overtopping, as overtopping is affected by several factors whose individual and combined influences are still largely unknown and difficult to predict. The most common hydraulic parameters which influence wave overtopping are the significant wave height, the wave period, the wave direction (obliquity), and the water depth at the structure toe. The structural parameters are the slope, the berm width and level, the crest width and level, and the geometry of any crest / parapet wall. Where rock or concrete armour are tested, the porosity, permeability and placement pattern of armour units affect overtopping as does the roughness of the individual structural elements.

Due to the large number of relevant parameters, and the very complex fluid motion at the structure, theoretical or numerical approaches to wave overtopping are not well developed, although progress is made every year, see Section 4.6. Physical model tests, such as wave flume studies, are therefore commonly used to develop empirical formulae for predicting wave overtopping. These formulae do not assess wave overtopping discharges and individual volumes very accurately, especially for low overtopping volumes. This is partially caused by scale and model effects and the fact that only very limited field data exists. These scale and model effects are briefly discussed in the Section 4.9.

Figure 4.28: Cross-section of a vertical caisson in a wave flume (left) with the overtopping chute and tank (right). Wave flume at INHA, ES

Figure 4.29: Testing wave overtopping of a dike slope 1:6 in a wave basin, including simulation of currents (from right to left). Part of the short-crested wave generator has also wind generators (upper left). Overtopping was measured in various boxes, middle right. Wave basin at DHI, DK

Limits in measuring mean overtopping discharges in laboratory tests can be found in Chapters 5, 6 and 7. Such overtopping discharges are given in a dimensionless way: $q/(gH_{m0}^3)^{0.5}$ and are given versus a dimensionless freeboard. In the graphs in Chapters 5 and 6, the (dimensionless) limit of $q/(gH_{m0}^3)^{0.5} = 10^{-6}$ is hardly exceeded so this limit might be used as a "zero overtopping" in the laboratory.

But zero overtopping may also depend on the method used to measure wave overtopping. Often a chute leads the overtopping water to a box. If a gauge measures the water level difference in the box before and

after the test, it will give the average overtopping discharge. But there should be a few millimetres difference, which sets the limit of zero overtopping. Sometimes an inner box is placed in the dry on a weighing scale, see Figure 4.30. The purpose of the outer box is to keep the inner space dry. The weighing scale is more accurate to measure wave by wave overtopping than one wave gauge in an overtopping tank. More gauges in the tank increase accuracy of measuring overtopping volumes. But even more determining for accuracy could be a short and wide chute. With respect to this issue, the width of the chute in Figure 4.30 is quite small.
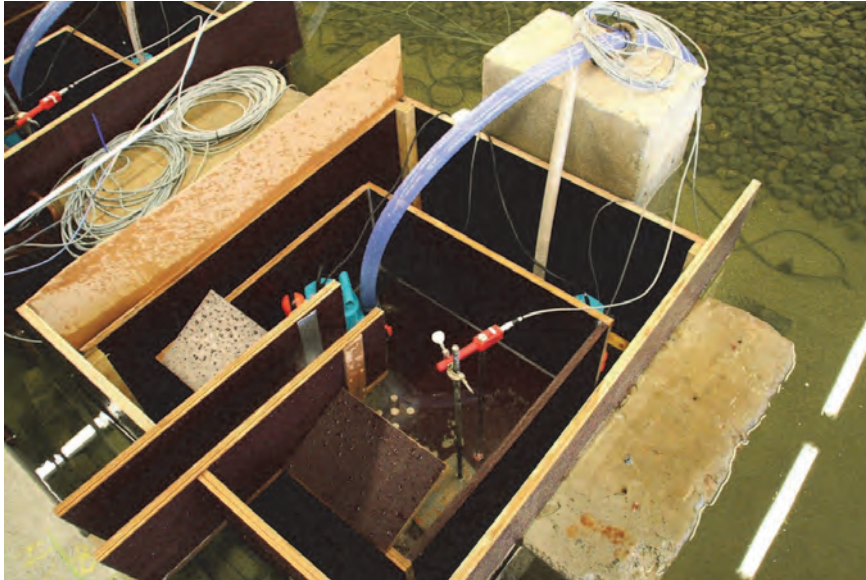
Figure 4.30: A chute (lower left) leading to the inner box, which is placed on a weighing scale. The outer box keeps a dry inner space for the second box. A reliable method to measure wave by wave overtopping. Set-up at wave basin at DHI, DK

Figure 4.31: Measuring wave overtopping at four locations (four chutes leading to an overtopping box) and at two crest levels; measuring flow velocities on the crest with micro-propellers (blue with red) and flow depth with small wave gauges (next to the micro-propellers). Wave run-up was measured by a capacitance wire along a non-overtopped slope (upper middle). Set-up at wave basin at DHI, DK

Physical models may also be able to measure wave overtopping related issues, that describe the actual required process or structural response more directly than an overtopping discharge or volume, like the flow velocity of waves overtopping a structure crest as a dike or embankment, or the flow depth of these overtopping waves. Figure 4.31 shows an example of measuring wave overtopping at four locations and at two crest levels, as well as measuring flow velocities and flow depths by micro-propellers and by small wave gauges. Also wave run-up was measured by making one part of the sloping structure very high.

Wave run-up may be measured by a capacitance wire along and just above the slope, but also by a run-up gauge with pins every 5 cm on the slope. These pins detect whether they are wet of not and give the run-up level at any moment. Another method is to use camera's or laser scanners and detect the maximum wave run-up level.

There are many cases where there are no reliable empirical overtopping prediction methods for a given structure geometry, or where the performance of a particular scheme to reduce overtopping is especially sensitive: e.g. where public safety is a concern. Alternatively, it may be that the consequences of overtopping are important: e.g. where overtopping waves cause secondary waves in the lee of the structure. For cases such as these, physical model testing may be the only reliable option for assessing overtopping.

4.8 Simulators of overtopping at dikes

Most key wave-structure processes in overtopping are simulated correctly using Froude scale physical models, wave flumes and wave basins (see Chapter 4), and it are these facilities that have provided measurements from which the prediction formulae of this manual have been derived.

Erosion of grassed slopes by wave attack is not however easy to test as the strength of clay and of grass roots cannot be scaled down. There are two ways to perform tests on real scale: bring (pieces of) the dike to a large scale facility that can produce significant wave heights of at least 1 m, or bring (simulated) wave attack to a real dike. Such large-scale facilities in Europe are principally the Delta Flume at Deltares, or the GWK in Hannover. For investigation in a large scale facility the main advantage will be that the waves are generated well so the wave-structure-interaction processes are generated well. The disadvantage is that the material to be tested has to be taken from a real dike in undisturbed pieces. This is difficult and expensive and real situations on a dike, like staircases, fences and trees are almost impossible to replicate. These tests are therefore often focused on the grass cover with under-lying clay only. Research on wave overtopping has however already suggested that it is often not the grass cover alone that will lead to protection failure, but an obstacle (tree; pole; staircase) or transition (dike crossing; from slope to toe or berm). Using Simulators on real dikes therefore has the significant advantage that undisturbed situations can be tested.

Three different Simulators have been developed, each to simulate one of the key processes in the wave run-up and overtopping processes that have been described in the following section. The main disadvantage of using Simulators is that only a part of the wave-structure-interaction can be simulated. The quality of simulation depends on the knowledge of the process to simulate, and the capabilities of the device. The experience of testing with the three simulators, on wave overtopping, run-up and wave impacts, over only seven years has given a tremendous increase in knowledge of dike strength, from which have been developed predictive models for safety assessment or design.

By simulating overtopping waves it is also possible to measure impact pressures and forces on structures that are hit by overtopping waves. Such a test will be at full scale and if necessary with salt water, giving realistic wave impacts without significant scale or model effects, see for instance Figure 4.37.

4.8.1 Run-up and overtopping processes at coastal structures

When waves reach a coastal structure such as dike or levee, they will often break onto the slope, perhaps causing impacts in zone 2, see Figure 4.32. When large waves attack such a dike the seaward side in this area will often be protected by a placed block revetment, concrete slabs, or asphalt.

Above the impact zone, there wave attack will be less direct with waves running up the slope and then back down until they meet the next up-rushing waves. This is the run-up zone on the seaward slope (zone 3 in Figure 4.32). Up-rushing waves that reach the crest will overtop the structure and then flow down the landward slope, see zones 4 and 5 in Figure 4.32.
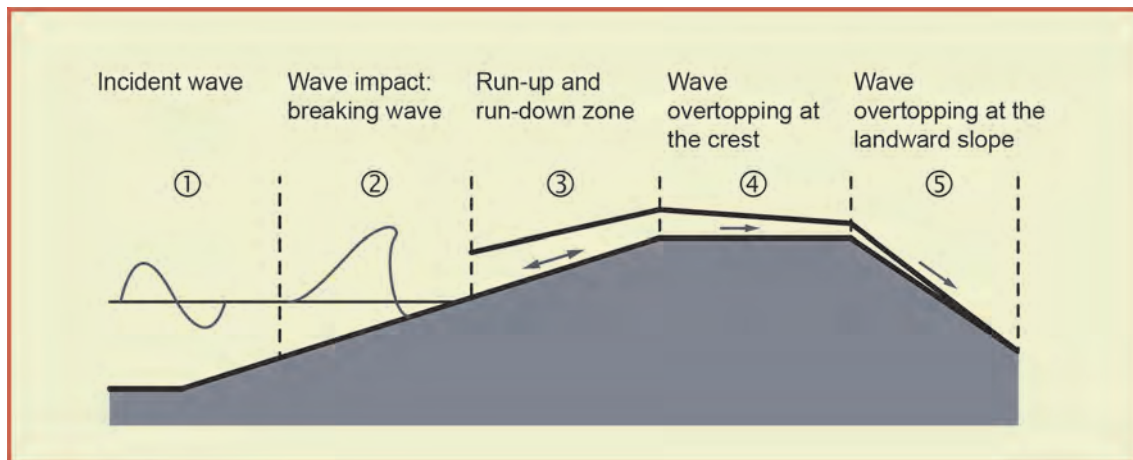
Figure 4.32   Wave breaking, run-up and overtopping at a dike (partly from Schüttrumpf , 2001)

Design of coastal structures is often focussed on deriving 'design' values for key parameters, like the $p_{max,2\%}$ or p_{max} for a design impact pressure, $R_{u2\%}$ for a wave run-up level and q as mean overtopping discharge or V_{max} as maximum overtopping wave volume. A structure can then be designed using the appropriate partial safety factors, or with a full probabilistic approach.

Three different wave-structure-interaction processes are recognized on a sloping dike, with general design parameters, but also with parameters for individual waves:

Impacts:

Design parameters: $p_{2\%}$; p_{max}
Description of process: distribution of impact pressures, rise times, impact durations, impact width ($B_{impact,50\%}$) and impact locations;

Wave run-up and run-down:

Design parameters: $R_{u2\%}$; $R_{d2\%}$
Description of process: distributions of run-up and run-down levels, velocities along the slope for each wave;

Wave overtopping:

Design parameters: q; V_{max}
Description of process: distributions of individual overtopping wave volumes, flow velocities, thicknesses and overtopping durations.

Wave run-up, run-down and wave overtopping are the subject of this manual and required parameters and processes have been described in Chapters 4–7.

To date three types of simulators have been developed in the Netherlands: on overtopping; wave run-up; and on impacts. The principle is similar for all three types: a box with a certain geometry is filled with water by a (large) pump at a constant rate. The box is equipped with one or more valves to hold and release the water and has a specifically designed outflow device to guide the water to match the slope of the part of the dike being tested. The magnitude of the wave-structure-interaction can be varied by changing the released volume(s) of water from the box. The three simulators have been described in the following sections.

4.8.2 Wave Overtopping Simulator

The first Wave Overtopping Simulator was constructed in 2006, and it (and later versions) has been used since then for 'strength' tests of protection on dike crest and landward slopes simulating loadings from overtopping waves. The development and use of these devices on dikes in the Netherlands, Germany and Belgium has been described by Van der Meer *et al.*, (2006, 2007, 2008, 2009, 2010, 2011, 2012), Akkerman *et al.*, (2007), Steendam *et al*, (2008, 2010, 2011) and Hoffmans *et al*, (2008). Adaptation and use in Vietnam is described by Le Hai Trung *et al*, (2010), and in the USA (Van der Meer *et al*, 2011) and (Thornton *et al*, 2011).

Figure 4.33   Set-up of the Wave Overtopping Simulator close to a highway

The general set-up of the Overtopping Simulator on a dike or levee is illustrated in Figure 4.33, where the simulator itself has been placed on the seaward slope and releases overtopping volumes directly onto the crest. These 'overtopping' flows are then guided down the landward side of the dike. To fill the device, water is pumped into the upper tank, from which it is released intermittently through a butterfly valve, each release discharging a known overtopping volume. Electrical and hydraulic power packs enable pumping and opening and closing of the valve. A measuring cabin has been placed close to the test section. The Overtopping Simulator is 4 m wide and has a maximum capacity of 22 m^3, or 5.5 m^3 per m width. The device in Vietnam has the same capacity, but that in the US has a capacity of 16 m^3 per m width (over a width of 1.8 m instead of 4 m). The sets of volumes to be released are calculated beforehand according to theoretical distributions of overtopping wave volumes (as described in Chapters 4 and 5) depending on assumed wave conditions at the sea side and crest freeboard.

Figure 4.34 shows the release of a large overtopping wave volume and Figure 4.35 shows one of the many examples of a failed dike section, here a sand dike covered with good quality grass.

Figure 4.34   Release of a large overtopping wave volume

Figure 4.35   Failure of a grass covered sand dike

Figure 4.36   Measuring wave forces on vertical plates under flows from the Overtopping Simulator

The crest of many defences, particularly in urban areas, includes a storm or wave wall to reduce overtopping landward. An important question is: what will be the wave forces onto such a storm wall when overtopping waves travel over the boulevard (promenade) and hit the wall? Small scale physical tests in a wave flume or wave basin may give flow velocities and flow thicknesses of the overtopping waves, but impact forces may well have significant model and scale effects, particularly when the water entrains much

air. One way to measure such wave forces might be to use full (or nearly full) scale tests in a large wave flume like the Delta flume in the Netherlands, or the GWK in Germany, or at medium scale at UPC in Spain.

Another option, however, is to use one of the simulators to produce in real scale, and if possible with salt water, overtopping flow velocities and thickness. Examples of tests to measure wave forces on sections of a storm wall is illustrated in Figure 4.36 and Figure 4.37.

Figure 4.37   Measuring wave impacts on a 0.46 m high vertical step of a stair case, caused by run-up flows on a promenade from the wave run-up simulator

4.8.3 Wave Run-up

Procedures for testing wave run-up were outlined by Van der Meer (2011) and Van der Meer *et al* (2012), and a pilot test was performed in 2012 adapting an existing Wave Overtopping Simulator. The test device was placed on a seaward berm and run-up levels were calibrated against released wave volumes. In this way the largest run-up levels of a hypothetical storm and storm surge, which would reach the upper slope above the seaward berm, were simulated.

Figure 4.38 gives the set-up of the pilot test and shows a run-up event that reached the crest, more than 3 m higher than the level of the Simulator. An example of damage developed by simulating wave run-up is shown in Figure 4.39. The up-rushing waves meets the upper slope of the dike and eats into it.

The pilot test gave valuable information on how testing could be improved, but also how the test device should be modified. A Wave Run-up Simulator should have a slender shape, different from the present Wave Overtopping Simulator, in order to release smaller volumes, but with higher velocities. At the end of 2013 such a new device was constructed and tested, and the first tests on the upper seaward slope of a sea dike were run before spring 2014. The box had a cross-section at the lower part of 0.4 m by 2 m, giving a test section of 2 m wide, see Figure 4.40. The upper part had a cross-section of 0.8 m by 1.0 m and this change was designed in order to have less wind forces on the Simulator, as it is more than 8m high. The cross-sectional area was the same over the full height of the Simulator in order not to dissipate energy during release of water.

Figure 4.38   Pilot wave run-up test at Tholen, using the existing Wave Overtopping Simulator

Figure 4.39   Final damage after the pilot run-up test

A drawer-type valve mechanism was designed to cope with the very high water pressures (> 7 m head) with two valves moving horizontally. This reduced leakage under high pressures as those pressures helped seal the valves. This new Wave Run-up Simulator was calibrated against a 1:2.7 slope. The largest run-up was about 13.5 m along the slope, about 4.7 m vertically. It was also used to test transitions from down-slope to berm, berm to grass upper-slope, also a set of steps, see Figure 4.41, as these are often a weak point in a dike.

Figure 4.40   The Wave Run-up Simulator

Figure 4.41   Testing a stair case with the new Wave Run-up Simulator in 2014

4.8.4 Wave Impacts

A Wave Impact Generator was developed in 2011 - 2012 under the WTI 2017-programme of the Dutch Rijkswaterstaat and Deltares, see Figure 4.42, and used for testing dikes from 2012. The purpose of this device was to measure effects of breaking waves on the front face of a dike. It is a box of 0.4 m wide, 2 m long and can be up to 2 m high (modular system). It has an advanced system of two flap valves of only 0.2 m wide, which open very rapidly to enable the water to reach the slope at almost the same moment

over the full width of 0.4 m, thus creating a consistent impact. Measured impacts are comparable with impacts measured in the Delta Flume.

Figure 4.42   Test with Wave Impact Generator

Figure 4.43   Failed road crossing by under-mining due to simulated wave impacts

As the location of impacts varies on the slope, the Wave Impact Generator has been attached to a tractor or excavator, which moves the test location a little up or down the slope. In this way the impact locations can be varied so that they do not occur all at the same location. Development and description of testing have been described by Van Steeg (2012a, 2012b and 2013).

The main application is simulation of wave impacts on grassed slopes of dikes where wave heights are limited to H_{m0} = 0.5 - 1 m, perhaps river dikes. In practice, it is used only to simulate the largest 30% of wave impacts. Slopes with various quality of grass, as well as soil (clay and sand), have been tested as well as a number of transitions, which are often found in dikes and which in many cases fail faster than a grassed slope. Figure 4.43 illustrates a road crossing of open blocks, which failed by undermining under simulated wave impacts.

4.9   Model and Scale effects

This section deals with model and scale effects resulting from scaled hydraulic models on wave overtopping. First, definitions will be given what scale effects and model effects are. Secondly, a methodology based on the current knowledge is introduced on how to account for these effects.

4.9.1 Scale effects

Scale and model effects result from incorrect reproduction of a prototype water-structure interaction in the scale model. Reliable results from scaled models can only be expected by fulfilling Froude's and Reynolds' law simultaneously. This is however not possible so that scale effects cannot be avoided when performing scaled model tests.

Since gravity, pressure and inertial forces are the relevant forces for wave motion most models are scaled according to Froude's law. Viscosity forces are governed by Reynolds' law, elasticity by Cauchy's law and surface tension forces by Weber's law, and these forces have to be neglected for most models. All effects and errors resulting from ignoring these forces are called scale effects. The problem of the quantification of all these scale effects is still unresolved, but the European research project CLASH gave a little more insight in scale effects with wave overtopping.

4.9.2 Model and measurement effects

Model or laboratory effects originate from the incorrect reproduction of the prototype structure, geometry and waves and currents, or due to the boundary conditions of a wave flume (side walls, wave paddle, etc.). Modelling techniques have developed significantly, but there are still influences of model effects on hydraulic model results to be expected.

Measurement effects result from different measurement equipment used for sampling the data in the prototype and model situations. These effects, which are referred to as "measurement effects" may significantly influence the comparison of results between prototype and model, or two identical models. It is therefore essential to quantify the effects and the uncertainty related to the different techniques available.

As an example, an important model effect is the width of an overtopping measurement that is often too small in terms of number of armour units (typically > 20 are advised) to obtain a reliable average overtopping discharge. When this is the case increasing the test duration above a certain limit will not give more certainty.

4.9.3 Methodology

Following the aforementioned definitions the reasons for differences between model and prototype data will sometimes be very difficult to assign to either model or scale effects. During CLASH, one of the major contributions to model effects was found to be wind since this is ignored in nearly all hydraulic models. Despite the lack of wind, additional differences were found and assigned to model effects, such as roughness and permeability of the structure.

The following phenomena may give indications of the contributions of the most important model effects in addition to wind. The repeatability of tests showed that the wave parameters (H_{m0}, T_p, $T_{m-1,0}$) have a coefficient of variation of $\sigma'{\sim}3\%$, and for wave overtopping the differences between two wave flumes were $\sigma'{\sim}13\%$ and $\sigma'{\sim}10\%$. Different time windows for wave analysis and different types of wave generation methods had hardly influence on the estimated wave parameters ($\sigma'{\sim}3\%$). The number of waves in the flume shows influence on wave overtopping, where a comparison of 200 to 1000 generated waves show differences in mean overtopping rates up to a value of 20%. Another element that generates variability is the seeding of the random phases of the generated time series. This variability, as shown in Romano *et al.* (2015), and is more pronounced if the overtopping probability is less than 5% and for $R_c/H_{m0} > 2$, while it decreases for high overtopping discharges.

The position of the overtopping tray at the side of the flume showed also differences in overtopping rates ($\sigma'{\sim}20\%$) from results where the tray was located at the centre of the crest. This could be because of the

different arrangement of the armour units in front of the overtopping tray or due to the influence of the side walls of the flume, hence the width of the test section was too small to accurately determine the real average overtopping discharge.

Scale effects have been investigated by various authors, and this has led to some generic rules that should be observed for physical model studies. Generally, water depths in the model should be much larger than h = 2.0 cm, wave periods larger than T = 0.35 s and wave heights larger than H_s = 5.0 cm to avoid the effects of surface tension; for rubble mound breakwaters the Reynolds number for the stability of the armour layer should exceed Re = $3x10^4$; for overtopping of coastal dikes Re > $1x10^3$; and the stone size in the core of rubble mound breakwaters has to be scaled according to the velocities in the core rather than the stone dimensions, especially for small models. The method for how this can be achieved is given in Burcharth *et al.* (1999). Furthermore, critical limits for the influence of viscosity and surface tension are given in Table 4.5, more details can be found in Schüttrumpf and Oumeraci (2005).

Table 4.5:   Scale effects and critical limits

Process	Relevant forces	Similitude law	Critical limits
Wave propagation	Gravity force Friction forces Surface tension	Fr_W Re_W We	$Re_W > Re_{W,crit} = 1x10^4$ T > 0,35 s; h > 2,0 cm
Wave breaking	Gravity force Friction forces Surface tension	Fr_W Re_W We	$Re_W > Re_{W,crit} = 1x10^4$ T > 0,35 s; h > 2,0 cm
Wave run-up	Gravity force Friction forces Surface tension	Fr_A, Fr_q Re_q We	$Re_q > Re_{q,crit} = 10^3$ $We > We_{crit} = 10$
Wave overtopping	Gravity force Friction forces Surface tension	Fr_A, Fr_q Re_q We	$Re_q > Re_{q,crit} = 10^3$ $We > We_{crit} = 10$

With: $Fr_W = c/(g \cdot h)^{1/2}$; $Fr_A = v_A/(g \cdot h_A)^{1/2}$; $Fr_q = v_A/(g \cdot R_u)^{1/2}$; $Re_W = c \cdot h/\nu$; $Re_q = (R_u - R_C)^2/(\nu \cdot T)$); $We = v_A \cdot h_A \cdot \rho_W/\sigma_W$

From observations in prototype and scaled models, a methodology was derived to account for those differences without specifically defining which model and measurement effects contribute how much. These recommendations are given in Sections 5.6 for dikes, 6.3.6 for rubble slopes, and 7.3.9 and 7.4.5 for vertical walls, respectively.

4.10 Uncertainties in predictions

Sections 4.2 to 4.7 have proposed various models to predict wave overtopping of coastal structures. These models will now be discussed with regard to their uncertainties.

4.10.1 Empirical Models

It has been discussed in section 1.5.4 that the model uncertainty concept uses a mean factor of 1.0 and often a Gaussian or log-normal distribution around the mean prediction. This manual describes the reliability of the formula often by taking one of the coefficients as a stochastic parameter (instead of m = 1) and giving a standard deviation (assuming a normal distribution). The standard deviation is derived from the comparison of model data and the model prediction.

This manual presents the following enhanced approaches:

- **Mean value approach**. Use the formula as given with the mean value of the stochastic parameter(s). This should be done to predict or compare with test data. In a graph also the 5%-exceedance lines or 90%-confidence band could be given to complete the comparison;
- **Design or assessment approach**. This is an easy semi-probabilistic approach with a partial safety factor; this is the mean value approach above, but now with the inclusion of the uncertainty of the prediction. The stochastic parameter(s) become(s) $\mu(m) + \sigma(m)$, where m is given in Equation 1.3;
- **Probabilistic approach**. Consider the stochastic parameter(s) with their given standard deviation and assuming a normal or log-normal distribution;
- The 5%-exceedance lines, or **90%-confidence band**, can be calculated by using $\mu(m) \pm 1.64\sigma(m)$ for the stochastic parameter(s).

In this manual, the formulae are given as a **mean value approach**. The formula(e) and 5%-exceedance curves are given in a graphical way. Key coefficients are taken as stochastic variables, and uncertainty is then described by giving the standard deviation, $\sigma(m)$. The coefficient to be used in the formula for the **design or assessment approach** will also be given.

4.10.2 Artificial Neural Network

When running the Artifical Neural Network (ANN) prediction model the user will be provided with wave overtopping ratios based on the new EurOtop database (Section 4.4) and the Neural Network prediction (Section 4.5). Together with these results the user will also obtain the uncertainties of the prediction through the 90% confidence interval that is given by the 5% and 95% exceedance probabilities.

Actually, the ANN-prediction is based on 500 neural networks where each neural network was trained on a different part of the database. In this way the 500 predictions give a distribution with mean value (the outcome of the prediction tool), but also the 90% confidence band or interval. The width of this 90% confidence interval largely depends on whether the neural network had data points in the database that were close to the geometry and conditions as calculated, or not. If this was indeed the case, then the 90% confidence band would be similar and maybe even a little smaller than with empirical models, described in the previous section. But if the structure geometry and/or the wave conditions would be far from data in the database, the 90% confidence band would increase significantly. Therefore, if the ANN is used to predict a trend in calculations, for example by increasing incrementally one parameter, then the widening of the confidence band would show directly the off-set from experience in the database.

4.10.3 EurOtop database

The new EurOtop database is described in Section 4.4. It provides a large dataset of available model data on wave overtopping of coastal structures. It should be mentioned that the model and scale effects approach introduced in Section 4.8 has not been applied to the database as all data were given as they were measured. Whenever these data are used for prototype predictions the user will have to check whether any scaling correction procedure is needed.

With respect to uncertainties all model results will contain variations in the measured overtopping ratios. Most of these variations will result from measurement and model effects as discussed earlier. Since the database is no real model but an additional source of data information no model uncertainty can be applied.

4.11 Guidance on use of methods

This manual is accompanied by an overall Calculation Tool outlined in Appendix A. This tool includes the elements:

- Empirical Calculator programmed with the main empirical overtopping equations in Chapters 5, 6 and 7 (limited to those that can be described explicitly, that is without iteration).

- PC-Overtopping. This tool codes all the prediction methods presented in Chapter 5 of EurOtop (2007) for 2%-wave run-up, mean overtopping discharge and individual overtopping wave volumes, for (generally shallow sloped) sea dikes, see Section 4.3. This tool has not been changed to the new formulae in this manual as given in Chapter 5.

- EurOtop Artificial Neural Network tool developed for this manual, starting from the CLASH research project, to calculate mean overtopping for many types of structures, see Section 4.4.

- EurOtop database, a listing of input parameters and mean overtopping discharge from each of more than 13,000 physical model tests on both idealised (research) test structures, and site specific designs. These data can be filtered to identify test results that may apply for configurations close to the reader's.

None of these methods give the universally 'best' results. The most reliable method to be used will depend on the type and complexity of the structures, and the closeness with which it conforms to simplifying assumptions used in previous model testing (on which all of the methods above are inherently based).

In selecting which method to use, or which set of results to prefer when using more than one method, the user will need to take account of the origins of each method. It may also be important in some circumstances to use an alternative method to give a check on a particular set of calculations. To assist these judgements, a set of simple rules of thumb are given here, but as ever, these should not be treated as universal truths.

- For simple vertical, composite, or battered walls which conform closely to the idealisations in Chapter 7, the results of the Empirical Calculator (i.e. the formulae in that chapter) are likely to have the same reliability than the Artificial Neural Network. PC-Overtopping is not applicable for these kind of structures.

- For simple sloped dikes with a single roughness, many test data have been used to develop the formulae in the Empirical Calculator, so this may be the most reliable, and simplest to use / check. For dikes with multiple slopes or roughness, PC-Overtopping is likely to be the most reliable, and easiest to use, although independent checking may be more complicated. The Database or Artificial Neural Network methods may become more reliable where the structure starts to include further elements.

- For armoured slopes and mounds, open mound structures that most closely conform to the simplifying models may best be described by the formulae in the Empirical Calculator. Structures of lower permeability may be modelled using PC-Overtopping. Mounds and slopes with crown walls may be best represented by application of the Database or Artificial Neural Network methods.

- For unusual or complex structures with multiple elements, mean overtopping discharge may be most reliably predicted by PC-Overtopping (if applicable) or by the Database or Artificial Neural Network methods.

- For structures that require use of the Artificial Neural Network method, it is possible that the use of many data for other configurations to develop a single Neural Network method may introduce some averaging. It may therefore be appropriate to check in the Database to see whether there

are already test data close to the configuration being considered. This procedure may require some familiarity with manipulating these types of test data.

In almost all instances, the use of any of these methods will involve some degree of simplification of the true situation. The further that the structure or design (analysis) conditions depart from the idealised configurations tested to generate the methods / tools discussed, the wider will be the uncertainties. Where the importance is high of the assets being defended, and/or the uncertainties in using these methods are large, then the design solution may require use of site specific physical model tests, as discussed in Section 4.7.

5 Coastal dikes and embankment seawalls

5.1 Introduction

Levees, coastal and river dikes and embankment seawalls are flood defence structures with often only water on one side, the seaward side; this in contrast to breakwaters. They are characterised by gentle and steep slopes, berms and the seaward protection consists of grass, placed block revetments, asphalt, rock, roughness elements and often a combination of these systems, see Figure 5.1 and Figure 5.2.

Figure 5.1:   Examples of coastal dikes, levees and seawalls. Delfzijl, NL; Busum, DE; Houtribdijk, NL; Rotterdamse Hoek, NL

An exact mathematical description of the wave run-up and wave overtopping process for coastal dikes or embankment seawalls is not possible due to the stochastic nature of wave breaking and wave run-up and the various factors influencing the wave run-up and wave overtopping process. Therefore, wave run-up and wave overtopping for coastal dikes and embankment seawalls are mainly determined by empirical formulae derived from experimental investigations. The influence of roughness elements, wave walls, berms, etc. is taken into account by introducing influence factors. A definition sketch is given in Figure 5.3 (see Section 1.4 for full descriptions).

The following chapter on coastal dikes and embankments is structured as follows. Section 5.2 describes wave run-up as a function of the wave breaking process on the seaward slope for simple smooth and straight slopes. Distinction is made between dike type slopes, roughly between 1:10 and 1:2 and much steeper slopes, even up to vertical walls. Another distinction is the effect of shallow and very shallow water including a change of the wave spectrum and breaker parameters to very large values. Section 5.3 gives prediction of the average wave overtopping discharge The influence factors on wave run-up and wave overtopping like berms, roughness or roughness elements, and oblique wave attack are handled in Section 5.4. Also a section on the influence of currents on wave overtopping is given here. Section 5.4.7 is completely dedicated to wave or storm walls on promenade type structures. Finally, distributions of overtopping wave volumes over the crest and the overtopping flow thicknesses and flow velocities are

discussed in Section 5.5 as the direct influencing parameters to the surface of the structure. The main calculation procedures assessing wave run-up and overtopping for coastal dikes and embankment seawalls is outlined in Table 5.1.

Figure 5.2: Examples of coastal dikes, levees and seawalls. Hanoi, Vietnam; Ile de Ré, FR; Boonweg, NL; Hondsbossche zeewering, NL
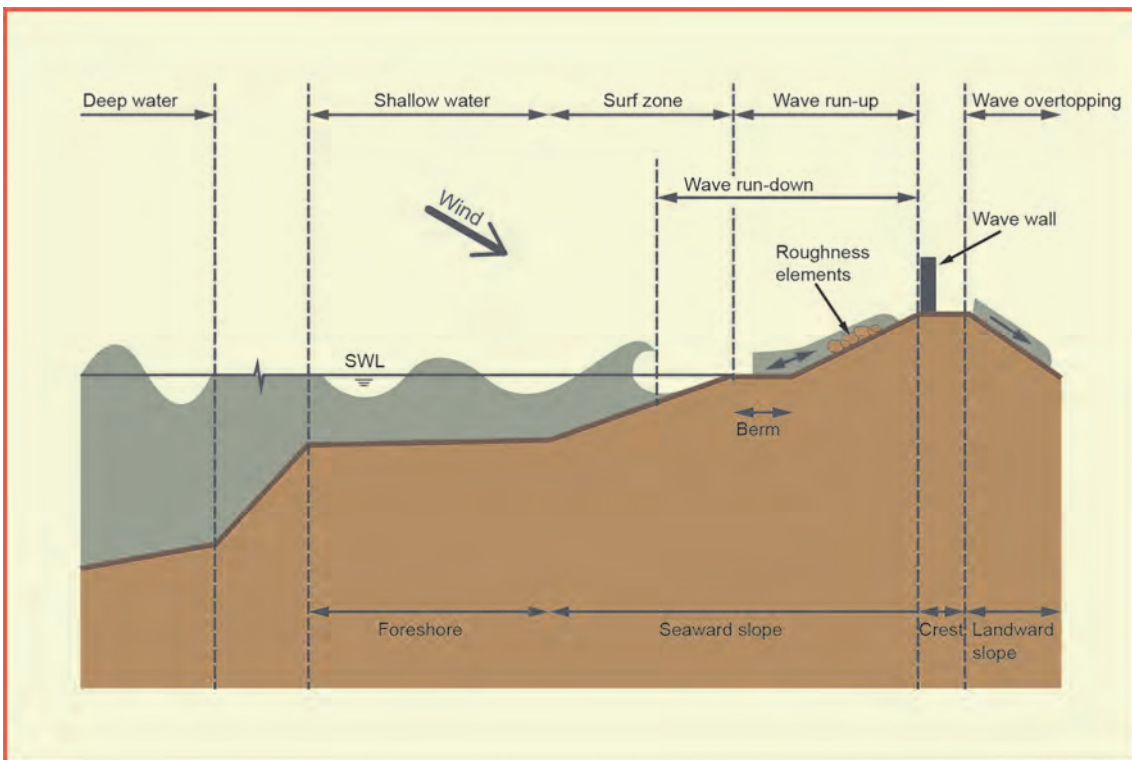
Figure 5.3: Wave run-up and overtopping for coastal dikes and embankment seawalls: definition sketch

Table 5.1: Main calculation procedure for coastal dikes and embankment seawalls

	Design approach		Mean value approach	
Wave run-up Relatively gentle slopes Very shallow foreshores Steep slopes up to vertical walls	Eqs. Eq. Eq.	5.4, 5.5 5.5 5.7	Eqs. Eq. Eq.	5.1, 5.2 5.2 5.6
Wave overtopping Relatively gentle slopes Very shallow foreshores Steep slopes up to vertical walls Negative freeboard	Eqs. Eq. Eq.	5.12, 5.13 5.16 5.18 + 1σ	Eqs. Eq. Eq. Eq.	5.10, 5.11 5.15 5.18 5.20
Influence factors Roughness Oblique waves Currents Composite slopes and berms Wave or storm walls	Eqs. Eqs. Eqs. Eq.	Table 5.2 5.28 - 5.30 5.33 - 5.37 5.38 - 5.43 5.44 - 5.51		
Overtopping wave characteristics Overtopping wave volumes Flow velocity and thickness – seaward Flow velocity and thickness – crest Flow velocity and thickness – landward	Eqs. Eqs. Eq. Eqs.	5.52 - 5.57 5.58 - 5.60 5.61 5.62 - 5.64		

5.2   Wave run-up

5.2.1   History of the 2%-value for wave run-up

The choice for 2% as the relative run-up height as a design basis for crest level assessment of dikes was made long ago and was probably arbitrary. The first international paper on wave run-up, mentioning the 2% wave run-up, is Asbeck *et al.*, 1953. The formula $R_{u2\%} = 8\,H_{m0}\tan\alpha$ is mentioned there (for 5% wave steepness and gentle smooth slopes), and this formula was used for the design of dikes until 1980.

The origin stems from the closing of the Southern Sea in the Netherlands in 1932 by the construction of a 32 km long dike (Afsluitdijk). This created the fresh water lake IJsselmeer and in the 45 years after closure about half of the lake was reclaimed as new land, called polders. The dikes for the first reclamation (Noordoostpolder) had to be designed in 1936/1937. It is for this reason that in 1935 to 1936 a new wind-wave flume was built at Delft Hydraulics (now Deltares) and the first tests on wave run-up were performed in 1936. The final report on measurements (report M101), however, was not issued until 1941 "due to lack of time". Nevertheless, the measurements had been analysed in 1936 to such a degree that "the dimensions of the dikes of the Noordoostpolder could be established". The M101 report gives only the 2% wave run-up value and this must have been the time that this value would be the right one to design the crest height of dikes.

Further tests from 1939 – 1941 on wave run-up, published in report M151 in 1941, however, used only the 1% wave run-up value. Other and later tests (Report M422, 1953; Report M500, 1956 and Report M544, 1957) report the 2%-value, but for completeness also give the 1%, 10%, 20% and 50% values.

It can be concluded that the choice for the 2% value was made in 1936, but the reason why is not clear as the design report itself could not be retrieved. More information, however, was retrieved from Professor Battjes (personal communication), who took notes during the lectures he attended from Professor Thijsse, the founder of Delft Hydraulics, and also the person who was involved in the model tests during 1936. The notes of Professor Battjes (from the sixties) gives, freely translated from Dutch:

"We see developments in design of dikes. Wind wave flumes have been built in laboratories. The run-up heights of the waves were visually recorded. To get better accuracy one needs more time for testing. Measurement series of 50 waves were performed. Till now steep slopes, as well as rough and gentle slopes have been compared. With 50 waves per test series the 2%-run-up level was created. Waves: a duration of one and a half hour with 8 second waves gives 600 waves and 2% means that only 12 waves will overtop the dike. This gives of course no disaster. With 1% there will be only 6 overtopping waves and 5% will be too much."

The notes of Professor Battjes show that probably the length of the test series of 50 waves determined the 2%-value. An anecdote from Jan Willem Seyffert (personal communication) says that at that time of testing the wave generator was personally driven by a bike type machine. The person would not be physically able to generate more than about 50 waves, before he had to rest.

100

5.2.2   Relatively gentle slopes

The wave run-up height is defined as the vertical difference between the highest point of wave run-up and the still water level (SWL) as shown in Figure 5.4. Due to the stochastic nature of the incoming waves, each wave will give a different run-up level. In the Netherlands, as well as in Germany, many dike heights have been designed to a wave run-up height $R_{u2\%}$. This is the wave run-up height which is exceeded by 2% of the number of incoming waves at the toe of the structure. The idea behind this was that if only 2% of the waves reach the crest of a dike or embankment during design conditions, the crest and inner slope do not need specific protection measures other than clay with grass. It is for this reason that much research in the past has been focused on the 2%-wave run-up height. The history of the 2%-value has been described in the previous section 5.2.1.
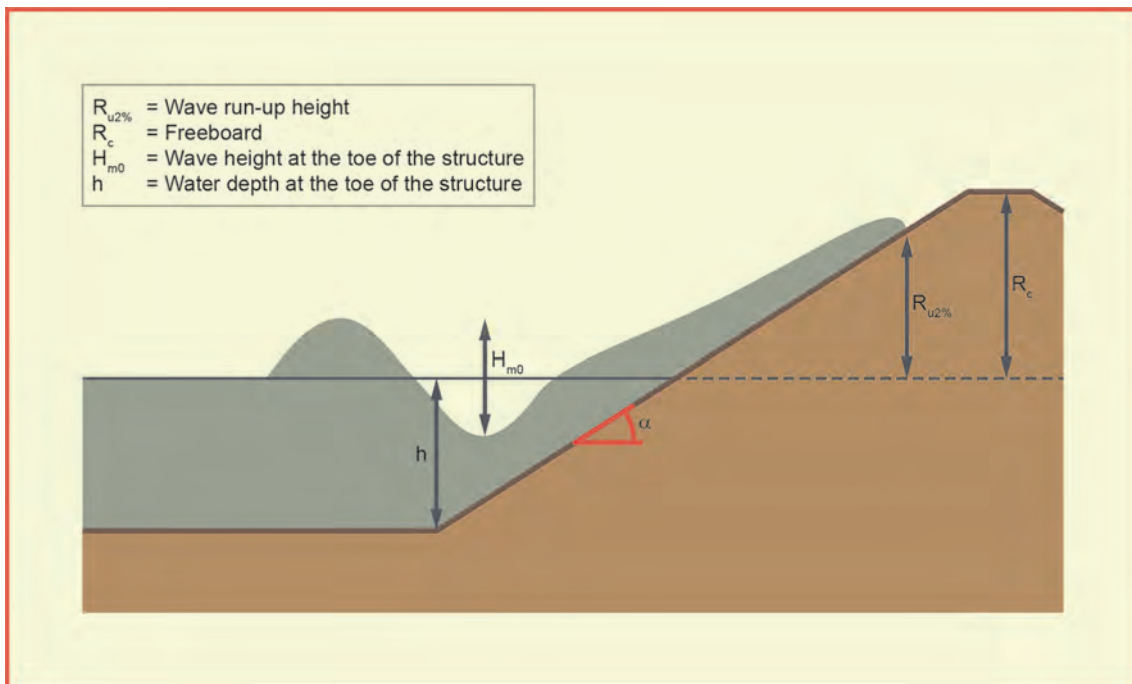
Figure 5.4:   Definition of the wave run-up height $R_{u2\%}$ on a smooth impermeable slope

In the past decade the design or safety assessment has been changed to allowable overtopping instead of wave run-up. Still a good prediction of wave run-up is valuable as it is the basic input for calculation of the number of overtopping waves over a coastal structure, which is required to calculate overtopping volumes, overtopping velocities and flow thicknesses.

The general formula that can be applied for the 2%-wave run-up height for relatively gentle slopes (1:2.0 and gentler) is given by Equations 5.1 and 5.2 and Figure 5.5. The relative wave run-up height $R_{u2\%}/H_{m0}$ in Equations 5.1 and 5.2 is related to the breaker parameter $\xi_{m-1,0}$. The breaker parameter or

surf similarity parameter $\xi_{m-1,0}$ relates the slope steepness $\tan \alpha$ to the wave steepness $s_{m-1,0}$ and is often used to distinguish different breaker types, see Section 1.4.3.

For relatively gentle slopes the breaker parameter is generally smaller than $\xi_{m-1,0} = 4$. In case larger values are found for slopes of 1:2.5 or gentler, this can only be due to very small wave steepnesses, probably caused by severe wave breaking on a (very) shallow foreshore; very shallow foreshores are discussed in Section 5.2.3. Steep slopes, say 1:2 up to vertical walls, give less wave run-up (and wave overtopping) than the maximum given in Equation 5.2, see Section 5.2.4. For a **mean value approach** the wave run-up is expressed as:

$$\frac{R_{u2\%}}{H_{m0}} = 1.65 \cdot \gamma_b \cdot \gamma_f \cdot \gamma_\beta \cdot \xi_{m-1,0} \qquad \qquad 5.1$$

with a maximum of $\dfrac{R_{u2\%}}{H_{m0}} = 1.0 \cdot \gamma_f \cdot \gamma_\beta \left(4 - \dfrac{1.5}{\sqrt{\gamma_b \cdot \xi_{m-1,0}}} \right)$ $\qquad \qquad 5.2$

where $R_{u2\%}$ is the wave run-up height exceeded by 2% of the incoming waves [m], γ_b is the influence factor for a berm [-], γ_f is the influence factor for roughness elements on a slope [-], γ_β is the influence factor for oblique wave attack [-] and $\xi_{m-1,0}$ is the breaker parameter [-].
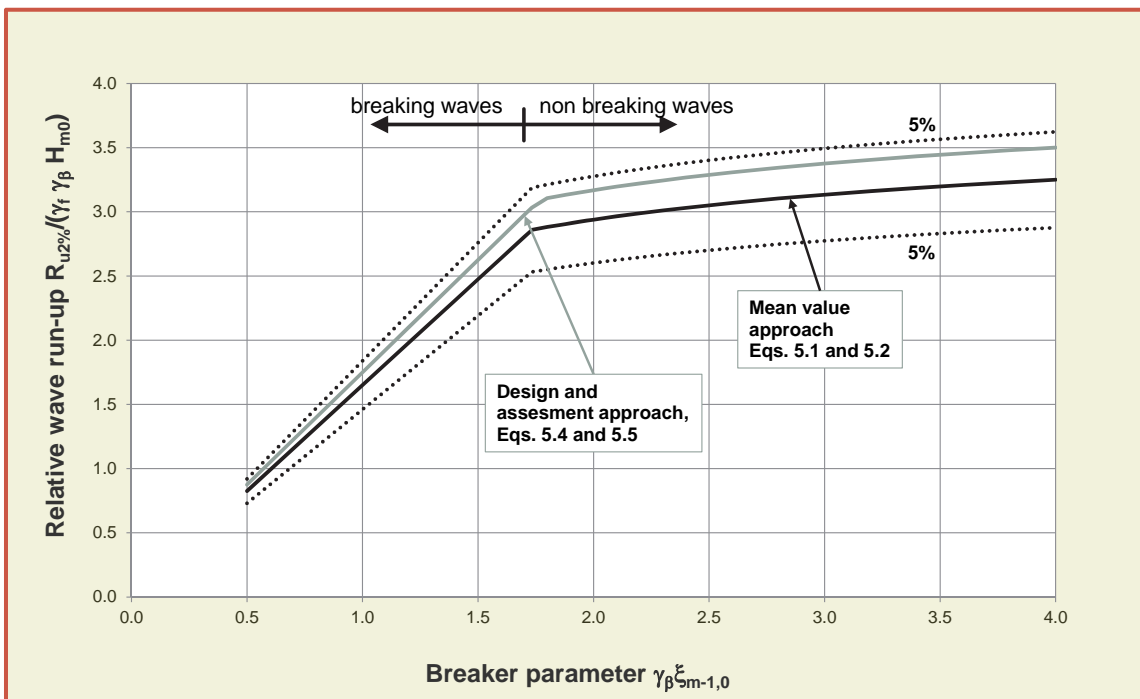
Figure 5.5: Relative 2%-wave run-up height $R_{u2\%}/H_{m0}$ for relatively gentle slopes, as a function of the breaker parameter $\xi_{m-1,0}$ and other influence factors

The relative wave run-up height increases linearly with increasing $\xi_{m-1,0}$ in the range of breaking waves and small breaker parameters less than about $\xi_{m-1,0} = 1.8$. For non-breaking waves and higher breaker parameter than this value, the increase is less steep as shown in Figure 5.5 and becomes more or less horizontal. In that area the influence of slope angle and wave steepness becomes much smaller. The relative wave run-up height $R_{u,2\%}/H_{m0}$ is also influenced by the geometry of the coastal dike or embankment seawall; the properties of the incoming waves; and possibly by the effect of wind.

The geometry of the coastal dike is considered by the (average) slope $\tan \alpha$, the influence factor for a berm γ_b, the influence factor for roughness or roughness elements on the slope γ_f; and the influence factor for a wave wall γ_V. The latter influence factor is only valid for wave overtopping, as wave run-up on a vertical wall is not an issue. The influence factors on geometry will be discussed in Sections 5.4 and 5.5.

The effect of wind on the wave run-up-height for smooth impermeable slopes will mainly be focused on the thin layer in the upper part of the run-up. As described in Section 1.4, very thin layers of wave run-up are not considered and the run-up height was defined where the run-up layer becomes less than 1-2 cm. Wind will not have a lot of effect then. This was also proven in the European programme OPTICREST, where wave run-up on an actual smooth dike was compared with small scale laboratory measurements. Scale and wind effects were not found in those tests. It is recommended not to consider the influence of wind on wave run-up for coastal dikes or embankment seawalls.

The properties of the incoming waves are considered in the breaker parameter $\xi_{m-1,0}$ and the influence factor for oblique wave attack γ_β, which is discussed in Section 5.4.3. As described in Section 1.4, the spectral wave period $T_{m-1,0}$ is most suitable for the calculation of the wave run-up height for complex spectral shapes as well as for theoretical wave spectra (JONSWAP, TMA, etc.). This spectral period $T_{m-1,0}$ gives more weight to the longer wave periods in the spectrum and is therefore well suited for all kinds of wave spectra including bimodal and multi-peaked wave spectra.

The peak period T_p, which was used in former investigations, is difficult to apply in the case of bimodal spectra and should not be applied for multi-peaked or flat wave spectra as this may lead to large inaccuracies. Nevertheless, the peak period T_p is still in use for single peak wave spectra and there is a clear relationship between the spectral period $T_{m-1,0}$ and the peak period T_p for conventional single peak wave spectra:

$$T_p = 1.1\, T_{m-1,0} \qquad\qquad 5.3$$

Similar relationships exist for theoretical wave spectra between $T_{m-1,0}$ and other period parameters like T_m and $T_{m0,1}$, see Section 1.4, where it is also recommended to use the spectral wave height H_{m0} for wave run-up height calculations.

The recommended formulae for wave run-up calculations, Equations 5.1 and 5.2, is based on a large (international) dataset, including roughness, berms, oblique wave attack, etc. As an example Figure 5.5 is given with data for relatively gentle, smooth and straight slopes. Due to the large dataset for all kind of sloping structures a significant scatter is present, which cannot be neglected for application. There are several ways to include this uncertainty for application, but all are based on the formula describing the mean and a description of the uncertainty around this mean; see Section 1.5.5 for a further explanation. In essence, the mean value approach gives the average expectation and should also give the reliability around this average, often by giving a standard deviation. The design or assessment approach includes some safety (one standard deviation) and can straightforwardly be used for design and assessment of coastal structures. The *mean value approach* (Equations 5.1 and 5.2) as well as the *design and assessment approach* (Equations 5.4 and 5.5) are given in Figure 5.5.

Coefficient 1.65 in Equation 5.1 can be considered as a stochastic variable with a mean value of 1.65 and a standard deviation of $\sigma = 0.10$. For a design and assessment approach one should use the value of 1.75. Coefficient 1.0 for the "maximum" in Equation 5.2 can be considered as a stochastic variable with a mean value of 1.00 and a standard deviation of $\sigma = 0.07$. For a design and assessment approach one should use the value of 1.07. For a design and assessment approach, using a partial safety factor of one standard deviation, the run-up formula becomes:

$$\frac{R_{u2\%}}{H_{m0}} = 1.75 \cdot \gamma_b \cdot \gamma_f \cdot \gamma_\beta \cdot \xi_{m-1,0} \qquad\qquad 5.4$$

with a maximum of
$$\frac{R_{u2\%}}{H_{m0}} = 1.07 \cdot \gamma_f \cdot \gamma_\beta \left(4.0 - \frac{1.5}{\sqrt{\gamma_b \cdot \xi_{m-1,0}}} \right)$$

5.5

The wave run-up formulae, Equations 5.1 and 5.2 are given in Figure 5.6 together with measured data from small and large scale model tests. In Figure 5.6 all data were measured under perpendicular wave attack on relatively gentle slopes and without significant wave breaking in front of the dike toe. Exceedance lines, for example, can be drawn by using $R_{u2\%} / H_{m0} = \mu \pm x \cdot \sigma = \mu \pm x \cdot \sigma' \cdot \mu$, where μ is the prediction by Equations 5.1 and 5.2, $\sigma = \sigma' \cdot \mu$ the standard deviation, and x a factor of exceedance percentage according to the normal distribution. For example x = 1.64 for the 5% exceedance limits and x = 1.96 for the 2.5% exceedance limits. The 5% exceedance limits are also given in Figure 5.5 and Figure 5.6. The area between the 5%-limits is the 90%-confidence band.
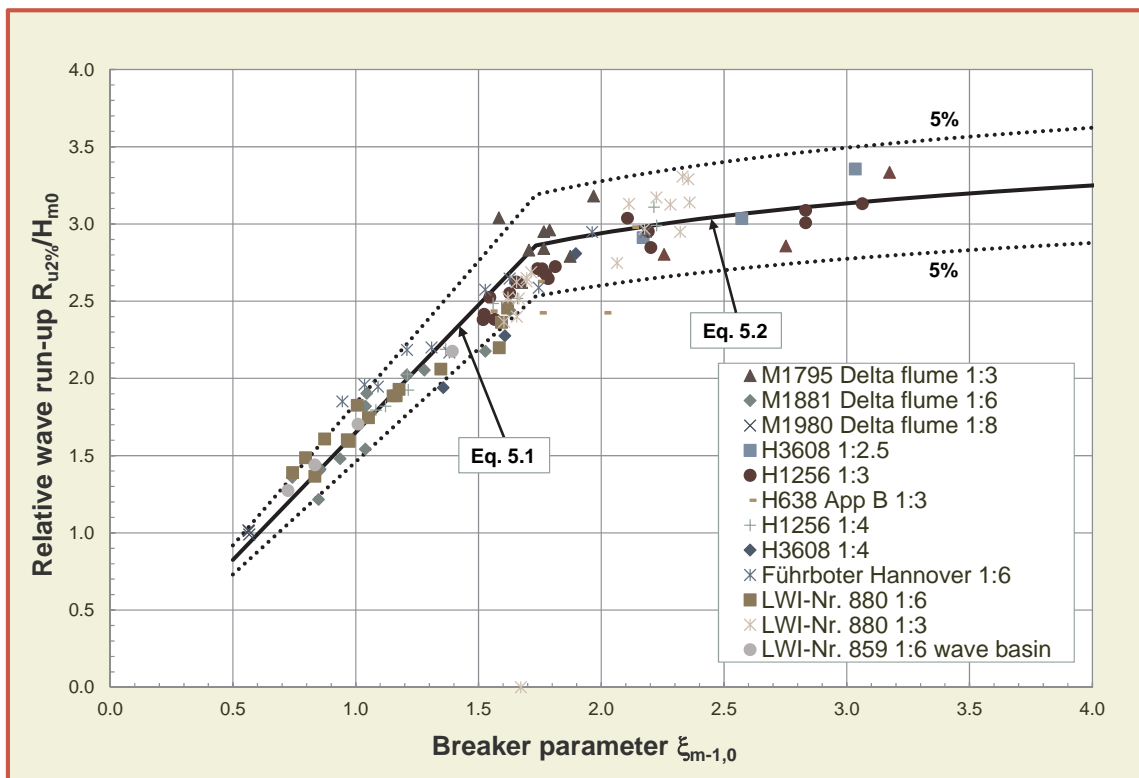
Figure 5.6:   Wave run-up for relatively gentle, smooth and straight slopes

The influence factors γ_b, γ_f and γ_β where derived from experimental investigations. A combination of influence factors is often required in practice which reduces wave run-up and wave overtopping significantly. Systematic investigations on the combined influence of wave obliquity and berms showed that both influence factors can be used independently without any interactions. Nevertheless, a systematic combination over the range of all influence factors and all combinations was not possible until now. *Therefore, further research is recommended if the overall influence factor $\gamma_b \gamma_f \gamma_\beta$ becomes lower than 0.4.*

5.2.3   Shallow and very shallow foreshores

Most wave conditions have wave steepnesses between $s_{m-1,0} = 0.01$ and 0.06. The largest values are found for wind waves and the smaller for swell conditions, or conditions where the wave height has been reduced a little due to breaking over a foreshore. If foreshores are (very) gentle and long and wave heights in deeper water are fairly high, the waves may break over a large part of the foreshore and may reduce significantly. Such deep water wave heights may reduce to less than 10%-20% of their original height, at the toe of the structure. With such severe wave breaking at shallow or very shallow foreshores,

other influences than just wave height and wave period start to play a role, like changing spectral shape (and period), infra gravity waves and surf beat. This process and the influence on wave run-up and wave overtopping is not fully understood yet, but from the investigation of Van Gent (1999) it is clear that there is a significant influence.

Van Gent (1999) made small scale model tests on a 1:100 and 1:250 foreshore with smooth structure slopes of 1:4 and 1:2.5. Due to the heavy breaking wave periods, $T_{m-1,0}$ changed sometimes from a few seconds at deep water to more than 8 s at the toe of the structure. This implies a significant change of spectral shape. Also wave heights reduced in some cases from roughly 0.14 m to less than 0.04 m. With such small wave heights and very long periods at the toe of the structure, the breaker parameter becomes very large, around $\xi_{m-1,0} = 14$ for a 1:4 slope and $\xi_{m-1,0} = 20$ for a 1:2.5 slope. Such values are far outside the range given in Figure 5.5 and Figure 5.6 of the previous section. Therefore shallow and very shallow foreshores have to be treated differently from situations where waves do not break, or only break to some extent.
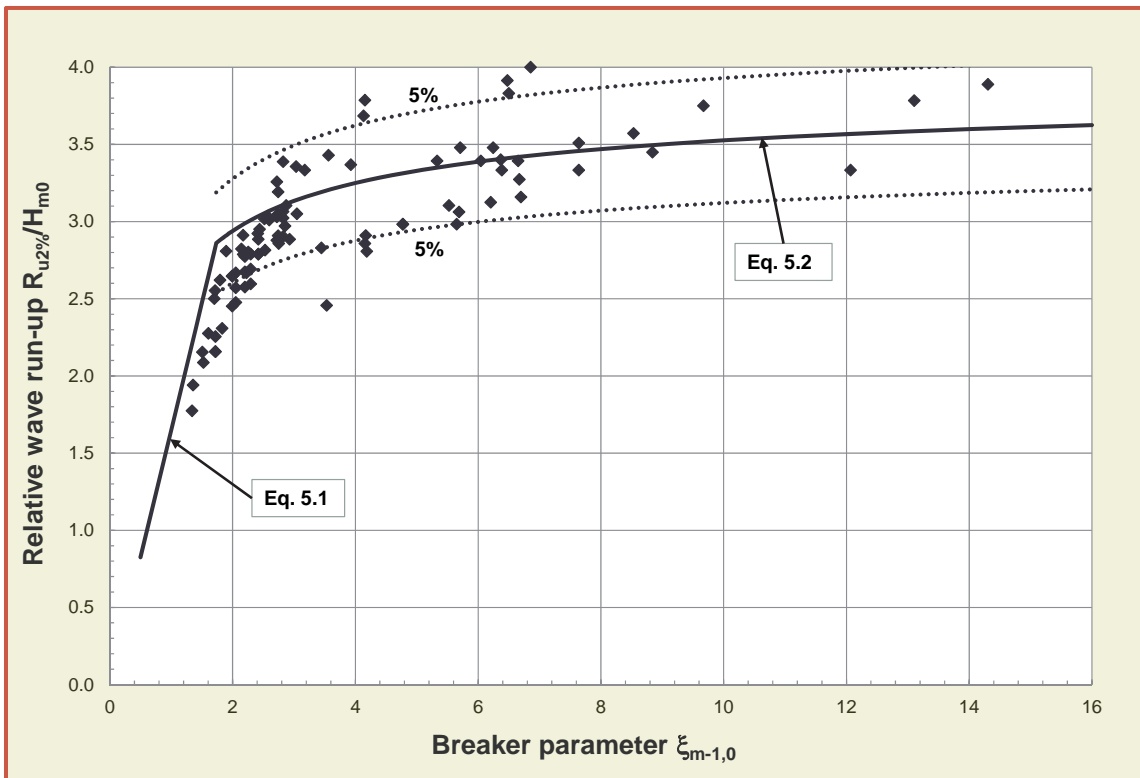
Figure 5.7:   Wave run-up for smooth straight slopes of 1:2.5 and 1:4 on shallow and very shallow foreshores of 1:100 and 1:250 (Van Gent, 1999)

Figure 5.7 gives the data of Van Gent (1999) with Equations 5.1 and 5.2 and the 5%-exceedance lines. The main point of interest is the area with breaker parameters $\xi_{m-1,0} > 4$, where significant wave breaking occurred. The "maximum" in Equation 5.2 describes the area of excessive wave breaking well, as it was originally fitted to these data. For very large breaker parameters, say $\xi_{m-1,0} > 15$, the relative wave run-up becomes almost horizontal, which means that it actually becomes independent of wave steepness as well as slope angle. For these conditions at very shallow foreshores, it does not make a difference whether the slope is 1:4, 1:2.5 or even much steeper like 1:1. The very low wave steepness and probably increased water level by wave set-up, surf beat or infra gravity waves, gives a relative run-up height $R_{u2\%}/H_{m0}$ of around 3.6, regardless of the structure slope angle.

The breaker parameter $\xi_{m-1,0}$ is a combination of slope angle and wave steepness. Large breaker parameters may be found for (very) steep slopes and/or (very) low wave steepness. In the case of a very shallow foreshore, as in Figure 5.7, it is the very low wave steepness. It means that this very low steepness may be a parameter to distinguish between very steep slopes with "normal" wave conditions and shallow and very shallow foreshores (with gentle as well as steep slopes). A wave steepness of

$s_{m-1,0} < 0.01$ gives generally conditions of severe wave breaking (unless it is very low and long swell). For a relatively steep slope it gives $\xi_{m-1,0} = 5$. As soon as this threshold is exceeded one should realise that the situation is probably for a (very) shallow foreshore with extensive breaking, and then Equation 5.2 should be used.

5.2.4 Steep slopes up to vertical walls

Dike slopes are often quite gentle, say gentler than 1:2.5. But seawalls and concrete structures may have steeper slopes. Steep slopes may give large breaker parameters exceeding the range as given in Figure 5.5 and Figure 5.6 for relatively gentle slopes. But the wave run-up will not be as high as in Figure 5.7, which is specifically for (very) shallow foreshores. Due to the work of Victor *et al.* (2012) it is possible to give a good prediction of waver run-up for steep slopes up to vertical walls, at relatively deep water (no very shallow foreshore). This investigation focussed on wave overtopping on very steep slopes and prediction formulae will be given in Section 5.3.3. Those formulae on wave overtopping on very steep slopes can be used to estimate the wave run-up level $R_{u2\%}/H_{m0}$. For these calculations a wave height of $H_{m0} = 3$ m was taken and it was assumed that an overtopping discharge of 1 l/s per m would be quite close to a run-up level of 2%. The required crest level for an overtopping discharge of 1 l/s per m was then taken as $R_{u2\%}$. Calculations were performed for various slope angles.
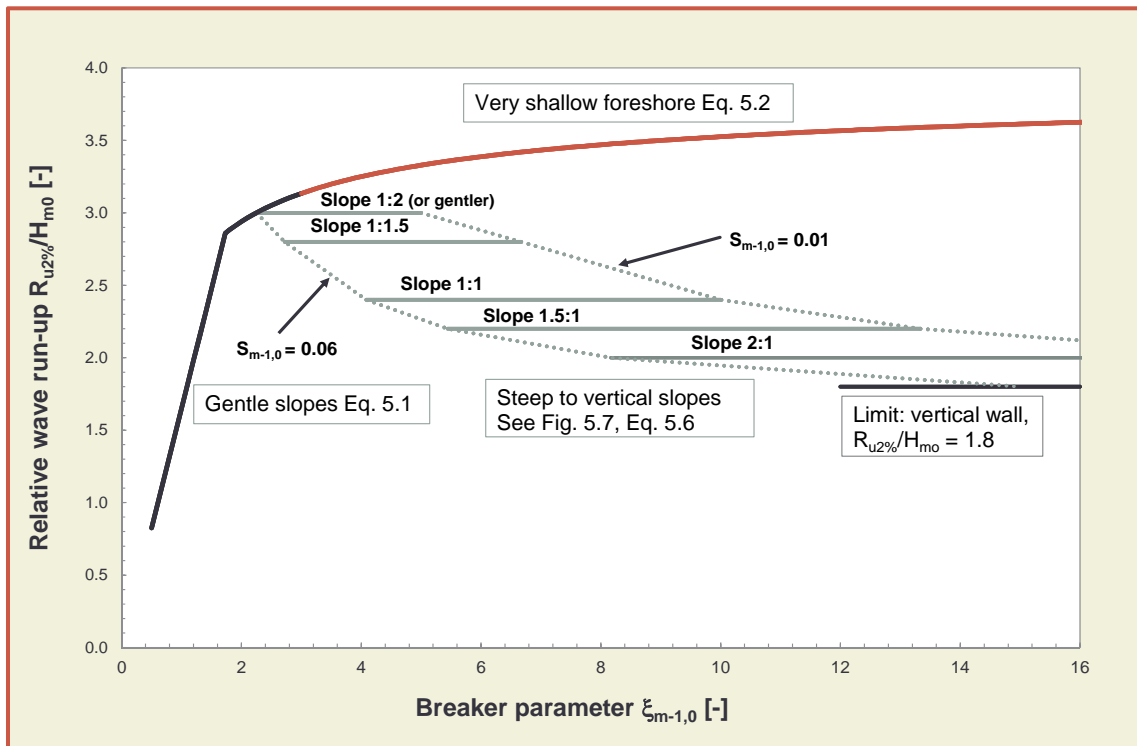
Figure 5.8:   Wave run-up for (very) steep slopes compared to gentle slopes and situations with (very) shallow foreshores – mean value approach. Based on Victor *et al.* (2010)

Figure 5.8 shows Equations 5.1 and 5.2 for relatively gentle slopes and for the situation of (very) shallow foreshores, but it also shows the relative wave run-up (calculated as described above) for slopes of 1:2 and steeper, up to the limit of a vertical wall. Actually, in the zone of surging or non-breaking waves, say $\xi_{m-1,0} > 2$, the wave period or wave steepness has no influence anymore on wave run-up and each slope angle shows a horizontal line. The length of the line is given by the range of wave steepness that was applied: $s_{m-1,0} = 0.01$ to 0.06. The graph shows that a steeper slope gives smaller wave run-up. The relative wave run-up against a vertical wall will be $R_{u2\%}/H_{m0} = 1.8$. Figure 5.8 shows clearly the difference between a (very) shallow foreshore and steep slopes without significant wave breaking on a foreshore, but in both situations large breaker parameters will be found. For application of wave run-up formulae one has to distinguish between the situation of no or limited wave breaking on a foreshore and (very) shallow foreshores.

As steep slopes show no influence of wave steepness on wave run-up it is possible to give a prediction formula that is only based on the slope angle cotα. Figure 5.9 shows the relative wave run-up for steep slopes up to a vertical wall as a function of the slope angle and excluding the influence of a foreshore. The prediction is given by Equation 5.6.

$$\frac{R_{u2\%}}{H_{m0}} = 0.8\cot\alpha + 1.6 \quad \text{with a minimum of 1.8 and a maximum of 3.0} \tag{5.6}$$

Figure 5.9 shows Equation 5.6 together with the 5%-exceedance lines, given by a variation coefficient of σ' = σ / μ = 0.07. For a design and assessment approach, with a partial safety factor of one standard deviation, one should then use Equation 5.7.

$$\frac{R_{u2\%}}{H_{m0}} = 0.86\cot\alpha + 1.71 \quad \text{with a minimum of 1.93 and a maximum of 3.21} \tag{5.7}$$
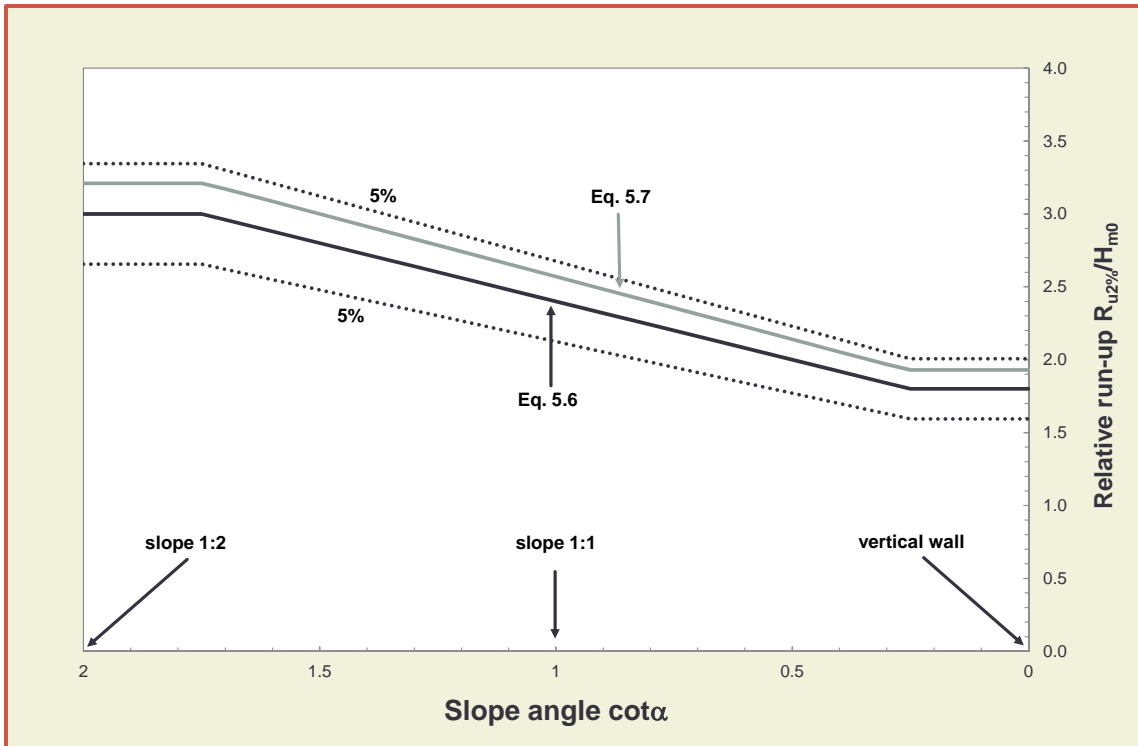
Figure 5.9: Wave run-up for very steep slopes up to vertical walls

The question is: what happens for very steep slopes on very gentle foreshores? The deviation in Figure 5.8 for breaker parameters $\xi_{m-1,0} > 10$ is very large between the curve of (very) shallow foreshores and the curves for the very steep slopes. The difference can be up to a factor of 2 in run-up height, but research has yet to be conducted in this area. The upper curve in the graph was developed for 1:2 and 1:4 slopes at (very) shallow foreshores, but not for steeper slope angles. Still one can imagine that the "very shallow water effect" of infra gravity waves or surf-beat may also increase wave run-up for very steep slopes. Therefore, it is proposed to use this maximum for (very) shallow water (the second part of Equation 5.1) always in the situation of shallow and very shallow water ($s_{m-1,0} < 0.01$), also for very steep slopes. This leads to the decision diagram in Figure 5.10 for wave run-up, which is applicable for the mean value approach. For the design and assessment approach, one should use Equations 5.4, 5.5 and 5.7 instead of Equations 5.1, 5.2 and 5.6.
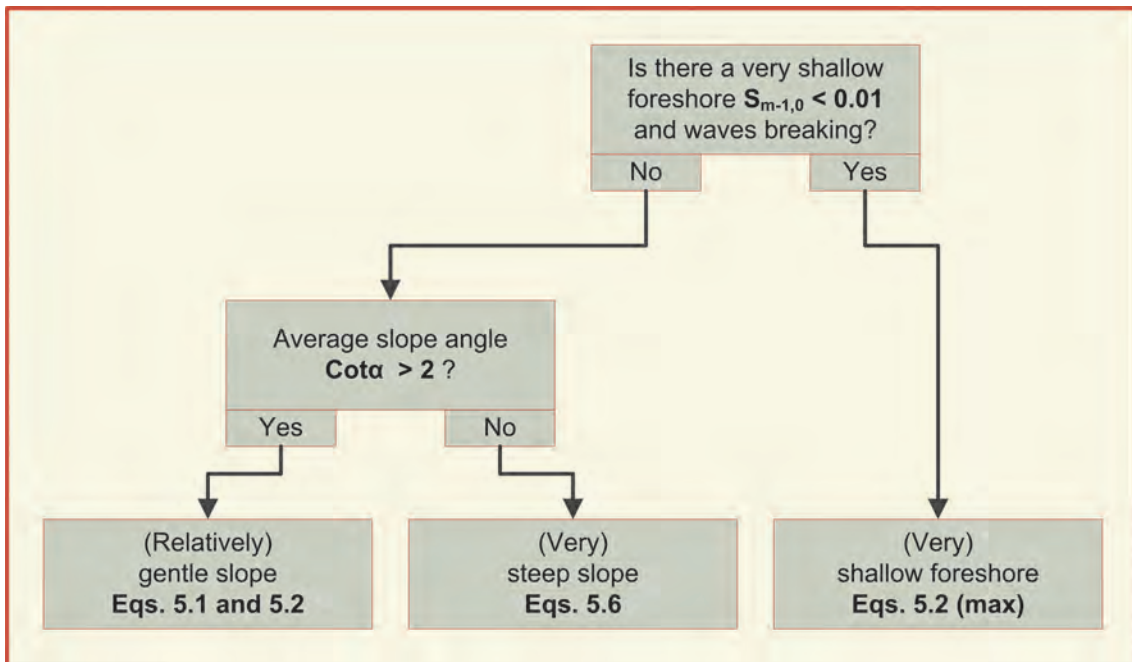
Figure 5.10: Decision diagram for wave run-up (mean value approach)

5.3 Wave overtopping discharges

5.3.1 General formulae

Wave overtopping occurs if the crest level of the dike or embankment seawall is lower than the highest wave run-up level R_{max}. In that case, the freeboard R_c defined as the vertical difference between the still water level (SWL) and the crest height becomes important (Figure 5.4). Wave overtopping depends on the freeboard R_c and increases for decreasing freeboard height R_c. Usually wave overtopping for dikes or coastal embankments is described by an average wave overtopping discharge q, which is given in m^3/s per m width, or in litres/s per m width.

An average overtopping discharge q can only be calculated for quasi-stationary wave and water level conditions. If the amount of water overtopping a structure during a storm is required, the average overtopping discharge has to be calculated for each, more or less constant, storm water level and constant wave conditions.

Many model studies were performed all over the world to investigate the average overtopping discharge for specific dike geometries or wave conditions. For practical purposes, empirical formulae were fitted through experimental model data. It is a long-established established method based on the original work of Owen (1980), that wave overtopping discharge, q, on many kinds of coastal structures generally decreases exponentially as the crest freeboard, R_c, increases, with a general form:

$$\frac{q}{\sqrt{gH_{m0}^3}} = a\exp\left(-b\frac{R_c}{H_{m0}}\right)$$

5.8

where H_{m0} is the spectral significant wave height, and a and b are fitted coefficients. This form of equation has become popular as it gives a straight line on a log-linear graph, and it has only two coefficients for fitting to the data. For sloping structures like dikes, levees or embankments EurOtop (2007) gave two design formulae with the general expression of Equation 5.8.

In the years since publication of EurOtop (2007), some co-authors continued exploration of wave overtopping phenomena and have identified areas of interest in need of further research. The developments have been described in Van der Meer and Bruce (2014). One of the needs for further research was overtopping at very low freeboards.

For sloping structures, overtopping at low and zero freeboard conditions has often been overlooked in physical model studies (perhaps due to the challenges of measurement of very large discharges) but they represent important situations, e.g. in analysis of performance of partially-constructed breakwaters, and of low-freeboard, lower-cost defences. It is clear that familiar, exponential-type formulae, like Equation 5.8, work poorly in these regions as they over-estimate the overtopping discharge.

Analysis has therefore been performed to bring together the conventional exponential formulae with the few reliable datasets including very low and zero freeboard. In doing so, Van der Meer and Bruce (2014) have revisited early Dutch work from the 1970s which offered a continuous prediction extending to zero freeboard. They proposed a curved line in an easy way, as the exponential function is a special case of the Weibull distribution, it is possible to go back to a Weibull-type function and use a fitted shape factor. Such a function looks still very much like Equation 5.8 and is described by:

$$\frac{q}{\sqrt{gH_{m0}^3}} = a \exp\left[-\left(b\frac{R_c}{H_{m0}}\right)^c\right] \quad \text{for } R_c \geq 0 \qquad\qquad 5.9$$

The main difference with Equation 5.8 is the addition of an extra exponent, c and that the equation is valid for the full range of $R_c \geq 0$. The effect of this exponent is that Equation 5.9 will be a curved line on a log-linear graph, except if c = 1 (then Equation 5.9 reverts back to Equation 5.8).
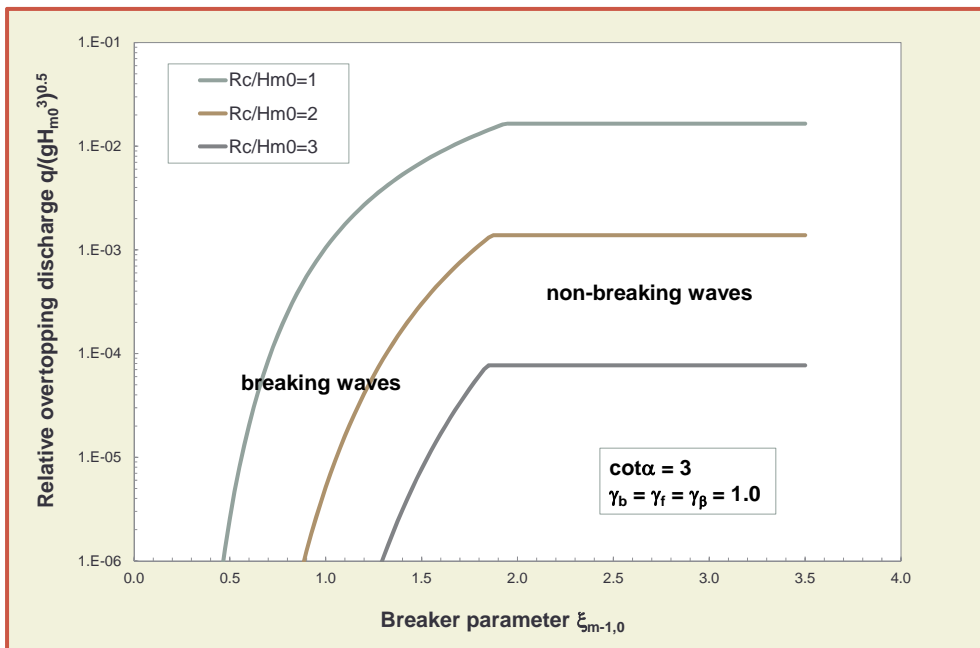
Figure 5.11: Wave overtopping discharge as a function of the breaker parameter $\xi_{m-1,0}$ and for three freeboards

The wave overtopping discharge can be described by two formulae, comparable with wave run-up, one for breaking (plunging) waves on the slope, and one for non-breaking (surging) waves. Also a similar curve can be made as in Figure 5.6, but now with the relative overtopping discharge as a function of the breaker parameter. Figure 5.11 shows the graph for three relative freeboards, where with increasing breaker parameter the wave overtopping discharges increases, until a maximum is reached for non-breaking waves. The graph was made for a smooth plane slope with cotα = 3.

The general formulae for the average overtopping discharge on a slope (dike, levee, embankment) are given by (*mean value approach*):

$$\frac{q}{\sqrt{g \cdot H_{m0}^3}} = \frac{0.023}{\sqrt{\tan \alpha}} \gamma_b \cdot \xi_{m-1,0} \cdot \exp\left[-\left(2.7 \frac{R_c}{\xi_{m-1,0} \cdot H_{m0} \cdot \gamma_b \cdot \gamma_f \cdot \gamma_\beta \cdot \gamma_v}\right)^{1.3}\right]$$

5.10

with a maximum of
$$\frac{q}{\sqrt{g \cdot H_{m0}^3}} = 0.09 \cdot \exp\left[-\left(1.5 \frac{R_c}{H_{m0} \cdot \gamma_f \cdot \gamma_\beta \cdot \gamma^*}\right)^{1.3}\right]$$

5.11

109

Equations 5.10 and 5.11 show quite a number of influence factors: γ_b is the influence factor for a berm [-], γ_f is the influence factor for roughness elements on a slope [-], γ_β is the influence factor for oblique wave attack [-] and γ_v is the influence factor for a wall at the end of a slope. All these influence factors have been described in depth in Section 5.4. Compared to EurOtop (2007), an influence factor γ^* [-] has been added for non-breaking waves (relatively steep slopes) for a storm wall on a slope or promenade. This influence factor γ^* is a combined factor of all kind of geometrical influences and full details will be given in Section 5.4.7.
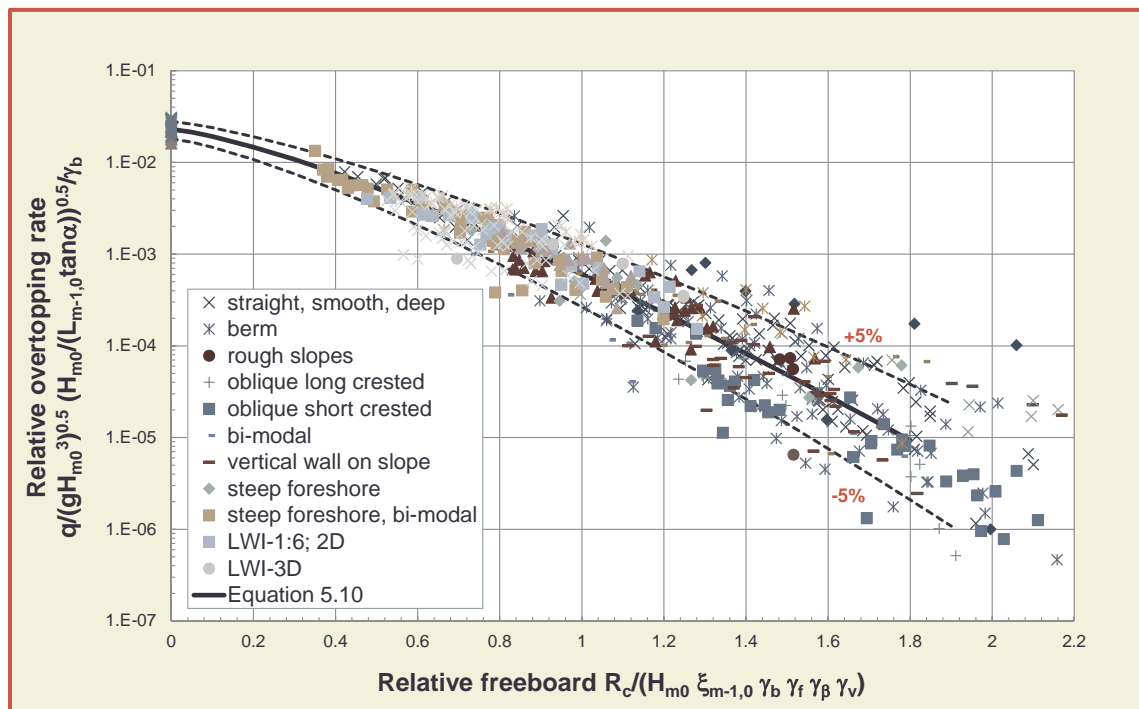
Figure 5.12:   Wave overtopping data for breaking waves and overtopping Equation 5.10 with 5% under and upper exceedance limits (= 90%-confidence band)

Equations 5.10 and 5.11 are given in Figure 5.12 together with measured data for breaking waves from different model tests in small and large scale as well as in wave flumes and wave basins. Note that data in the graph are not all data that exist, as it is mainly the data used to come to the prediction formulae for EurOtop (2007). In addition to the mean prediction line in the graph, the 5% lower and upper confidence limits have been plotted.

Data for non-breaking waves are presented in Figure 5.13 together with measured data, the overtopping formula 5.11 for non-breaking waves and the 5% lower and upper confidence limits. Equations 5.10 and 5.11 give the averages of the measured data (mean value approach) and can be used for predictions and comparisons with measurements.
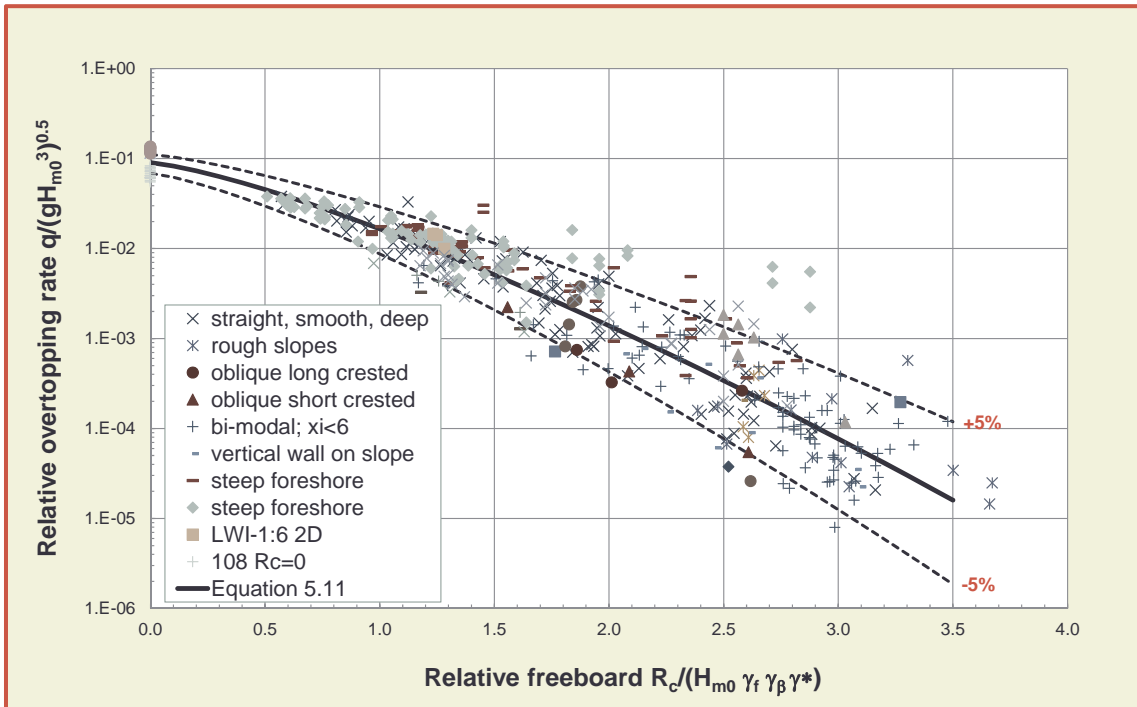
Figure 5.13: Wave overtopping data for non-breaking waves and overtopping Equation 5.11 with 5% under and upper exceedance limits (= 90%-confidence band)

The reliability of Equation 5.10 is given by $\sigma(0.023) = 0.003$ and $\sigma(2.7) = 0.20$, and of Equation 5.11 by $\sigma(0.09) = 0.0135$ and $\sigma(1.5) = 0.15$. For a *design or assessment approach* it is strongly recommended to increase the average discharge by about one standard deviation. Thus, Equations 5.12 and 5.13 should be used in design and safety assessments:

$$\frac{q}{\sqrt{g \cdot H_{m0}^3}} = \frac{0.026}{\sqrt{\tan \alpha}} \gamma_b \cdot \xi_{m-1,0} \cdot \exp\left[-\left(2.5 \frac{R_c}{\xi_{m-1,0} \cdot H_{m0} \cdot \gamma_b \cdot \gamma_f \cdot \gamma_\beta \cdot \gamma_v} \right)^{1.3} \right] \tag{5.12}$$

with a maximum of:
$$\frac{q}{\sqrt{g \cdot H_{m0}^3}} = 0.1035 \cdot \exp\left[-\left(1.35 \frac{R_c}{H_{m0} \cdot \gamma_f \cdot \gamma_\beta \cdot \gamma^*} \right)^{1.3} \right] \tag{5.13}$$

A comparison of the two formulae that give a prediction of the average discharge or *mean value approach* (Equations 5.10 and 5.11) and for the *design and assessment approach* (Equations 5.12 and 5.13) for breaking and non-breaking waves is given in Figure 5.14 and Figure 5.15.

EurOtop (2007) gave overtopping formulae according to Equation 5.8, i.e. a straight line on a log-linear graph, see also Section 4.2.1 where the old and new formulae were given. The application area was for $R_c/H_{m0} > 0.5$, where the new equations in this update of the manual are valid for $R_c/H_{m0} > 0$. The new formulae widen the application area, but are very similar in the area with $R_c/H_{m0} > 0.5$. In order to compare the old EurOtop (2007) and the new formulae, including the effect of the roughness, Figure 5.16 was made for non-breaking waves (Equation 5.11 in this manual with Equation 5.8 in EurOtop (2007), or Equation 4.2 in Section 4.2.1). It is clear that the differences are very small, except in the area $R_c/H_{m0} < 0.5$.

Mathematically speaking, one would expect that due to the exponent $c = 1.3$ in Equation 5.13, the effect of the influence factors would change, as the part within the exponential function becomes different for $c = 1$ (the old formula) and $c = 1.3$ (the new formula). This is indeed true for the same (large) value of R_c/H_{m0}, but the effect of an influence factor is that the curve shifts to the left and remains in the same overtopping range. The actual difference between the old and new formulae is similar with and without an influence

factor different from 1.0, see also Figure 5.16. In Section 4.2.1 the difference was described as follows: for breaking waves the new formulae may give up to 4% more overtopping discharge and up to 30% less than the old formulae. For non-breaking waves it was up to 27% more and also about 30% less for the new formulae. Compared to the reliability of wave overtopping discharge prediction, which is estimated for a confidence band of 90% between a factor 2.5 and up to 20 or more (for very small overtopping) a deviation of up to 30% is small and insignificant.
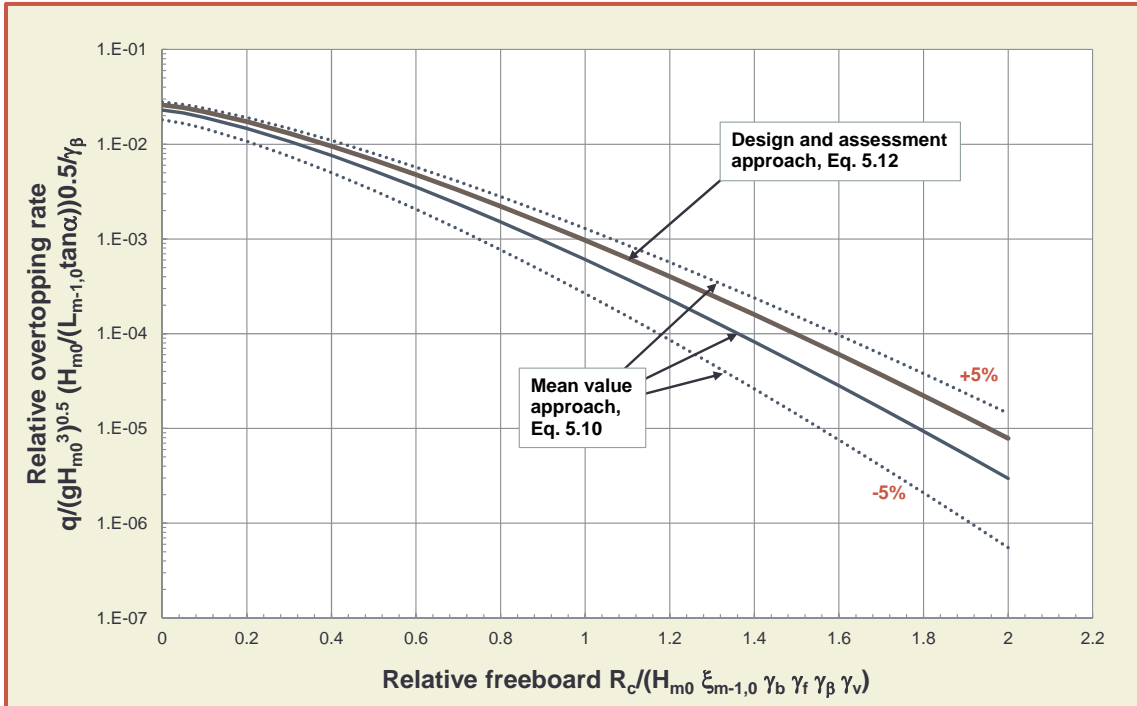
Figure 5.14 : Wave overtopping for breaking waves – Comparison of formulae for *mean value approach* and *design and assessment approach*
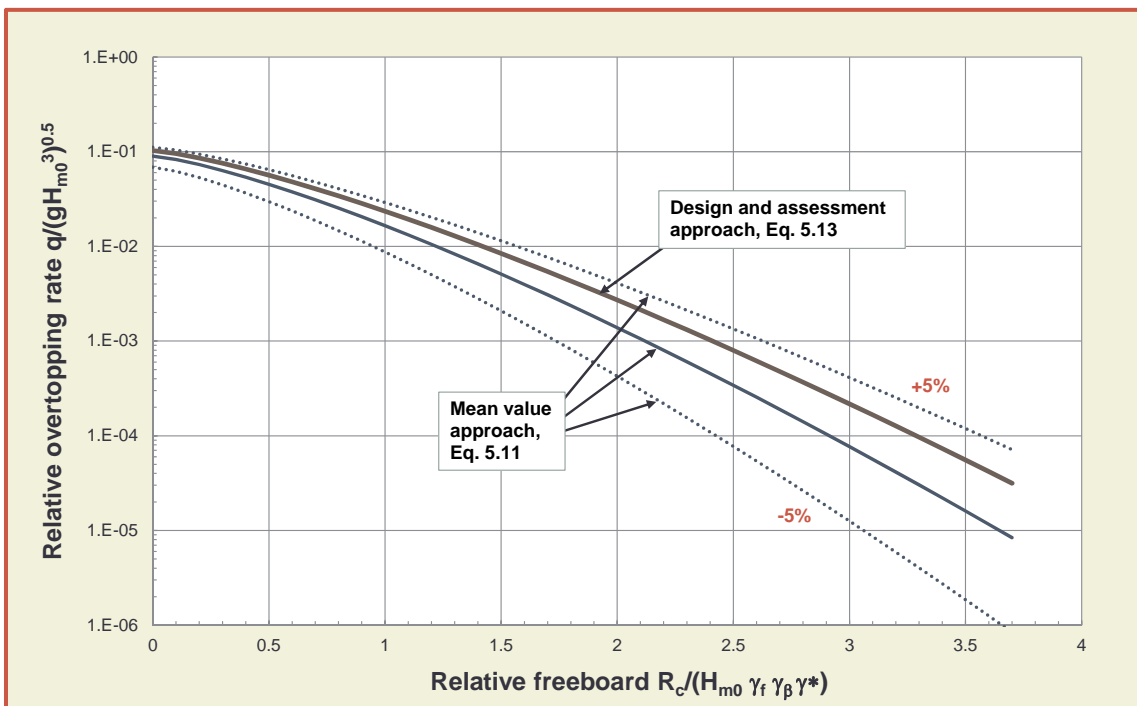
Figure 5.15: Wave overtopping for non-breaking waves – Comparison of formulae for *mean value approach* and *design and assessment approach*
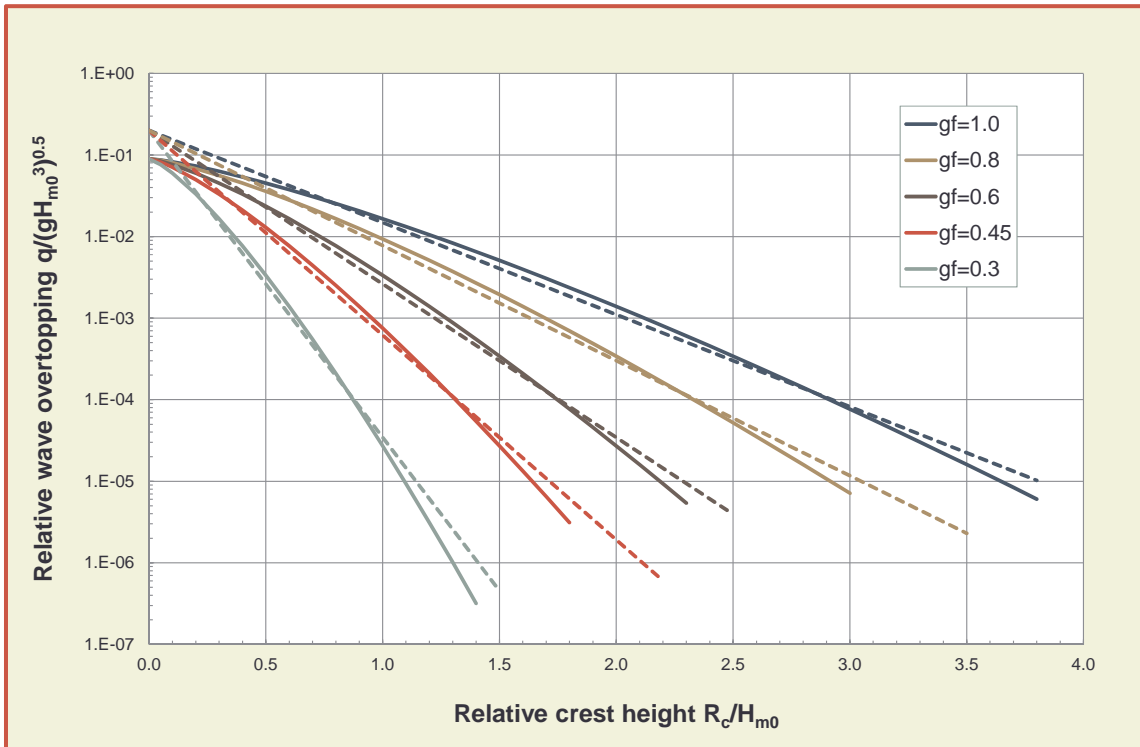
Figure 5.16:   Comparison of Equation 5.11 with the original Equation 5.8 in EurOtop (2007), for various values of the influence factor for roughness

5.3.2 Shallow and very shallow foreshores

In the case of very heavy breaking on a shallow foreshore the wave spectrum is often transformed into a flat spectrum with no significant peak. In that case, long waves are present and influencing the breaker parameter $\xi_{m-1,0}$. In Section 5.2.3 the effect of (very) shallow foreshores on wave run-up has been described and similar effects may be expected for wave overtopping. As described in Section 5.2.3 very shallow foreshores may be present if the wave steepness at the toe of the structure becomes smaller than $s_{m-1,0} < 0.01$. It then generally gives conditions of severe wave breaking (unless it is very low and long swell). As soon as this threshold is exceeded one should realise that the situation is probably for a (very) shallow foreshore with extensive breaking, and then Equations 5.10 - 5.13 should not be used.

Another wave overtopping formula (Equation 5.15 – *mean value approach*) is recommended for shallow and very shallow foreshores to avoid a large underestimation of wave overtopping prediction, using the formulae in Section 5.3.1. Equations 5.10 - 5.13 are roughly valid for breaker parameters $\xi_{m-1,0} < 5$, whereas Equation 5.15 is valid for larger values. In this case also the criterion $s_{m-1,0} < 0.01$ should apply and a check whether waves are indeed breaking and the low wave steepness is not caused by a low long swell. In order to create a continuous approach a linear interpolation is recommended for breaker parameters $5 < \xi_{m-1,0} < 7$. Equation 5.16 gives the *design and assessment approach.*

Equations 5.15 and 5.16 are based on the work of Altomare *et al.* (2016) and are a slight modification with the equations in EurOtop (2007), which was based on the work of Van Gent (1999) only. The area of application was widened to very small water depths near the toe of the sloping structure, even up to zero water depth. The data and equations are shown in Figure 5.17 and are mainly based on foreshore slopes ranging from 1:250 up to 1:35.

The transition from shallow to very shallow foreshores is given when the relative water depth becomes small: if $h_t/H_{m0} \leq 1.5$. In that case one should not take the average slope of the sloping structure (see Section 5.4.6, Figure 5.41 and Figure 5.42), but the average slope between *the point on the foreshore* with a depth of $1.5H_{m0}$ and the run-up level $R_{u2\%}$, see Altomare *et al.* (2016). For the 2% run-up level Equation 5.2 has to be used. This gives the following equation for the average slope for a very shallow foreshore, $\tan \alpha_{sf,}$ assuming one straight slope with cot α without berm:
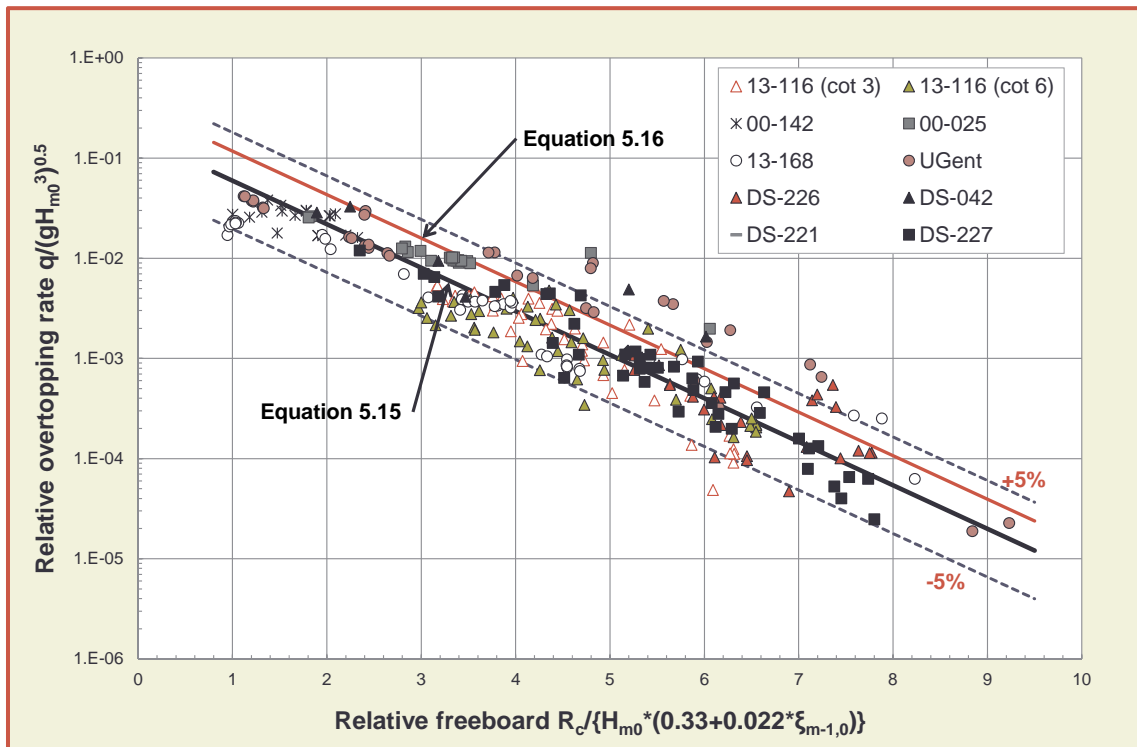
Figure 5.17:   Wave overtopping for (very) shallow foreshore with $\xi_{m-1,0} > 5$ and $s_{m-1,0} < 0.01$. From Altomare *et al.* (2016); see that reference for information on the legend

$$\tan \alpha_{sf} = \frac{\left(1.5H_{m0} + R_{u2\%}\right)}{\left(1.5H_{m0} - h_t\right) \cdot m + \left(h_t + R_{u2\%}\right) \cdot \cot \alpha} \quad \text{if } h_t/H_{m0} \leq 1.5 \qquad 5.14$$

So, for very shallow foreshores, a part of the foreshore is taken as "belonging" to the structure. With this modification one can calculate the adjusted breaker parameter $\xi_{m-1,0}$ and then Equations 5.15 and 5.16 are still valid.

The general formula for wave overtopping at (very) shallow foreshores, with $\xi_{m-1,0} > 7$ and $s_{m-1,0} < 0.01$, is given as *mean value approach* by:

$$\frac{q}{\sqrt{g \cdot H_{m0}^3}} = 10^{-0.79} \cdot \exp\left(- \frac{R_c}{\gamma_f \cdot \gamma_\beta \cdot H_{m0} \cdot (0.33 + 0.022 \cdot \xi_{m-1,0})}\right) \qquad 5.15$$

The exponent -0.79 was derived from measurements and can be considered as a stochastic variable with mean -0.79 and a standard deviation of $\sigma(-0.79) = 0.29$. For a *mean value approach* of wave overtopping through Equation 5.15 one should use -0.79, which gives $10^{-0.79} = 0.16$. For a *design and assessment approach* one should use -0.79 + 0.29 = -0.50, giving $10^{-0.50} = 0.32$, leading to Equation 5.16.

$$\frac{q}{\sqrt{g \cdot H_{m0}^3}} = 10^{-0.50} \cdot \exp\left(- \frac{R_c}{\gamma_f \cdot \gamma_\beta \cdot H_{m0} \cdot (0.33 + 0.022 \cdot \xi_{m-1,0})}\right) \qquad 5.16$$

5.3.3 Steep slopes up to vertical walls

Section 4.2.3 and Figure 4.3 give an overall view of overtopping on various types of structures. Figure 4.4 shows that smooth steep sloping structures with non-breaking wave conditions give largest wave overtopping and this decreases for very steep (battered) and vertical walls. What happens if slopes become steeper than say 1:2 or 1.5? The two boundaries are known: the formula for steep smooth slopes with non-breaking waves (Equation 5.10) and a formula for vertical walls, see Chapter 7. Chapter 7 describes that for vertical walls a distinction has to be made for vertical walls at relatively deep water without an influencing foreshore and walls at the end of a influencing foreshore. Here we consider only vertical walls at relatively deep water, where waves are not (significantly) influenced by a sloping foreshore. The question can be answered quite easily as both situations have been based upon similar equations. For example Equation 5.11 for sloping structures has a fixed exponent c = 1.3, as well as Equation 7.1 in Section 7.3.2 for vertical walls at relatively deep water, without sloping foreshore. The *mean value approach* for the vertical wall is given by:

$$\frac{q}{\sqrt{g \cdot H_{m0}^3}} = 0.047 \cdot \exp\left[-\left(2.35\frac{R_c}{H_{m0} \cdot \gamma_f \cdot \gamma_\beta}\right)^{1.3}\right]$$

5.17

Figure 5.18 gives Equations 5.11 and 5.17 and shows the difference for steep sloping structures with non-breaking waves and a vertical wall. It is clear that if slopes become very steep, up to vertical, the overtopping discharge should decrease (for similar wave conditions).
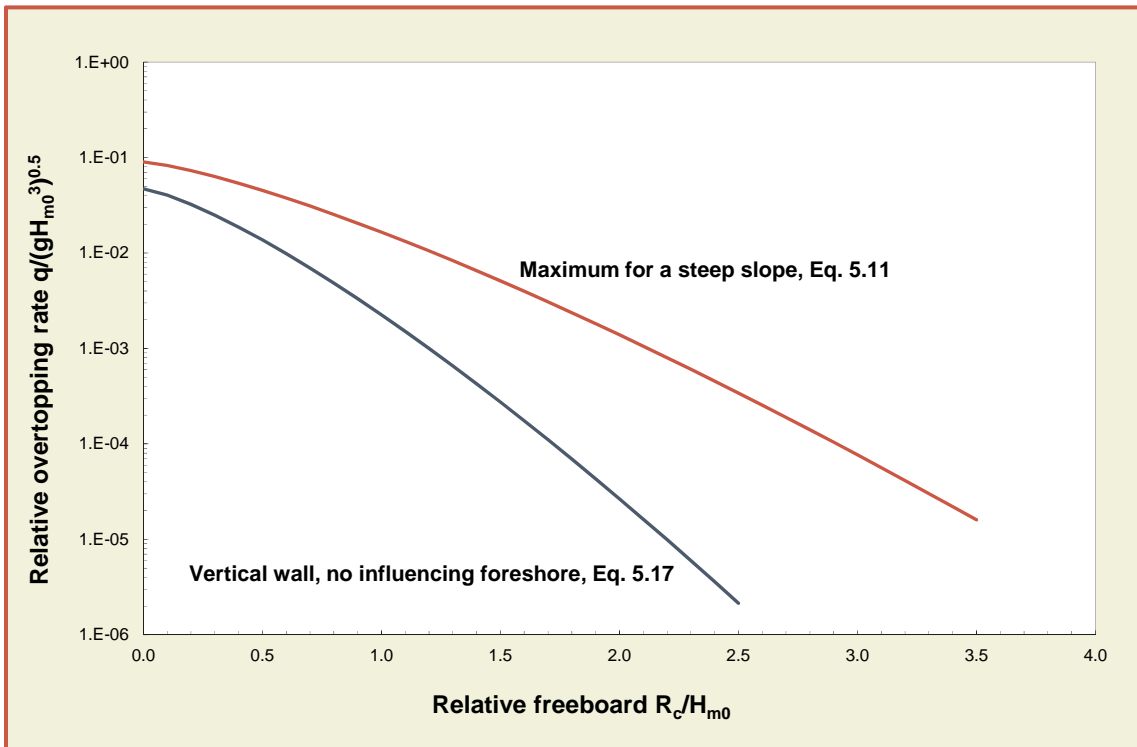
Figure 5.18: Wave overtopping data for vertical walls (see Chapter 7) with Eq. 5.17 and Eq. 5.10 for slopes and non-breaking waves

Equation 5.10, for steep slopes and non-breaking waves, and Equation 5.17 for vertical walls, have the same shape, and only differ in coefficient and exponent. The connecting parameter is the slope angle cot α. Without any data one would probably choose a linear influence to combine Equations 5.10 and 5.17 to one general formula.

Very interesting data by Victor *et al.* (2012) became available, however, with tests on steep and very steep smooth slopes with relatively low freeboards. Tested slope angles ranged from cot α = 0.36 (almost

3V:1H) to cot α = 2.75. Data of some selected slopes have been given in Figure 5.19, together with Equations 5.10 and 5.17, but also with an overall formula that combines these two equations with cot α as the changing parameter. This formula is given in Equation 5.18 and is only applicable for smooth slopes. For this reason γ_f has been omitted in Equation 5.18. The tests by Victor *et al.* (2012) were performed by perpendicular wave attack only, therefore the inclusion of γ_β in the equation is an assumption.

$$\frac{q}{\sqrt{g \cdot H_{m0}^3}} = a \cdot \exp\left[-\left(b\frac{R_C}{H_{m0} \cdot \gamma_\beta}\right)^{1.3}\right] \quad \text{(non-breaking waves)}$$

5.18

a = 0.09 - 0.01 (2 – cot α)$^{2.1}$ for cotα < 2 and a = 0.09 for cotα ≥ 2

b = 1.5 + 0.42 (2 – cotα)$^{1.5}$, with a maximum of b = 2.35 and b = 1.5 for cotα ≥ 2

The reliability of Equation 5.18 can be described by giving a variation coefficient σ' = σ / μ for coefficient a as well as b: σ(a) = 0.15 and σ'(b) = 0.10. Equation 5.18 gives the *mean value approach* of wave overtopping and for a *design or safety assessment approach* one should add one standard deviation. For the two coefficients a and b in Equation 5.18 this means that one should take (1+ σ'(a))•a = 1.15•a and (1- σ'(b)•b = 0.9•b, where a and b are calculated by Equation 5.18. For example Equation 5.18 gives for a slope angle of 2.5:1 (cot α = 0.4): a = 0.632 and b = 2.35. These values should be used for *mean value approach* of the overtopping discharge.
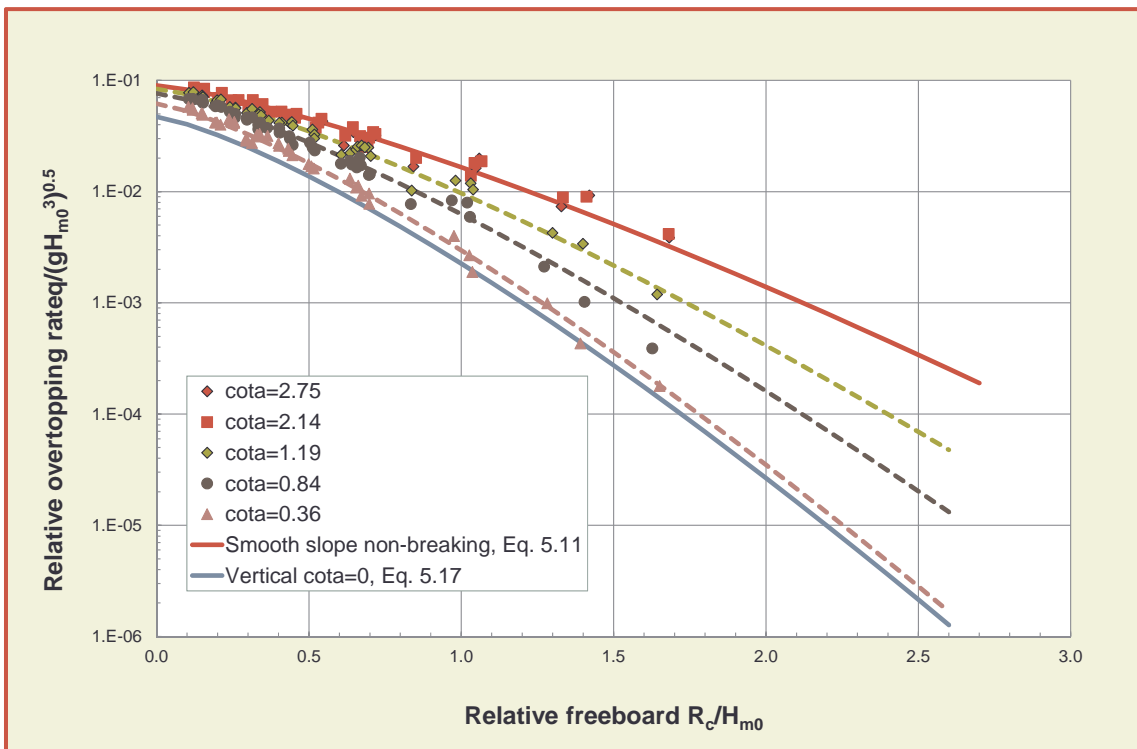
Figure 5.19:   Wave overtopping data for very steep slopes up to vertical with Eq. 5.18 as overall formula

For a *design or assessment approach* one should take a = 1.15•0.632 = 0.727 and b = 0.9•2.35 = 2.115. For a vertical wall, the *design and assessment approach* is given by a = 0.054 and b = 2.11. Note that Equation 5.18 gives a maximum for cot α ≥ 2, where for breaking waves one should of course use Equation 5.10 (or 5.12). Slopes steeper than 1:2 show smaller wave overtopping, although the difference between a slope 1:2 and 1:1.5 will be small.

Another item to discuss relates to the use of influence factors. Influence factors γ_b (influence factor for a berm), γ_f (influence factor for roughness elements on a slope), γ_β (influence factor for oblique wave attack), γ_v (influence factor for a wave wall) and γ^* (combined influence factor for a storm wall on a slope or promenade) will be described in Section 5.4 and are related to gentle and steep slopes. Similar influence factors for a vertical wall are described in Chapter 7.

What about the very steep slopes, up to vertical, in Equation 5.18? If cot α = 2 the influence factors of a slope should be used and for cotα = 0 (vertical wall) this should be the influence factors from Chapter 7. Equation 5.18 only gives γ_β, as only smooth slopes are considered with γ_f = 1. For oblique wave attack the following approach could be considered. For cot α ≥ 1 one should use the γ_β as described in Section 5.4 and for vertical slopes with cot α = 0 the γ_β as described in Section 7.3.5. Interpolation is than recommended between 0 < cot α < 1, as in Equation 5.19:

$$\gamma_\beta\text{(very steep slope)} = \gamma_\beta\text{(vertical wall)} + \cot \alpha \cdot [\gamma_\beta\text{(vertical wall)} - \gamma_\beta\text{(slope)}] \qquad 5.19$$

5.3.4 Negative freeboard

If the water level is higher than the crest of the dike or embankment seawall, large overtopping quantities overflow or overtop the structure. In this situation, the amount of water flowing to the landward side of the structure is composed by a part which can be attributed to overflow ($q_{overflow}$) and a part which can be attributed to overtopping ($q_{overtop}$), see also Figure 5.20. The part of overflowing water can be calculated by the well-known weir formula for a broad crested structure:

$$q_{overflow} = 0.54 \cdot \sqrt{g \cdot \left| - R_c^3 \right|} \qquad 5.20$$

where R_c is the (negative) crest height and $-R_c$ is the overflow depth [m]. The coefficient 0.54 may vary depending on the shape and width of the crest, but gave a fairly good prediction of overflow and overtopping tests on a submerged dike or levee by Hughes and Nadal (2009). Those tests also showed that the effect of wave overtopping becomes negligible as soon as the relative submergence R_c/H_{m0} < -0.3. In that case the overflow is completely governing the process.
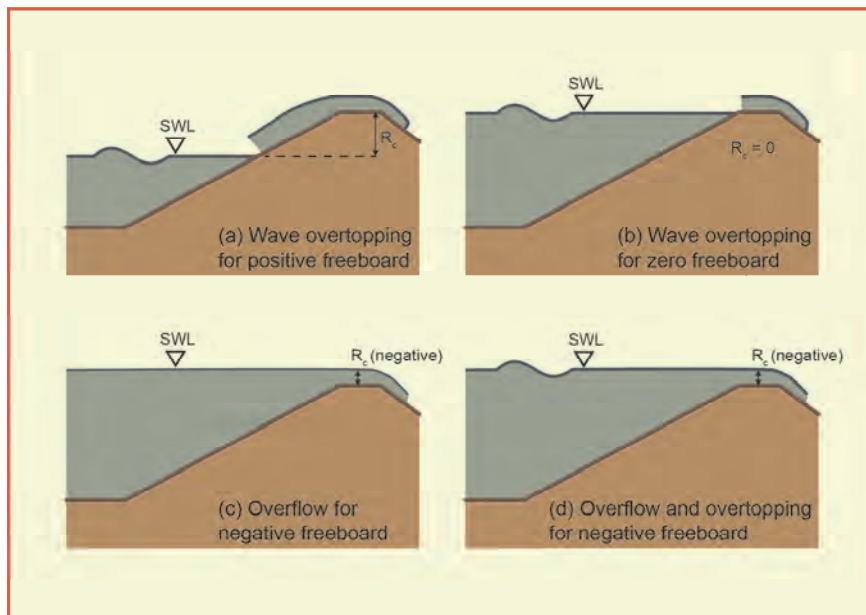
Figure 5.20: Wave overtopping and overflow for positive, zero and negative freeboard

The effect of wave overtopping ($q_{overtop}$) is accounted for by the overtopping discharge at zero freeboard. This depends on the type of structure: for gentle slopes this is Equation 5.10, for the maximum for steep slopes (non-breaking waves) this is Equation 5.11, for a vertical structures it is Equation 5.17 and, finally, for a very steep slope it is the value of "a" in Equation 5.18. The discharge at zero freeboard can be calculated in these equations by using R_c = 0 m, which means that the part with the exponent can be deleted. This discharge should be added to the discharge calculated by Equation 5.20.

5.4 Influence factors on wave run-up and wave overtopping

5.4.1 General

Many of the formulae on wave run-up and wave overtopping in Sections 5.1 to 5.3 include one or more influence factors, like: γ_f = influence factor for roughness elements on a slope; γ_β = influence factor for oblique wave attack; γ_b = influence factor for a berm; γ_v = influence factor for a wall on a slope; and γ^* = combined influence factor for a storm wall on a slope or promenade. This section 5.4 gives values for these influence factors, or methods to derive them. When the influence is not present, the influence factor becomes 1.0. If a certain influence is present, the value of the influence factor becomes smaller than 1.0 and the wave run-up and wave overtopping discharge will decrease. A value smaller than 1 as used in the horizontal axis of Figure 5.12 to Figure 5.15, acts as a virtual increase of the relative freeboard.

The influence factors for roughness and a berm, respectively γ_f and γ_b, are similar for wave run-up and for wave overtopping. Only the influence factor for oblique wave attack, γ_β, differs. The influence factor for wave overtopping is smaller than for wave run-up. The reason is that the wave overtopping discharge is measured as a discharge per m width along the structure and the effective width of oblique wave attack on this metre along the structure decreases with increasing obliquity. The difference is roughly a factor $\cos\beta$.

The general way to establish influence factors is to compare tests with reference tests, for example a smooth straight slope with perpendicular wave attack, or with a well-known formula for that kind of structure. In principal the influence factor is determined, for exactly the same wave conditions and freeboard, as follows:

$$\gamma = \frac{R_{u2\%;\text{influence}}}{R_{u2\%;\text{no influence}}} \quad \text{for wave run-up} \qquad 5.21$$

$$\gamma = \frac{\ln(q_{\text{no influence}})}{\ln(q_{\text{influence}})} \quad \text{for wave overtopping} \qquad 5.22$$

It is not always possible to find the influence factor directly through Equations 5.21 or 5.22, as a requirement is that the wave conditions for both tests should be exactly the same. A more practical way is to compare a fit through one or more test results with a reference curve, like the run-up and overtopping formulae in this chapter with all influence factors equal to 1.0 and with the influence factor as only unknown in the fit through those data points with the influence present.

5.4.2 Effect of roughness

On the seaward side of most seadikes and embankment seawalls there will typically be a grass, asphalt, concrete or natural block revetment systems; as shown in Figure 5.21. Therefore, these types of surface roughness (generally described as smooth slopes) were often used as reference in hydraulic model investigations and the influence factor for surface roughness, γ_f, of these smooth slopes for wave heights greater than about 0.75 m is equal to γ_f = 1.0, or in case of a block revetment sometimes a little smaller.

117

Figure 5.21:   Typical seaward faces of dikes / embankments with (relatively) smooth slopes

The description of possible roughness on a smooth slope in this section is quite extensive. This is partly caused by the investigations that have been performed over a long period of time, as well as recent developments. First investigations were performed to find the influence factors for different types of placed block revetments, that were quite close to smooth slopes. By realising that roughness may have quite an influence on the required crest level of a dike or embankment, quite some research has been performed on artificial roughness, like blocks and ribs on top of existing fairly smooth placed block revetments. But artificial roughness has to be added on a slope, which in practice is not so easy. With the extensive programme in the Netherlands in the past fifteen years on replacing and improving placed block revetments, this has led to new inventions, both by mechanically placement of blocks as well as by invention of new types of block shapes with not only roughness, but also permeability. All of this has been described in this section.
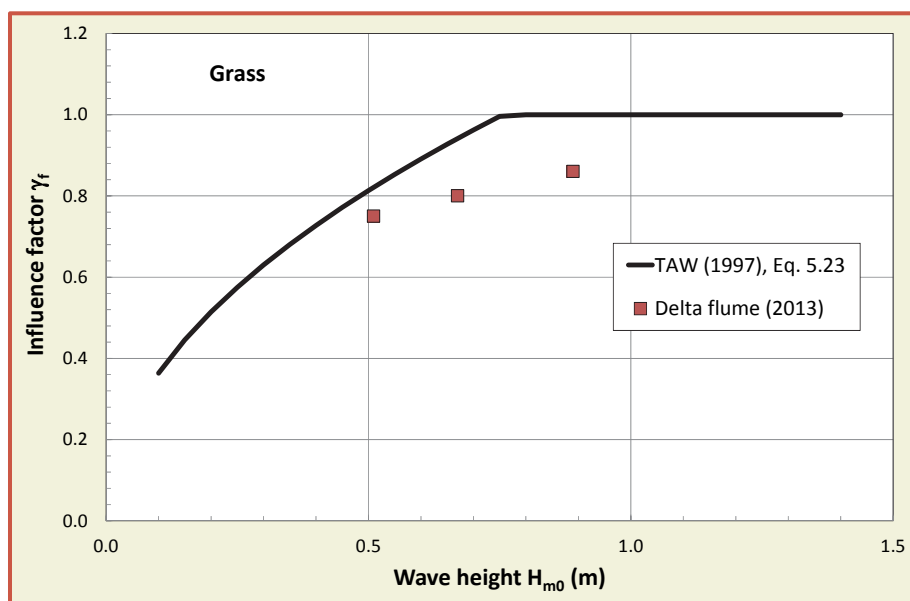
Figure 5.22:   Influence factor for grass surface, compared with measurements in the Delta flume

For significant wave heights H_{m0} less than 0.75 m, grass influences the run-up process and lower influence factors γ_f are recommended by TAW (1997). This is due to the relatively greater hydraulic roughness of

the grass surface for thin wave run-up depths. The relationship given by TAW (1997) is described by Equation 5.23 which is shown graphically in Figure 5.22. During recent tests in Deltares' large Delta flume (Van Steeg, 2014) run-up on a grass slopes was directly compared with run-up on a concrete slope. Those tests showed that there was a clear difference for relatively small waves, smaller than 0.75 m, and are shown in Figure 5.22 below the predictions of Equation 5.23. Nevertheless, to be conservative, it is advised to use Equation 5.23.

$$\gamma_f = 1.15 H_{m0}^{0.5} \text{ for grass and } H_{m0} < 0.75 \text{ m} \qquad\qquad 5.23$$

The effect of larger influence of roughness if the wave height is relatively small, may also be present for other structure types. Table 5.2 gives influence factors for roughness for (relatively) smooth slopes.

Table 5.2: Surface roughness factors for typical embankment revetments

Reference type	γ_f	Figure
Concrete	1.0	
Asphalt	1.0	Figure 5.21b
Closed concrete blocks	1.0	Figure 5.21c
Grass	1.0	Figure 5.21a
Basalt, basalton	0.90	Figure 5.21d
Placed revetment blocks (Haringman, Fixtone)	0.90	Figure 5.21d

Figure 5.23:   Performance of roughness elements showing the degree of turbulence

Roughness elements on slopes can be used to increase the surface roughness and to reduce the wave run-up height and the wave overtopping rate with as main objective to reduce the design crest height. Roughness elements may influence the wave run-up as well as the wave run-down process, and Figure 5.23 shows the influence of artificial roughness elements on the turbulence. Roughness elements are applied either across the entire slope or for parts of the slope which should be considered during the calculation process. Available data on the influence of surface roughness on wave run-up and wave overtopping are based on model tests at small, but if possible at large scale, in order to avoid scale effects. A summary of typical types of surface roughness, as investigated in the 1990's, is given in Table 5.2 and more detailed information is given below. Recent developments on roughness at placed block revetments in the Netherlands are given in the next section.

The efficiency of artificial roughness elements on embankments, such as blocks or ribs (or battens), depends on the width of the block or rib f_b, the height of the blocks f_h and the distance between the ribs f_L, see Figure 5.24. The optimal ratio between the height and the width of the blocks was found to be f_h/f_b = 5 to 8 and the optimal distance between ribs is f_L/f_b = 7. When the total surface is covered by blocks

or ribs and if the height is at least $f_h/H_{m0} = 0.15$, then the following minimum influence factors are found for the following three examples of artificial roughness, with examples shown in Figure 5.25:

Block, 1/25 of total surface covered $\quad\quad\quad \gamma_{f,min} = 0.85$

Block, 1/9 of total surface covered $\quad\quad\quad \gamma_{f,min} = 0.80$

Ribs, $f_L/f_b = 7$ apart (optimal) $\quad\quad\quad \gamma_{f,min} = 0.75$
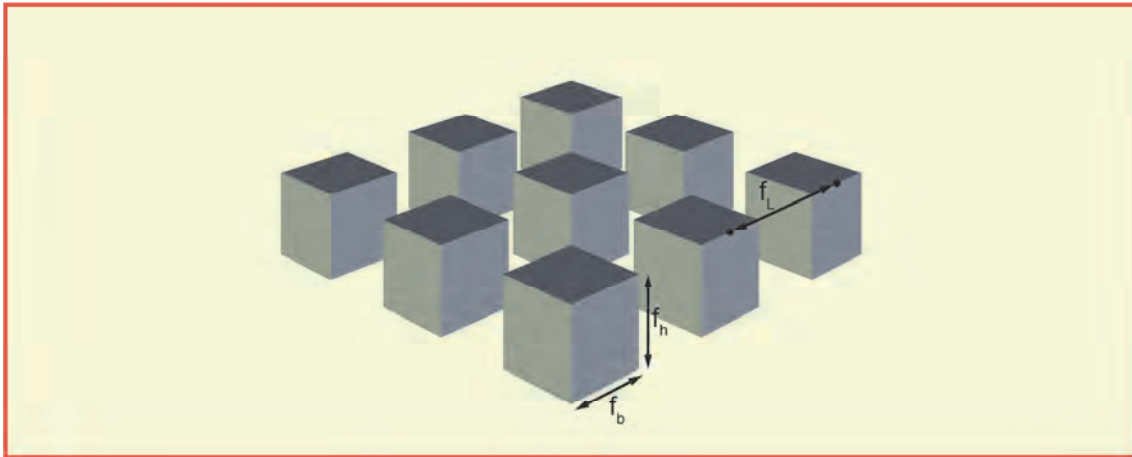
Figure 5.24: Dimensions of artificial roughness elements

A block or rib height than greater $f_h/H_{m0} = 0.15$ has no further reducing effect. If the height is less, then an interpolation is required:

$$\gamma_f = 1 - (1 - \gamma_{f,min}) \cdot \left(\frac{f_h}{0.15 \cdot H_{m0}} \right) \quad \text{for: } f_h/H_{m0} < 0,15 \qquad\qquad 5.24$$

In the Delta flume another option was tested, where revetments consisted of blocks of 0.50 m by 0.50 m, and in another one quarter of the blocks were placed 0.088 m above the surface, see Figure 5.25 upper and lower left, respectively. The influence factor for roughness was found to be $\gamma_{f,min} = 0.90$, which appeared to be less effective than smaller blocks. Figure 5.25 shows on the right side testing of artificial blocks on small scale (upper picture) and preparation of a slope with ribs (lower picture). An example of ribs in practice is given in Figure 5.26 and an overall view of influence factors for artificial roughness elements is given in Table 5.3.

Table 5.3: Influence factors for artificial roughness elements on a smooth slope

Reference type	γ_f	Figure
Small blocks over 1/25 of surface, optimum height	0.85	Figure 5.25a
Small blocks over 1/9 of surface, optimum height	0.80	Figure 5.25b
¼ of revetment blocks 8.8 cm higher	0.90	Figure 5.25c
Ribs (optimum dimensions)	0.75	Figure 5.25d

The influence factors for roughness elements apply for $\gamma_b \xi_{m-1,0} < 1.8$, increasing linearly up to 1.0 for $\gamma_b \xi_{m-1,0} = 10$ and remain constant for greater values. For more explanation see Chapter 6; specifically Section 6.2 and Figure 6.3; where discussion concerning influence factors for roughness for rock and concrete armour layers can be found.
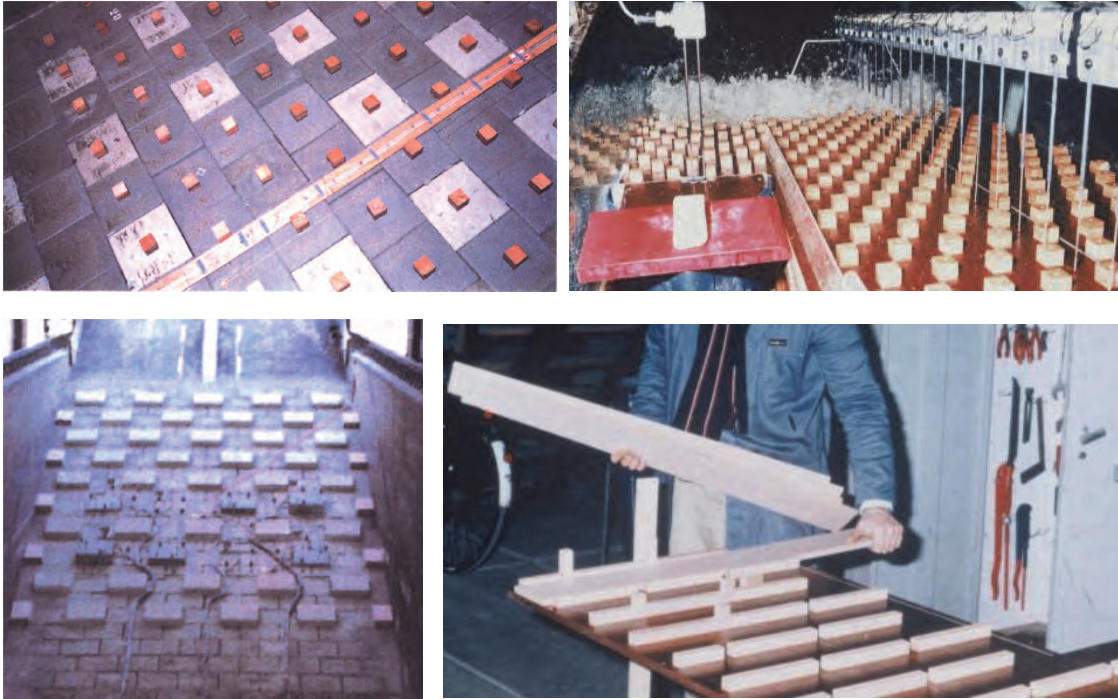
Figure 5.25:   Artificial roughness by blocks and battens or ribs. Fig. a: blocks covering 1/25 of surface;
Fig. b: blocks covering 1/9 of surface; Fig. c: blocks 8 cm higher for ¼ of surface;
Fig. d: preparing battens or ribs on smooth surface for testing

Figure 5.26:   Example of battens or ribs in reality

As already mentioned, roughness elements are mostly applied for parts of the slope. Therefore, a reduction factor is required which takes only this part of the slope into account. It can be shown that roughness elements have little or no effect 0.25 $R_{u2\%,smooth}$ below the still water line or 0.50 $R_{u2\%,smooth}$ above the still water line. The resulting influence factor γ_f is calculated by weighting the various influence factors $\gamma_{f,i}$ and by including the lengths L_i of the appropriate sections i in between SWL-0.25·$R_{u2\%smooth}$ and SWL+0.50·$R_{u2\%smooth}$ as follows:

$$\gamma_f = \frac{\sum_{i=1}^{n} \gamma_{f,i} \cdot L_i}{\sum_{i=1}^{n} L_i} \qquad\qquad 5.25$$

It appears that roughness elements applied only under water (with a smooth upper slope) have no effect and, in such a case, should be considered as a smooth slope. For construction purposes, it is recommended to restrict roughness elements to their area of influence. The construction costs will be less than covering the entire slope by roughness elements. As a final point to be considered, the effect of roughness elements on wave run-up may be reduced by debris accumulating between the elements.

5.4.3 Recent developments on roughness for placed block revetments

In the Netherlands many seaward faced dike protections have been improved in the past fifteen years and still quite a number have to be improved in the near future. The originally smooth protections as partly in Figure 5.1 and Figure 5.2 and all examples in Figure 5.21, do not reduce wave run-up and overtopping much. Not only the protection had to be improved, but also in many cases the wave overtopping had to be reduced. For this reason new systems of placed block revetments have been developed with as main objectives that they should be placed easily on large surfaces and that they should reduce wave run-up and overtopping. Two different systems will be described here. The first system is partly open and has porosity within the revetment. The second system is placed with a pattern of different thickness, creating roughness in this way.

Figure 5.27, Figure 5.28 and Figure 5.29 give three new types of block revetments. They all have the property to absorb some of the up-rushing water and to dissipate some of the wave energy that is rushing up the slope of a dike. The open volume per square meter protection, $d_{channel}$, determines the porosity of the protection. It is emphasized that only the hollow sections around the 'neck' of the block are taken into account and not the volume around the 'toe' or the 'head' of the block. An important condition for this approach is that the openings in the head of the blocs are large enough to allow the wave run-up tongue to enter the channels.

Figure 5.27: Impression of Hillblocks®. Left: type 'Slim', middle: type 'Basic', right: during placing procedure on a dike. Courtesy Deltares

Figure 5.28: Impression of RONA®Taille. Left and middle: single element. Right: placing pattern seen from above. Courtesy Deltares
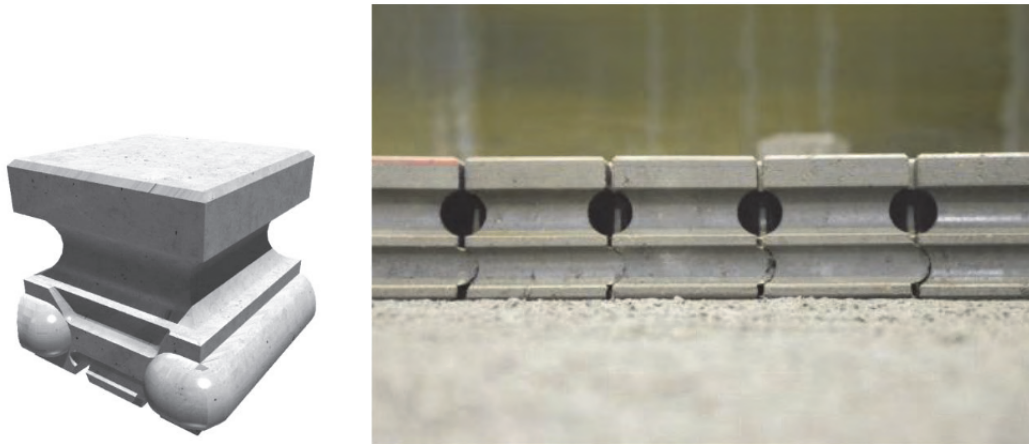
Figure 5.29: Impression of Verkalit® GOR. Left: single element. Right: placed in a pattern. Courtesy Deltares

In describing the effectiveness of the system on wave run-up and overtopping, the dimensionless form $H_{m0}/d_{channel}$ will be used. The thickness of the revetment determines the stability of the protection against wave attack. That thickness should be applied up to the crest level of the dike. One may want to reduce the thickness of the protection further up the slope, as wave forces will be less there, but then the effectiveness with respect to wave run-up and overtopping will reduce. In that case $H_{m0}/d_{channel}$ will become larger, resulting in a larger influence factor.

The influence factors of the systems described above on wave run-up and overtopping have been determined by Van Steeg *et al.* (2016) through tests in the large Delta flume of Deltares. The final results, with influence factor versus $H_{m0}/d_{channel}$ are given in Figure 5.30. Taking all results together there is a clear tendency that the influence factor increases (is less effective) with larger $H_{m0}/d_{channel}$. Within one system this was not always the case, as then some trends are more or less horizontal.
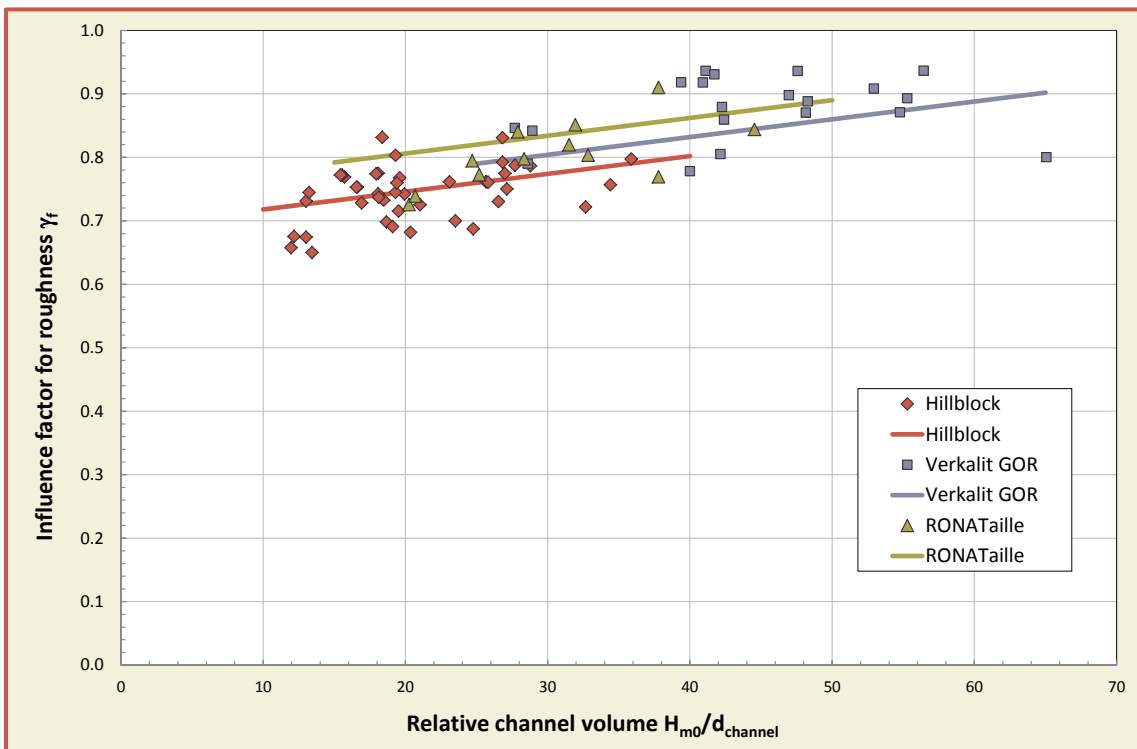
Figure 5.30: Influence factor of roughness/porosity as function of the dimensionless channel volume for open placed block revetments

The influence factor for these three systems can be described by:

$$\gamma_f = 0.0028 H_{m0}/d_{channel} + f \qquad\qquad 5.26$$

with f = 0.69, 0.72, and 0.75 for respectively Hillblock®, RONA®Taille, and Verkalit® GOR. The tests showed that the influence factor for wave overtopping might increase a little if the overtopping becomes relatively large (say $q/(gH_{m0}^3)^{0.5} > 3.2.10^{-4}$). This is in agreement with the effect that was found for grass, see Figure 5.22, where small wave height gave lower run-up.

Another type of system to reduce wave run-up and overtopping, that was developed recently in the Netherlands, was placement patterns with higher and lower surfaces of blocks, in a chessboard pattern (Figure 5.31) or in a rib pattern (Figure 5.32). Each area of 4 by 4 units is placed mechanically in one move. Due to the different heights a kind of roughness has been created, not porosity as in the examples described before. Tests were performed at small scale and the test set-up is shown in Figure 5.33.

Figure 5.31: Chessboard pattern produced with two thicknesses of placed block revetments. The roughness has only been placed in the run-up zone, above the wide asphalt berm

Figure 5.32: Rib pattern produced with two thicknesses of place block revetments. Each area of 4 by 5 units is placed mechanically in one move. Courtesy Projectbureau Zeeweringen

Figure 5.33: Testing block pattern on a scale of 1:22. Courtesy Deltares

124

The results of the tests on a chessboard and rib pattern can be summarised as follows:

- The chessboard and rib patterns have f_L/f_h = 6-10 and f_h/H_{m0} = 0.08-0.19;
- Chessboard and rib patterns have similar roughness if they have similar geometry, ie. height and distance in the pattern;
- A fully covered slope gives γ_f = 0.73;
- If the coverage is only above SWL, γ_f = 0.77;
- If the coverage is only around SWL, γ_f = 0.83;
- If the height of the pattern is 50% higher the influence factor reduces by 0.03.

5.4.4 Effect of oblique waves

Wave run-up and wave overtopping can be assumed to be equally distributed along the longitudinal axis of a dike. If this axis is curved, wave run-up or wave overtopping will certainly increase for concave curves; with respect to the seaward face; due to the accumulation of wave run-up energy. Similarly, wave run-up and overtopping will decrease for convex curves, due to the distribution of wave run-up energy. Recently an experimental investigation has been performed concerning the influence of a curved dike axis and the spatial distribution of wave run-up and wave overtopping. This HYDRALAB-project CornerDike has not yet been analysed to its fully, but initial results are given by Pohl *et al.* (2014).

Only limited research is available on the influence of oblique wave attack on wave run-up and wave overtopping due to the complexity and the high costs of model tests in wave basins. Most of the relevant research was performed on the influence of long crested waves and only few investigations are available on the influence of short-crested waves (see Figure 5.34) on wave run-up and wave overtopping.

Figure 5.34: Short-crested waves resulting in wave run-up and wave overtopping (photo: Zitscher)

Long crested waves have no directional distribution and wave crests are parallel and of infinite width. Only swell coming from the ocean can sometimes be regarded as a long crested wave. In nature, storm waves are short crested. This means, that wave crests are not parallel, the direction of the individual waves is scattered around the main direction and the crests of the waves have a finite width. The directional spreading might be characterized by the directional spreading width σ or the spreading factor s. Relations between these parameters are given by Equation 5.27. The directional spreading width is $\sigma = 0°$ (s = ∞) for long crested waves.

$$s = \frac{2-\sigma^2}{\sigma^2} \text{ or: } \sigma = \sqrt{\frac{2}{s+1}}$$

5.27

The angle of wave attack β is defined at the toe of the structure after any transformation on the foreshore by refraction or diffraction as the angle between the direction of the waves and the perpendicular to the long axis of the dike or revetment as shown in Figure 5.35. Thus, the direction of wave crests approaching parallel to the dike axis is defined as β = 0° (perpendicular wave attack).
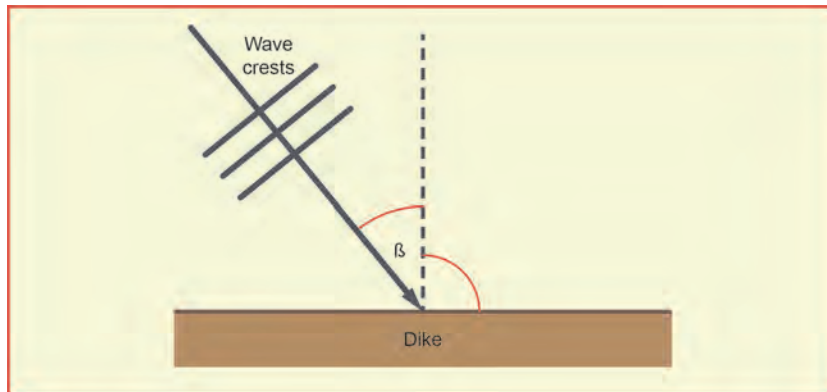
Figure 5.35: Definition of angle of wave attack β

The influence of the wave direction on wave run-up or wave overtopping is defined by an influence factor γ_β. As described in Section 5.4.1, the influence factor for oblique wave attack differs for wave run-up and wave overtopping. The reason is that the effective width of oblique waves approaching one metre width along the dike or structure (the way overtopping discharge is measured), reduces for increasing obliquity. The influence factor also differs for long-crested and short-crested waves.

For practical purposes, it is recommended to use the following expressions for short-crested waves to calculate the influence factor γ_β for *wave run-up*:

$$\gamma_\beta = 1 - 0.0022|\beta| \quad \text{for:} 0° \leq \beta \leq 80° \text{(short-crested waves)}$$
$$\gamma_\beta = 0.824 \quad \text{for:} |\beta| > 80°$$

5.28

and for *wave overtopping*:

$$\gamma_\beta = 1 - 0.0033|\beta| \quad \text{for:} 0° \leq \beta \leq 80° \text{(short-crested waves)}$$
$$\gamma_\beta = 0.736 \quad \text{for:} |\beta| > 80°$$

5.29

Equations 5.28 and 5.29 are shown graphically in Figure 5.36. In special cases one could use the influence factor for long-crested waves. This might be for comparison with other test results, obtained with long-crested wave attack, or if really long swell is present that looks like long-crested waves. In such cases Equation 5.30 can be applied, which gives the influence factor for wave overtopping with long-crested waves. In general it can be said that the curves for short-crested waves, Equations 5.28 and 5.29, are based on limited research, but the range of angles of wave attack tested was from β = 0° - 80°. The curve for long-crested waves, Equation 5.30, was based on at least four independent investigations and can be regarded as quite reliable, see Van der Meer (2010). The application is of course limited as the assumption of long-crested waves will not always be valid.

$$\gamma_\beta = \cos^2(|\beta| - 10°) \text{ with a minimum of } \gamma_\beta = 0.6 \text{ (long-crested waves)}$$
$$\gamma_\beta = 1 \text{ for } |\beta| = 0° \text{ - } 10°$$

5.30

For wave directions 80° < |β| ≤110° waves are diffracted around the structure and an adjustment of the wave height H_{m0} and the wave period $T_{m-1,0}$ are recommended:

$$H_{m0} \text{ is multiplied by } \frac{110-|\beta|}{30} \quad \text{ and } T_{m-1,0} \text{ is multiplied by } \sqrt{\frac{110-|\beta|}{30}} \qquad 5.31$$

This reduces run-up and overtopping linearly to zero for β = 80° to 110°, the latter being 20° offshore. For wave directions between 110° < |β| ≤180° wave run-up and overtopping are set to $R_{u2\%} = 0$ and q = 0.

No significant influence of different spreading widths s (s = ∞, 65, 15 and 6) was found in model tests. As long as some spreading is present, short-crested waves behave similarly and independently of the spreading width. The main point is that short-crested oblique waves give different wave run-up and wave overtopping than long-crested waves.
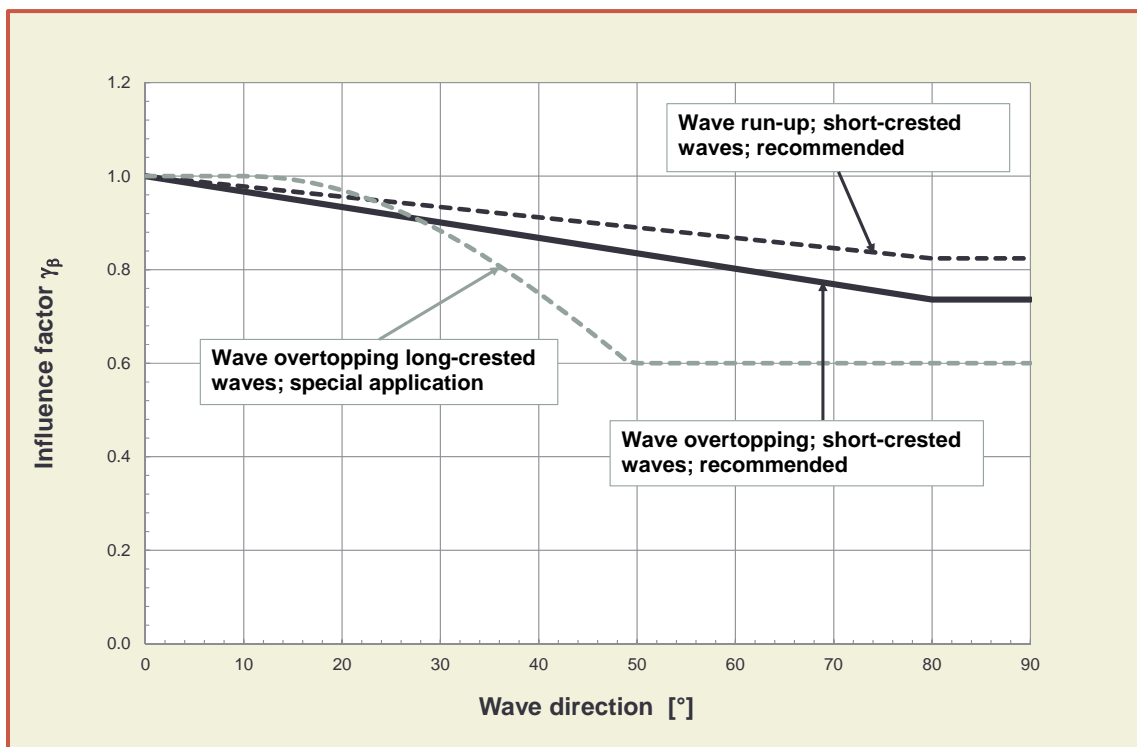
Figure 5.36:   Influence factor γ_β for oblique wave attack and short crested waves, measured data are for wave run-up

5.4.5 Effect of currents

Often the influence of currents on wave overtopping can be neglected, but in some cases currents may exist along the dike or structure during wave conditions where wave overtopping could be expected. This could be due to tides and storm surges, although the peak of the water level often coincides with slower currents. Another example may be a river with extreme discharge and very high water levels, together with a storm. The water level may be close to the crest level, where the storm may generate relatively small waves under an angle with the dike and with the direction of the current, which could cause wave overtopping. The question is then: how does the current influence the wave overtopping?

The EU-project FlowDike was performed to get an answer on that question. The overall report of the project is given by Lorke *et al.* (2012) and the in depth analysis of the influence of currents on wave overtopping in Van der Meer (2010). Currents were generated in a canal and waves were generated with angles of 45° against the current up to 45° along with the current and a number of wave angles in

between. Wave overtopping was measured in two investigations, one on a 1:3 slope and one on a 1:6 slope.

The first conclusion was that if currents are not too strong, the effect of currents on wave overtopping can be given by the influence of the angle of wave attack only, without considering the current. Any effect disappeared in the scatter by applying Equation 5.30 (long-crested waves only were used in the FlowDike project to determine the effects of currents). For stronger currents effects on overtopping were noticed. It is not an easy theory to describe the effect of currents, and it is therefore valuable to give a threshold where below that the simpler method could be used (applying Equations 5.28 or 5.29, without considering current effect) and where above this threshold the guideline in the remainder of this section should be followed.

The investigation was performed with wave heights roughly between 0.1 and 0.15 m. The currents generate were 0, 0.15, 0.3 and 0.4 m/s. Significant influence was found for the highest current of 0.4 m/s and a little less for 0.3 m/s. Taking wave heights during a storm at high river discharges around 0.5 to 1 m, the threshold for the influence of currents on wave overtopping would be around 0.7 to 0.8 m/s and effects would certainly be significant for currents exceeding 1 m/s. For sea dikes with an assumed wave height of 2 m, the threshold would become about 1 m/s with significant influences for currents larger than 1.5 m/s. Based on these elaborations, the following thresholds for the influence of currents on wave overtopping can be formulated:

> For wave heights $H_{m0} = 0.5 - 1$ m: effects of current starts for U > 0.75 m/s
>
> For wave heights $H_{m0} \sim 2$ m: effects of current starts for U > 1 m/s   5.32
>
> Below the thresholds, Equations 5.28 or 5.29 above can be used.

Currents may change the wave height, wave period and angle of energy towards the dike slope. The wave height was measured in the model at the toe of the dike. The *relative* wave period, measured going along with the current, will be different from the *absolute* wave period, which is the wave period measured in a fixed point, like with a wave gauge. Relative wave periods become shorter if the waves are against the current and longer when they are along with the current. It was analysed whether the influence of currents on wave overtopping could (partly) be described by using this relative wave period. It turned out that this resulted in large influences for waves against fairly high currents. The wave periods and wave steepnesses to be used were also out of the physical range (too short periods and too large steepnesses). For this reason the influence of change of relative wave period was not taken to describe the influence of currents on wave overtopping, but the usual absolute wave period.

Another effect is the change of direction of wave energy, β_e. Some wave energy will travel along the wave crest. Including the angle of wave energy instead of the generated wave angle resulted in a strong influence for the largest generated currents. As it might well be the case that actual currents are a little smaller near and on the slope of the dike than in the channel, river or sea, there is good reason to decrease the influence of the angle of wave energy a little. Arbitrarily a combined wave angle of $0.5(\beta + \beta_e)$ was chosen and this gave good results for the 1:3 slope as well as the 1:6 slope. Figure 5.37 gives all test results. The reliability in Figure 5.37 can be described by a standard deviation of $\sigma(\gamma_\beta) = 0.045$. Therefore, the influence of currents above the threshold in Equation 5.32 on wave overtopping can be described by using the combined wave angle $0.5(\beta + \beta_e)$ in existing formulae for the effect of angle of wave attack, such as Equations 5.28 or 5.29. The method to come to the angle of wave energy β_e is given below.

For a more in depth description of the influence of currents on waves one is referred to Holthuijsen (2007), and the following is partly from there. The absolute frequency $\omega = 2\pi/T_{m-1,0}$ is a function of the wave number $k = 1/L$ and the current velocity in the wave direction U_n.

> $$\omega = (g\,k\,\tanh(kd))^{0.5} + k\,U_n \qquad\qquad 5.33$$
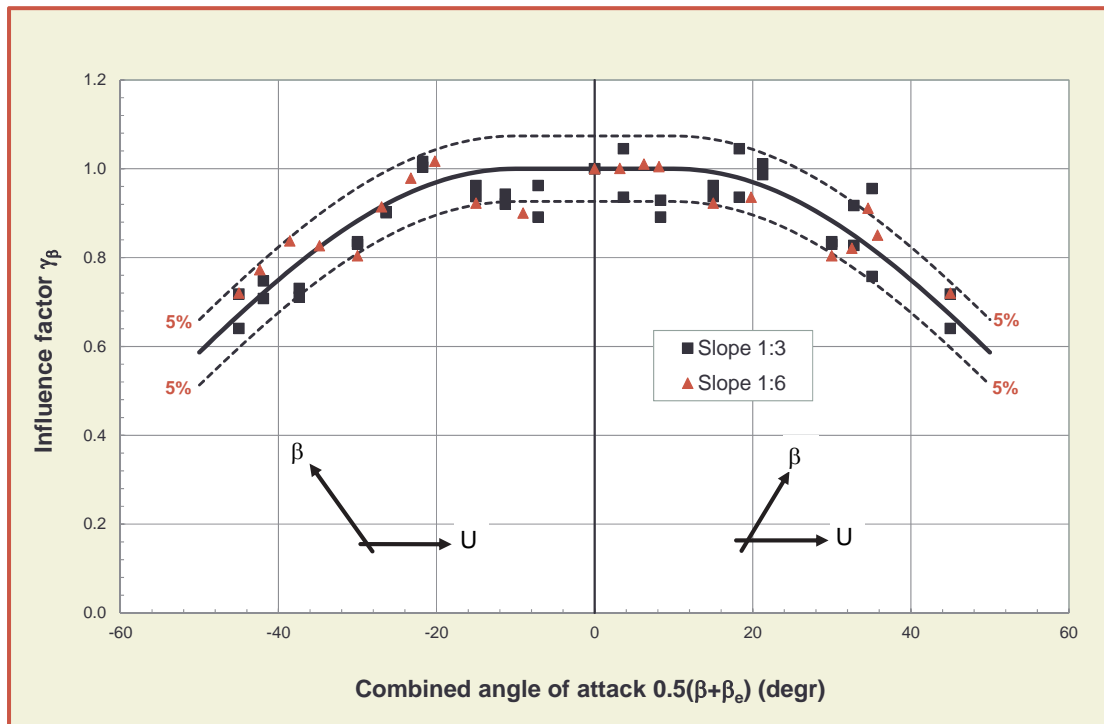
Figure 5.37: Results on the influence of currents and oblique wave attack on wave overtopping, by using the combined angle of wave attack $0.5(\beta + \beta_e)$ in Equation 5.30

where $\omega = 2\pi/T_{m-1,0}$ is the absolute frequency, $k = 2\pi/L$ is the wave number, L the local wave length, d the water depth and U_n the current component normal to the wave crest. The current in the tests was along the dike and with oblique wave attack U_n can be calculated as shown in Figure 5.38:

$$U_n = U \sin\beta$$

5.34

where β = angle of wave attack ($\beta = 0°$ for waves perpendicular to the structure)
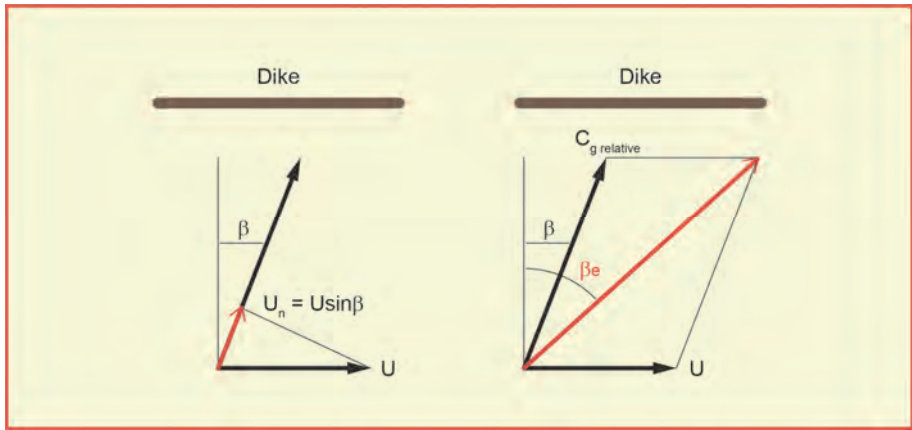
Figure 5.38: Definition of U_n and the angle of wave energy β_e

With ω and U_n as known variables, Equation 5.33 becomes an implicit function with k, which has to be solved by iteration. The solved k gives with Equation 5.33 the relative frequency σ:

$$\sigma^2 = g\,k\,\tanh(kd) \tag{5.35}$$

The relative group velocity c_g (see Figure 5.38) becomes:

$$c_{g,\,relative} = 0.5\sigma/k\,(1 + 2kd/\sinh(2kd)) \tag{5.36}$$

Vector summation shown above gives the angle of energy β_e (with respect to the normal of the dike, just like the angle of wave attack):

$$\beta_e = \arctan\{(c_{g,\,relative}\,\sin\beta + U)/(c_{g,\,relative}\,\cos\beta)\} \tag{5.37}$$

As an Example – *Find t*he angle of wave energy β_e .*Given* $H_{m0} = 0.127$ m; $T_p = 2.05$ s; $\beta = 15°$ (along with the current); $U = 0.30$ m/s and water depth 0.5 m.

Solution

> $\omega = 2\pi/T_{m-1,0} = 3.37$ (s^{-1}).
> $U_n = 0.0776$ m/s - Equation 5.34.
> Iterative solving of equation 5.33 gives: $k = 1.611$ (m^{-1}).
> $\sigma = 3.246$ s^{-1} – Equation 5.35
> $c_{g,\,relative} = 1.68$ m/s - Equation 5.36.
> $\beta_e = 24.3°$ - Equation 5.37.

The angle of energy $\beta_e = 24.3°$ is a little larger than the angle of wave attack $\beta = 15°$. The combined angle $0.5(\beta + \beta_e) = 19.65°$ should be used in Equations 5.28 or 5.29 for short-crested waves and in Equation 5.30 for long-crested waves.

5.4.6 Composite slopes and berms

Definition of a berm

A berm is a part of a dike profile in which the slope varies between horizontal and 1:15 (see Section 1.4 for a detailed definition). Typical berms are given in Figure 5.39. A berm is defined by the width of the berm B and by the vertical difference d_B between the middle of the berm and the still water level (Figure 5.40). The width of the berm B may not be greater than $0.25 \cdot L_{m-1,0}$. If the berm is not horizontal, the horizontal berm width B has to be calculated according to Figure 5.40. It is the horizontal berm width that is used in further calculations. The lower and the upper slope are extended to draw a horizontal berm without changing the berm height d_B. The horizontal berm width is therefore shorter than the angled berm width. Here, d_b is zero if the berm lies on the still water line. The characteristic parameters of a berm, with L_{berm}, are defined in Figure 5.40.

The benefit of a berm is that the equivalent slope angle becomes smaller, which reduces overtopping and leads to a lower required crest level for the dike or embankment. The best location for a berm is around the design water level and the effect reduces if the berm is below or above the water level during wave attack. A difference exists between a berm and a promenade. Section 5.4.7 describes the effect of a storm wall on a promenade, with or without storm wall. A promenade by definition is much closer to the crest than a berm, and often is the crest of the seawall. Berms and promenades may be similar in slope angle (gentler than 1:20) and size, but the difference is the level where they are present in the geometry. A berm is given by a width B, a promenade by a width G_c.

Figure 5.39: Typical berms
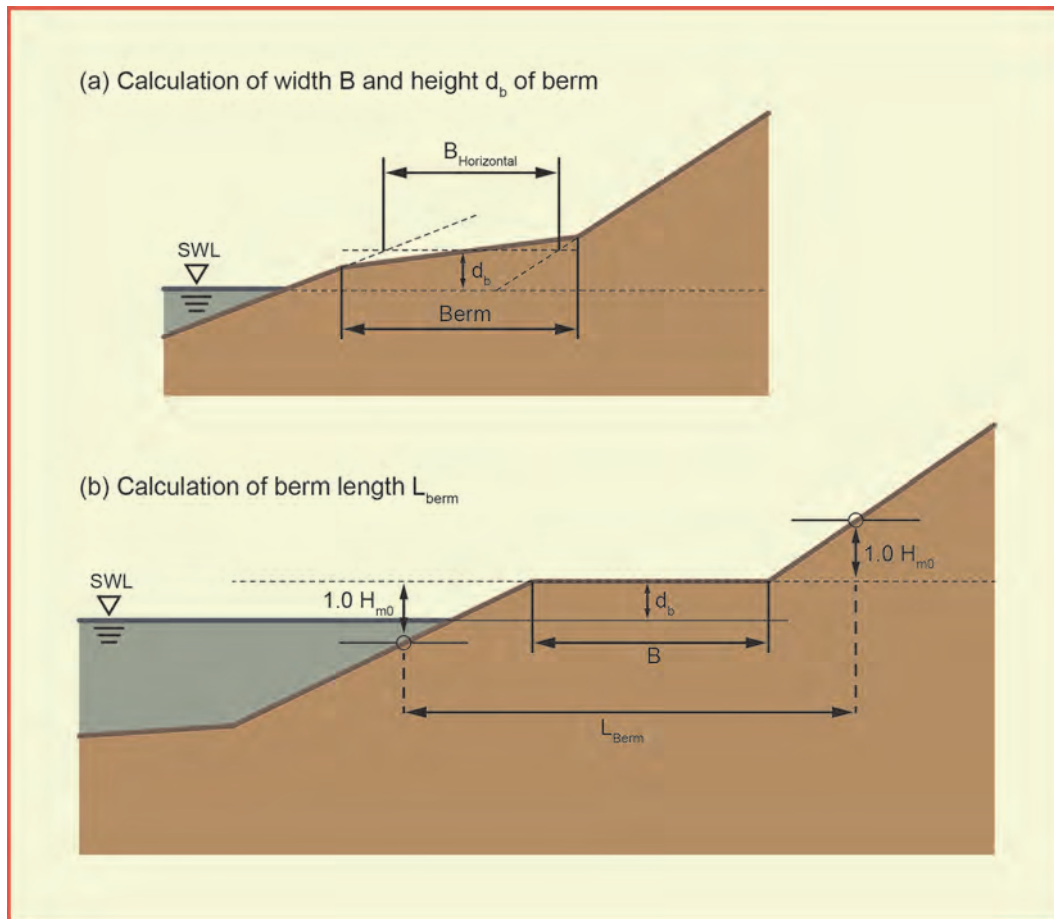
Figure 5.40: Definition of horizontal berm B and characteristic berm length L_{Berm}

Average slopes

Many dikes do not have a straight slope from the toe to the crest, but consist of a composite profile with different slopes, a berm or multiple berms. A characteristic slope is required to be used in the breaker parameter $\xi_{m-1,0}$ for composite profiles or bermed profiles to calculate wave run-up or wave overtopping. Theoretically, the run-up process is influenced by a change of slope from the breaking point to the maximum wave run-up height. Therefore, often it has been recommended to calculate the characteristic slope from the point of wave breaking to the maximum wave run-up height. This approach needs some calculation effort, because of the *iterative solution* since the wave run-up height $R_{u2\%}$ is unknown. For the breaking limit a point on the slope can be chosen which is 1.5 H_{m0} below the still water line.

It is recommended to use also a point on the slope 1.5 H_{m0} above water as a first estimate to calculate the characteristic slope and to exclude the berm, see Figure 5.41 and Equation 5.38. As a second estimate, the wave run-up height from the first estimate is used to calculate the average slope (L_{Slope} has to be

adapted see Figure 5.41) as in Equation 5.39. If the run-up height or 1.5 H_{m0} comes above the crest level, then the crest level must be taken as the characteristic point above SWL.

$$1^{st} \text{ estimate: } \tan\alpha = \frac{3 \cdot H_{m0}}{L_{Slope} - B} \tag{5.38}$$

$$2^{nd} \text{ estimate: } \tan\alpha = \frac{\left(1.5 \cdot H_{m0} + R_{u2\% \, (from \, 1st \, estimate)}\right)}{L_{Slope} - B} \tag{5.39}$$

132
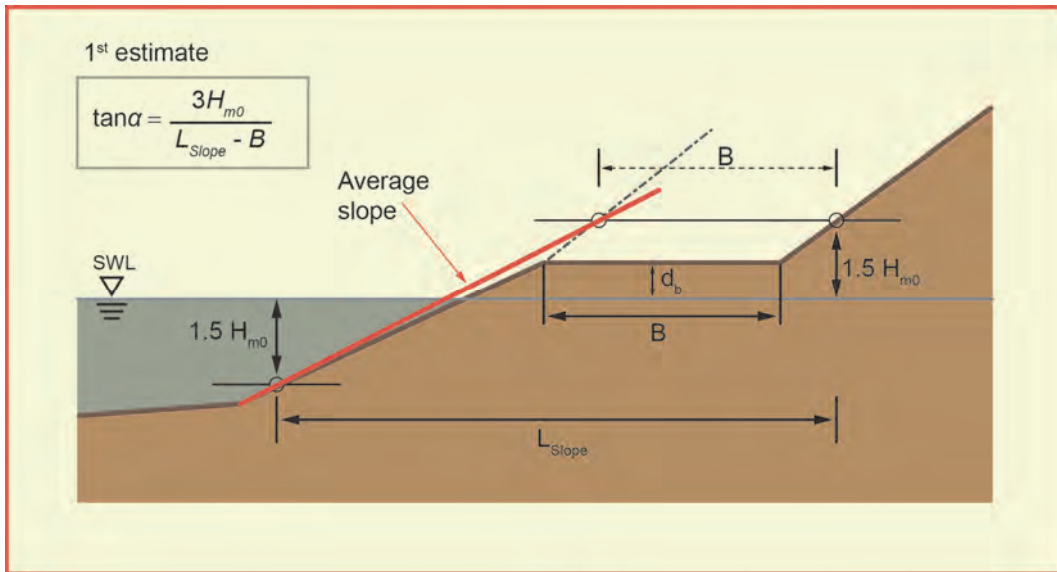
Figure 5.41: Determination of the average slope (1st estimate)
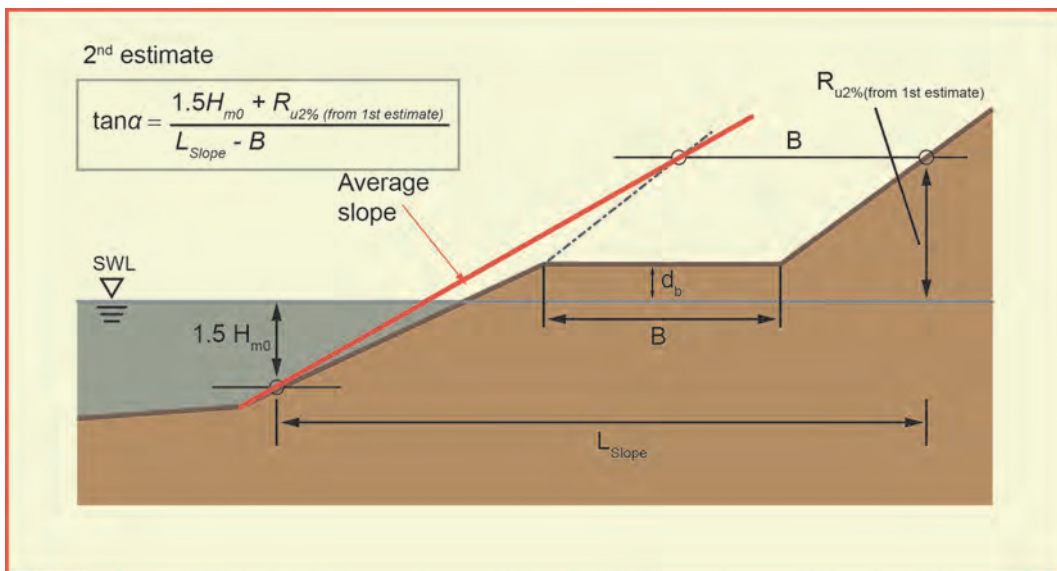
Figure 5.42: Determination of the average slope (2nd estimate)

Influence of berms

A berm reduces wave run-up or wave overtopping. The influence factor γ_b for a berm consists of two parts, given by r_B and r_{db}.

$$\gamma_b = 1 - r_B\left(1 - r_{db}\right) \quad \text{for}: 0.6 \le \gamma_b \le 1.0$$

5.40

The first part (r_B) stands for the influence of the width of the berm L_{Berm} and becomes zero if no berm is present, see Equation 5.41. The second part (r_{db}) stands for the vertical difference d_b between the still water level (SWL) and the middle of the berm and becomes zero if the berm lies on the still water line, see Equation 5.42. The reduction of wave run-up or wave overtopping is maximum for a berm on the still water line and decreases with increasing d_b. Thus, a berm lying on the still water line is most effective. A berm lying below $2 \cdot H_{m0}$ or above $R_{u2\%}$ has no influence on wave run-up and wave overtopping.

133

$$r_B = \frac{B}{L_{Berm}}$$

5.41

Different expressions are used for r_{dB} in Europe. Here an expression using a cosine-function for r_{db} (Figure 5.43) is recommended which is also used in PC-Overtopping, see Section 4.3.

$$r_{db} = 0.5 - 0.5\cos\left(\pi \frac{d_b}{R_{u2\%}}\right) \quad \text{for a berm above still water line}$$

$$r_{db} = 0.5 - 0.5\cos\left(\pi \frac{d_b}{2 \cdot H_{m0}}\right) \quad \text{for a berm below still water line}$$

5.42

$r_{db}=1$ for berms lying outside the area of influence

The influence of the berm depth d_b on the factor r_{db} is given in a graphical way in Figure 5.43.
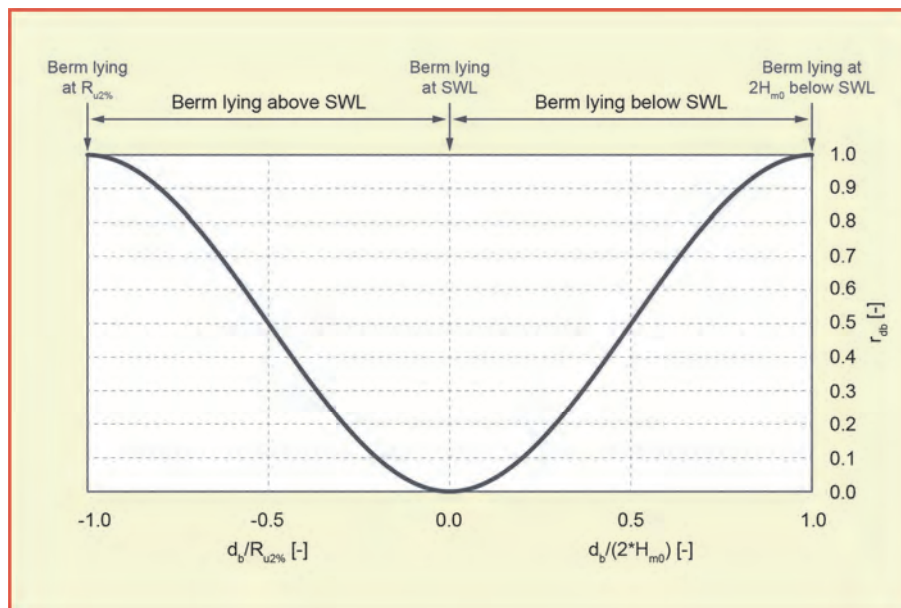
Figure 5.43: Influence of the berm depth d_b on factor r_{db}, which is part of Equation 5.42

The maximum influence of a berm is actually always limited to $\gamma_B = 0.6$. This corresponds to an optimal berm width of $B = 0.4\, L_{berm}$ on the still water line.

The definition of a berm is made for a slope smoother than 1:15 while the definition of a slope is made for slopes steeper than 1:8, see Section 1.4. If a slope or a part of the slope lies in between 1:8 and 1:15 it is required to interpolate between a bermed profile and a straight profile. For wave run-up this interpolation is written by Equation 5.43. A similar interpolation procedure should be followed for wave overtopping.

$$R_{u2\%} = R_{u2\%(1:8slope)} + \left(R_{u2\%,(Berm)} - R_{u2\%,(1:8slope)}\right) \cdot \frac{(1/8 - \tan\alpha)}{(1/8 - 1/15)} \qquad 5.43$$

5.4.7 Effect of a wave wall on a slope or promenade

Besides the roughness of the dike's slope (γ_f), wave obliqueness (γ_β) and a berm (γ_b), as discussed in the previous sub-sections of Section 5.4, measures at the crest level of a slope, such as vertical wave walls, can also reduce wave overtopping discharges. These wave walls in general are relatively small compared to the whole geometry of the structure, otherwise they would fall into the category of vertical walls described in Chapter 7.

If the structure is a dike-type structure, such a wall will be directly on the top of the slope or just behind on the crest. But specific situations exist where the crest of the dike has a (wide) promenade with at the end possibly buildings such as apartments. One cannot easily increase the crest level in such a case and a possible solution to reduce wave overtopping may then be to construct a wave wall with limited height somewhere on the promenade. The wave wall may even be a removable one, see for example Figure 3.13.

In order to limit wave overtopping even further, it is possible to design a parapet, wave return structure or bullnose at the top of the wall. In this section it will be called a bullnose.

This section will give guidance on wave walls on a slope or somewhere on a promenade, with or without a bullnose. It is divided into four areas of application:

- A relatively large wave wall with the foot of the wall below SWL (guidance as in EurOtop, 2007);
- A wave wall at the end of a gentle slope 1:6 (breaking waves on the slope);
- A wave wall with the foot of the wall above swl, on a slope or promenade (non-breaking waves on the slope). Most of this work is based on extensive research at Ghent University (Van Doorslaer *et al.* 2015) and is the main body of this section;
- Stilling wave basins.

Wave wall with submerged foot, $h_{wall}/R_c > 1$

Limited guidance on wave walls was given in EurOtop (2007), Section 5.3.5. Part of that guidance has now been replaced by the work of Van Doorslaer *et al, (*2015), as long as the foot of the wall is above SWL (see further in this section). If the wall is relatively large with the foot below SWL, the guidance as in EurOtop (2007) is still valid. In that case one has to schematise a vertical wall as a 1:1 slope, keeping the same relative freeboard, in order to determine the average slope of the structure and to determine whether the overtopping formula for breaking waves (Equation 5.10 or 5.12) should be used, or for non-breaking waves (Equation 5.11 or 5.13). In this case breaking waves are defined as $\gamma_b \cdot \xi_{m-1,0} < 3$. In case of breaking waves the influence factor γ_v for a wave wall was suggested to be 0.65. For non-breaking waves the wave wall itself had no extra influence other than increasing the crest freeboard (there is no influence factor γ_v in Equation 5.11 or 5.13). The application was limited to slopes below the wave wall between 1:2.5 and 1:3.5 and the foot of the wall may not be lower than $1.2H_{m0}$.

Wave wall at the end of a gentle slope 1:6 (breaking waves on the slope)

New model test were performed at Ghent University on a much gentler smooth dike slope 1:6, with and without storm wall, where only breaking waves were measured, (Van Doorslaer *et al.*, 2016). In the

analysis the slope angle α remained 1:6 and no equivalent slope was calculated: $\tan(\alpha)$ = 1:6, this in contrast to the general method in this manual. The results showed that γ_v is not as low as was estimated in the EurOtop, (2007) where guidance was given for steeper slopes only, and has, within certain limits, no dependency on the height of the storm wall, taking the crest freeboard as a constant. It is suggested to use a fixed value γ_v = 0.92 for breaking waves in Equation 5.10 for a slope of 1:6 with a wave wall. Figure 5.44 shows the test results with and without a wall on top of a 1:6 slope.
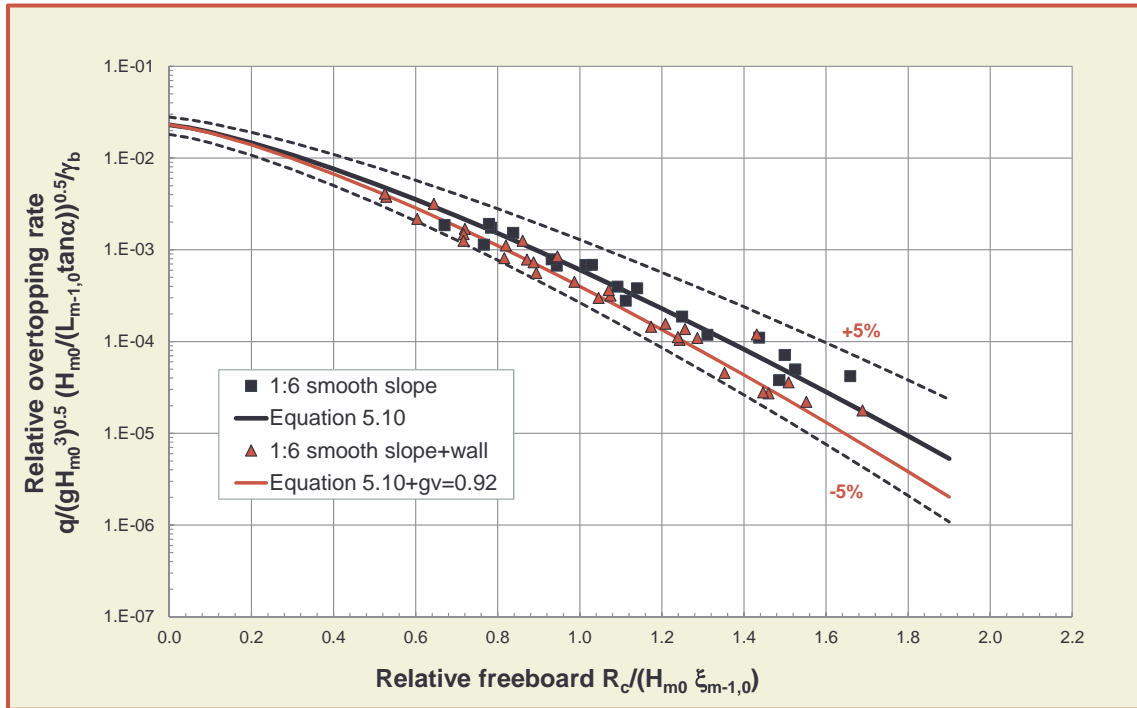
Figure 5.44   Results of a storm wall on top of a smooth 1:6 dike slope (breaking waves). The data points with storm wall are located slightly below the data without storm wall, giving γ_v = 0.92

Wave wall on top of emerged slope or promenade (non-breaking waves on the slope)

The main improvement, however, in this manual is based on Van Doorslaer *et al.* (2015) and relates to a straight smooth seaward slope of 1:2 or 1:3 with a wave wall or storm wall on top of the slope or somewhere on a promenade, with or without bullnose. In order to give an overall view and an impression of the possible effects of storm walls and a bullnose, Figure 5.45 and Figure 5.46 were produced. The first figure gives all test results with the trend line for a smooth straight 1:2 or 1:3 slope as reference. The 5% exceedance lines (or 90% confidence band) are based on the reliability given for Equation 5.10 in Section 5.3.1.

Figure 5.45 shows that a smooth slope gave always the largest wave overtopping and that any measure, such as a promenade, a storm wall, with or without a bullnose, reduces wave overtopping. The smallest influences are found for extending the top of the slope with a promenade only (no storm wall) and with a storm wall directly on the slope, without promenade or bullnose. Those data points are closest to the trend line for a smooth slope and mostly within the 90% confidence band. Most effective are a wall with bullnose on a slope or a wall with or without bullnose on a promenade. Those data points give often overtopping that is a factor of 10-100 smaller than for a smooth straight slope, with the same crest level.

If all the reduction factors have been applied that have been described further on in this section, it gives Figure 5.46. The test results have been analysed into great detail, leading to a graph with limited scatter around the main curve. Actually, the scatter for these specific tests is significantly smaller than for the overall Equation 5.11, which is given in the graph by the 5% exceedance lines. Note that the graphs are for non-breaking waves only, as the tested seaward slopes of 1:2 and 1:3 always gave non-breaking waves and the actual slope was used to calculate the breaker parameter, $\xi_{m-1,0}$.
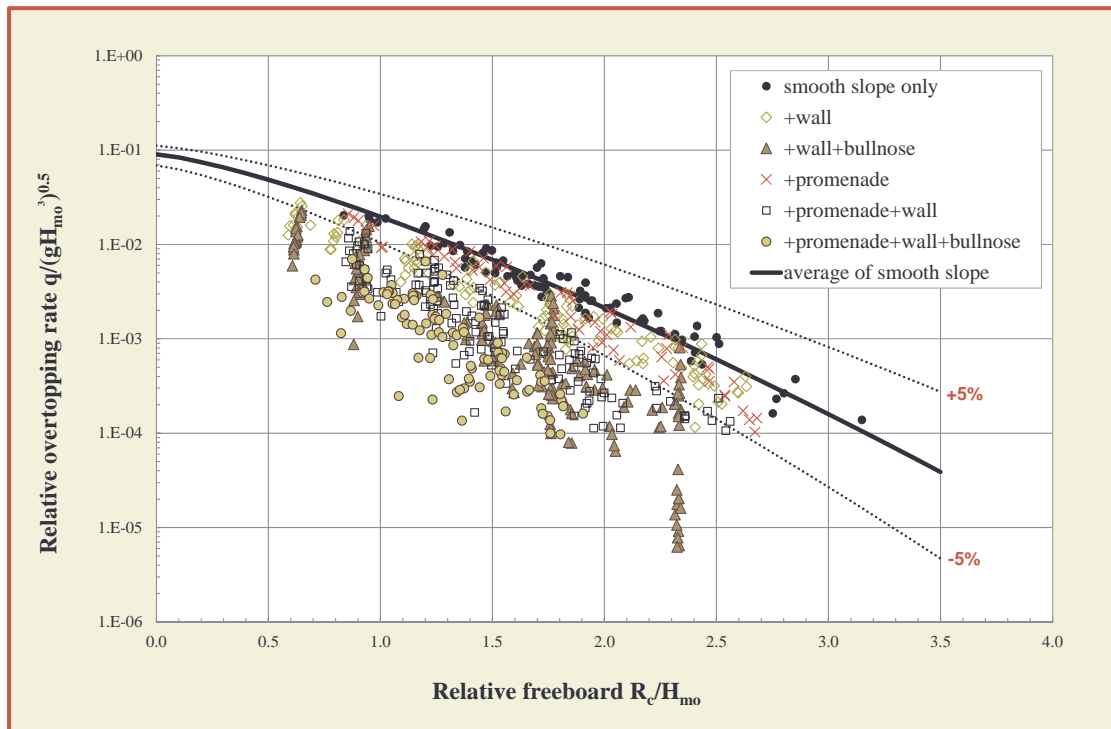
Figure 5.45.   All test results of Van Doorslaer *et al.* (2015) on wave walls with or without bullnose, without applying all reduction factors as described in this section
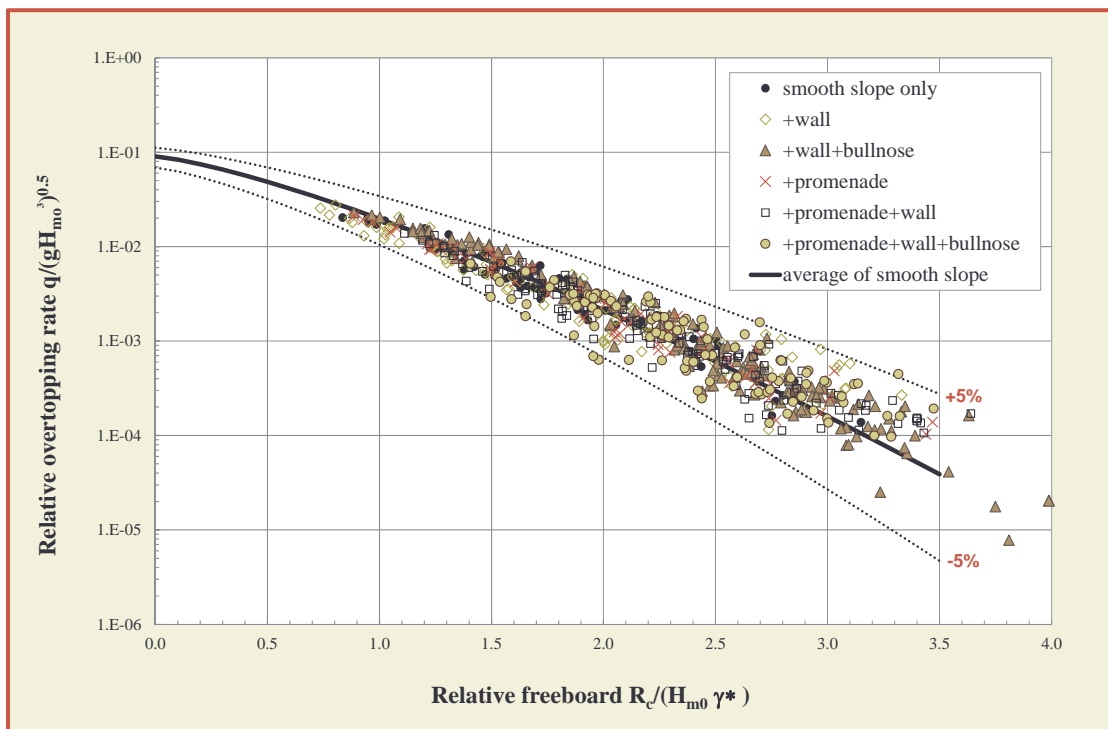
Figure 5.46:   All test results of Van Doorslaer *et al.* (2015) on wave walls with or without bullnose, applying all reduction factors as described in this section

The range of application of a storm wall on a slope or promenade can be given as follows:
- the foot of the storm wall is above swl
- cot α = 2 - 3 (this could also be an average slope)
- $s_{m-1,0} = 0.01 – 0.05$
- $\xi_{m-1,0} = 2.2 – 4.8$ (based on the seaward slope only)
- $R_c/H_{m0} > 0.6$
- Promenade slope 1% and 2%

Influence factors or reduction coefficients are proposed for different geometrical configurations at the top of a smooth sloping dike. Such configurations can be summarized as follows:

a)   smooth dike slope + storm wall;
b)   smooth dike slope + storm wall and bullnose;
c)   smooth dike slope + promenade;
d)   smooth dike slope + promenade + storm wall;
e)   smooth dike slope + promenade + storm wall and bullnose;

The influence factors are to be included in the general formula for non-breaking waves, Equation 5.11, in the denominator of the exponential part of the formula:

$$\frac{q}{\sqrt{gH_{m0}^3}} = 0.09 \cdot exp\left(-\left[1.5\frac{R_c}{H_{m0}\gamma^*}\right]^{1.3}\right) \qquad 5.44$$

where γ^* is the combined influence factor that will be detailed for each configuration a) to e) above. No roughness, obliqueness or presence of a berm was used throughout the model tests. This that $\gamma_f = \gamma_\beta = \gamma_b = 1$, but these influence factors could be applied in practice, assuming that they are also valid when a wave wall is present.

a)   Smooth dike slope + storm wall (γ^* = γ_v)

The case of a smooth dike with a storm wall, Figure 5.47, corresponds to the situation where a vertical wall (with height h_{wall}) is built on the top of the slope of the dike. The height of this storm wall is included in the definition of the crest freeboard R_c ($R_c = A_c + h_{wall}$). The influence factor γ^* = γ_v is defined as follows:

$$\gamma_v = exp\left(-0.56\frac{h_{wall}}{R_c}\right) \qquad 5.45$$

Figure 5.47:   Configuration of a slope with a storm wall

The range of application for the dimensions of the wall are given by $h_{wall}/R_c = 0.08 - 1.00$.

b) Smooth dike slope + wall + bullnose ($\gamma^* = \gamma_v \cdot \gamma_{bn} \cdot \gamma_{s0,bn}$)

The influence factor for a geometry with a smooth dike slope with on top a wave wall with a bullnose, see Figure 5.48, is a combination of three factors: the influence of the wall, the influence of the bullnose, and the influence of the wave period or wave steepness. This last influence ($s_{m-1,0}$) only appears for this specific geometry where a storm wall with bullnose is directly situated at the top of the slope.
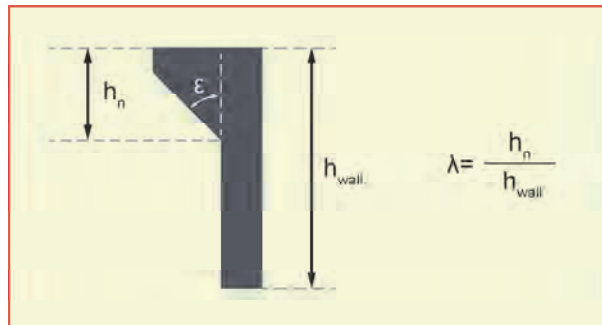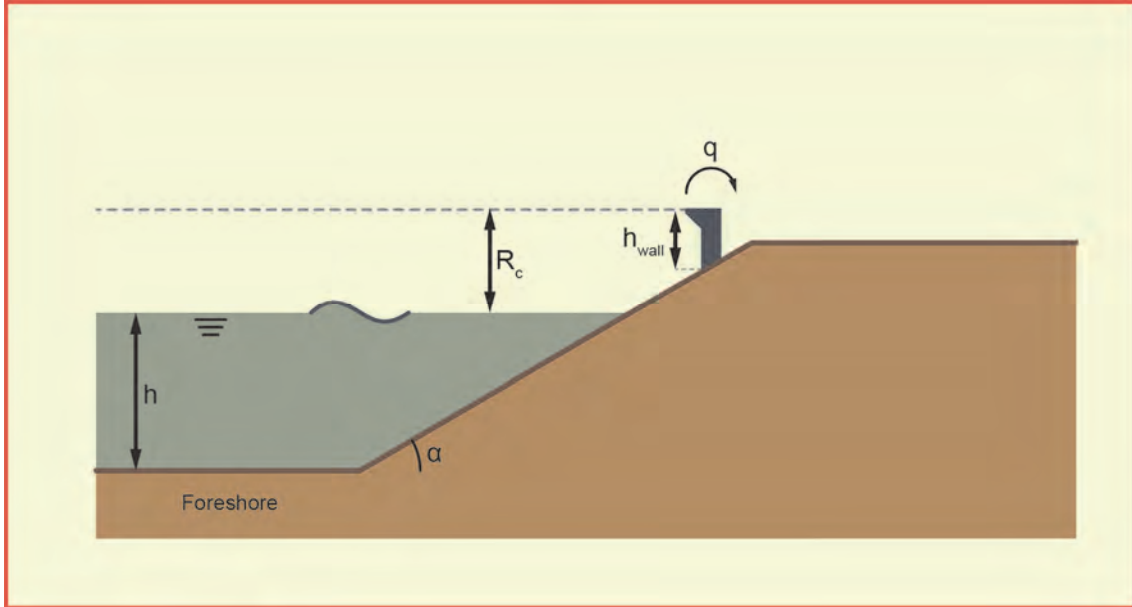
Figure 5.48: Configuration of a slope with a storm wall and bullnose

The first factor, γ_v, is calculated with Equation 5.45. The coefficient, γ_{bn}, depends on the angle ε and the position λ of the bullnose and is defined by Equations 5.46 and 5.47:

$$\gamma_{bn} = 1.8\gamma_\varepsilon\gamma_\lambda \qquad \text{for } h_{wall}/R_c \geq 0.25 \qquad\qquad 5.46$$

where:
$$\gamma_\varepsilon = 1.53 \cdot 10^{-4}\varepsilon^2 - 1.63 \cdot 10^{-2}\varepsilon + 1 \qquad \text{if } 15° \leq \varepsilon \leq 50°$$
$$\gamma_\varepsilon = 0.56 \qquad\qquad\qquad\qquad\qquad\qquad \text{if } \varepsilon > 50°$$
$$\gamma_\lambda = 0.75 - 0.20\lambda \qquad\qquad\qquad\qquad \text{if } 0.125 \leq \lambda \leq 0.6$$

$$\gamma_{bn} = 1.8\gamma_\varepsilon\gamma_\lambda - 0.53 \qquad \text{for } h_{wall}/R_c < 0.25 \qquad\qquad 5.47$$

where:

$$\gamma_\varepsilon = 1 - 0.003\varepsilon \qquad \text{if } 15 \le \varepsilon \le 60$$
$$\gamma_\lambda = 1 - 0.144\lambda \qquad \text{if } 0.1 \le \lambda \le 1$$

The overtopping discharge over a smooth dike with storm wall and bullnose is dependent on the wave period or wave steepness. A wave with long wave period has the tendency to fill the space underneath the bullnose, so the rest of the incident wave observes the structure as a normal vertical storm wall. A wave with short wave period does not have this behaviour. An influence factor, $\gamma_{s0,bn}$, is then introduced for this geometry as:

$$\gamma_{s0,bn} = 1.33 - 10s_{m-1,0} \tag{5.48}$$

The range of application is given by $h_{wall}/R_c = 0.11 - 0.90$; $\lambda = 0.125 - 1$; and $\varepsilon = 15°$, $30°$, $45°$ and $60°$.

c) Smooth dike slope + promenade ($\gamma^* = \gamma_{prom}$)

The case with a smooth dike slope with a promenade corresponds to cases with a sloping dike with quite a wide crest, which can serve as tourist promenade (e.g. Belgian coastline, see Figure 3.13). This promenade is quasi horizontal, it only has a 1% or 2% slope seawards to stimulate drainage from overtopping or rainfall back towards the sea. The overtopping discharge is measured at the end of the promenade, see Figure 5.49. The freeboard R_c is measured at this location, so includes the height differences on the promenade.
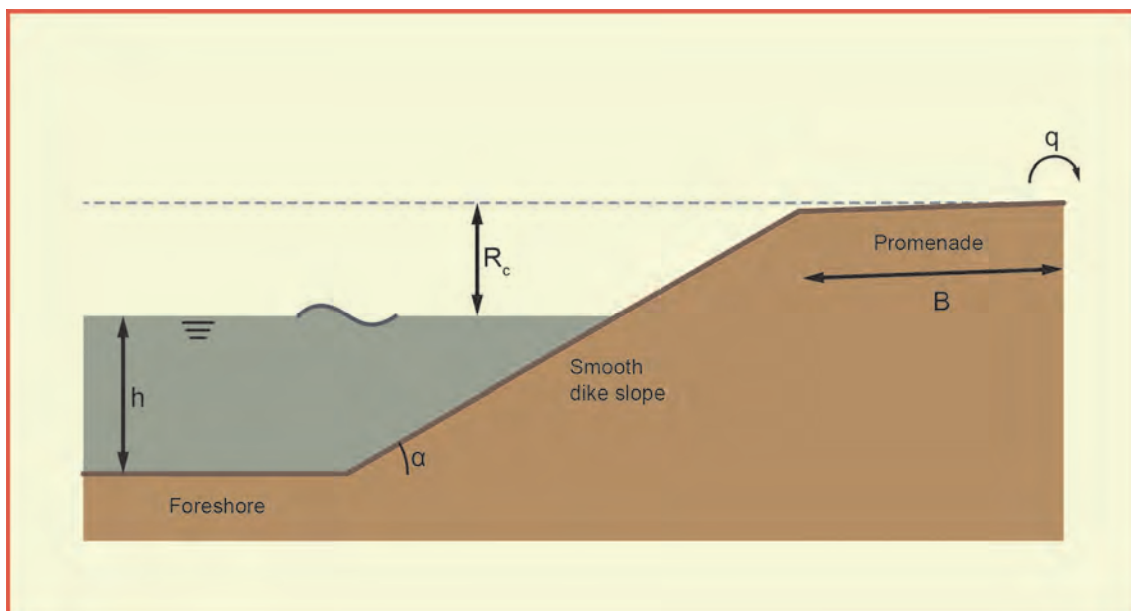
Figure 5.49: Configuration of a slope with a promenade

The influence factor is a function of the dimensionless promenade width G_c (with $L_{m-1,0}$ the deep water wave length and $T_{m-1,0}$ measured at the toe of the structure) and is expressed as follows:

$$\gamma_{prom} = 1 - 0.47\frac{G_c}{L_{m-1,0}} \tag{5.49}$$

The range of application for $G_c/L_{m-1,0} = 0.05 - 0.5$.

d) Smooth dike slope + promenade + wall ($\gamma^* = \gamma_{prom\_v}$)

When a storm wall is built at the end of a promenade, see Figure 5.50, a new influence factor γ_{prom_v} is introduced, as a combination of γ_{prom} (Equation 5.49) and γ_v (Equation 5.45). Van Doorslaer *et al.* (2015) showed that simply multiplying both independent influence factors underestimated the reductive effect of a storm wall placed at the end of a promenade. It is a post-overtopping process, where an overtopped bore over the top of the slope once again overtops a (vertical) structure, and due to this changed physical behaviour influence factors cannot just be multiplied.
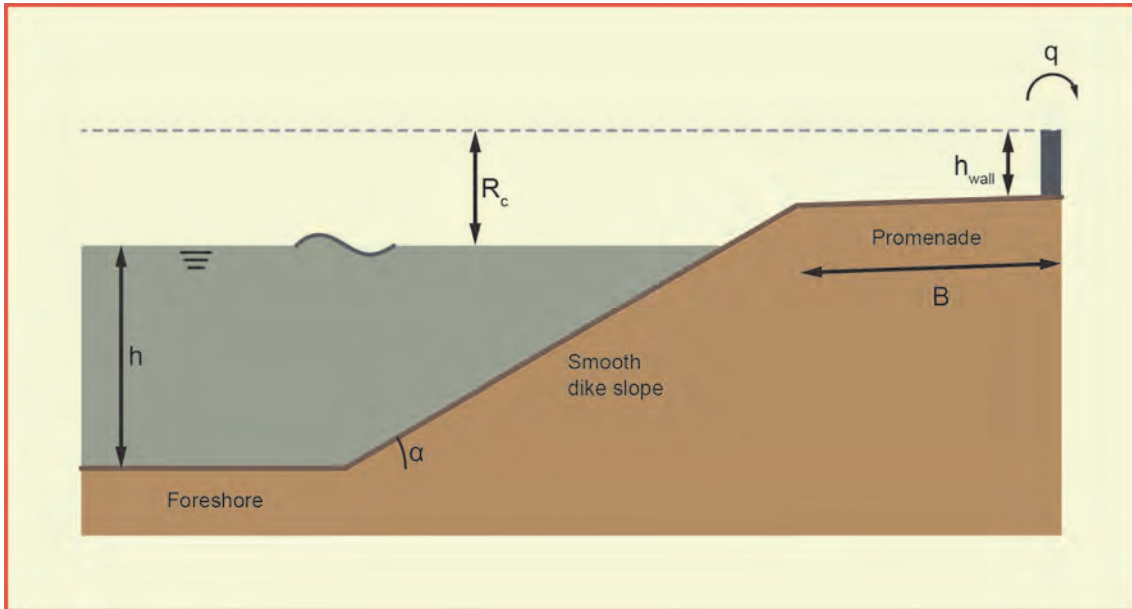
Figure 5.50: Configuration of a slope with a promenade and a storm wall

The new influence factor becomes:

$$\gamma_{prom\_v} = 0.87\gamma_{prom}\gamma_v \qquad\qquad 5.50$$

The range of application is given by $G_c/L_{m-1,0} = 0.05 - 0.4$ and $h_{wall}/R_c = 0.07 - 0.80$.

e) Smooth dike slope + promenade + wall + bullnose ($\gamma^* = \gamma_{prom\_v\_bn}$)

When a storm wall with bullnose is built at the end of a promenade, see Figure 5.51, the influence factor $\gamma_{prom\_v\_bn}$ is introduced:

$$\gamma_{prom\_v\_bn} = 1.19\gamma_{prom\_v}\,\gamma_{bn} \qquad\qquad 5.51$$

Also here the physics are different when an overtopped bore on a promenade faces a storm wall with bullnose (like here), than when a wave faces a slope with storm wall and parapet on top. Thereby, this geometry reduces less than the multiplication of γ_{bn} (Equations 5.46 and 5.47) and γ_{prom_v} (Equation 5.50). Note that overtopping over this geometry is independent of the wave period (unlike the geometry in Figure 5.48).

The range of application is given by $G_c/L_{m-1,0} = 0.04 - 0.4$; $h_{wall}/R_c = 0.17 - 0.80$, $\varepsilon = 30°, 45°$; and $\lambda = 0.25 - 0.38$.
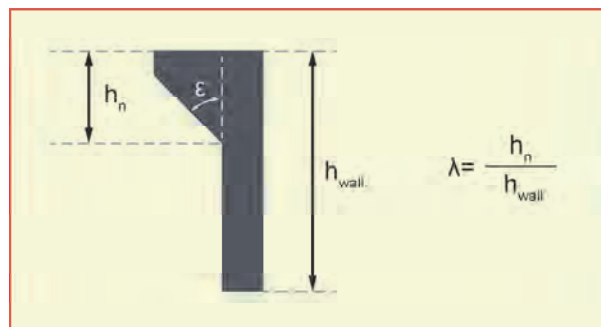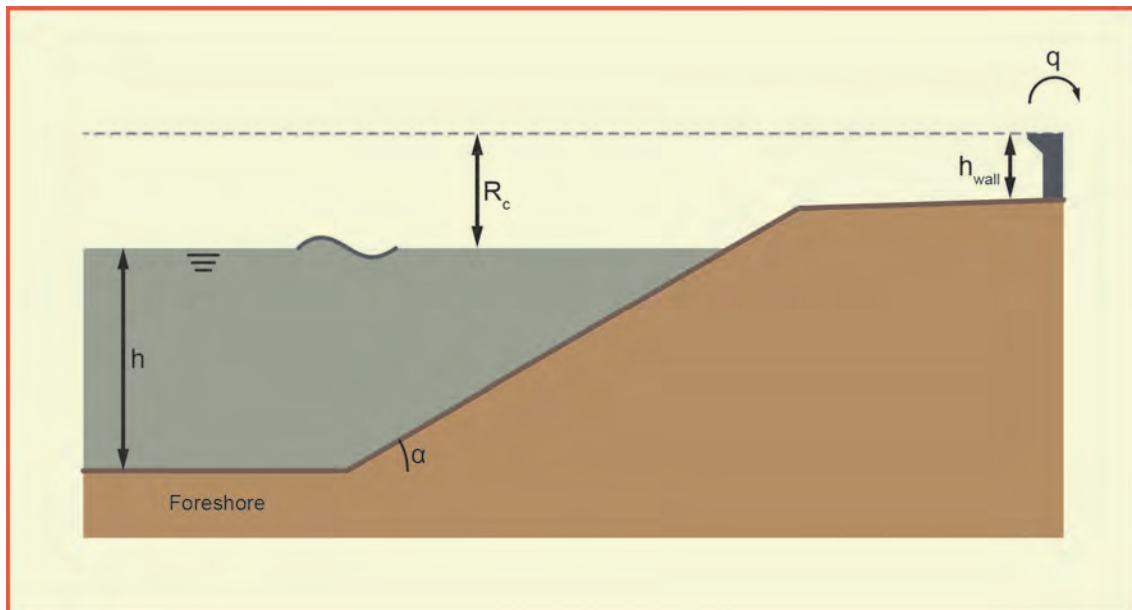
Figure 5.51:   Configuration of a slope with a promenade and a storm wall with bullnose

Stilling wave basin

The concept of a Stilling Wave Basin (SWB) was introduced by Cavani *et al.* (1999) and Aminti and Franco (2001) for rubble mound breakwaters. Geeraerts *et al.* (2006) used the principle at a smooth dike slope and promenade. A Stilling Wave Basin (SWB) is based on the principle of the wave energy dissipation between two walls forming the basin. A wave that overtops the first wall drops in the basin and loses (most of) its energy to overtop the second (landward) wall. The first wall may actually consist of a double row of shifted walls or can be a single wall with some gaps to evacuate the overtopped water or rainfall towards the sea. An example of a Stilling Wave Basin is shown in Figure 5.52.

The study by Geeraerts *et al.* (2006) investigated some geometric parameters, such as the length of the basin, the height of the front wall, the opening ratio of every wall, etc. The optimal influence factor was around 0.45. The set-up of a dike slope with Stilling Wave Basin is given in the Figure 5.53.

Figure 5.52:   A stilling wave basin at Oostende, BE
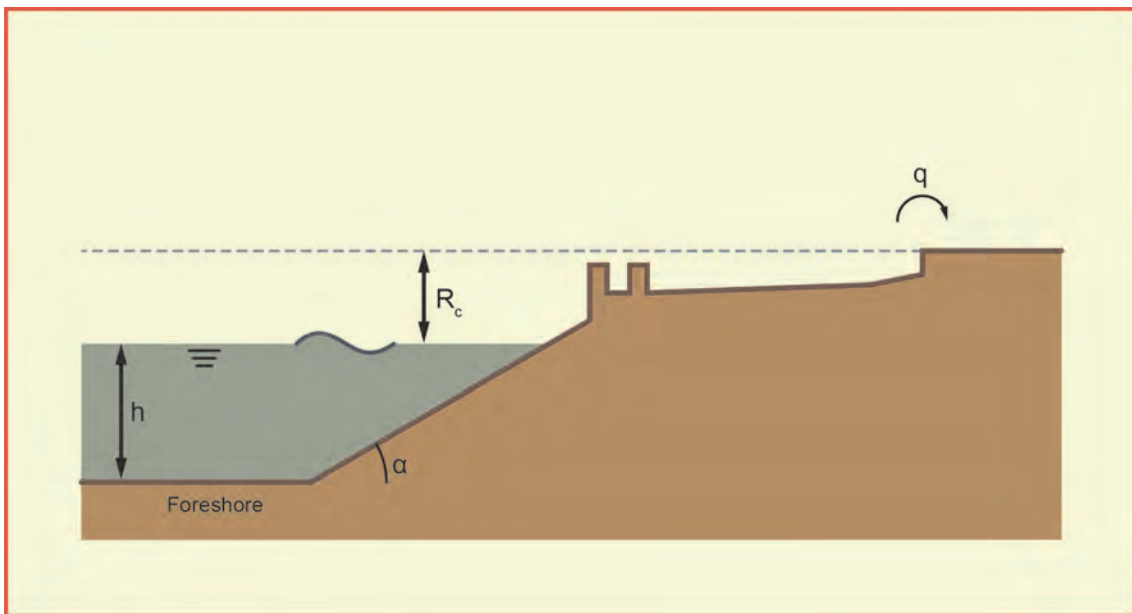
Figure 5.53. Concept of a stilling wave basin to reduce wave overtopping

5.5 Overtopping wave characteristics

5.5.1 Introduction

The average overtopping discharge, q, has been the main parameter in the previous Sections 5.3 and 5.4 to describe wave overtopping. It is simply the amount of water that comes over the crest, divided by the time that the amount of water was measured. For example, if 5 m^3 water has been measured per m width and over one hour, the average overtopping discharge becomes q = 5000/3600 = 1.39 l/s per m. The actual behaviour at the structure is completely different.

Figure 5.54 gives an idea of the irregular behaviour of wave overtopping in time, where the wave height in the model test was H_{m0} = 0.065 m and the average overtopping discharge was q = 0.048 l/s per m. The red record in the top of the graph shows the random waves that have been generated in a physical model facility. Only some of the largest waves will reach the crest and generate wave overtopping. The black record gives the height measurement of a wave gauge placed on top of the crest of the structure and actually gives the flow thickness of overtopping wave volumes. The graph shows that overtopping wave volumes are irregular, all different and that there are less overtopping wave volumes than incident waves. Only a certain percentage of the incident waves reach the crest and cause wave overtopping. This section deals with individual waves that reach the crest and cause wave overtopping.
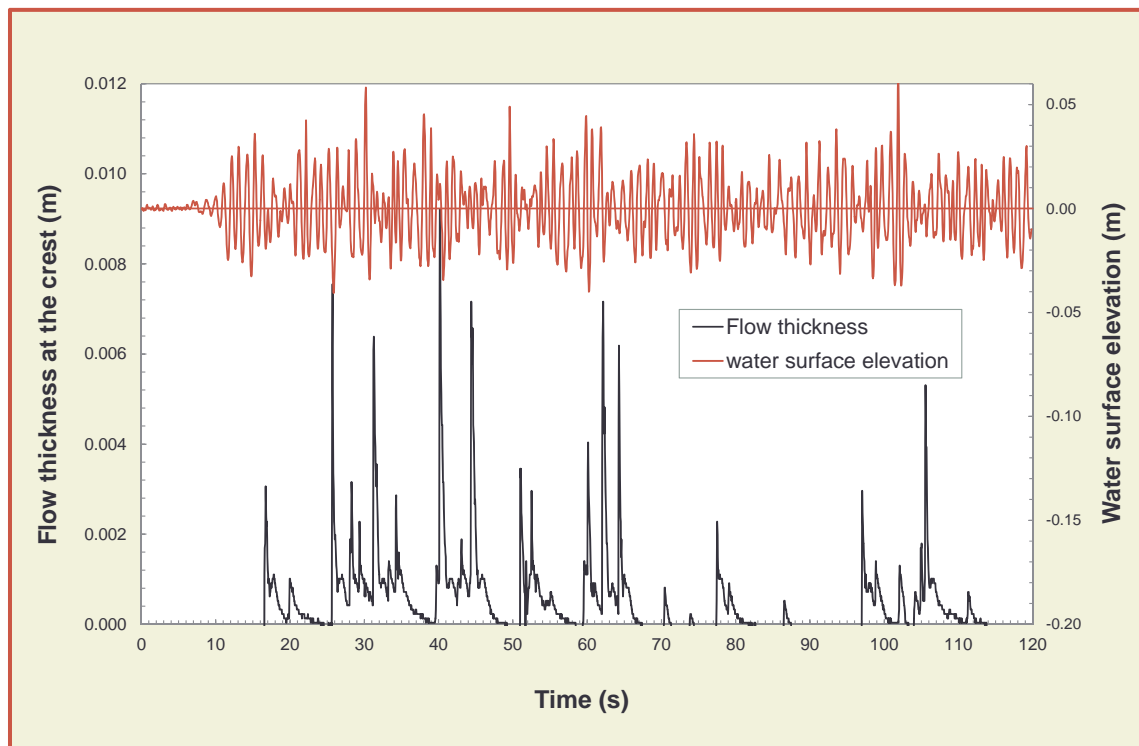
Figure 5.54:   Example of irregular wave overtopping, as measured by a wave gauge at the crest of a structure (flow thickness) and the wave record in front of the structure

Figure 5.55 shows the process of a wave reaching a structure and gives then the wave-structure-interaction. A wave may break in the breaking zone 2, runs up the slope to its highest point and then runs down the slope in zone 3 till it meets the next wave. If the up-rushing wave reaches the crest, the process of wave overtopping starts, first along the crest in zone 4 and finally down the landward slope in zone 5. A picture of wave overtopping in reality was already given in Figure 3.19. It shows that wave overtopping is not only irregular in time, but also irregular along the dike.
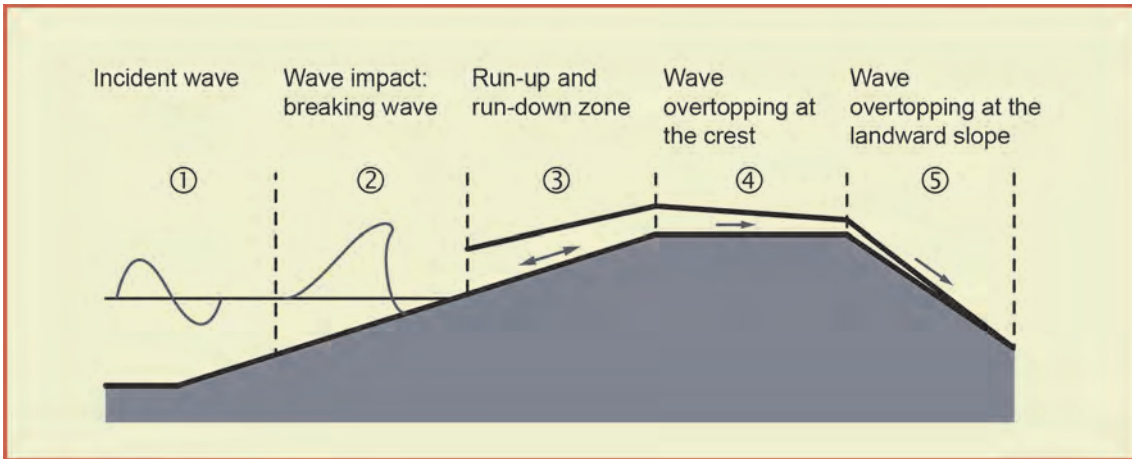
Figure 5.55: Process of wave breaking, run-up and overtopping at a dike (graph partly from Schüttrumpf, 2001)

Figure 5.56 gives the measurements of an overtopping wave at the crest of a dike (simulated by the overtopping simulator, see Section 4.8). The flow velocity as well as the flow thickness were recorded over time. Data processing of records like Figure 5.56 lead to a maximum flow thickness, h, and maximum flow velocity, v. Statistics of these parameters h and v are described in Section 5.5.3 to 5.5.5, whereas Section 5.5.2 will describe the overtopping wave volumes. Note that even for one event, like in Figure 5.56, the maximum values do not occur at the same time. Multiplication of the records for h and v and integrating over the duration gives the total volume in the overtopping wave, V. In the case of Figure 5.56 the overtopping wave volume was V = 0.9 m^3 per m width.
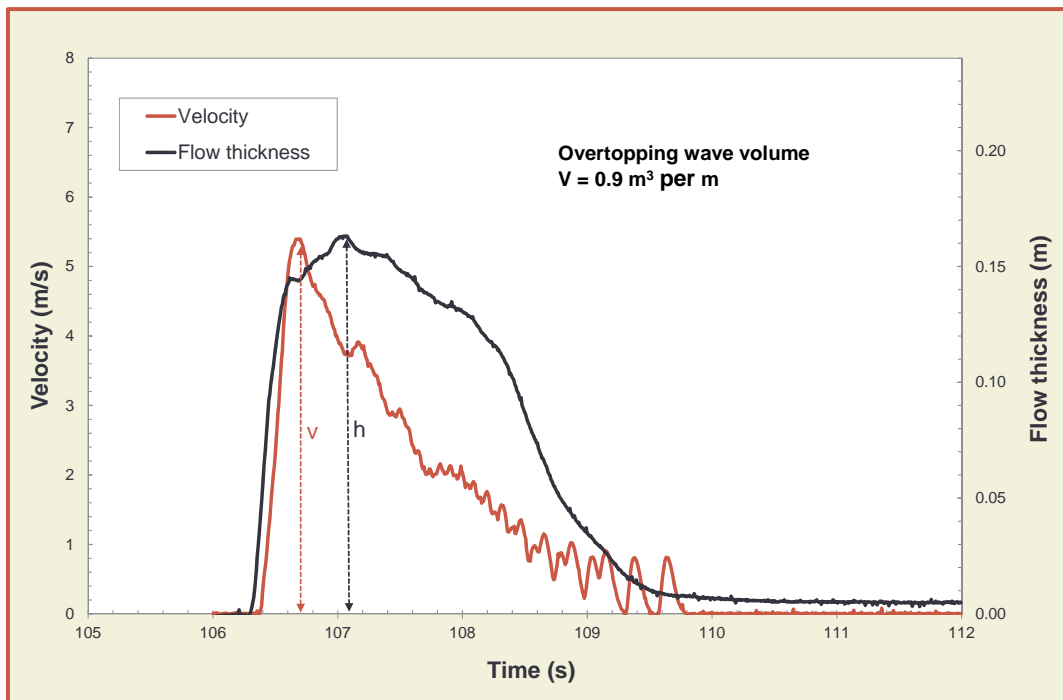
Figure 5.56: Measurement of an overtopping wave at the crest of a dike

5.5.2 Overtopping wave volumes

The distribution of individual overtopping wave volumes can be represented by the two parameter Weibull probability distribution, given by the percent exceedance distribution in Equation 5.52.

$$P_{V\%} = P(V_i \geq V) = \exp\left[-\left(\frac{V}{a}\right)^b\right] \cdot (100\%) \text{ and } P_{V\%} = P_V \cdot (100\%)$$

5.52

where P_V is the *probability* (between 0 and 1) that an individual wave volume (V_i) will be less than a specified volume (V), and $P_{V\%}$ is the *percentage* of wave volumes that will exceed the specified volume (V). The two parameters of the Weibull distribution are the non-dimensional shape factor, b, that helps define the extreme tail of the distribution and the dimensional scale factor, a, that normalizes the distribution.

$$a = \left(\frac{1}{\Gamma\left(1 + \frac{1}{b}\right)}\right)\left(\frac{qT_m}{P_{ov}}\right)$$

5.53

where Γ is the mathematical gamma function. This gamma function can be entered into MS Excel© as = 1 / EXP(GAMMALN(1+1/b)). The relationship between the shape parameter b and the part in Equation 5.53 with the gamma function $1/[\Gamma(1+1/b)]$ is given in Figure 5.57.
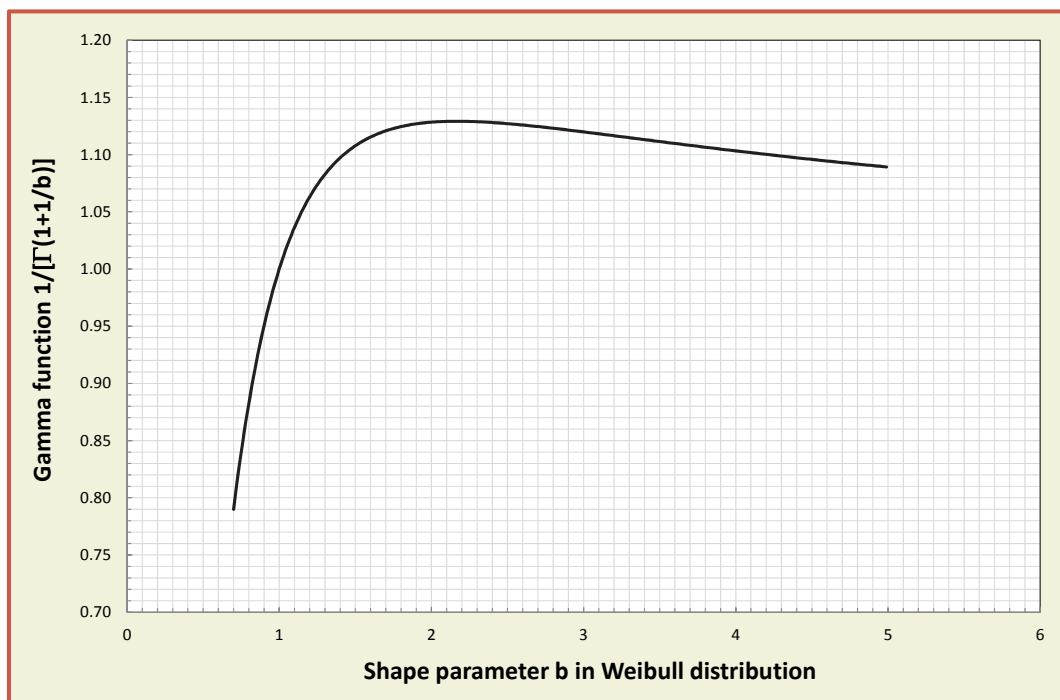
Figure 5.57:   Relationship between the shape parameter b and the mathematical gamma function in Equation 5.53

Recent improvements in describing wave overtopping processes have been described by Hughes *et al.* (2012) and Zanuttigh *et al.* (2013). Zanuttigh *et al.* (2013) give for b the following relationship (Figure 5.58):

$$b=0.73+55 \left(\frac{q}{gH_{m0}T_{m-1,0}} \right)^{0.8}$$

$\qquad$ 5.54

Figure 5.58 shows that for a relative discharge of $q/(gH_{m0}T_{m-1,0}) < 10^{-4}$ the average value of b is about 0.75 and this value has long been used to describe overtopping of individual wave volumes (as given in EurOtop, 2007). But the graph shows that with larger relative discharge the b-value may increase significantly, leading to a gentler distribution of overtopping wave volumes.

This new knowledge may have an effect on design and usage of wave overtopping simulators and also on describing the damage effects of wave overtopping on the landward side, or on allowable overtopping. Note that b-values larger than 2 give distributions that are flatter than a Rayleigh-distribution and that these values only appear for submerged structures, where there is overtopping as well as overflow. For emerged structures the b-value is always smaller than 2. See also Figure 4.5 on the effect of the b-value on the shape of the distribution.

Equation 5.52 is applied on the number waves that actually reach the crest and cause wave overtopping, it is not applied on the number of incident waves in a storm. It means that there are a certain number of overtopping wave volumes, N_{ow}, out of a total number of incident waves, N_w, and there is also a maximum overtopping wave volume, V_{max}. This V_{max} depends on the storm duration and a longer storm may end up with a larger V_{max}. In order to apply Equation 5.52 for a specific case, one has to calculate the probability of overtopping, P_{ov}, or the number of overtopping waves, N_{ow}, where the relationship is given by:

$$P_{ov} = \frac{N_{ow}}{N_w}$$

$\qquad$ 5.55
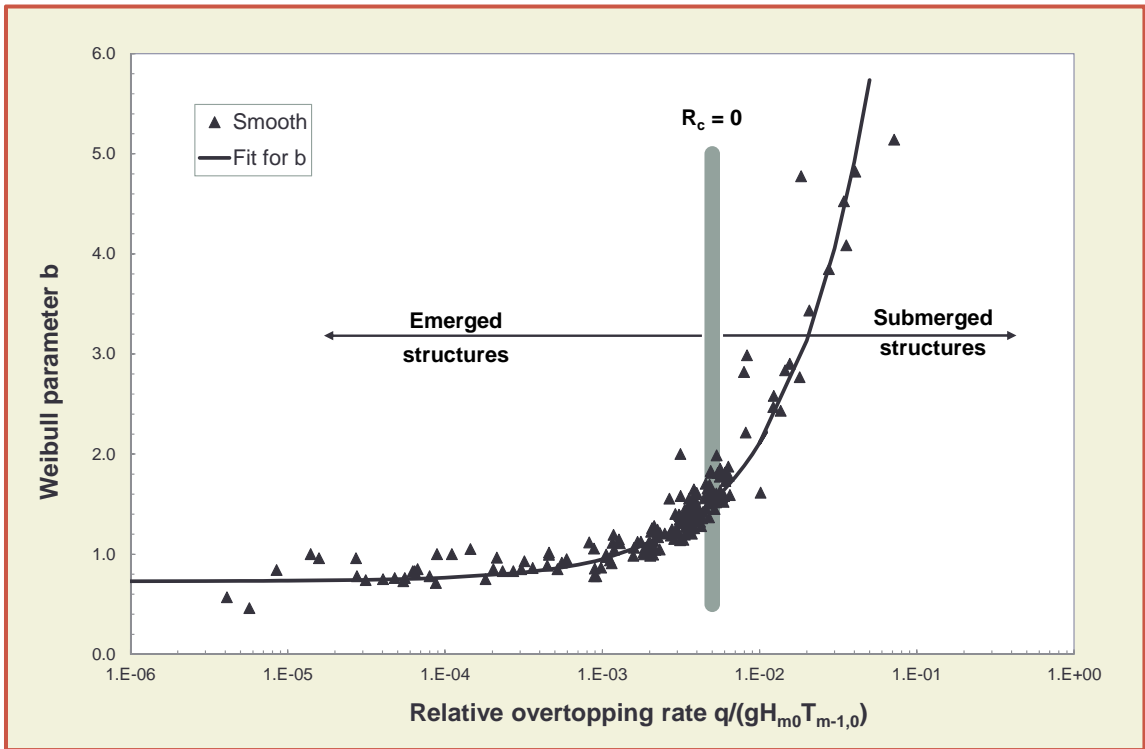
Figure 5.58: New Weibull shape factor, b, for smooth structures, spanning a large range of relative freeboards (Zanuttigh *et al.*, 2013)

Here the 2% run-up level, $R_{u2\%}$, becomes important, which has been described in Section 5.2. Although the 2% run-up level is no longer a direct design parameter for the required crest height, it still plays an important role in describing individual overtopping wave volumes. The probability of overtopping per wave can be calculated by assuming a Rayleigh-distribution of the wave run-up heights and taking $R_{u2\%}$ as a basis:

$$P_{ov} = \exp\left[-\left(\sqrt{-\ln 0.02}\,\frac{R_c}{R_{u2\%}}\right)^2\right]$$ (5.56)

For the prediction of the maximum overtopping volume in a given distribution the following formula can be used, by filling in the number of overtopping waves N_{ow}. Note that the prediction of this maximum volume is subject to some uncertainty, which is always the case for a maximum in a distribution.

$$V_{max} = a \cdot \left[\ln(N_{ow})\right]^{1/b}$$ (5.57)

Example

The probability distribution function for wave overtopping volumes per wave is calculated for a smooth dike with $\cot\alpha = 3$ and a freeboard of $R_c = 1.41$ m. The wave conditions are given by an incident wave height at the toe of the dike $H_{m0} = 1.0$ m, a peak period of $T_p = 4.0$ s (a wave steepness of $s_{op} = 0.040$), a spectral period of $T_{m-1,0} = T_p/1.1 = 3.63$ s and a mean period of $T_m = T_p/1.2 = 3.33$ s. The storm duration is 2 hours.

For these conditions, the wave run-up height is $R_{u2\%} = 2.65$ m (higher than the crest height) – Equations 5.4 and 5.5 and the average overtopping rate q = 10 l/s per m – Equations 5.12 and 5.13. The probability of overtopping per wave is $P_{ov} = 0.33$ – Equation 5.56. The b-value becomes b = 0.809 – Equation 5.54, and the scale factor becomes a = 0.090. The storm duration is 2 hours, resulting in 2159 incoming waves and 771 overtopping waves (about one-third of the waves). The largest predicted overtopping wave volume, based on the given distribution, will be $V_{max} = 922$ l per m – Equation 5.57.
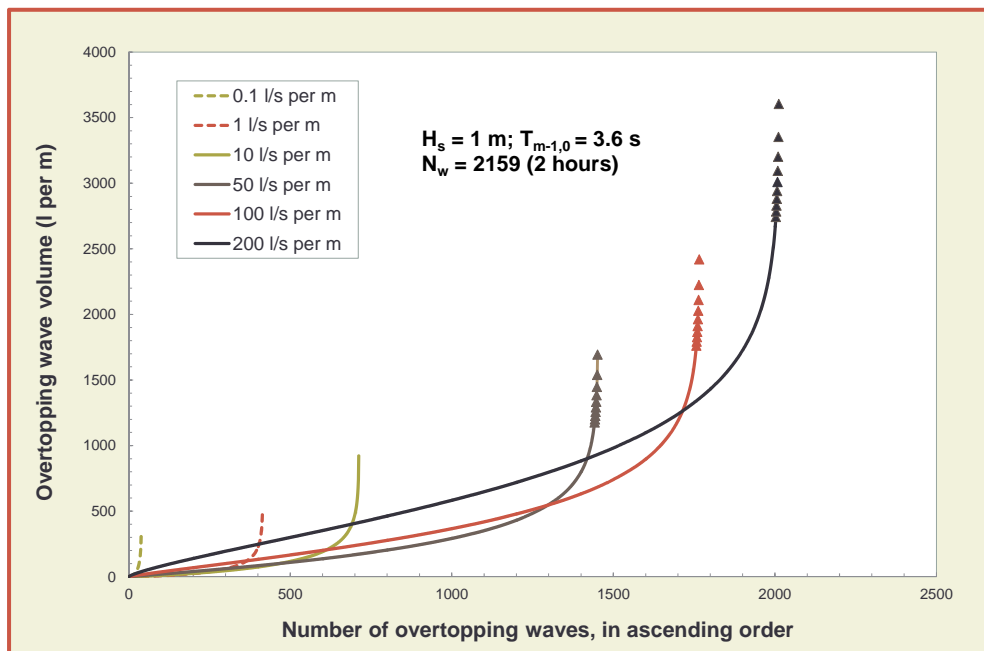
Figure 5.59: Distributions for overtopping wave volumes for a wave height of 1 m and various overtopping discharges. The triangles give the largest individual volumes
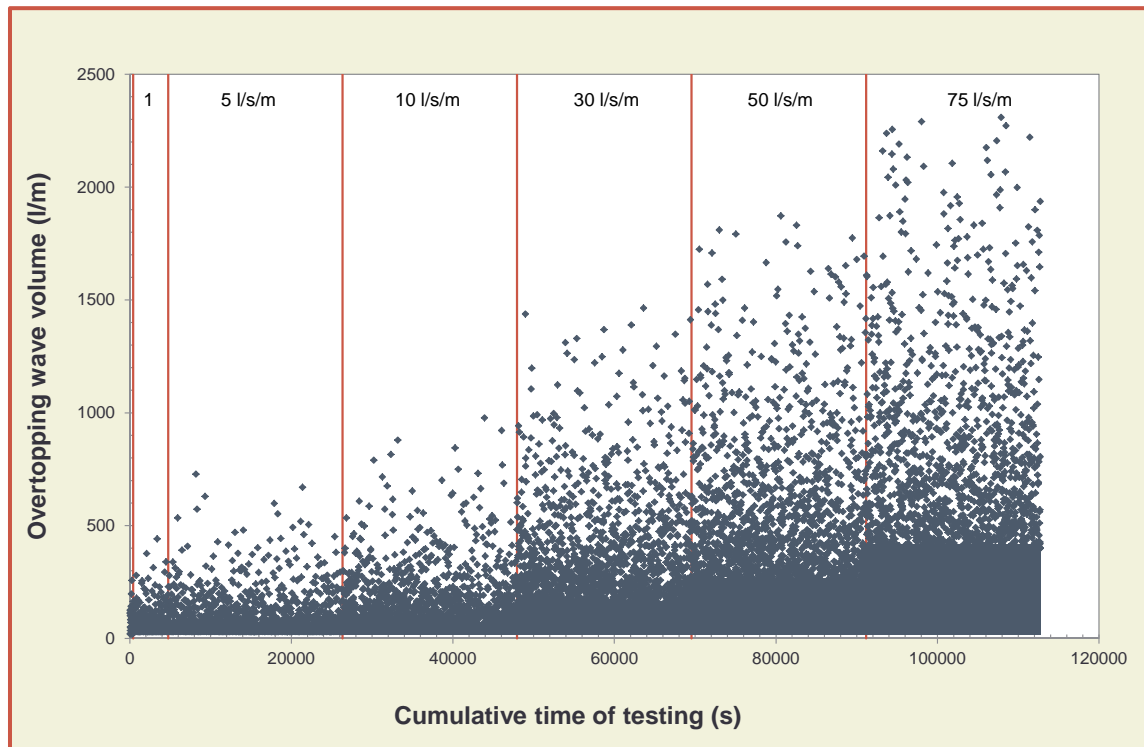
Figure 5.60:   Simulated overtopping wave volumes for increasing overtopping discharge, for a storm duration per sea state of 6 hours and for a wave height of $H_{m0} = 1.0$ m

The distribution of overtopping wave volumes is given in Figure 5.59 where the line for q = 10 l/s per m shows 771 overtopping waves and a maximum of 922 l per m. In order to show the difference with other overtopping discharges, for the same wave conditions but another freeboard to meet the given overtopping discharge, Figure 5.59 also gives the distributions for q = 0.1 l/s per m (almost nothing), 1; 50; 100 and 200 l/s per m. With increasing overtopping discharge the number of overtopping waves increase as well as the maximum overtopping wave volume.

Another way to show the random behaviour of wave overtopping and the differences between various overtopping discharges, is given in Figure 5.60. Here a simulation in time is given of storms with increasing overtopping discharges, where each condition has a duration of 6 hours. The wave conditions are the same as for the example (H_{m0} = 1 m and $T_{m-1,0}$ = 3.63 s). Wave overtopping gives a large number with relative small overtopping wave volumes (most points are close to the horizontal axis) and a limited number with larger volumes (the data points higher in the graph).

5.5.3 Overtopping flow velocities and thicknesses at the seaward slope

Average overtopping rates are not appropriate to describe the interaction between the overtopping flow and the failure mechanisms (infiltration and erosion) of a dike or similar structure. Also, the overtopping wave volumes are not the direct input to this kind of calculation, rather it are the flow velocities and flow thicknesses of overtopping wave volumes. Research has been carried out in small and large scale model tests to investigate the overtopping flow, where first results have been described in Schüttrumpf and Van Gent (2003), later added by results from the FlowDike-project, Lorke *et al.* (2012). All results together have been analysed by Van der Meer (2011) and Van der Meer *et al.* (2012) and a summary is given here. Distinction is made between flow velocities and related flow depths on the seaward slope, the dike crest and the landward slope.

The engineering design parameter for wave run-up is the level on the slope that is exceeded by 2% of the up-rushing waves ($R_{u2\%}$). Sections 5.2 to 5.4 give methods to calculate the overtopping discharge as well as the 2% run-up level for all kinds of wave conditions and for many types of coastal structures. Knowing the 2% run-up level for a certain condition is the starting point to describe the wave run-up process.

Assuming a Rayleigh distribution of the run-up levels and knowing $R_{u2\%}$ gives all the required run-up levels, see Equation 5.56 in the previous section.

The wave run-up level is a start, but also run-up velocities and flow thicknesses are required. From the wave overtopping tests it is known that the front velocity is the governing parameter in initiating damage to a grassed slope. Focus should therefore be on describing this front velocity along the upper slope, the crest and the landward slope. In the run-up phase, however, front velocities and maximum velocities at a certain location may be different, due to the preceding breaking of the wave; this will be explained later. By only considering random waves and the 2%-values, the equations for (maximum) run-up velocity and (maximum) flow thickness at a certain location on the seaward slope become, see also Figure 5.61:

$$v_{A,2\%} = c_{v2\%}(g(R_{u2\%} - z_A))^{0.5}$$

5.58

$$h_{A,2\%} = c_{h2\%}(R_{u2\%} - z_A)$$

5.59

where $v_{A,2\%}$ is the run-up velocity exceeded by 2% of the up-rushing waves, $c_{v2\%}$ is a coefficient, g the acceleration due to gravity, $R_{u2\%}$ the 2%-level of wave run-up related to the still water level, z_A the location on the seaward slope (in the run-up zone, related to SWL), $h_{A,2\%}$ the flow thickness exceeded by 2% of the up-rushing waves and $c_{h2\%}$ is a coefficient. No distinction is required for breaking and non-breaking waves since wave breaking is considered in the calculation of the wave run-up height $R_{u2\%}$.
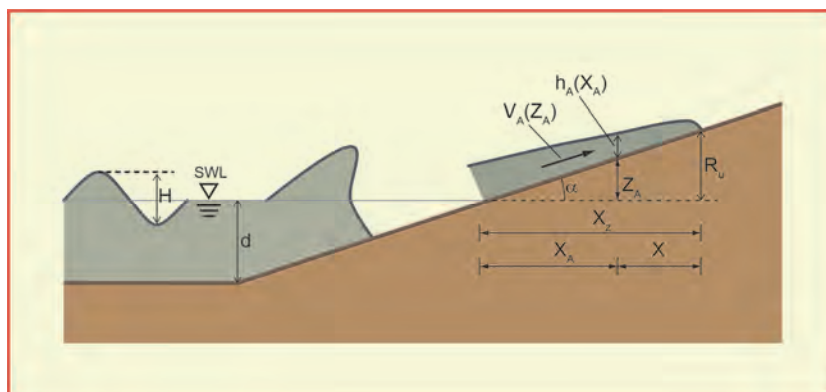
Figure 5.61: Definition sketch for flow thickness and wave run-up velocities on the seaward slope

The main issue is to find the correct values of $c_{v2\%}$ and $c_{h2\%}$, but comparing the results of various research studies (Van der Meer *et al.*, 2012) gives the conclusion that they are not consistent. The best conclusion at this moment is to take $c_{h2\%} = 0.20$ for slopes of 1:3 and 1:4 and $c_{h2\%} = 0.30$ for a slope of 1:6. Consequently, a slope of 1:5 would then by interpolation give $c_{h2\%} = 0.25$. This procedure is better than to use a formula like $c_{h2\%} = 0.055 \cot\alpha$, as given in EurOtop [2007]. One can take $c_{v2\%} = 1.4$-1.5 for slopes between 1:3 and 1:6.

Moreover, the general form of Equation 5.58 for the maximum velocity somewhere on a slope, may differ from the front velocity of the up-rushing wave. Van der Meer (2011) analysed individual waves rushing up the slope. Front velocities were obtained from a record of the wave run-up by taking a certain distance that the front has passed over the slope in a certain time. Part of the (smoothed) record of one test has been given in Figure 5.62, including the method of analysis.

Maximum velocities, the location of this velocity on the slope and the maximum wave run-up of that specific wave were found by data processing. A closer inspection of Figure 5.62 shows that often the first part of the wave run-up record is almost straight and the front velocity slows down quickly only close to the maximum run-up level. The velocity records in Figure 5.62 show a certain duration where the velocity is quite close to the maximum velocity (which is always a little peaked), say within about 20% of the peak

value. For this reason the combined record of wave run-up and front velocity was judged by eye and three other locations were established from the data. In total the following locations where derived, see also Figure 5.62.

1. $R_{u\ start}$:   the location where the run-down changes into run-up
2. $R_{u\ min}$ at $\sim u_{max}$:   the lowest location where the velocity is within about 20% of its maximum velocity
3. R_u at u_{max}:   the location where u_{max} has been calculated (data processing)
4. $R_{u\ max}$ at $\sim u_{max}$: the highest location where the velocity is within about 20% of its maximum velocity
5. $R_{u\ max}$:   the maximum run-up level (data processing)
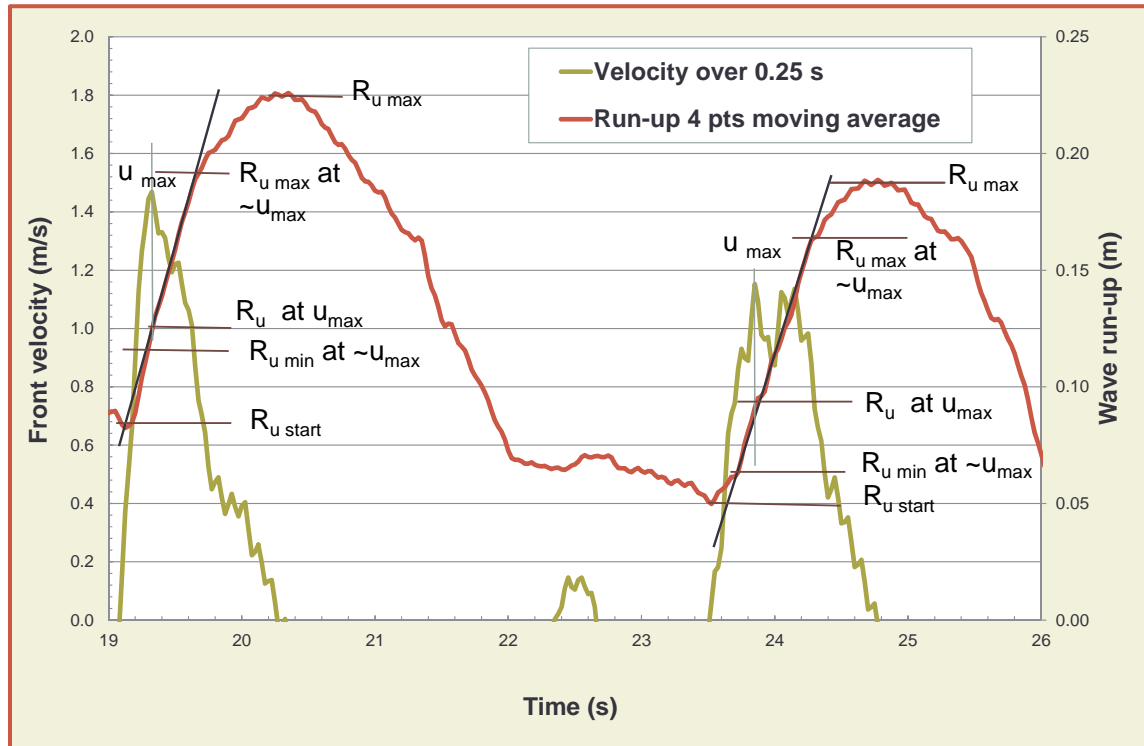
Figure 5.62:   Record of two up-rushing waves with derived velocity from this record. Definition of five run-up levels

The total analysis can be found in Van der Meer (2011). Based on this analysis the following conclusion on the location of maximum or large velocities and front velocities in the run-up of waves on the seaward slope of a smooth dike can be drawn, which is also shown graphically in Figure 5.63.

On average, the run-up starts at a level of 15% of the maximum run-up level, with a front velocity close to the maximum front velocity and this velocity is more or less constant until a level of 75% of the maximum run-up level. The real maximum front velocity on average is reached between 30%-40% of the maximum run-up level. Figure 5.63 also shows that a square root function as assumed in Equation 5.58,which is valid for a maximum velocity at a certain location (not the front velocity) is different from the front velocity. The process of a breaking and impacting wave on the slope has influence on the run-up, it gives a kind of acceleration to the up-rushing water. This is the reason why the front velocity is quite constant over a large part of the run-up area.

Further analysis showed that there is a clear trend between the maximum front velocity in each up-rushing wave and the (maximum) run-up level itself, although there is considerable scatter. Figure 5.64 shows the final overall figure (detailed analysis in Van der Meer, 2011), where front velocity and maximum run-up level of each wave were made dimensionless. Note that only the largest front velocities have been analysed and that the lower left corner of the graph in reality has a lot of data, but will be less significant with respect to effect on failure mechanisms.
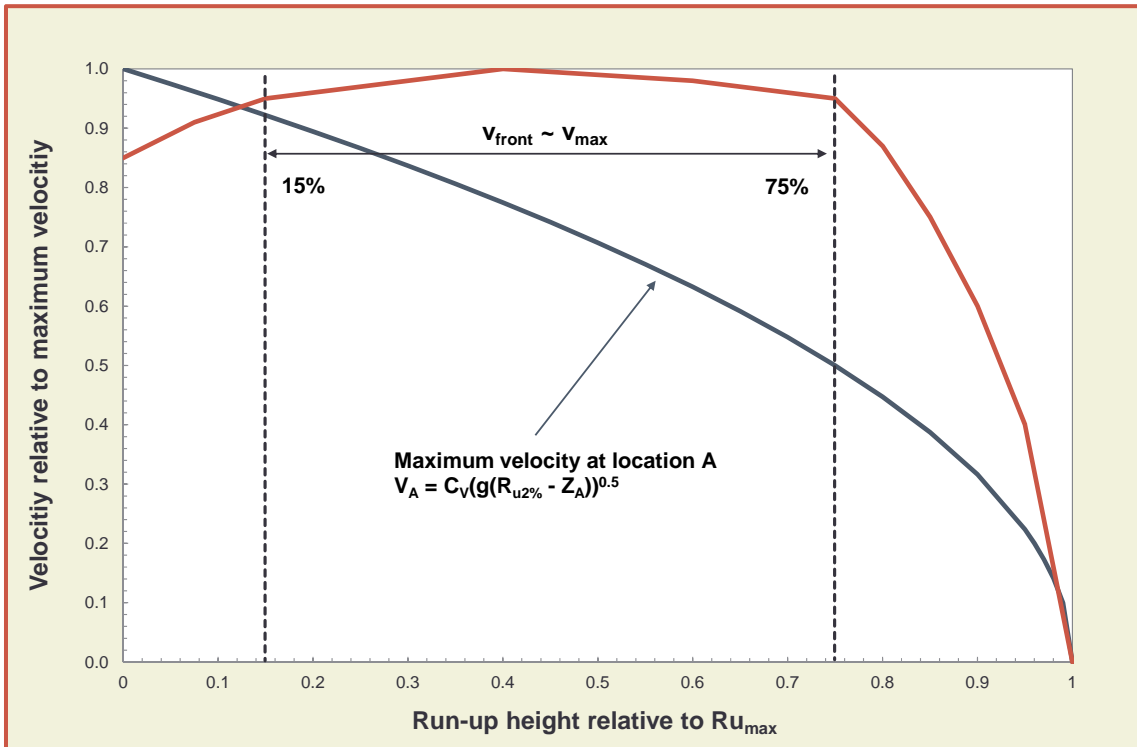
Figure 5.63: General trend of front velocity over the slope during up-rush (red line), compared to the theoretical maximum velocity at a certain location (dark line)
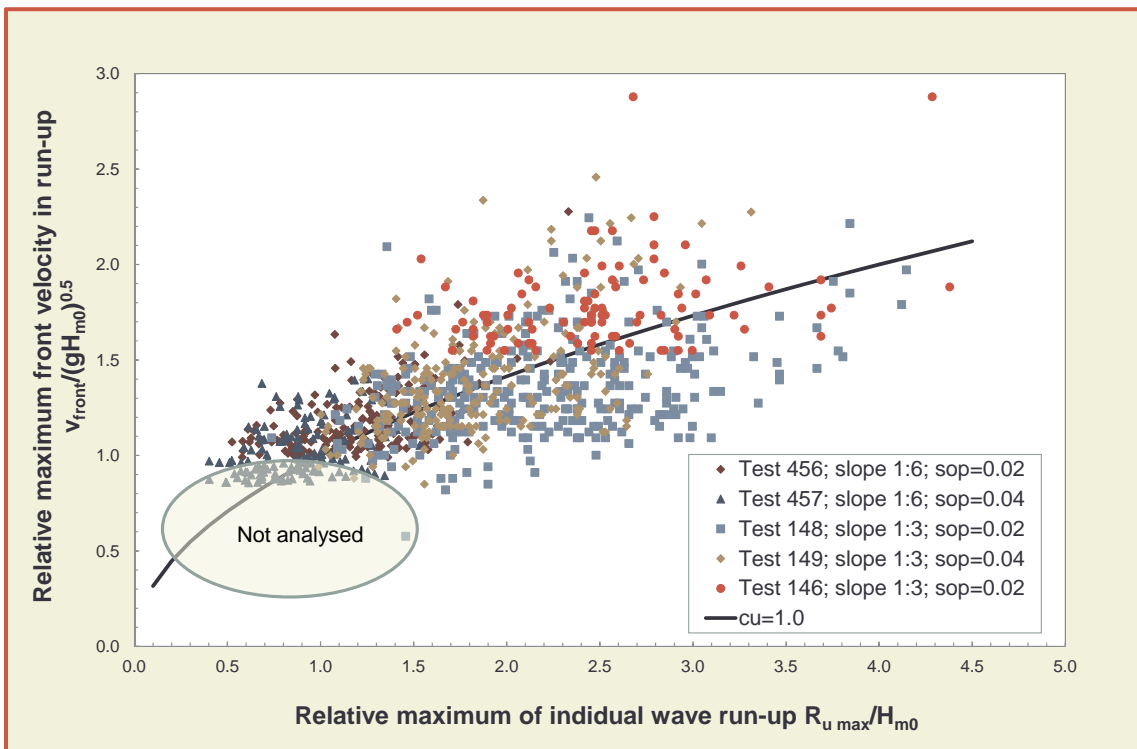
Figure 5.64: Relative maximum front velocity versus relative run-up on the slope; all tests

The trend and conclusion in Figure 5.63 explains, in part, why the relationship between the maximum front velocity and the maximum run-up in Figure 5.64 gives a lot of scatter. A front velocity close to the maximum velocity is present over a large part of the slope and the actual location of the maximum velocity may be more or less "by accident". The trend given in Figure 5.64 can be described by:

$$\frac{\mathrm{v}_{front}}{\sqrt{(gH_{m0}}}=c_u\sqrt{\frac{Ru_{max}}{H_{m0}}}$$

5.60

with c_u is a stochastic variable $\mu(c_u) = 1.0$, a normal distribution with coefficient of variation $\sigma' = 0.25$.

An application is shown in Figure 5.65 for a wave height of $H_{m0} = 2.0$ m with a peak period of $T_p = 5.7$ s (a wave steepness of $s_{op} = 0.040$), a spectral period of $T_{m-1,0} = 5.18$ s, a mean period of $T_m = 4.75$ s and a duration of 1 hour. The slope of the structure is $\cot\alpha = 3$. The 2% run-up becomes $R_{u2\%} = 5.34$ m from Equations 5.4 and 5.5 and is given by the crossing with the red line in Figure 5.65. The run-up distribution is a straight line on a Rayleigh scale and this scale has been used in the graph. For each run-up level the front velocity can be calculated with 5.60, which gives the curved line in the graph. The front velocity at the 2%-level is just over 7 m/s where the largest run-up gives a front velocity of more than 8 m/s. Note that in these calculations the average line in Figure 5.64 has been taken and that the significant scatter has not been taken into account.
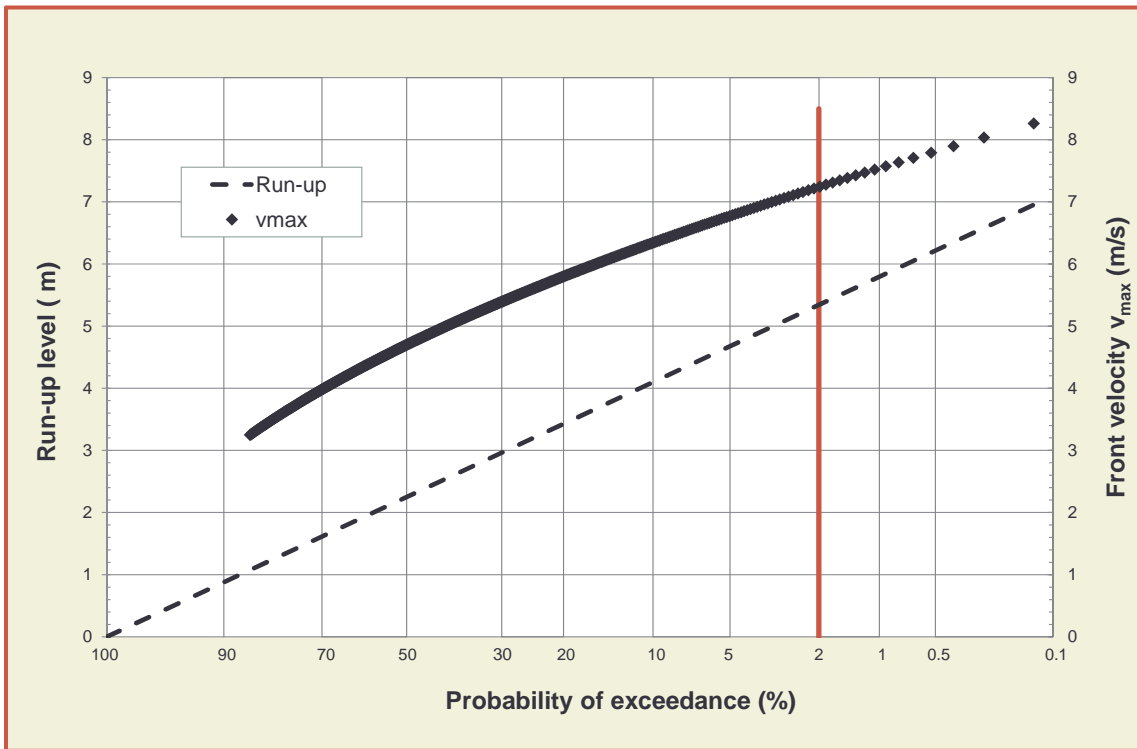
Figure 5.65: Distribution of wave run-up levels and front velocities on a slope of 1:3 and a wave height of $H_{m0} = 2$ m

5.5.4 Overtopping flow velocities and thicknesses at the crest

If an up-rushing wave reaches the crest, it will flow over the crest and Figure 5.66 shows a sequence for a regular wave of 1 m height and period of 9.5 s running over the crest of a smooth dike. Note that the overtopping tongue arrives as a very turbulent flow at the dike crest. The water is full of air bubbles and the flow can be called "white water flow". The overtopping flow separates slightly from the dike surface at the front edge of the crest. No flow separation occurs at the middle or at the rear edge of the crest. In the second overtopping phase, the overtopping flow has crossed the crest. Less air is in the overtopping flow but the flow itself is still very turbulent with waves in flow direction and normal to flow direction. In the third overtopping phase, a second peak arrives at the crest resulting in nearly the same flow thickness as the first peak. In the fourth overtopping phase, the air has disappeared from the overtopping flow and both overtopping velocity and flow thickness are decreasing. Finally, the overtopping flow nearly stops on the

dike crest for small overtopping flow thicknesses. Little air is in the overtopping water. At the end of this phase, the overtopping water on the dike crest starts flowing seaward.

Note that with shorter and random waves, and waves over a crest covered with grass, the flow may show a different behaviour, certainly with respect to a second peak coming over (see also Figure 5.56, where no second peak is present).

The flow parameters at the transition line between the seaward slope and dike crest are the initial conditions for the overtopping flow on the dike crest. The evolution of the overtopping flow parameters on the dike crest will be described below. The overtopping flow thickness on the dike crest depends on the width of the crest B and the co-ordinate on the crest x_C (Figure 5.67). The overtopping flow thickness on the dike crest decreases directly behind the seaward crest and remains almost constant along the crest, for a smooth crest. This decrease in flow thickness may be explained by the change in flow direction, from up the slope to horizontal (Van der Meer *et al.* 2012). This decrease is to about two thirds of the flow thickness at the seaward slope (Equation 5.59). This differs from guidance in EurOtop (2007) and not much is known about the distance it takes to reduce to two thirds of the initial flow thickness.

The decay of flow velocity along the crest is a function of the distance from the seaward edge, made dimensionless with the wave length $L_{m-1,0} = gT^2_{m-1,0}/(2\pi)$ and is given by Equation 5.61. If the crest would be very wide, like for a promenade, Equation 5.61, might not be accurate anymore.

$$v_{2\%}(x_C)/v_{2\%}(x_C=0) = \exp(-1.4\, x_C / L_{m-1,0}) \qquad 5.61$$

Test conditions:
Regular wave: H=1.0m; T=9.5s; h=5.0m
Dike geometry: R_C=1.0m; 1:n = 1:6; 1:m = 1:3; B_C=2.0m
Average overtopping discharge: q=120 l/(sm)
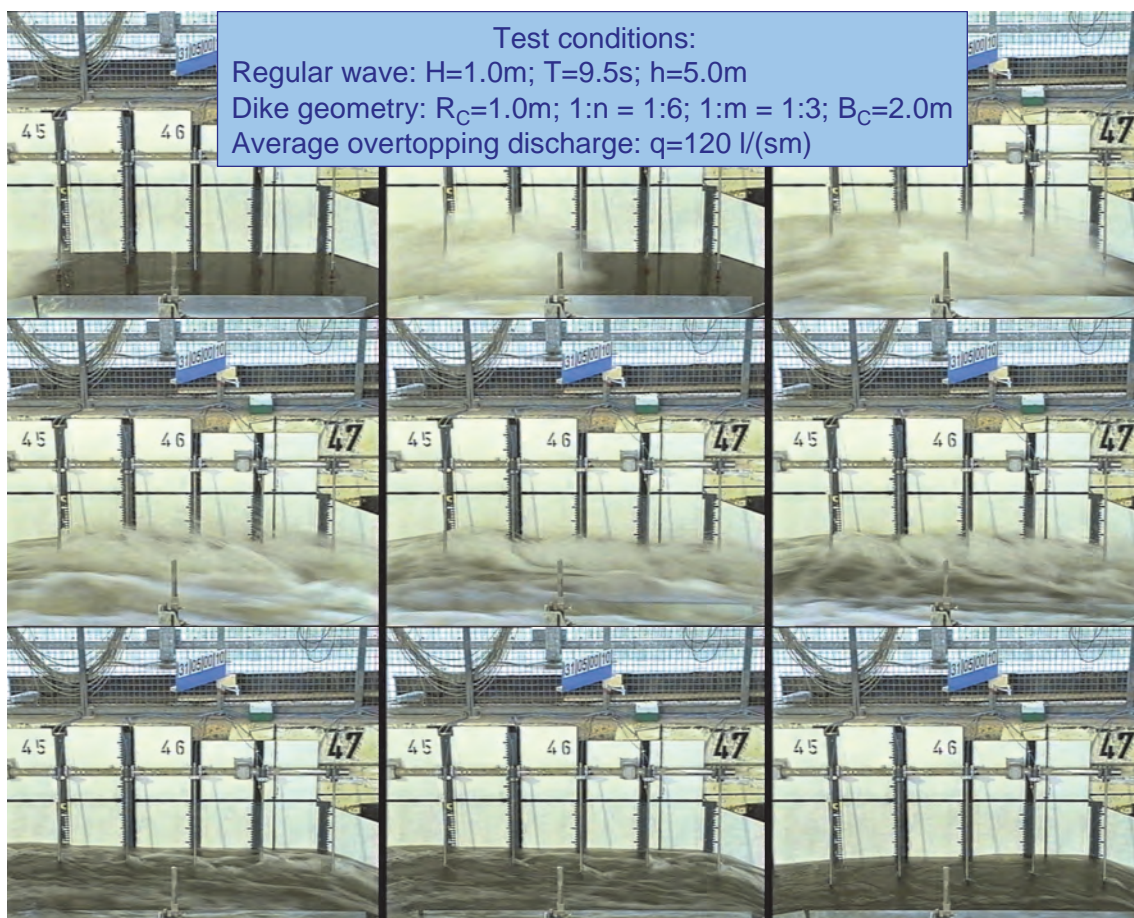
Figure 5.66:   Sequence showing the transition of overtopping flow on a dike crest (1 m regular wave with a period of 9.5 s; Large Wave Flume, Hannover)
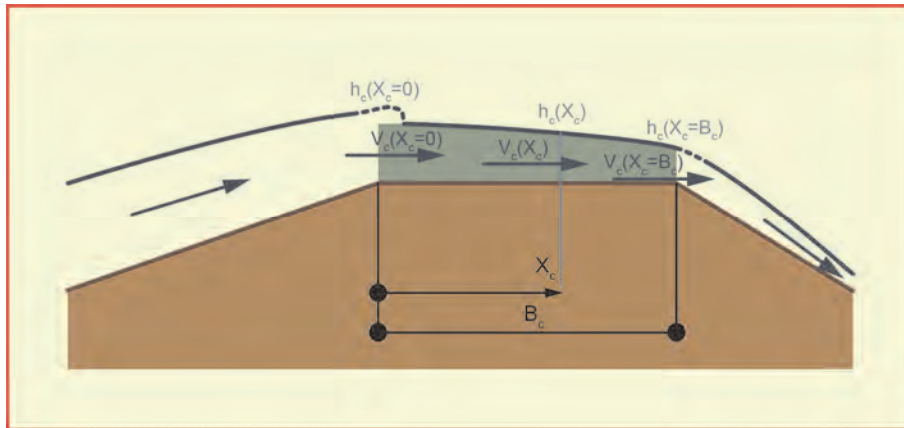
Figure 5.67:   Definition sketch for overtopping flow parameters on the dike crest

5.5.5 Overtopping flow velocities and thicknesses at the landward slope

The overtopping water flows from the dike crest to the landward slope of the dike. The description of the overtopping process on the landward slope is very important with respect to dike failures which often occurred on the landward slope in the past. Figure 5.68 shows overtopping waves over a dike, for overtopping tests in the Large Wave Flume in Hannover, where the landward slope was quite smooth.

Figure 5.69 shows overtopping waves over a dike, where the sequence was taken during simulation of a very large overtopping wave of 5.5 m^3 per m, or 22 m^3 for the 4 m width shown, from the wave overtopping simulator on a real grass dike. The turbulence and air entrainment in real situations is clear (and probably much larger than in small scale investigations).
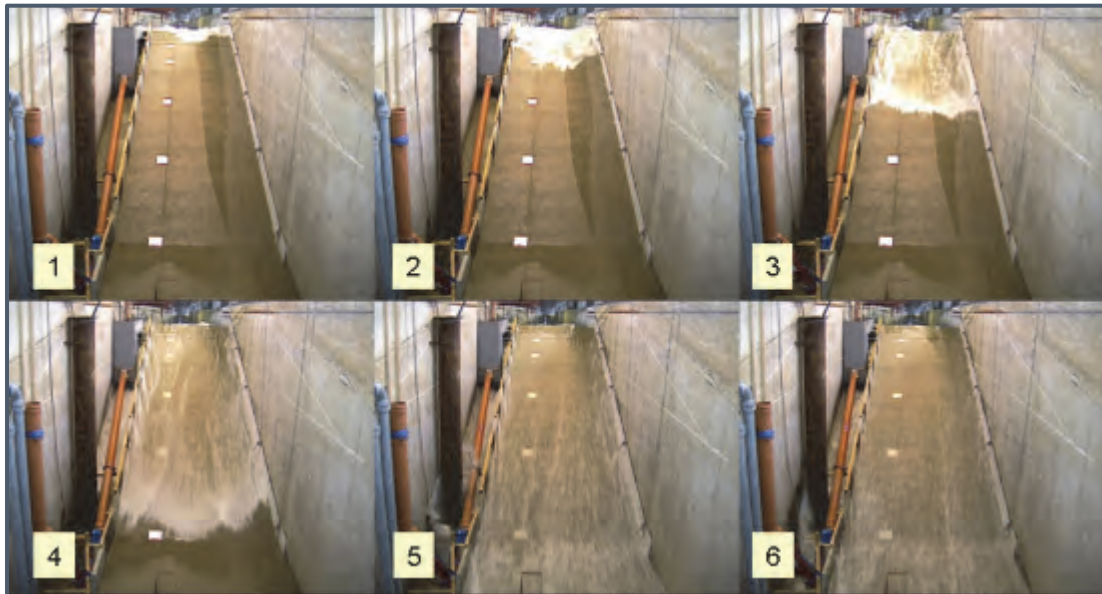
Figure 5.68:   Overtopping flow on the landward slope (Large Wave Flume, Hannover)

An analytical function was developed which describes overtopping flow velocities and overtopping flow thicknesses on the landward slope as a function of the overtopping flow velocity at the end of the dike crest ($v_{b,0} = v_C(x_C = B)$), the slope angle β of the landward side and the position s_B on the landward side with $s_B = 0$ at the intersection between dike crest and landward slope. A definition sketch is given in Figure 5.70.
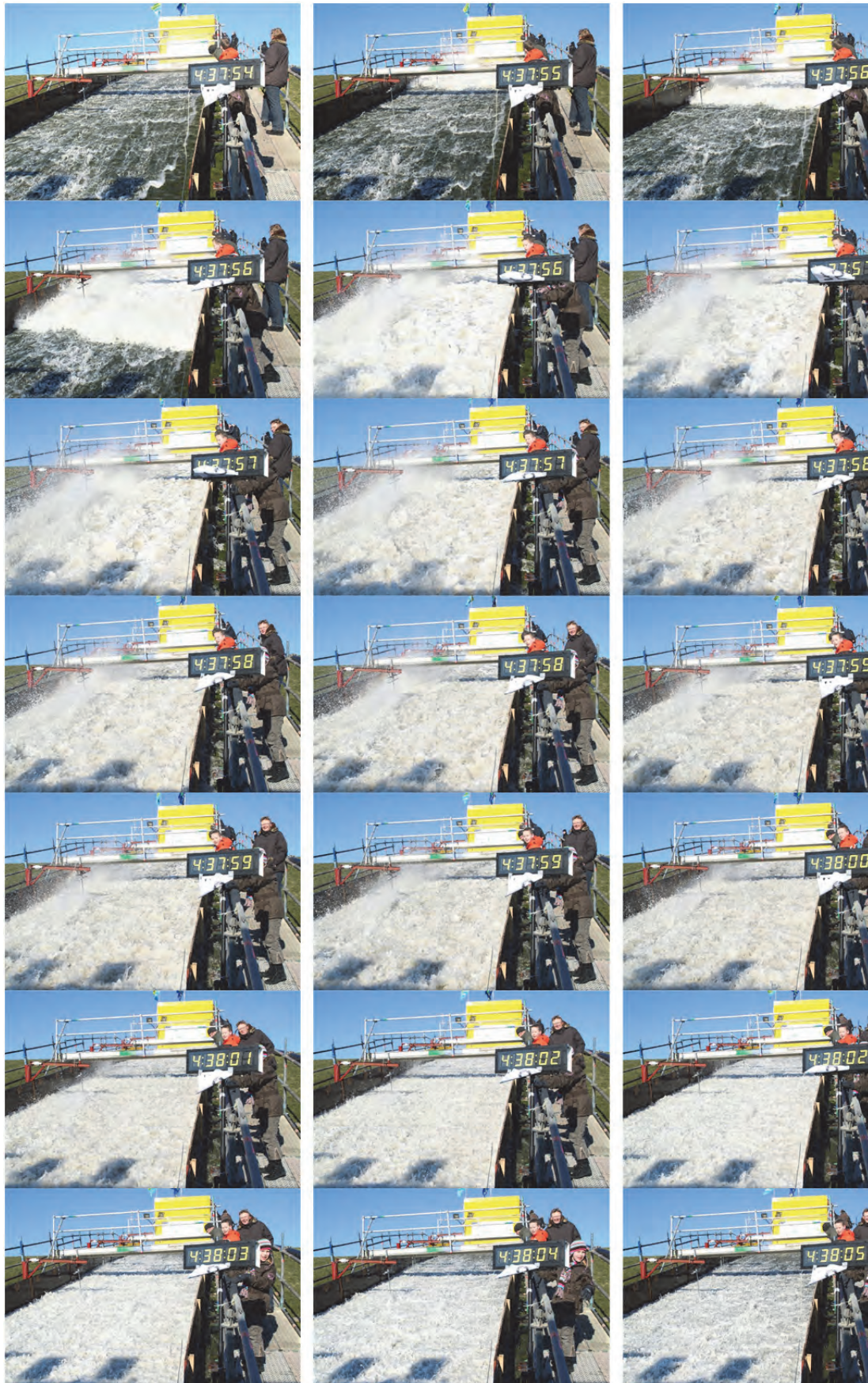
Figure 5.69:   Release of an overtopping wave of 5.5 m^3 per m by the wave overtopping simulator
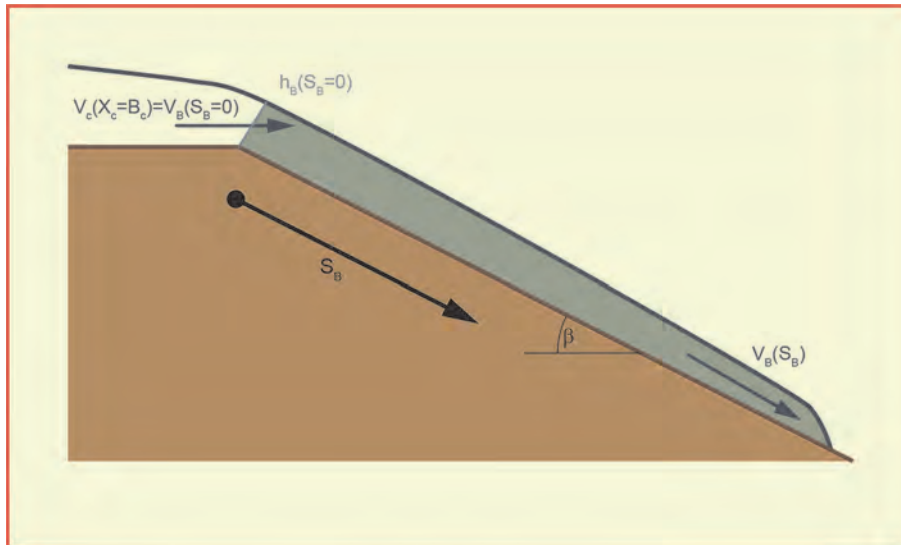
Figure 5.70: Definition of overtopping flow parameters on the landward slope

The following assumptions were made to derive an analytical function from the Navier-Stokes equations: velocities vertical to the dike slope can be neglected; the pressure term is almost constant over the dike crest; and the viscous effects in the flow direction are small. This results in the following formula for overtopping flow velocities:

$$v_b = \cfrac{v_{b,0} + \cfrac{k_1 h_b}{f} \tanh\left(\cfrac{k_1\, t}{2}\right)}{1 + \cfrac{f\, v_{b,0}}{h_b\, k_1} \tanh\left(\cfrac{k_1\, t}{2}\right)}$$

with:

$$t \approx -\frac{v_{b,0}}{g\,\sin\beta} + \sqrt{\frac{v_b^{\,2}}{g^2 \sin^2\beta} + \frac{2\,s_b}{g\,\sin\beta}} \quad \text{and} \quad k_1 = \sqrt{\frac{2\,f\,g\,\sin\beta}{h_b}}$$

5.62

Equation 5.62 needs an iterative solution since the overtopping flow thickness h_b and the overtopping flow velocity v_b on the landward slope are unknown. The overtopping flow thickness h_b can be replaced in a first step by:

$$h_b = \frac{v_{b,0} \cdot h_{b,0}}{v_b}$$

5.63

with $v_{b,0}$ the overtopping flow velocity at the beginning of the landward slope ($v_{b,0} = v_B(s_B = 0)$); and $h_{b,0}$ the overtopping flow thickness at the beginning of the landward slope ($h_{b,0} = h_B(s_B = 0)$).

The overtopping flow on the landward slope tends towards an asymptote for $s_b \to \infty$ which is given by:

$$v_b = \sqrt{\frac{2 \cdot g \cdot h_b \cdot \sin\beta}{f}}$$

5.64

An important factor influencing the overtopping flow on the landward slope is the bottom friction coefficient f which has to be determined experimentally. References in the past were all based on smooth slopes,

often made of plywood or mortar in physical scale facilities and the mean value amounted to about f = 0.02. Specific hydraulic measurements were performed recently with overtopping wave volumes released by the wave overtopping simulator on a landward slope, covered with grass, of about 1:3, see Figure 5.71. The length of this slope was about 18 m and measurements were concentrated around the upper half, as the theory given by Equation 5.62 predicts a fast increase in velocity over the first 5 m. Seven velocity meters were placed over about 7 m length and a final one 14 m from the crest line. The measurements were repeated three times.

Figure 5.71 shows the crest and landward slope with the location of the measurements and gives with the black line the prediction by Equation 5.62. In this calculation (and also for other test situations) a friction factor of f = 0.01 was found to give the best correlation with measurements, which is a little smaller than the value of 0.02 above. The value of f = 0.01 was found, however, on a real dike with flow velocities at the crest between 4 m/s and 6 m/s. Figure 5.71 gives the measurements for a flow velocity at the crest of about 6 m/s. The measurements showed that the flow *thickness* was under-predicted by Equation 5.63 and the main reason may be that these overtopping waves may have 20% to 30% air entrained, where the measurements included this air entrainment. For wave overtopping on real dikes covered with grass, it is recommended to use a friction factor f = 0.01 in Equation 5.62.
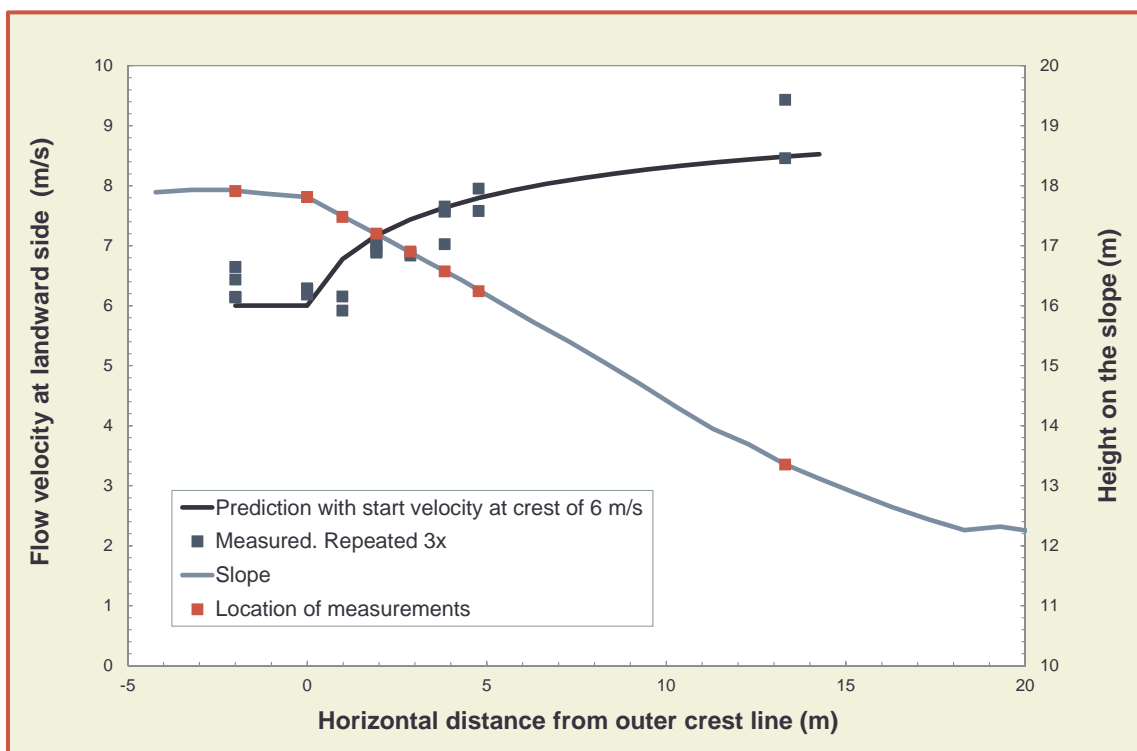
Figure 5.71:   Increase of flow velocity over the landward side of a grass covered dike, measured and predicted (Equation 5.62) with f = 0.01

In Figure 5.72, the influence of the landward slope on overtopping flow velocities is shown, based on Equation 5.62 with f = 0.01 and where the solid lines are for an initial velocity at the crest of 4 m/s and the dashed lines for an initial velocity of 6 m/s. The landward slope was varied between 1:2.4 and 1:5, which is a practical range. The graph does not show the flow velocity itself, but the velocity increase with respect to the initial velocity at the edge of the crest. An increase factor of 1.4 means that the velocity over the slope has increased by 40%. It is obvious that overtopping flow velocities increase for steeper slopes. The increase for a gentle slope of 1:5 is limited to about 20%, but for a steep 1:2.4 slope an initial velocity at the crest of the dike of 6 m/s may end up near the toe of the dike with a velocity of 9 m/s (50% increase). The trend for flow thickness is of course opposite, due to the larger velocity the flow thickness will naturally decrease. The graph shows a clear reason why wave overtopping at grass covered dikes

often occurs at the lower part of the slope: the front velocity is much larger in this area than close to the crest of the dike or levee.
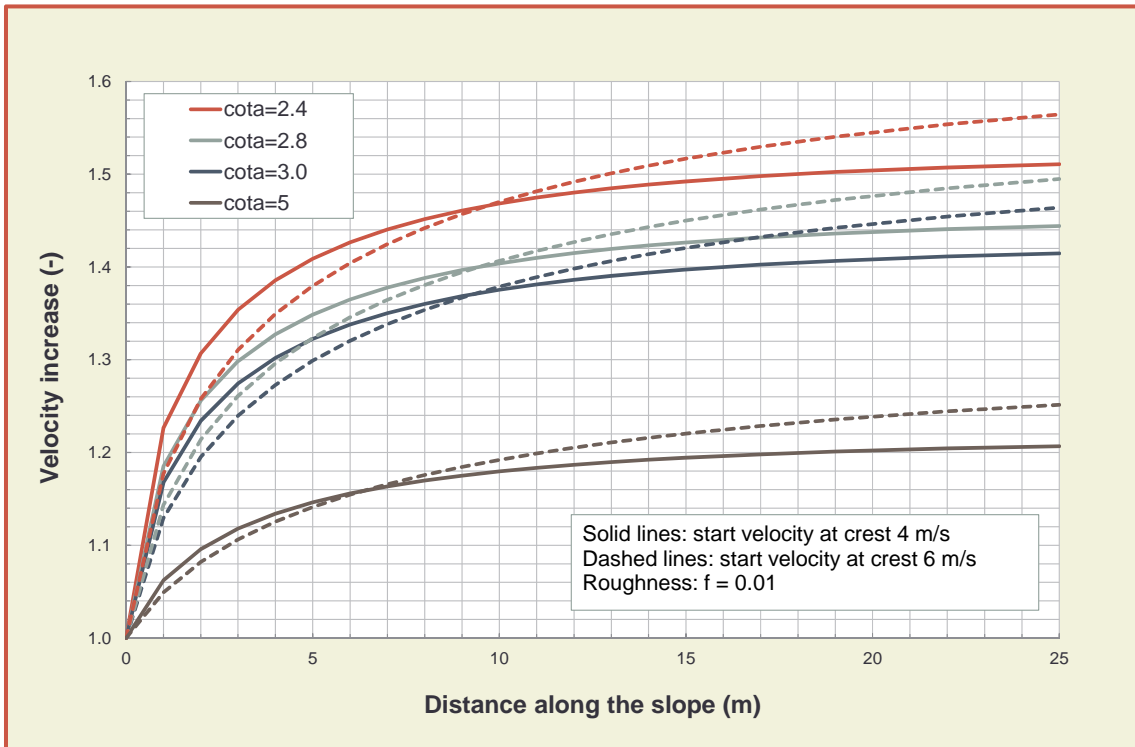
Figure 5.72: Increase of flow velocities over a grass covered landward slope of a dike, for various slope angles

5.6 Scale effects and uncertainties for dikes and embankments

A couple of investigations on the influence of wind and scale effects are available for sloping structures, mainly based on the CLASH-project or the predecessor OPTICREST. The results for rubble mound (rough) structures will be described in Section 6.3.6. The investigation did not show significant influence of wind on wave overtopping at dikes, levees or embankments, as they are generally smooth and covered e.g. by grass, revetment stones or asphalt which all have roughness coefficients larger than $\gamma_f = 0.9$. Hence, there are no significant scale effects for these large influence factors on roughness. This is however only true if the model requirements as given in Table 4.5 in Section 4.9 are respected.

For rough slopes as they e.g. occur for any roughness elements on the seaward slope, scale effects for low overtopping rates cannot be excluded and therefore, the procedure as given in Section 6.3.6 should be applied.

The model uncertainty is considered as the accuracy, with which a model or method can describe a physical process or a limit state function. Therefore, the model uncertainty describes the deviation of the prediction from the measured data due to this method. In this chapter often graphs have been given with the mean prediction line, the data and the 5% exceedance lines, giving the 90% confidence band. The definition of model uncertainty has been given by Equation 1.3 and model uncertainty has been described in Section 1.5.4.

The explicit model uncertainty has often been given by taking one or two coefficients in the equation as a stochastic variable. For example, the reliability of Equation 5.10 is given by $\sigma(0.023) = 0.003$ and $\sigma(2.7) = 0.20$, and of Equation 5.11 by $\sigma(0.09) = 0.0135$ and $\sigma(1.5) = 0.15$ and graphs were given in Figure 5.12 and Figure 5.13. The model effects include repeatability of tests, model effects, uncertainties in wave measurements and also the accuracy of the equation itself by the assumption of the shape of the equation to represent nature. The uncertainties for the assessment of design parameters in reality, such as the wave height, the wave period, the water depth, the angle of wave attack, geometrical parameters

such as the crest height and the slope angle and real roughness and or permeability of the slope, are not included.

The uncertainties of part of these parameters may be estimated following an analysis of expert opinions from Schüttrumpf *et al.* (2006) using coefficients of variations (σ') for the wave height H_{m0} (3.6%), the wave period (4.0%), and the slope angle (2.0%). Other parameters are independent of their mean values so that standard deviations (prototype measures) can be used for the water depth (0.1 m), the crest height and the height of the berm (0.06 m), and the friction factor (0.05). It should be noted that these uncertainties should only be used if no better information (e.g. measurements of waves) are obtainable.

Using these values of uncertainty together with the already proposed model uncertainties for the parameters for Equation 5.10, crude Monte Carlo simulations were performed to obtain the uncertainty in the resulting mean overtopping discharges.

Results are shown in Figure 5.73. The data points come from the calculations of the Monte Carlo simulations. The graph gives the mean value approach as well as the design and assessment approach (+1σ) and the 5%-exceedance lines for Equation 5.10 with black lines. Then the resulting +σ and –σ lines from the Monte Carlo simulations are given by respectively red and green dashed lines. Finally the +5% and -5%-exceedance lines from the Monte Carlo simulations are given by bold red and green lines.

By comparison of the lines from the equation and the simulations, it can be seen that the resulting curves from the Monte Carlo simulations are only giving slightly larger uncertainty bands than the lines resulting from calculations with model uncertainty only. This suggests a very large influence of the model uncertainty so that no other uncertainties, if assumed to be in the range as given above, need to be considered. It is therefore proposed to use Equations 5.10 and 5.11 as suggested in Section 5.3.1. In case of a design and assessment approach, Equations 5.12 and 5.13 should be used with no further adaptation of parameters. In case of probabilistic calculations, Equations 5.10 and 5.11 should be used and uncertainties of all input parameters should be considered in addition to the model uncertainty. If detailed information of some of these parameters is not available, the uncertainties as proposed above may be used.
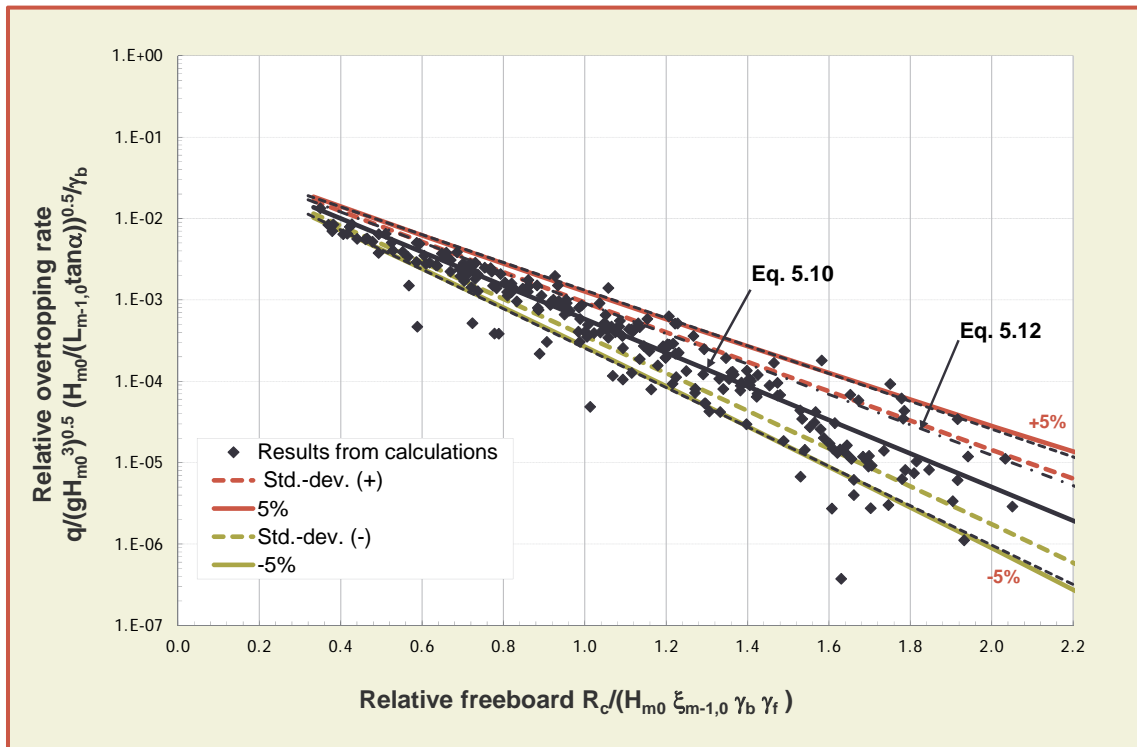
Figure 5.73: Wave overtopping over smooth slopes, showing results from Monte Carlo simulations, including uncertainty calculations

It should be noted that only uncertainties for mean wave overtopping rates are considered here. Other methods such as flow velocities and flow depths were not considered here but can be dealt with using the principal procedure as discussed in Section 1.5.

It should be noted that only uncertainties for mean wave overtopping rates are considered here. Other methods such as flow velocities and flow depths were not considered here but can be dealt with using the principal procedure as discussed in Section 1.5.

6 Armoured rubble slopes and mounds

6.1 Introduction

Armoured rubble slopes and mounds are characterized by a mound with some porosity or permeability, covered by a sloping porous armour layer consisting of large rock, see Figure 6.1, or concrete units, see Figure 6.2. Also shingle beaches belong to the rubble mound structures, see Figure 6.2 upper left. In contrast to dikes and embankment seawalls the permeability of the structure and armour layer plays a role in wave run-up and overtopping. The cross-section of a rubble mound slope, however, may have great similarities with an embankment seawall and may consist of various slopes, but generally they have steeper slopes.

Figure 6.1:   Rock armoured structures: seawall; rock breakwater; berm breakwater; berm breakwater head

As rubble mound structures are to some extent similar to dikes and embankment seawalls, the basic wave run-up and overtopping formulae are taken from Chapter 5, and it is strongly proposed that users of this manual take note of Chapter 5 before applying Chapter 6. The design formulae in Chapter 5 will then be modified, if necessary, to fit for rubble mound structures. Also for most definitions the reader is referred to Chapter 5 (or Section 1.4). More in particular:

- the definition of wave run-up (Figure 5.4)

- the general wave run-up formula (Equations 5.1 and 5.2)

- the general wave overtopping formula (Equations 5.10 and 5.11)

- the influence factors γ_b, γ_f and γ_β (Section 5.4)

- the spectral wave period $T_{m-1,0}$ (Section 1.4.2)

- the mean value approach and the design and assessment approach (Section 1.5.5).

Figure 6.2: Shingle beach and rubble mound structures: shingle beach; antifer cubes; tetrapode; accropode II

The main calculation procedure for armoured rubble slopes and mounds is given in Table 6.1, which gives also guidance through the chapter. First wave run-up and proportion or percentage of overtopping waves will be described and a graph for wave run-down has been given. Then overtopping for three types of structures has been given, rubble mound breakwaters or seawalls, berm breakwaters and shingle beaches (defined by 2%-run-up level). Influence factors will be discussed for roughness/permeability, oblique waves and the width of the rubble mound armour crest. Overtopping wave volumes have been described and finally scale effects in wave overtopping which are present in small scale models for small overtopping rates.

Table 6.1: Main calculation procedure for armoured rubble slopes and mounds

	Design approach		Mean value approach	
Wave run-up				
Wave run-up height (2%)	Eq.	6.2	Eq.	6.1
Wave run-up height for shingle beaches				
Percentage of overtopping waves	Eqs.	6.3 or 6.4	Eqs.	6.3 or 6.4
Wave overtopping				
Rubble mound breakwaters	Eq.	6.6	Eq.	6.5
Berm breakwaters	Eqs.	6.10-6.12	Eqs.	6.9, 6.11, 6.12
Overtopping wave volumes	Eqs.	6.16-6.18	Eqs.	6.16-6.18
Overtopping velocities			Eqs.	6.19-6.20
Influence factors				
Roughness	Table 6.2, Eq. 6.7			
Oblique waves	Eq.	6.9		
Width of armour crest	Eq.	6.8		
Scale effects	Eqs.	6.13-6.15		

6.2   Wave run-up and run-down levels, number of overtopping waves

Through civil engineering history the wave run-up and particularly the 2% run-up height was important for the design of dikes and coastal embankments, see also Section 5.2.1. Till quite recently the 2% run-up height under design conditions was considered a good measure for the required dike height. With only 2% of overtopping waves the load on the crest and inner side were considered so small that no special measurements had to be taken with respect to the strength of these parts of a dike. Recently, the requirements for dikes changed to allowable wave overtopping, making the 2% run-up value less important in engineering practice.

Wave run-up has always been less important for rock slopes and rubble mound structures and the crest height of these type of structures has mostly been based on allowable overtopping, or even on allowable transmission (low-crested structures). Still an estimation or prediction of wave run-up is valuable as it gives a prediction of the number or percentage of waves which will reach the crest of the structure and eventually give wave overtopping. And this number is needed for a good prediction of individual overtopping wave volumes.

Figure 6.3 gives 2% wave run-up heights for various rocks slopes with $\cot\alpha$ = 1.5, 2, 3 and 4 and for an impermeable and permeable core of the rubble mound. These run-up measurements were performed during the stability tests on rock slopes of Van der Meer (1988). First of all the graph gives values for a large range of the breaker parameter $\xi_{m-1,0}$, due to the fact that various slope angles were tested, but also with long wave periods (giving large $\xi_{m-1,0}$-values). Most breakwaters have steep slopes 1:1.5 or 1:2 only and then the range of breaker parameters is often limited to $\xi_{m-1,0}$ = 2-4. The graph gives rock slope information outside this range, which may be useful also for slopes with concrete armour units.
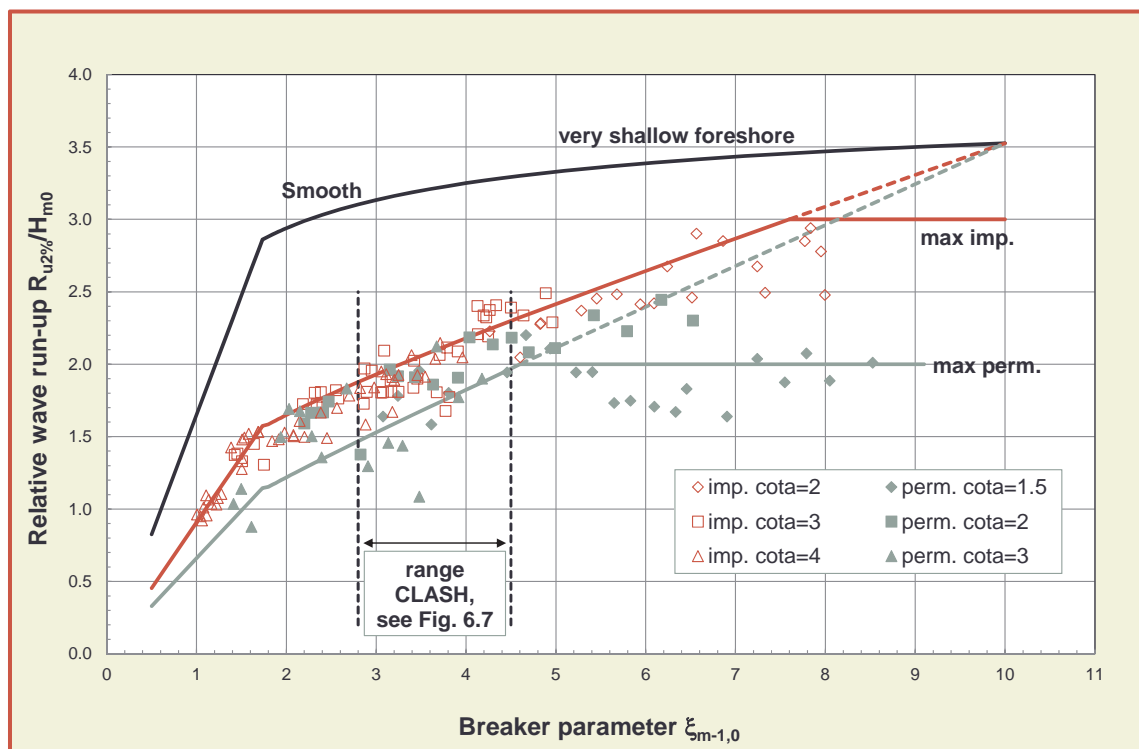
Figure 6.3:   Relative run-up on straight rock slopes with permeable and impermeable core, compared to smooth impermeable slopes

The highest curve in Figure 6.3 gives the prediction for smooth straight slopes, see Figure 5.5 and Equations 5.1 and 5.2, where for large breaker parameters the maximum found is for very shallow water (see also Section 5.2.3). The maximum for steep smooth slopes at more deeper water is around $R_{u2\%}/H_{m0}$ = 2.8 to 3.0 and is also given in the graph. A rubble mound slope dissipates significantly more

163

wave energy than an equivalent smooth and impermeable slope. Both the roughness and porosity of the armour layer cause this effect, but also the permeability of the under layer and core contribute to it. Figure 6.3 shows the data for an impermeable core (geotextile on sand or clay underneath a thin under layer) and for a conventional under layer with a permeable core (such as most breakwaters). The difference is most significant for large breaker parameters.

Equations 5.1 and 5.2 include the influence factor for roughness γ_f. For two layers of rock on an impermeable core $\gamma_f = 0.55$. This reduces to $\gamma_f = 0.40$ for two layers of rock on a permeable core. Both values were based on Figure 6.3 and on comparison of run-up levels. This influence factor is used in the linear part of the run-up formula, say for $\xi_0 \leq 1.8$. From $\xi_{m-1,0} = 1.8$ the roughness factor increases linearly up to 1 for $\xi_{m-1,0} = 10$, although it does not reach this value of 1.

For an impermeable core a maximum is reached for $R_{u2\%}/H_{m0} = 3.0$, which is only a little lower than the maximum of about 3.5. For the permeable core the maximum is $R_{u2\%}/H_{m0} = 2.0$. The physical explanation for this is that if the slope becomes very steep (large $\xi_{m-1,0}$-value) and the core is impermeable, the surging waves slowly run up and down the slope and all the water stays in the armour layer, leading to fairly high run-up. The surging wave actually does not "feel" too much roughness anymore and acts as a wave on a very steep smooth slope. For an permeable core, however, the water can penetrate into the core which decreases the actual run-up to a constant maximum (the horizontal line in Figure 6.3).

Most influence factors for roughness of concrete units (to be discussed later) were based on the CLASH work. A slope angle of 1:1.5 was tested there with a range in breaker parameters between $\xi_{m--1,0} = 2.8$ and 4.5. This relatively small range (wave steepnesses of 0.02, 0.035 and 0.05) is also given in Figure 6.3.

The prediction for the 2% mean wave run-up value for rock or rough slopes can be described by Equation 6.1

Mean value approach

$$\frac{R_{u2\%}}{H_{m0}} = 1.65 \cdot \gamma_b \cdot \gamma_f \cdot \gamma_\beta \cdot \xi_{m-1,0}$$

with a maximum of $\dfrac{R_{u2\%}}{H_{m0}} = 1.00 \cdot \gamma_{f\,surging} \cdot \gamma_\beta \left(4.0 - \dfrac{1.5}{\sqrt{\gamma_b \cdot \xi_{m-1,0}}} \right)$

6.1

From $\xi_{m-1,0} = 1.8$ the roughness factor $\gamma_{f\,surging}$ increases linearly up to 1 for $\xi_{m-1,0} = 10$:

$\gamma_{f\,surging} = \gamma_f + (\xi_{m-1,0} - 1.8)*(1 - \gamma_f)/8.2$

Maximum $R_{u2\%}/H_{m0} = 3.0$ for structures with an impermeable core and 2.0 for a permeable core.

Equation 6.1 may also give a good prediction for run-up on slopes armoured with concrete armour units, if the right roughness factor is applied (see Section 6.3).

The coefficient 1.65 in Equation 6.1 can be considered as a stochastic variable with a mean value of 1.65 and a standard deviation of $\sigma = 0.10$. This is the *mean value approach*. For a *design or assessment approach* one should use the value of 1.75. The coefficient 1.0 for the "maximum" in Equation 6.1 can be considered as a stochastic variable with a mean value of 1.00 and a standard deviation of $\sigma = 0.07$. For a design or assessment approach one should use the value of 1.07 and the run-up formula is given in Equation 6.2.

Design and assessment approach

$$\frac{R_{u2\%}}{H_{m0}} = 1.75 \cdot \gamma_b \cdot \gamma_f \cdot \gamma_\beta \cdot \xi_{m-1,0}$$

with a maximum of $\dfrac{R_{u2\%}}{H_{m0}} = 1.07 \cdot \gamma_{f\,surging} \cdot \gamma_\beta \left(4.0 - \dfrac{1.5}{\sqrt{\gamma_b \cdot \xi_{m-1,0}}} \right)$

6.2

From $\xi_{m-1,0} = 1.8$ the roughness factor $\gamma_{f\,surging}$ increases linearly up to 1 for $\xi_{m-1,0} = 10$:

$\gamma_{f\,surging} = \gamma_f + (\xi_{m-1,0} - 1.8)*(1 - \gamma_f)/8.2$

With a maximum $R_{u2\%}/H_{m0} = 3.21$ for structures with an impermeable core and 2.14 for a permeable core.

Until now, only the 2% run-up value has been described. It might be that there is interest in another percentage, for example for design of breakwaters where the crest height may be determined by an allowable percentage of overtopping waves, say 10-15%. A few ways exist to calculate run-up heights for other percentages, or to calculate the number of overtopping waves for a given crest height. Van der Meer and Stam (1992) give two methods. One is an equation like Equation 6.1 with a table of coefficients for the 0.1%, 1%, 2%, 5%, 10% and 50% (median). Interpolation is then needed for other percentages.

The second method gives a formula for the run-up distribution as a function of wave conditions, slope angle and permeability of the structure. The distribution is a two parameter Weibull distribution. With this method the run-up can be calculated for every percentage wanted. Both methods apply to straight rock slopes only and will not be described here. The given references, however, give all details.

The easiest way to calculate run-up (or overtopping percentage) different from 2% is to take the 2% value and assume a Rayleigh distribution. This is similar to the method in Chapter 5 for dikes and embankment seawalls. The probability of overtopping $P_{ov} = N_{ow}/N_w$ (the percentage is simply 100 times larger) can be calculated by:

$$P_{ov} = N_{ow} / N_w = \exp\left[-\left(\sqrt{-\ln 0.02}\, \frac{R_c}{R_{u,2\%}} \right)^2 \right]$$

6.3

Equation 6.3 can be used to calculate the probability of overtopping, given a crest freeboard R_c or to calculate the required crest freeboard, given an allowable probability or percentage of overtopping waves.

One warning should be given in applying Equations 6.1, 6.2 and 6.3. The equations give the run-up level in percentage or height on a straight (rock) slope. This is not the same as the number of overtopping waves or overtopping percentage and Figure 6.4 shows the difference. The run-up is always a point on a straight slope, whether for a rock slope or armoured mound the overtopping is measured some distance away from the seaward slope and on the crest; often behind a crown wall. This means that Equations 6.1, 6.2 and 6.3 always give an over estimation of the number of overtopping waves.

Figure 6.5 shows measured data for rubble mound breakwaters armoured with Tetrapods (De Jong 1996), Accropode™ or a single layer of cubes (Van Gent *et al.* 1999). All tests were performed at Delft Hydraulics, now Deltares. The test set-up was more or less similar to Figure 6.4 with a crown wall height R_c a little lower than the armour freeboard A_c. CLASH data on specific overtopping tests (see Section 6.3) for various rock and concrete armoured slopes were added to Figure 6.5.
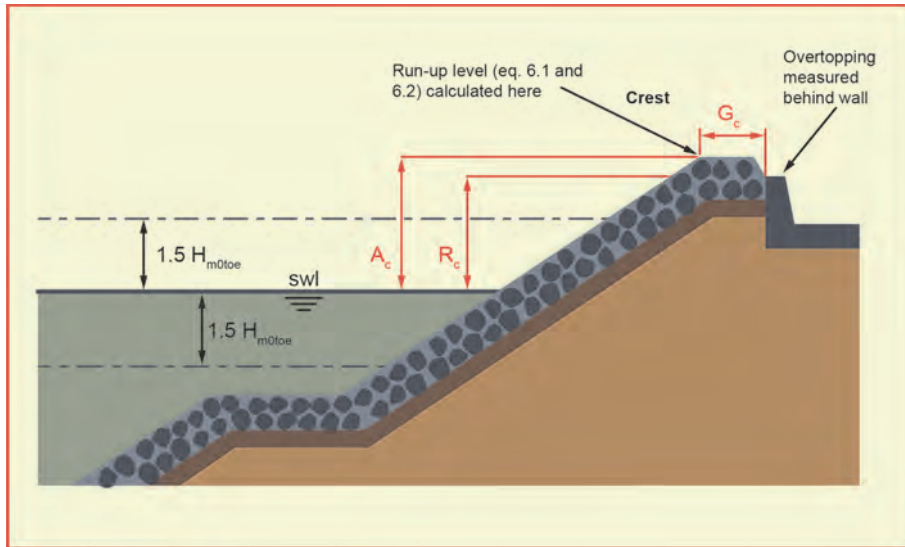
Figure 6.4:   Run-up level and location for overtopping differ

This Figure 6.5gives only the percentage of overtopping waves passing the crown wall. Analysis showed that the size of the armour unit relative to the wave height had influence, which gave a combined parameter A_c*D_n/H_{m0}^2, where D_n is the nominal diameter of the armour unit. The figure covers the whole range of overtopping percentages, from complete overtopping with the crest at or lower than SWL to no overtopping at all. The CLASH data give maximum overtopping percentages of about 30%. Larger percentages mean that overtopping is so large that it can hardly be measured and that wave transmission starts to play a role.
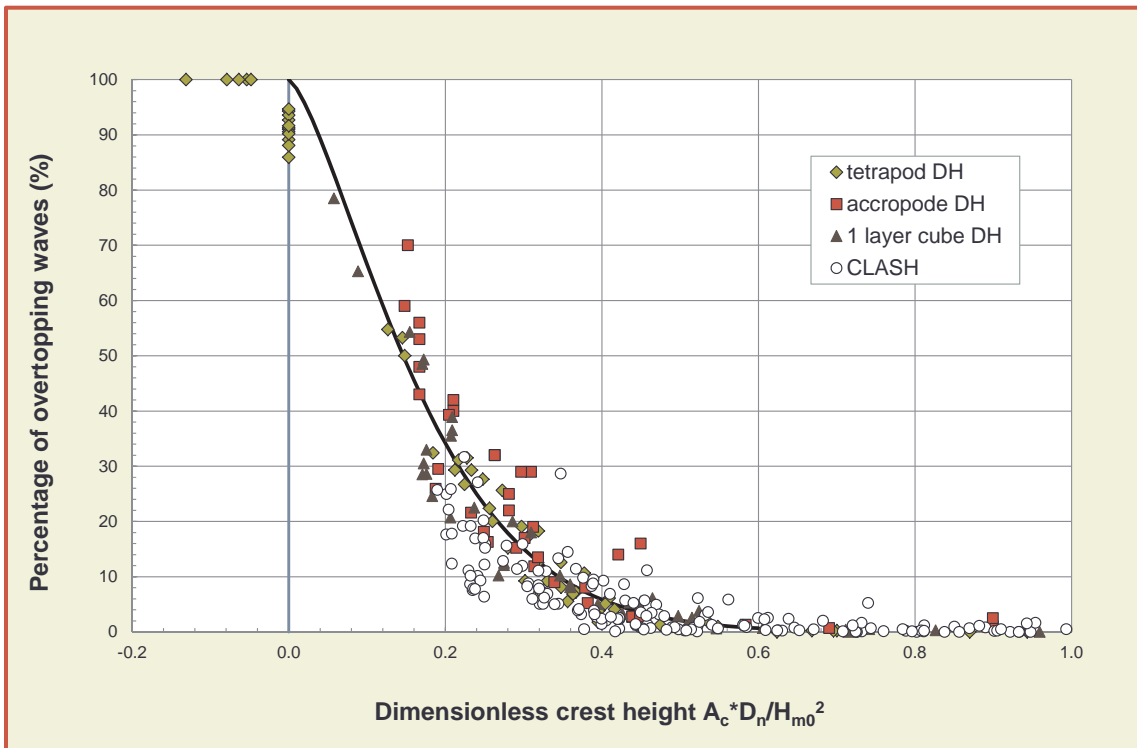
Figure 6.5:   Percentage of overtopping waves for rubble mound breakwaters as a function of relative (armour) crest height and armour size ($R_c \leq A_c$)

Taking 100% overtopping for zero freeboard (the actual data are only a little lower), a Weibull curve can be fitted through the data. Equation 6.4 can be used to predict the number or percentage of overtopping waves or to establish the armour crest level for an allowable percentage of overtopping waves.

$$P_{ov} = N_{ow} / N_w = \exp\left[-\left(\frac{A_c D_n}{0.19 H_{m0}^2}\right)^{1.4}\right] \qquad 6.4$$

It is clear that Equations 6.1 to 6.3 will give more overtopping waves than Equation 6.4, but both estimations together give a designer enough information to establish the required crest height of a structure given an allowable overtopping percentage.

When a wave on a structure has reached its highest point it will run down on the slope till the next wave meets this water and run-up starts again. The lowest point to where the water retreats, measured vertically to SWL, is called the run-down level. Run-down often is less, or not, important compared to wave run-up, but both together they may give an idea of the total water excursion on the slope. Therefore, only a first estimate of run-down on straight rock slopes is given here, based on the same tests of Van der Meer (1988), but re-analysed with respect to the use of the spectral wave period $T_{m-1,0}$.

Figure 6.6 gives an overall view, where it shows clearly the influence of the permeability of the structure as the solid data points (impermeable core) generally show larger run-down than the open data symbols of the permeable core. Furthermore, the breaker parameter $\xi_{m-1,0}$ gives a fairly clear trend of run-down for various slope angles and wave periods. Figure 6.6 can be used directly for design purposes, as it also gives a good idea of the scatter.
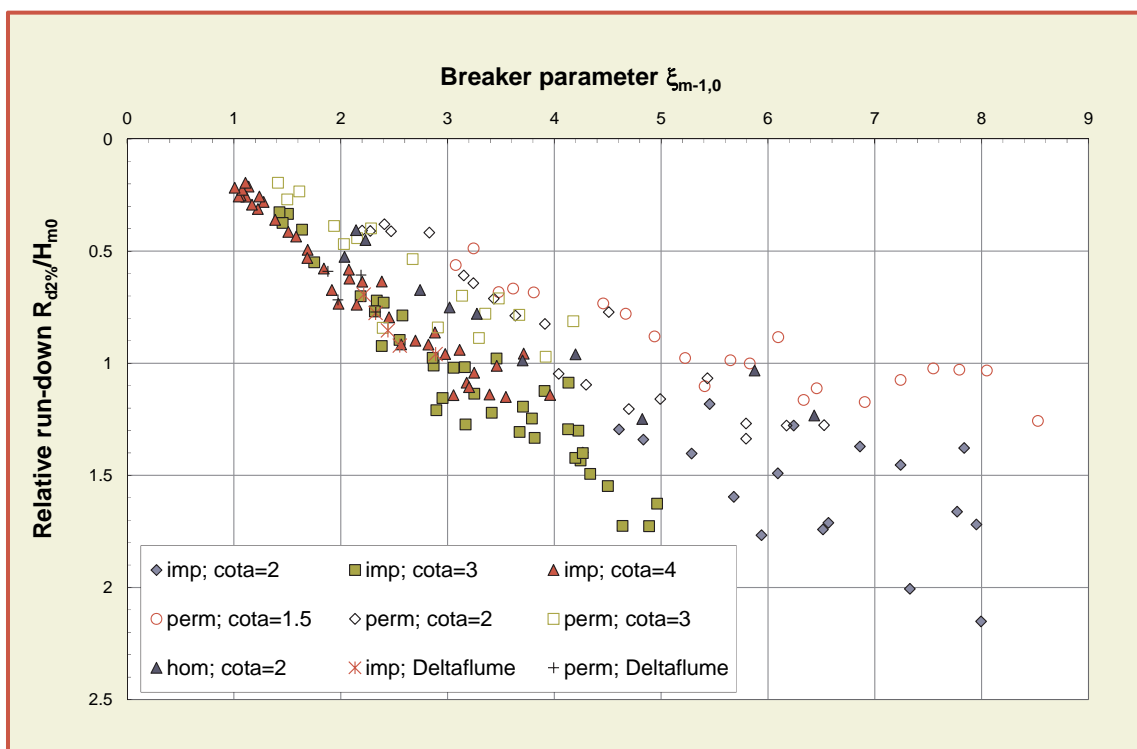
Figure 6.6:   Relative 2% run-down on straight rock slopes with impermeable core (imp), permeable core (perm) and homogeneous structure (hom)

6.3   Overtopping discharges

6.3.1   Simple armoured slopes

The mean overtopping discharge or overtopping rate is often used to judge allowable overtopping. It is easy to measure and an extensive database on mean overtopping discharge was gathered for CLASH. This mean discharge does of course not describe the real behaviour of wave overtopping, where only large waves will reach the top of the structure and give overtopping. Random individual wave overtopping means random in time and each wave gives a different overtopping volume, see also Figure 5.54. But the description of individual overtopping is based on the mean overtopping, as the duration of overtopping multiplied with this mean overtopping discharge gives the total volume of water overtopped by a certain number of overtopping waves. The mean overtopping discharge has been described in this section. The individual overtopping wave volumes is the subject in Section 6.4

Just as for run-up, the basic formula for mean wave overtopping discharge has been described in Chapter 5 for smooth slopes (Equations 5.10 and 5.11). The influence factor for roughness should take into account rough structures. Rubble mound structures often have steep slopes of about 1:1.5, leading to the overtopping equation that gives the maximum (Eq. 5.11). Section 5.3.3 described very steep slopes up to vertical walls. It should be noted that the physical maximum slope angle for rubble mound structures is about 1:4/3. This means that formulae in Section 5.3.3 cannot be applied to rubble mound slopes and that mainly Equation 5.11 has to be used, repeated here as Equation 6.5.

$$\frac{q}{\sqrt{g \cdot H_{m0}^3}} = 0.09 \cdot \exp\left[-\left(1.5 \frac{R_c}{H_{m0} \cdot \gamma_f \cdot \gamma_\beta}\right)^{1.3}\right] \quad \text{for steep slopes 1:2 to 1:4/3} \qquad \text{6.5}$$

Equation 6.5 gives the average of the measured data and can be used for predictions and comparisons with measurements (*mean value approach*). The reliability of Equation 6.5 is described by σ(0.09) = 0.0135 and σ(1.5) = 0.15. For a *design and assessment approach* it is strongly recommended to increase the average discharge by about one standard deviation, see Equation 6.6:

$$\frac{q}{\sqrt{g \cdot H_{m0}^3}} = 0.1035 \cdot \exp\left[-\left(1.35 \frac{R_c}{H_{m0} \cdot \gamma_f \cdot \gamma_\beta}\right)^{1.3}\right] \quad \text{for steep slopes 1:2 to 1:4/3} \qquad \text{6.6}$$

As part of the EU research programme CLASH (Bruce *et al.* 2009) tests were undertaken to derive roughness factors for rock slopes and different armour units on sloping permeable structures. Overtopping was measured for a 1:1.5 sloping permeable structure at a reference point 3 D_n from the crest edge, where D_n is the nominal diameter. The wave wall had the same height as the armour crest, so $R_c = A_c$. As discussed in Section 6.2 and Figure 6.4, the point to where run-up can be measured and the location of overtopping may differ. Normally, a rubble mound structure has a crest width of at least 3 D_n. Waves rushing up the slope reach the crest with an upward velocity. For this reason, it is assumed that overtopping waves reaching the crest will also reach the location 3 D_n farther. Pictures of the various units tested are shown in Figure 6.8 to Figure 6.9.

Results of the CLASH-work are shown in Table 6.2 and Figure 6.7, where all data are shown together in one graph. Two lines are given, one for a smooth slope, Equation 6.5 with $\gamma_f = 1.0$, and one for rubble mound 1:1.5 slopes with the same equation, but with $\gamma_f = 0.45$. The lower line only gives an average, but shows clearly the very large influence of roughness and permeability on wave overtopping. The required crest height for a steep rubble mound structure is at least half of that for a steep smooth structure with similar overtopping discharge. It is also for this reason that smooth slopes are often more gentle in order to reduce the crest heights.
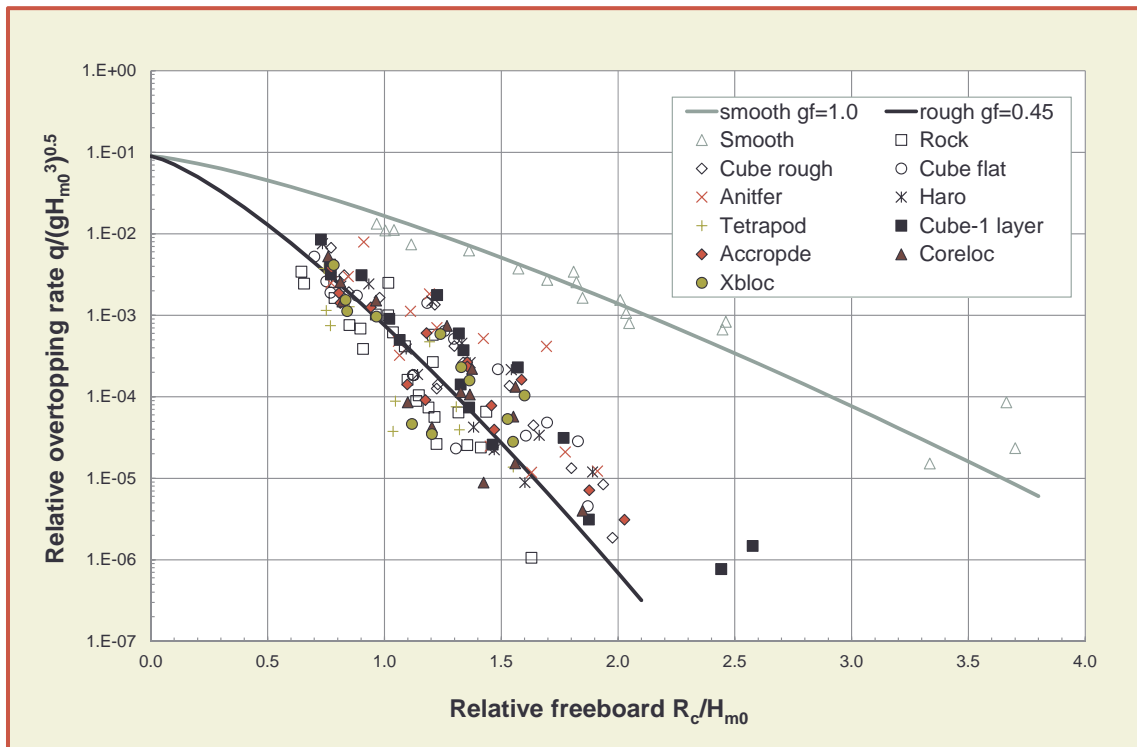
Figure 6.7: Mean overtopping discharge for 1:1.5 smooth and rubble mound slopes. CLASH-project

Table 6.2: Values for roughness factor γ_f for permeable rubble mound structures with slope of 1:1.5. Values in italics are estimated/extrapolated

Type of armour layer	γ_f	Figure
Smooth impermeable surface	1.00	Figure 6.8
Rocks (1 layer, impermeable core)	0.60	
Rocks (1 layer, permeable core)	0.45	
Rocks (2 layers, impermeable core)	0.55	
Rocks (2 layers, permeable core)	0.40	Figure 6.8
Cubes (1 layer, flat positioning)	0.49	
Cubes (2 layers, random positioning)	0.47	Figure 6.8
Antifers	0.50	Figure 6.8
HARO's	0.47	Figure 6.9
Tetrapods	0.38	Figure 6.9
Dolosse	*0.43*	
Accropode™ I	0.46	Figure 6.9
Xbloc®; CORE-LOC®; Accropode™ II	0.44	Figure 6.9
Cubipods one layer	*0.49*	
Cubipods two layers	*0.47*	
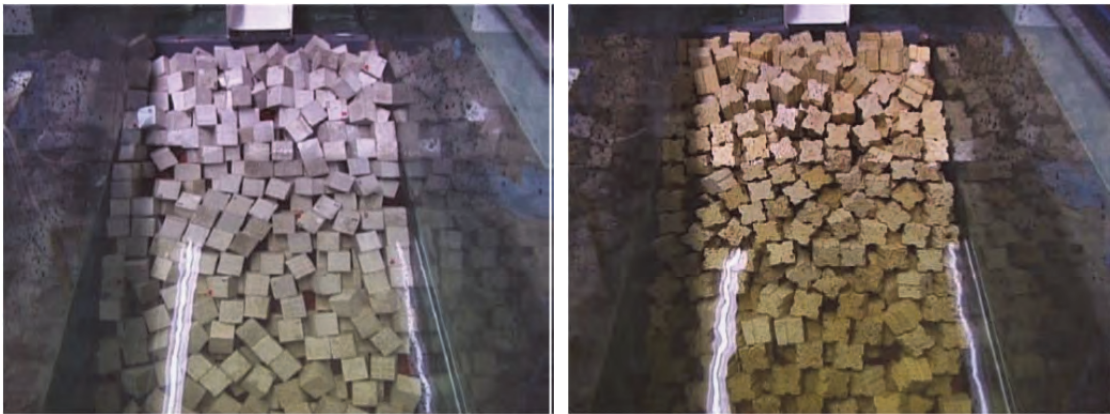
Figure 6.8:   Clockwise from top left: smooth, rocks, cubes and Antifer cubes; Test set-up in CLASH
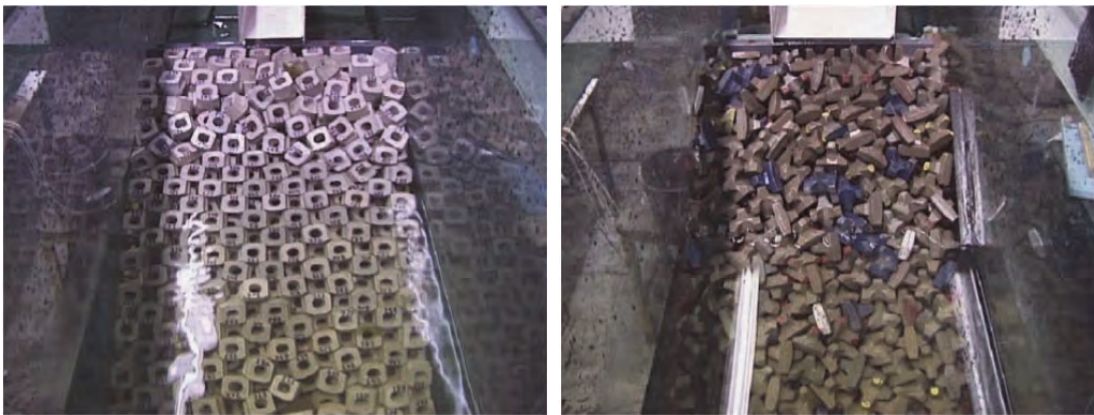
Figure 6.9:   Clockwise from top left: Haros, Accropode I, Xbloc and Tetrapods; Test set-up in CLASH

EurOtop (2007) gave overtopping formulae according to Equation 5.8, ie. a straight line on a log-linear graph. The range of application was for $R_c/H_{m0} > 0.5$, whereas the new equations in this update of the manual are valid for $R_c/H_{m0} > 0$. The new formulae widen the application area, but are very similar in the area with $R_c/H_{m0} > 0.5$. To compare the old EurOtop (2007) and the new formulae, like Equation 6.6, Figure 5.16 was made for non-breaking waves, where also the curve for $\gamma_f = 0.45$ as presented in Figure 6.7 is given.

In Figure 6.7, one-layer systems like Accropode™, CORE-LOC®, Xbloc® and 1 layer of cubes have solid symbols, whereas two-layer systems are shown as open symbols. There is a slight tendency that one-layer systems give a little more overtopping than two-layer systems, which is also clear from Table 6.2. Equation 6.5 and 6.6 can be used with the roughness factors in Table 6.2 for prediction of mean overtopping discharges for rubble mound breakwaters. Values in italics in Table 6.2 have been estimated / extrapolated, based on the CLASH results, but slightly modified according to Bruce *et al.* 2009).

Since the CLASH-project a new concrete armour unit was invented and tested, see Molines and Medina (2015). There was, however, a large difference in testing compared to the CLASH set-up, where R_c and A_c were equal, ie. the armour freeboard was the same as the freeboard by the crest wall. The tests with a double layer of cubipods were performed with $A_c/R_c = 0.57\text{-}0.79$ and for one layer of cubipods $A_c/R_c = 0.42\text{-}0.63$. This means that in many cases the crest wall was far above the armour freeboard and this configuration has effect on the overtopping formula in general. Considering the results of the tests, compared to other data and formulae in the mentioned paper, it seems that cubipods gave more or less similar results as cubes in one or two layers. For this reason they got these influence factors in Table 6.2, but they must be seen as tentative. Other tests, more close to the CLASH set-up, may in future give more accurate figures.

Note that influence factors on roughness in Table 6.2 were derived for breaker parameters in the range $\xi_{m-1,0} = 2.8$ and 4.5, which is a fairly small range; see Figure 6.3 also. In this range the influence factor is shown to be fairly constant, although there was a slight tendency that larger wave periods gave slightly larger overtopping discharges. In application of Equations 6.5 or 6.6 it is recommended to check whether the breaker parameter is in the right range. For breaker parameters $\xi_{m-1,0} > 5$, meaning a large wave period, it may be wise to increase the influence factor as described in Equations 6.1 or 6.2:

From $\xi_{m-1,0} > 5.0$ the roughness factor $\gamma_{f\,mod}$ increases linearly up to 1 for $\xi_{m-1,0} = 10$, which can be described by:

$$\gamma_{f\,mod} = \gamma_f + (\xi_{m-1,0} - 5)*(1 - \gamma_f)/5.0 \qquad 6.7$$

With a maximum $\gamma_{f\,mod} = 0.60$ for rubble mound structures with a permeable core.

6.3.2 Effect of armoured crest berm

Simple straight slopes including an armoured crest berm of less than about 3 nominal diameters ($G_c \approx 3D_n$) will have a little increased overtopping with respect to Equation 6.5. It is, however, possible to reduce overtopping with a wide crest as much more energy can be dissipated in a wider crest. Besley (1999) described in a simple and effective way the influence of a wide crest. First the wave overtopping discharge should be calculated for a simple slope, with a crest width up to 3 D_n. Then the following reduction factor on the overtopping discharge can be applied:

$$C_r = 3.06 \exp(-1.5G_c/H_{m0}) \quad \text{with maximum } C_r = 1 \qquad 6.8$$

Equation 6.8 gives no reduction for a crest width smaller than about 0.75 H_{m0}. This is fairly close to about 3 D_n and is, therefore, consistent. A crest width of 1 H_{m0} reduces the overtopping discharge to 68%, a

crest width of 2 H_{m0} gives a reduction to 15% and for a wide crest of 3 H_{m0} the overtopping reduces to only 3.4%. In all cases the crest has the same height as the armour crest: i.e. $R_c = A_c$. Equation 6.8 was determined for a rock slope with permeable under layer and core and can be considered as conservative; an Accropode slope showed more reduction which might then also be the case for other single layer units. If the under layer and/or core are not permeable, the overtopping may be larger for a wide crest as given by the equation, as more water will then remain in the armour layer.

6.3.3 Effect of oblique waves

Section 5.4.3 describes the effect of oblique waves on run-up and overtopping on smooth slopes (including some roughness), but specific tests on rubble mound slopes were not performed at that time. During CLASH, however, this omission was discovered and specific tests on a rubble mound breakwaters were performed with a slope of 1:2 and armoured with rock or cubes (Andersen and Burcharth, 2004a). The structure was tested both with long-crested and short-crested waves, but only the results by short-crested waves will be given.

For oblique waves the angle of wave attack β (deg.) is defined as the angle between the direction of propagation of waves and the axis perpendicular to the structure (for perpendicular wave attack: $\beta = 0°$). The direction of wave attack is the angle after any change of direction of the waves on the foreshore due to refraction. As with smooth slopes, the influence of the angle of wave attack is described by the influence factor γ_β. Just as for smooth slopes, there is a linear relationship between the influence factor and the angle of wave attack, but for permeable slopes the reduction in overtopping is much faster with increasing angle (compare with Equation 5.28):

$$\gamma_\beta = 1 - 0.0063|\beta| \text{ for } 0° \leq |\beta| \leq 80°$$

for $|\beta| > 80°$ the result $\beta = 80°$ can be applied

6.9

The wave height and period are linearly reduced to zero for $80° \leq |\beta| \leq 110°$, just like for smooth slopes, see Section 5.4.3. For $|\beta| > 110°$ the wave overtopping is assumed to be q = 0 m³/s per m.

6.3.4 Composite slopes and berms, including berm breakwaters

In every formula where a $\cot\alpha$ or breaker parameter $\xi_{m-1,0}$ is present, a procedure is required to deal with a composite slope. Hardly any specific research exists for rubble mound structures and, therefore, the procedure for composite slopes at sloping impermeable structures like dikes and sloping seawalls is assumed to be applicable. That procedure has been described in Section 5.4.6.

Also the influence of a berm in a sloping profile has been described in Section 5.4.6 and can be used for rubble mound structures. There is, however, often a difference in response of composite slopes or berms for rubble mound and smooth gentle slopes. On gentle slopes the breaker parameter $\xi_{m-1,0}$ has large influence on wave overtopping, see Equations 5.10 and 5.11 as the breaker parameter will be quite small. Rubble mound structures often have a steep slope, leading to the formula for "non-breaking" waves, Equations 6.5 and 6.6. In these equations there is no influence factor present for a berm.

This means that a composite slope and even a, not too long, berm leads to the same overtopping discharge as for a simple straight rubble mound slope. Only when the average slope becomes so gentle that the maximum in Equation 6.6 does not apply anymore, then a berm and a composite slope will have an effect on the overtopping discharge. Generally, average slopes around 1:2 or steeper do not show influence of the slope angle, or only to a limited extent.

A specific type of rubble mound structure is the berm breakwater (see Figure 6.10 and also Figure 6.1 the two lowest pictures). The original idea behind the berm breakwater is that a large berm, consisting of fairly large rock, is constructed into the sea with a steep seaward face. The berm height is higher or equal than the minimum required for construction with land based equipment. Due to the steep seaward face the first

storms will reshape the berm to a certain extent and may even become a structure with a fully reshaped S-profile. Such a profile has then a gentle 1:4 or 1:5 slope just below the water level and steep upper and lower slopes, see Figure 6.11 (top). Such a structure is called a fully reshaping mass armoured berm breakwater, see Van der Meer and Sigurdarson (2016). Sometimes not the whole berm reshapes and a part is left. Then it is called a partly reshaping mass armoured berm breakwater.

The idea of the reshaping berm breakwater has evolved in Iceland to a more stable berm breakwater, now called partly or hardly reshaping Icelandic-type berm breakwater. The main difference is that during rock production from the quarry care is taken to gather a few percent of really big rock. Only a few percent is required to strengthen the corner of the berm and part of the down slope and upper layer of the berm in such a way that reshaping will hardly occur. An example with various rock classes (class I being the largest) is given in Figure 6.11 (bottom). Rock classes could be for example: Class I 16-20 t; Class II 10-16 t; Class III 4-10 t: and Class IV 1-4 t. Therefore distinction has been made between fully reshaping mass armoured berm breakwaters and hardly or partly reshaping Icelandic-type berm breakwaters.

Figure 6.10   Icelandic-type berm breakwater
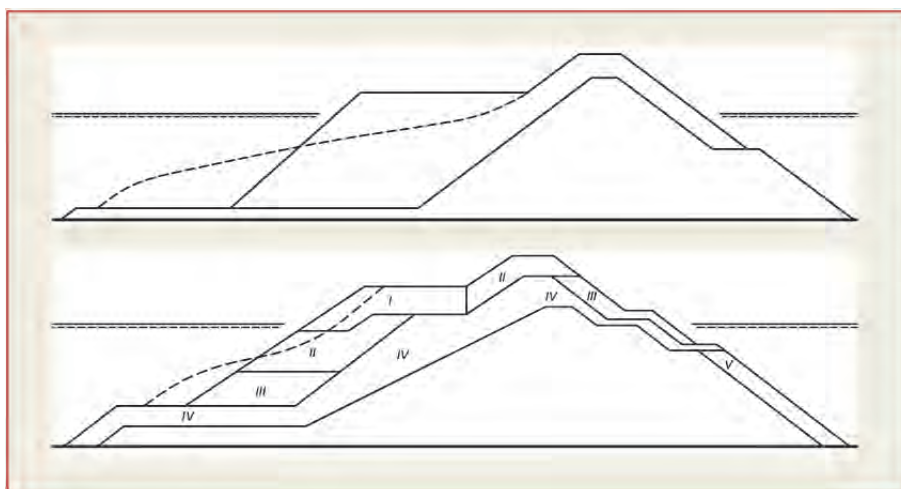
Figure 6.11:   Fully reshaping berm breakwater (top) and hardly or partly reshaping Icelandic-type berm breakwater

Basic information on berm breakwaters has been described by Lykke Andersen (2006). Only part of his research was included in the CLASH database (2004) and consequently in the Neural Network prediction method. All his data on wave overtopping on berm breakwaters has now been included in the new EurOtop database and the accompanying prediction neural network, see Sections 4.4 and 4.5. He performed about 600 tests on reshaping berm breakwaters and some 60 on non-reshaping berm breakwaters (fixing the steep slopes by a steel net). The true non-reshaping Icelandic type of berm breakwaters with large rock classes, has not been tested on stability and, therefore, his results might lead to an overestimation. The final result of the work of Lykke Andersen (2006) is a quite complicated formula, based on multi-parameter fitting. The advantage of such a fitting is that by using a large number of parameters, the data set used will be quite well described by the formula. The disadvantage is that physical understanding of the working of the formula, certainly outside the ranges tested, is limited. Also, due to the fact that so many structures were tested, this effect may be negligible.

The formulae in Lykke Andersen (2006) span a wider range of structures than only berm breakwaters. A breakwater should be statically stable, meaning that after (some) reshaping, the structure should be stable like a conventional structure. Dynamically stable structures may reshape during every significant event, like rock and shingle beaches. There longshore transport under oblique wave attack may be present, which should always be avoided for breakwaters. The transition from statically stable berm breakwaters to dynamically stable structures (not called breakwaters) is around $H_{m0}/\Delta D_{n50} = 3.0$, where Δ is the relative mass density and D_{n50} the nominal diameter and where H_{m0} is the design wave height for a return period of 100 years . If one is interested in the overtopping behaviour of dynamically stable structures, the work of Lykke Andersen (2006) is recommended to be used.

A berm breakwater is also a rubble mound breakwater with large roughness and permeability without a straight slope, like the data points in Figure 6.4, but a steep seaward slope with a berm and often a partly or fully reshaped berm. Nevertheless, it may be expected that overtopping data for berm breakwaters will give a graph similar to Figure 6.7. The influence factor may then be a function of the geometry of the berm breakwater and wave conditions. It should be noted that the starting point is the initial geometry of the berm breakwater that should be taken, not the (partly) reshaped profile after wave attack. For berm breakwaters a CLASH-type prediction method has been developed (Van der Meer and Sigurdarson, 2016), Equation 6.9.

Mean value approach

$$\frac{q}{\sqrt{g \cdot H_{m0}^3}} = 0.09 \cdot \exp\left[-\left(1.5\frac{R_c}{H_{m0} \cdot \gamma_{BB} \cdot \gamma_\beta}\right)^{1.3}\right]$$

<div align="right">6.9</div>

where γ_{BB} is the influence factor for a berm breakwater. Note that Equation 6.9 is similar to Equation 6.5, but γ_f has been changed by γ_{BB}. Equation 6.10 with application of γ_{BB} should be used if a design and assessment approach is needed.

Design and assessment approach

$$\frac{q}{\sqrt{g \cdot H_{m0}^3}} = 0.1035 \cdot \exp\left[-\left(1.35\frac{R_c}{H_{m0} \cdot \gamma_{BB} \cdot \gamma_\beta}\right)^{1.3}\right]$$

<div align="right">6.10</div>

Data on overtopping at berm breakwaters have been gathered, partly from research and partly from projects, and reanalysed in line with the procedure in Chapter 5 (Sigurdarson and van der Meer (2012) and Van der Meer and Sigurdarson, 2016). The data has a large variation in wave period or wave steepness and shows a clear dependency on those parameters. The data were grouped according to the two types of berm breakwaters shown in Figure 6.11 for fully reshaping mass armoured type and partly reshaping Icelandic-type, as these may respond differently with regard to wave overtopping.

It is known that the wave period has influence on overtopping at berm breakwaters, this in contrast to steep smooth slopes and also to conventional breakwaters with a straight and steep slope, although Equation 6.7 gives an increase of the influence factor on roughness for large breaker parameters. The reason may be the berm itself, which is very permeable and is most effective for dissipation of energy of short waves. The influence of wave steepness on the influence factor γ_{BB} is shown in Figure 6.12, for hardly and partly reshaping Icelandic-type of berm breakwaters.
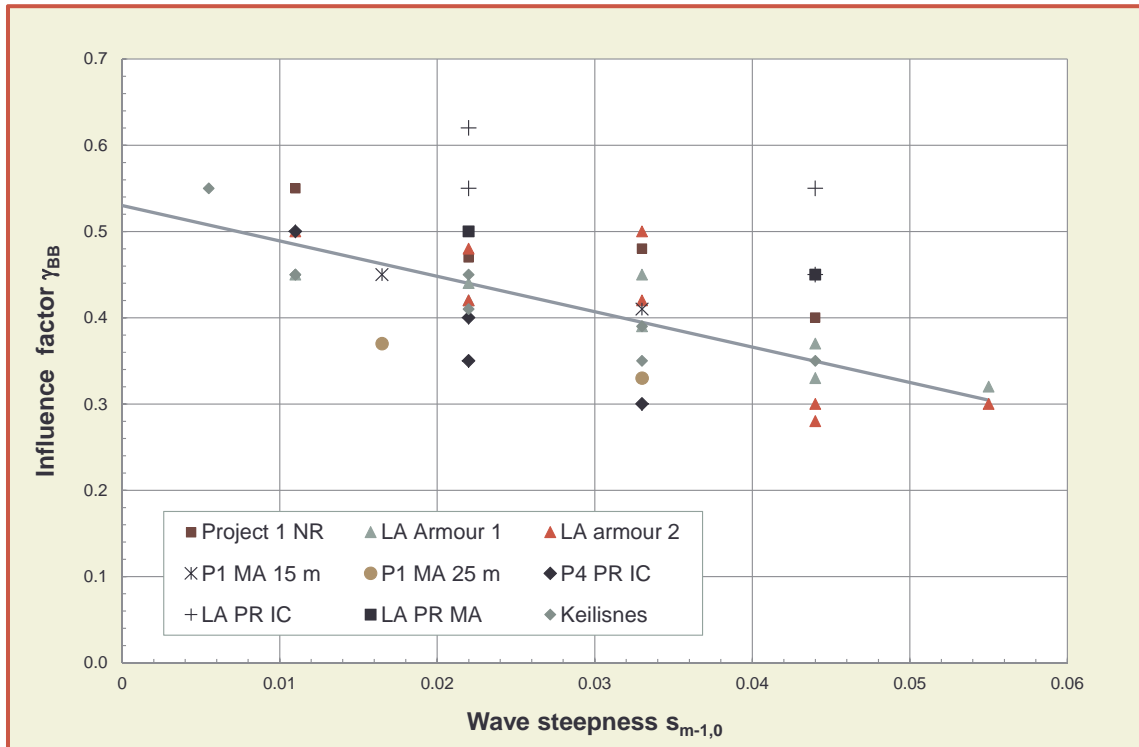
Figure 6.12: Influence of wave steepness on γ_{BB} for a hardly or partly reshaping Icelandic-type berm breakwater. For explanation of legend, see Sigurdarson and Van der Meer, 2012

The graph gives very low influence factors up to $\gamma_{BB} = 0.3$ for very large steepness, but these values may grow up to 0.5 and even a little larger for very low wave steepness. A similar influence was found for reshaping berm breakwaters and there maximum influence factors of 0.6 were found for very low wave steepness, comparable to the maximum value in Equation 6.7 for straight rubble mound slopes.

The influence factor γ_{BB} can be described by Equations 6.11 and 6.12.

$$\gamma_{BB} = 0.68 - 4.1s_{m-1,0} - 0.05B/H_{m0} \quad \text{for hardly and partly reshaping berm breakwaters} \quad 6.11$$

$$\gamma_{BB} = 0.70 - 8.2s_{m-1,0} \quad \text{for fully reshaping berm breakwaters} \quad 6.12$$

Figure 6.13 and Figure 6.14 give the final results with all data available. The graphs can be directly compared with Figure 5.13, where all influence factors have been included in the parameters of the horizontal axis and the results are then directly compared with the curve for a smooth slope.

Overtopping in a laboratory can be measured very accurately, but the meaning of very small overtopping is not always realistic. Overtopping rates lower than 1 l/s per m are affected by scale effects. Wave overtopping graphs are given in relative form, using $q/(gH_{m0}^3)^{0.5}$ as dimensionless overtopping rate, see Figure 6.13 and Figure 6.14. A value of $q/(gH_{m0}^3)^{0.5} < 10^{-5}$ will mostly give an overtopping rate less than 0.5 l/s per m. This is already a threshold where scale effects play a role, and the graphs show data below

this threshold and it should be realised that in those situations only a few waves may overtop during a storm.
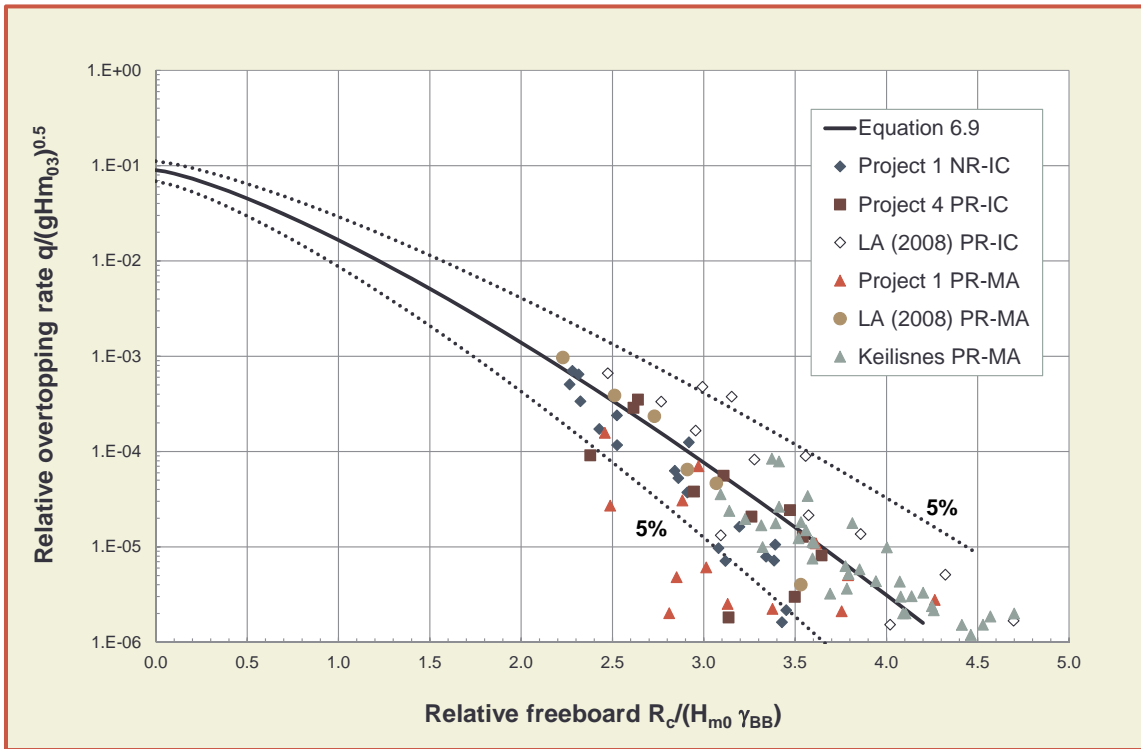
Figure 6.13: Wave overtopping for a hardly or partly reshaping Icelandic type berm breakwater. For explanation of legend, see Sigurdarson and Van der Meer, 2012
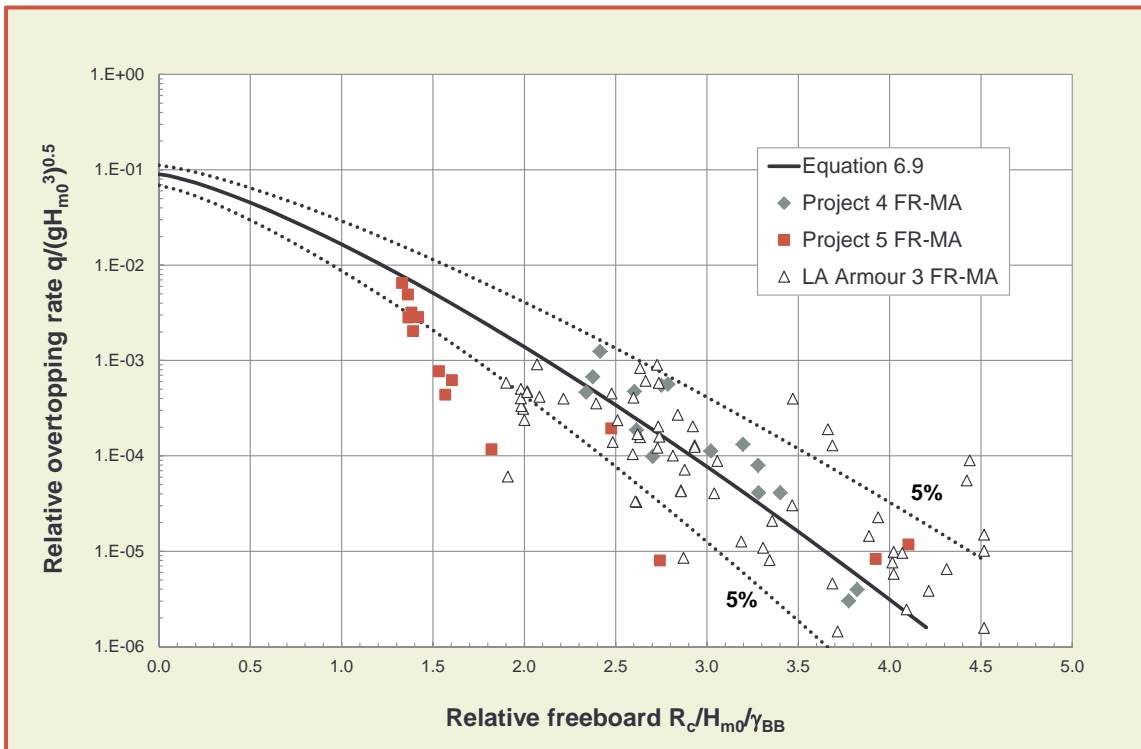
Figure 6.14: Wave overtopping for a fully reshaping berm breakwater. For explanation of legend, see Sigurdarson and Van der Meer, 2012

Berm breakwaters often have no crest wall to limit wave overtopping. It means that wave overtopping may not only be generated over the crest, but also through the upper armour layers. The two photos in

Figure 6.15 show the overtopping at the Bakkafjordur berm breakwater in Iceland during a storm in October 1995. The upper photo shows overtopping over the breakwater crest while the lower photo shows sea water flowing through the crest structure. Similar flow has been seen in hydraulic model tests.

Figure 6.15:   Rear side of the Bakkafjordur breakwater during a storm in 25 October 1995, overtopping over the crest and through the crest. Courtesy S. Sigurdarson

6.3.5 Effect of wave walls

Most breakwaters have a wave wall, capping wall or crest unit on the crest, simply to end the armour layer in a good way and to create access to the breakwater. For design, it is advised not to design a wave wall much higher than the armour crest, for the simple reason that wave forces on the wall will increase drastically if directly attacked by waves and not hidden behind the armour crest. For rubble mound slopes as a shore protection, design waves might be a little lower than for breakwaters and a wave wall might be one of the solutions to reduce wave overtopping. Nevertheless, one should realise the increase in wave forces if designing a wave wall significantly above the armour crest.

Equations 6.5 and 6.6 for a simple rubble mound slope includes a berm of 3 D_n wide and a wave wall at the same level as the armour crest: $A_c = R_c$. A slightly lower wave wall will not give larger overtopping, but no wave wall at all would certainly increase overtopping. Part of the overtopping waves will then penetrate through the crest armour. No formulae are present to cope with such a situation, unless the use of the Neural Network prediction method (Section 4.5), but the neural network tool actually takes the maximum of A_c and R_c to calculate the overtopping discharge.

Various researchers have investigated wave walls higher than the armour crest. None of them compared their results with a graph like Figure 6.7 for simple rubble mound slopes. During the writing of this manual some of the published equations were plotted in Figure 6.7 and most curves fell within the scatter of the data. Data with a wider crest gave significantly lower overtopping, but that was due to the wider crest, not the higher wave wall. In essence the message is: use the height of the wave wall R_c and not the height of

the armoured crest A_c in Equations 6.5 and 6.6 if the wall is higher than the crest. For a wave wall lower than the crest armour the height of this crest armour should be used. The Neural Network prediction might be able to give more precise predictions.

6.3.6   Scale and model effect corrections

Results of the CLASH project suggested significant differences between field and model results on wave overtopping. This has been verified for different sloping rubble mound structures. Results of the comparisons in that project have led to a scaling procedure which is mainly dependent on the roughness of the structure γ_f [-]; the seaward slope cot α of the structure [-]; and the mean overtopping discharge, based on small scale tests or predictions, but *up-scaled to prototype*, q_{us} [m³/s per m].

Data from the field are naturally scarce, and hence the method can only be regarded as tentative. It is furthermore only relevant if mean overtopping rates are lower than about 1.0 l/s per m, but may include significant adjustment factors for these rates (i.e. lower than about 1 l/s per m). Due to the inherent uncertainties, the proposed approach in EurOtop (20007) tried to be conservative, it gave the upper envelope of the results. The approach in this manual is, however, to give a *mean value approach* with describing the uncertainty around the mean, or a *design and assessment approach*, which has an explicit safety factor of one standard deviation of the model factor. Therefore it is better to base the influence of scale and model effects on average values and consequently the method in EurOtop (2007) has been changed in this version, but using the same data.

The adjustment factor f_q for model and scale effects for rubble mound slopes can be determined as follows and is also given in Figure 6.16 as the bold black line:

$$f_q = \left(-\log q_{us} - 2\right)^5 / 14 + 1 \qquad \text{with as maximum Equation 6.14} \qquad\qquad 6.13$$

The upper bound or maximum in Equation 6.13 of the adjustment factor f_q is dependent on the slope angle cot α and can be calculated by Equation 6.14. This equation is given in Figure 6.16 by the horizontal dashed red lines and shows that a gentler slope gives a larger maximum.

$$f_{q\max} = 10 \cot a - 9 \qquad \text{with as maximum } f_{qmax} = 31 \qquad\qquad 6.14$$

Equations 6.13 and 6.14 are based on prototype and small scale measurements at Zeebrugge (Antifer cubes on a slope of 1:1.4) and at Ostia (rock slope 1:4). They are valid for rubble mound slopes with large roughness and permeability and consequently with a small influence factor for roughness γ_f. The steepest slope angle that may be applied is cot α = 4/3 as that is the steepest slope that is used for single layer armour units. The maximum adjustment factor f_q = 4.33 for this steep slope. The slope at Zeebrugge was also steep, which gives a maximum adjustment factor f_q = 5.0. For slopes of 1:4 (as at Ostia) and gentler a maximum adjustment factor is found of f_q = 31. Note that such a large adjustment factor is found for very small overtopping discharges of smaller than 4.5 10⁻⁶ m³/s per m, or 0.045 l/s per m. Very often such small overtopping discharges can be regarded as "no overtopping", see also Section 3.3.7.

The adjustment factor becomes significantly larger than 1 for wave overtopping discharges smaller than 1 to 2 l/s per m. For q_{us} = 3 l/s per m the adjustment factor f_q = 1.002; for q_{us} = 2 l/s per m it becomes f_q = 1.012 and for q_{us} = 1 l/s per m it becomes f_q = 1.071.

Wind may also influence the overtopping at rubble mound structures, but it is assumed that this will only be the case for (very) small overtopping, often regarded as spray.
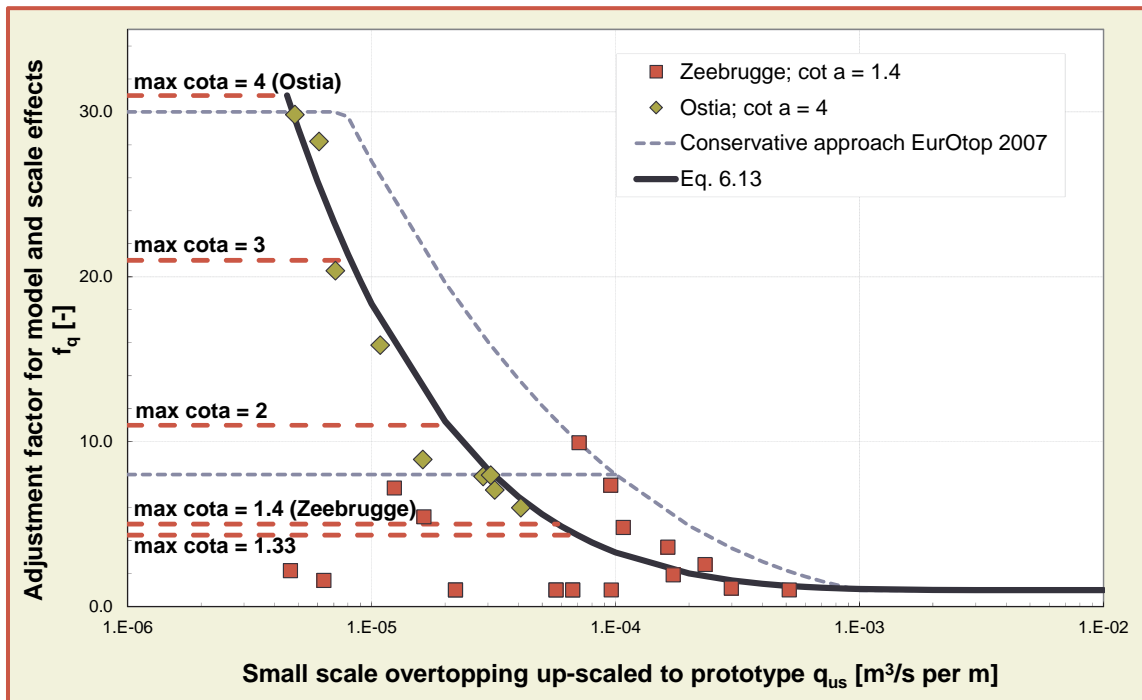
Figure 6.16: Proposed adjustment factor applied to data from two field sites: Zeebrugge 1:1.4 rubble mound breakwater (Antifer cubes) and Ostia 1:4 (rock slope)

The CLASH-project showed that smooth slopes do not show significant model or scale effects, in contrast to rubble mound structures. It is probably the roughness and permeability that have caused the differences between small scale model tests and prototype measurements, as resulted from the CLASH project. But there are also slopes with some roughness, with or without permeability, that cannot be regarded as a rubble mound slope (mainly given by $\gamma_f < 0.6$, see Table 6.2) and are also not smooth or almost smooth with $\gamma_f \geq 0.9$ (see Table 5.2). Such structures have been described in Sections 5.4.2 and 5.4.3. It are often fairly gentle slopes with artificial roughness and or permeability, such as blocks, ribs, chess pattern blocks or specially shaped block revetments. In general the roughness coefficients are between $0.7 < \gamma_f < 0.9$. Some of these slopes have been tested in the large Delta flume with waves well over 1 m. Then scale and model effects will be small or non-existent. But what about results of small scale testing? EurOtop (2007) proposed to use the method on scale effects up to an influence factor for roughness of $\gamma_f = 0.7$ and to consider $\gamma_f > 0.9$ as a smooth slope with $f_q = 1$.

EurOtop (2007) proposed to use the method (Equation 6.13 above) also for these slopes with roughness (but not rubble mound slopes), but to limit the maximum f_{qmax} in Equation 6.14 to a lower maximum $f_{qmax\ red}$. This is also proposed here. The maximum $f_{qmax\ red}$ is then given by Equation 6.15.

$$f_{q\max red} = 5 \cdot \gamma_f \cdot \left(1 - f_{q\max}\right) + 4.5 \cdot \left(f_{q\max} - 1\right) + 1 \text{ for } 0.7 < \gamma_f < 0.9$$
and f_{qmax} from Equation 6.14

6.15

As dike-type slopes like in Chapter 5 are often quite gentle with cot $\alpha = 3$ or 4, the maximum adjustment factor may still become 10 – 15 with $\gamma_f = 0.8$ for these slopes, although it will be for very small overtopping discharges. The proposal given in Equation 6.15 is based on interpolation between rough and permeable rubble mound slopes and smooth gentle slopes. It might well be that it gives an over-estimation and is a little on the conservative side. The main influence is on structures described in Sections 5.4.2 and 5.4.3.

The consequence of the model and scale effects as described in this section is that during physical scale model testing in a flume or basin the wave overtopping measurements may show zero overtopping, where in reality there might be overtopping over the structure! The CLASH-project clearly showed for measured

wave conditions and overtopping in reality, that the simulation by small scale modelling showed no overtopping. This asks for a procedure how to determine small overtopping rates in reality from physical small scale tests showing no overtopping. This procedure is given below with an example.

Suppose that model tests have been performed on a scale 1:20 on a rubble mound slope with slope angle cot α = 2.5. In total 17 tests have been performed, 14 of them showed measurable wave overtopping and 3 tests gave no measurable overtopping. Water level and wave heights were varied, where the wave height in prototype on average was H_{m0} = 2.5 m. The results can then be plotted in a conventional graph with relative overtopping rate $q/(gH_{m0})^3)^{0.5}$ versus the relative freeboard R_c/H_{m0}, see Figure 6.17. The model test data have been given by red diamonds. The three tests with no overtopping have been given for the correct relative freeboard R_c/H_{m0} and the relative overtopping rate $q/(gH_{m0})^3)^{0.5}$ at a fixed low value of 10^{-7} (on the horizontal axis).
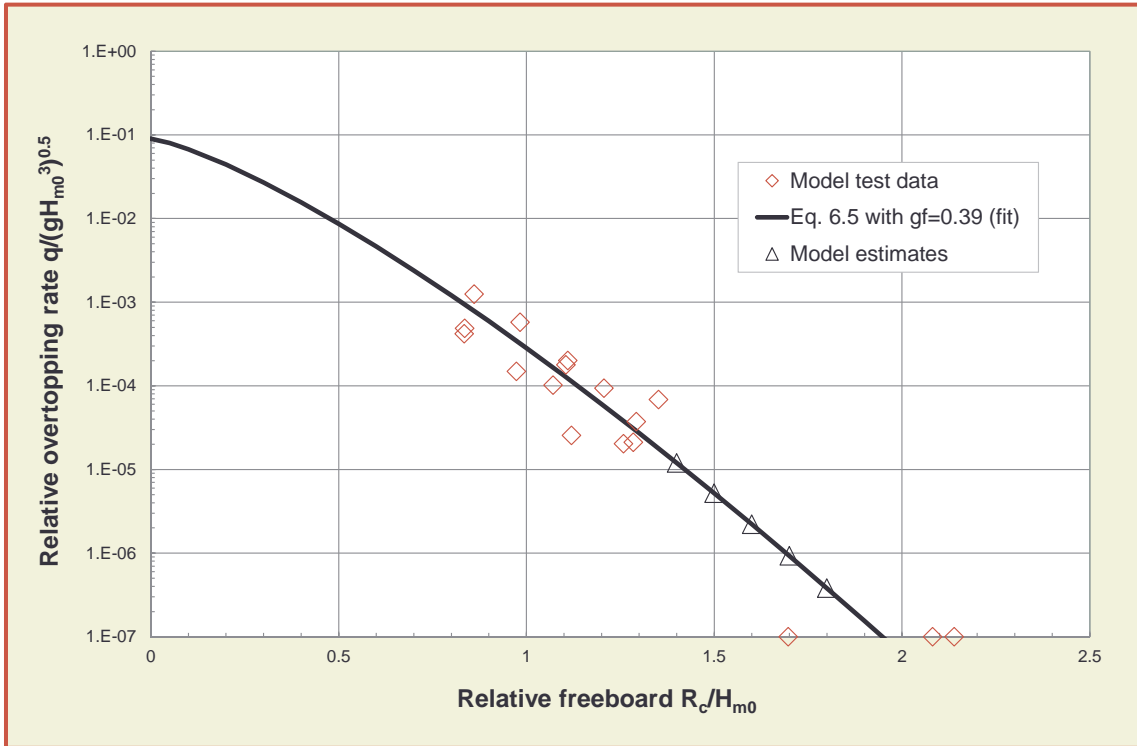
Figure 6.17: Model test results for an example with a fit through the results and an estimate for larger relative freeboards.

The model tests show that no measurements of wave overtopping are available for relative crest freeboards of R_c/H_{m0} > 1.4. In reality it could be possible that there still will be wave overtopping for these freeboards. The next step is then to fit Equation 6.5 through the data points with a measured quantity of q, with the best value of γ_f. In the example of Figure 6.17 this appears to be γ_f = 0.39. Now relative overtopping rates can be estimated by this fit for relative freeboards of for example R_c/H_{m0} = 1.4; 1.5; 1.6; 1.7; and 1.8. They are given as green triangles in the graph.

Now the relative overtopping rates, model test data as well as estimates, can be up-scaled by a linear scale factor of 20: $q_{us} = 20^{1.5} q$. Figure 6.18 gives the results where the up-scaled wave overtopping rate in m^3/s per m is given as function of the relative freeboard R_c/H_{m0}. They are given by the open symbols, similar as in Figure 6.17. Equations 6.13 and 6.14 can now be applied to calculated the corrected overtopping rates for prototype conditions. Equation 6.14 shows that for cot α = 2.5 the maximum adjustment factor $f_{q\,max}$ = 16. This adjustment factor is reached for the estimates with R_c/H_{m0} = 1.7 and 1.8. The solid symbols give the corrected overtopping rates. For overtopping rates q > 2.10^{-3} m^3/s per m, or 2 l/s per m, there is no adjustment and the up-scaled and corrected values are the same with the data points on top of each other. For smaller measured up-scaled overtopping rates, the corrected overtopping rates are a factor 1.1 to 2.2 larger. This ratio increases from 2.5 to 16 for the up-scaled estimates.

Section 3.3.7 describes that "zero overtopping" in prototype conditions will be close to a relative overtopping rate of $q/(gH_{m0})^3)^{0.5} = 10^{-5}$, giving with a wave height in this example of $H_{m0} = 2.5$ m, an overtopping rate of $1.2 \, 10^{-4}$ m³/s per m, or 0.12 l/s per m. This value is found in Figure 6.18 for a relative freeboard of $R_c/H_{m0} = 1.7$.

The conclusion of this exercise and example is that the model tests did not show wave overtopping for a relative freeboard of $R_c/H_{m0} = 1.4$, where through correction for model and scale effects "zero overtopping" may only be expected for relative freeboards of $R_c/H_{m0} > 1.7$. In order to design for such "zero overtopping" the crest freeboard has to be increased by 21%.
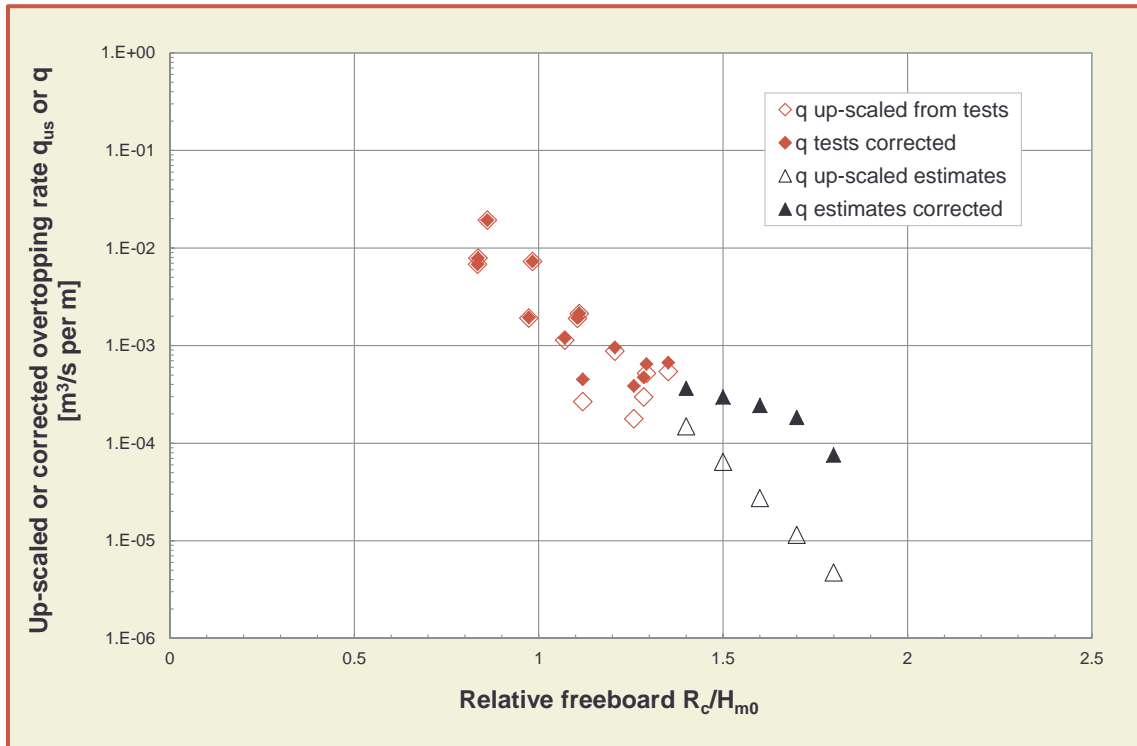
Figure 6.18:   Up-scaled and corrected overtopping rate, for model test results as well as estimates.

The method on up-scaling small and even zero overtopping discharges as given above, is based on small scale measurements as well as on a prototype situation that is significantly larger than small scale. If this is not the case, the multiplication factors as in Equations 6.13 and 6.14 do not have to be applied. The following boundary conditions are proposed, which are more based on experience than on real data:

- If the overtopping measurements are based on large scale testing with $H_{m0} > \sim 1$ m, multiplication factors do not have to be applied;
- If the wave height in prototype conditions $H_{m0} < \sim 1$ m, multiplication factors do not have to be applied

6.4 Overtopping wave characteristics

6.4.1 Overtopping wave volumes

Wave overtopping is a dynamic and irregular process and the mean overtopping discharge, q, does not cover this aspect. But by knowing the storm duration, t, and the number of overtopping waves in that period, N_{ow}, it is possible to describe this irregular and dynamic overtopping, if the overtopping discharge, q, is known. Each overtopping wave gives a certain overtopping volume of water, V. The distribution of overtopping wave volumes for coastal structures has been described in Section 5.5, Equations 5.52 and 5.53, which are repeated here.

182

$$P_{V\%} = P(V_i \geq V) = \exp\left[-\left(\frac{V}{a}\right)^b\right] \cdot (100\%) \text{ and } P_{V\%} = P_V \cdot (100\%) \qquad 6.16$$

$$a = \left(\frac{1}{\Gamma(1 + \frac{1}{b})}\right)\left(\frac{qT_m}{P_{ov}}\right) \qquad 6.17$$

Equation 6.17 shows that the scale parameter, a, depends on the overtopping discharge, but also on the mean period and probability of overtopping, or which is similar, on the storm duration and the actual number of overtopping waves. (Γ is the mathematical gamma function, and can be entered into MS Excel© as = 1 / EXP(GAMMALN(1+1/b)). It is graphically shown in Figure 5.57).

The probability of wave overtopping for rubble mound structures has been described in Section 6.2, Equation 6.3 and Equation 6.4. With the number of overtopping wave volumes known, Equations 6.16 and 6.17 give the distribution of overtopping wave volumes. The shape parameter, b, for structures likes dikes and embankments, is given by Equation 5.54 and Figure 5.58. Recent research showed that for rubble mound structures the shape parameter may be a little different (Zanuttigh *et al.*, 2013):
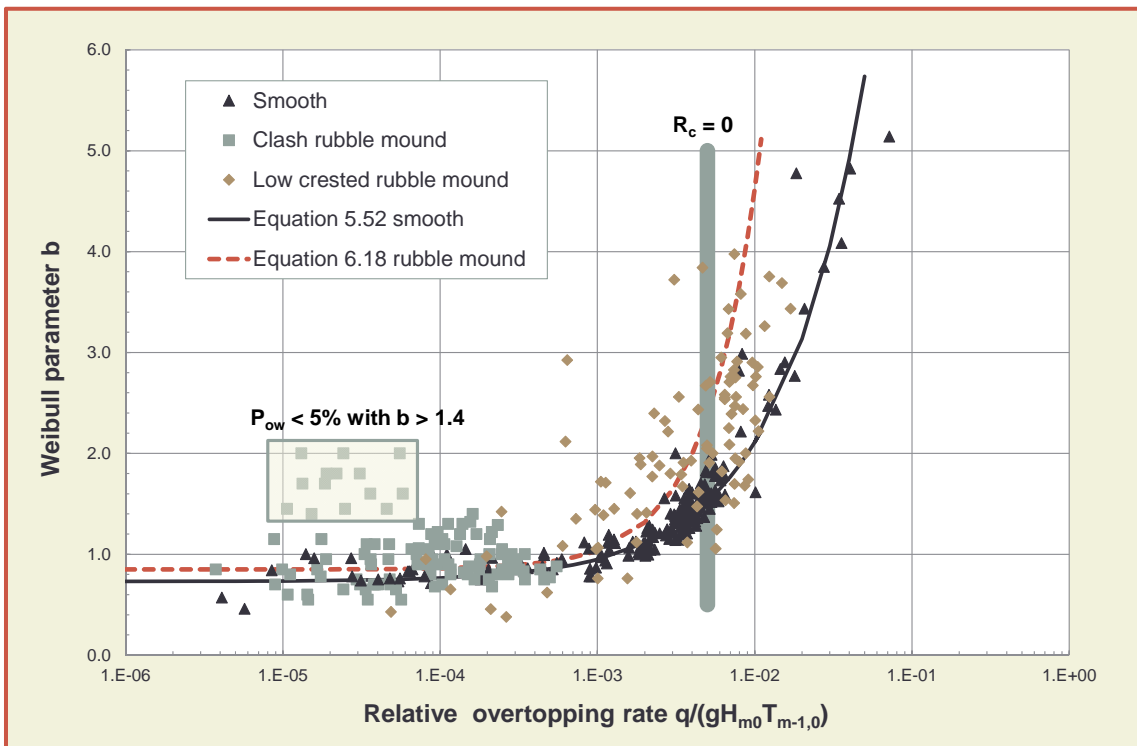
Figure 6.19: New Weibull shape factor, b, for rubble mound structures, spanning a large range of relative freeboards (Zanuttigh *et al.*, 2013)

$$b = 0.85 + 1500 \left(\frac{q}{gH_{m0}T_{m-1,0}} \right)^{1.3} \qquad\qquad 6.18$$

Equation 6.18 is given in Figure 6.19, including the data and fit for smooth slopes. It is clear that the scatter is significantly larger for rubble mound structures than for smooth slopes. Also the minimum value of b = 0.85 is a little larger than the minimum value of 0.73 for smooth structures.

The maximum overtopping during a certain event is fairly uncertain, as most maxima, but depends on the duration of the event. In a 6 hours period one may expect a larger maximum than only during 15 minutes. The maximum during an event can be calculated by Equation 5.57.

6.4.2 Overtopping velocities and spatial distribution

The hydraulic behaviour of waves on rubble mound slopes and on smooth slopes like dikes, is generally based on similar formulae, as clearly shown in this chapter. This is different, however, for overtopping velocities and spatial distribution of the overtopping water. A dike or sloping impermeable seawall generally has an impermeable and more or less horizontal crest. Up-rushing and overtopping waves flow over the crest and each overtopping wave can be described by a maximum velocity and flow depth, see Section 5.5.3. These velocities and flow depths form the description of the hydraulic loads on crest and inner slope and are part of the failure mechanism "failure or erosion of inner slopes by wave overtopping".

This is different for rubble mound slopes or breakwaters where wave energy is dissipated in the rough and permeable crest and where often overtopping water falls over a crest wall onto a crest road or even on the rear slope of a breakwater. A lot of overtopping water travels over the crest and through the air before it hits something else.

In CLASH, and a few other projects at Aalborg University, attention has been paid to the spatial distribution of overtopping water at breakwaters with a crest wall (Lykke Andersen and Burcharth, 2004b). The spatial distribution was measured by various trays behind the crest wall. Figure 6.20 gives different cross-sections with a set-up of three arrays, and the spatial distribution depends on the level with respect to the rear side of the crest wall and the distance from this rear wall, see Figure 6.21. The coordinate system (x, y) starts at the rear side and at the top of the crest wall, with the positive y-axis downward.
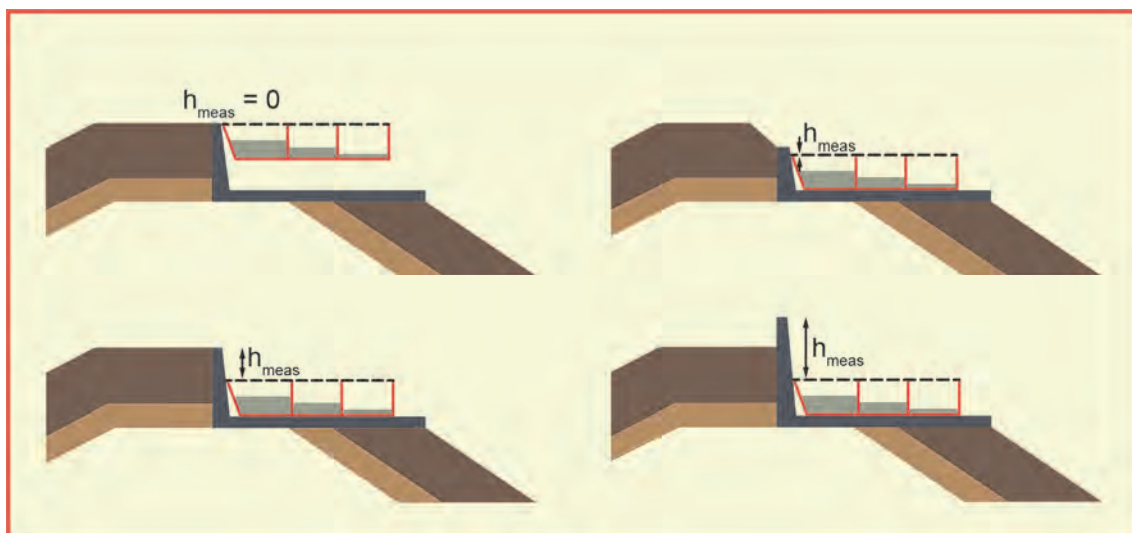
Figure 6.20:   Definition of y for various cross-sections

14
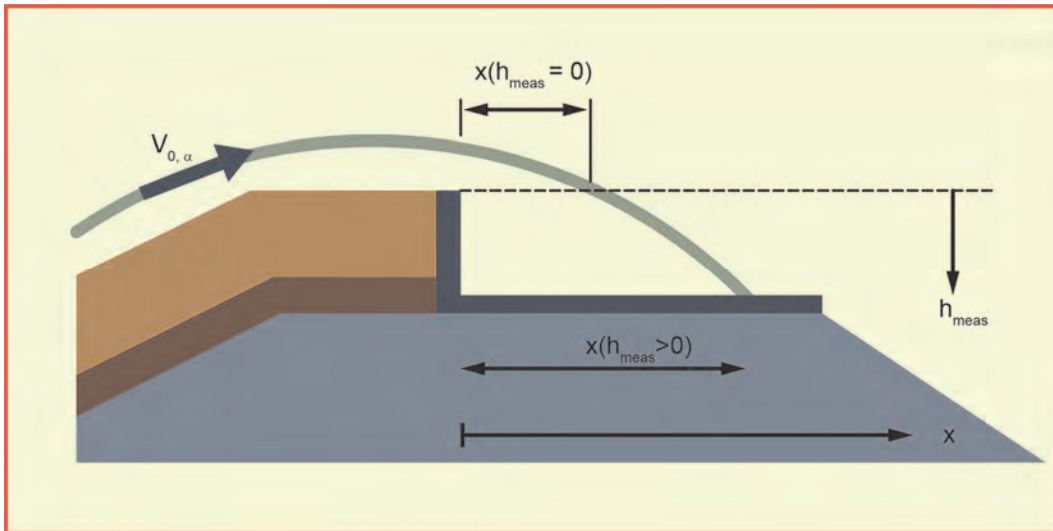
Figure 6.21: Definition of x- and y-coordinate for spatial distribution

The exceedance probability F of the travel distance is defined as the volume of overtopping water passing a given x- and y-coordinate, divided by the total overtopping volume. The probability, therefore, lies between 0 and 1, with 1 at the crest wall. The spatial distribution can be described with the following equations, which have slightly been rewritten and modified with respect to the original formulae by Lykke Andersen and Burcharth (2006). The probability F at a certain location can be described by:

$$F(x, y) = \exp\left(\frac{-1.3}{H_{m0}} \cdot \left\{ \max\left(\frac{x}{\cos\beta} - 2.7\, y\, s_{op}^{0.15}, 0\right)\right\}\right) \qquad 6.19$$

Equation 6.19 can be rewritten to calculate the travel distance x directly (at a certain level y) by rewriting the above equation:

$$\frac{x}{\cos\beta} = -0.77\, H_{m0} \ln(F) + 2.7\, y\, s_{op}^{0.15} \qquad 6.20$$

Suppose $\cos\beta = 0$, then we get $F = 1$ at $x = 0$, $F = 0.1$ at $x = 1.77\, H_s$ and $F = 0.01$ at $x = 3.55\, H_s$. It means that 10% of the volume of water travels almost two wave heights through the air and 1% of the volume travels more than 3.5 times the wave height. These percentages will be higher if $y \neq 0$, which is often the case with a crest unit.

The validity of Equations 6.19 and 6.20 is for rubble mound slopes of approximately 1:2 and for angles of wave attack between $0° \leq |\beta| < 45°$. It should be noted that the equation is valid for the spatial distribution of the water through the air behind the crest wall. All water falling on the basement of the crest unit will of course travel on and will fall into the water behind and/or on the slope behind.

6.5   Overtopping levels of shingle beaches

Beaches consisting of gravel or shingle (2 mm to 64 mm) are generally known as coarse beaches or shingle beaches and can be found in many parts (formerly glaciated) of the world (England, Iceland, Canada, etc.). Gravel barrier behaviour depends upon a number of factors such as sediment properties (porosity, permeability, grainsize), geological setting and wave climate.

Gravel beaches are highly efficient and practical forms of coastal protection and flood defence and overtopping and overwash processes play an important role in the evolution of these beaches, which can

trigger migration onshore over time by the rollover mechanism. This mechanism involves sediment transport from the front of the barrier, across the barrier crest and consequence deposition at the back of the barrier in the form of washover deposits.

The occurrence of overwash in areas of human occupation represents an hazard that can lead to damage to coastal properties and infrastructure, intrusion of salt and sand into agriculture soils, interference with back-barrier channel navigation, and loss of human life.

It is known that when wave run-up exceeds the barrier crest elevation, the following main outcomes, dependently on the level of exceedance, are possible. When wave run-up just overtops the barrier crest and flow velocities are very weak this cause insignificant morphological change. Vice versa if the combination of wave and water level conditions are severe, relative to the beach geometry, overtopping occurs more frequently. A range of features may result from this process; these include throat-confined overwash fans, or more wide-spread sluicing overwash, accretion on the barrier crest region and barrier stabilisation. Finally if the barrier beach is subjected to significant overwashing, erosion, lowering of the crest region and ultimately breaching can result.

Due to the dynamic and irregular overwash processes, i.e., rollover mechanism and/or accretion / lowering of the crest it is not possible to consistently measuring the mean overtopping discharge. Mobile beach wave overtopping cannot be therefore measured unless a solid/fixed structure is located behind the ridge. This is also not needed, as the mechanism is describing erosion and breaching, not the overtopping discharge.

Presently, understanding of run-up, overtopping and overwash of gravel beaches is considered to be poor and approaches to calculate run-up usually rely on formulae developed for structures or have been largely developed in laboratory environments using single grain size with associated problems in applying results to mixed sediments.

A classical formula to predict wave run-up on shingle beaches was described in EurOtop (2007). This formula was based on the assumption that a shingle beach may adjust its profile to the incident wave conditions, provided that sufficient material is available, therefore run-up and overtopping levels on shingle beaches are predicted considering the profile that will be formed under maximum wave conditions. The equations to predict the reshaped beach profile has been given in Van der Meer (1998) and is available in the program Breakwat (commercial software of Deltares). In this method the most important profile parameter for run-up is the crest height (h_c) above the (maximum) still water level (SWL). The largest waves will overtop this crest level and therefore h_c can be assumed more or less equal to $R_{u2\%}$.

The crest height (h_c) is only a function of the wave height and wave steepness, therefore the run-up level is defined as:

$$\frac{h_c}{H_{m0}} = 0.3 s_{om}^{-0.5} \qquad\qquad 6.21$$

where H_{m0} is the spectral significant wave height, s_{om} is the wave steepness using the wave mean period and not the spectral wave period $T_{m-1,0}$. See Section 1.4.2 for conversion.

A study on shingle beaches in Southeast England (Polidoro *et al.* 2013) used almost 400 field measurements (provided by the Environment Agency) of maximum wave run-up from several together with concurrent wave and water level data. Also wave flume tests were performed, where a selection of wave storms were extracted from the data set of events from wave buoys to reproduce a generic range of typical storm conditions. A prediction tool was developed during this work and a more detailed literature review on the present understanding of wave run-up on shingle beach and application of the tool is reported in the HR Wallingford research report "CAS0942-RT001-R03-00"

185

7 Vertical and steep walls

7.1 Introduction

This chapter presents guidance for the assessment of overtopping and post-overtopping processes at vertical and steep-fronted coastal structures such as caisson and blockwork breakwaters and vertical seawalls (see Figure 7.1). Also included are composite vertical wall structures, where the emergent part of the structure is vertical, fronted by a modest berm or toe mound, and vertical structures which include a bull-nose or wave return wall (as defined in Section 1.4.10 as the upper part of the defence.

Modern, large vertical breakwaters are almost universally formed of sand-filled concrete caissons usually resting on a small rock mound (e.g. Figure 7.1, upper left), or a larger rock mound if the water water depth becomes larger. Such caisson breakwaters may reach depths greater than 50 m, under which conditions no wave breaking at all at the wall would be expected. Sometimes the wall of a caisson is fully vertical, sometimes the upper part has a shifted parapet (to reduce wave forces), as in Figure 7.1, upper left. Conversely, older breakwaters may, out of necessity, have been constructed in shallower water or indeed, built directly on natural rock "skerries". As such, these structures may find themselves exposed to breaking wave, or "impulsive conditions", when the water depth in front of them is sufficiently low. These older breakwaters may be of stone or concrete blockwork construction (e.g. Figure 7.1, upper right). Urban seawalls (see examples in Figure 7.1, lower left and right) are almost universally fronted by shallow water, and are likely to be exposed to breaking or broken wave conditions, especially in areas of significant tidal range and possible high storm surges. The structure in Figure 7.1, lower right, shows a bull nose to reduce small wave overtopping even further.

Figure 7.1: Vertical structures: (clockwise top left) modern caisson breakwater with shifted parapet (Civitavecchia, Italy), old blockwork breakwater (St Andrews, UK), modern concrete seawall and older stone blockwork seawall with bull nose

The guidance in EurOtop (2007) was drawn largely from the predecessor UK Environment Agency "Overtopping of Seawalls: Design and Assessment Manual" (EA, 1999) with adjustments to many formulae based upon additional published work over the period 1999-2006. Those familiar with EurOtop (2007) should note that the differences between this second edition and the first arise principally from a bringing-

together of the approaches for sloping, steep and vertical structures according to a more uniform set of formulae. The adjusted set of formulae is anticipated to be simpler, with principal methods focussing on three classes of structure, and more transparent in terms of the physical processes being modelled. As these adjusted formulae are partly the result of algebraic manipulation of the previous formulae, in most cases, the final predictions will be unaltered, or hardly altered.

The principal changes are:

- A clear separation of situations based upon the presence or absence of an influencing foreshore in front of the vertical or steep structure (Section 7.3.5);

- For the case of structures without any influence of foreshore, the method for vertical and very steep "battered" walls is now the same as for the sloping structures presented in Chapter 5, which now extends from mildly sloping structures through to fully vertical walls;

- For plain vertical walls with influence of foreshore, an adjusted "discriminator" to identify impulsive overtopping conditions is used (replacing the previous h* parameter, see Section 1.4.4);

- A clearer integration of the methods for composite vertical structures with those for plain vertical structures;

- A new section on overtopping at perforated seawalls and caissons (Section 7.3.7);

- For prediction of the proportion of waves overtopping, there is an enhanced presentation of the existing formulae with clearer indication of the combined influences of impulsiveness and the obliquity of wave attack.
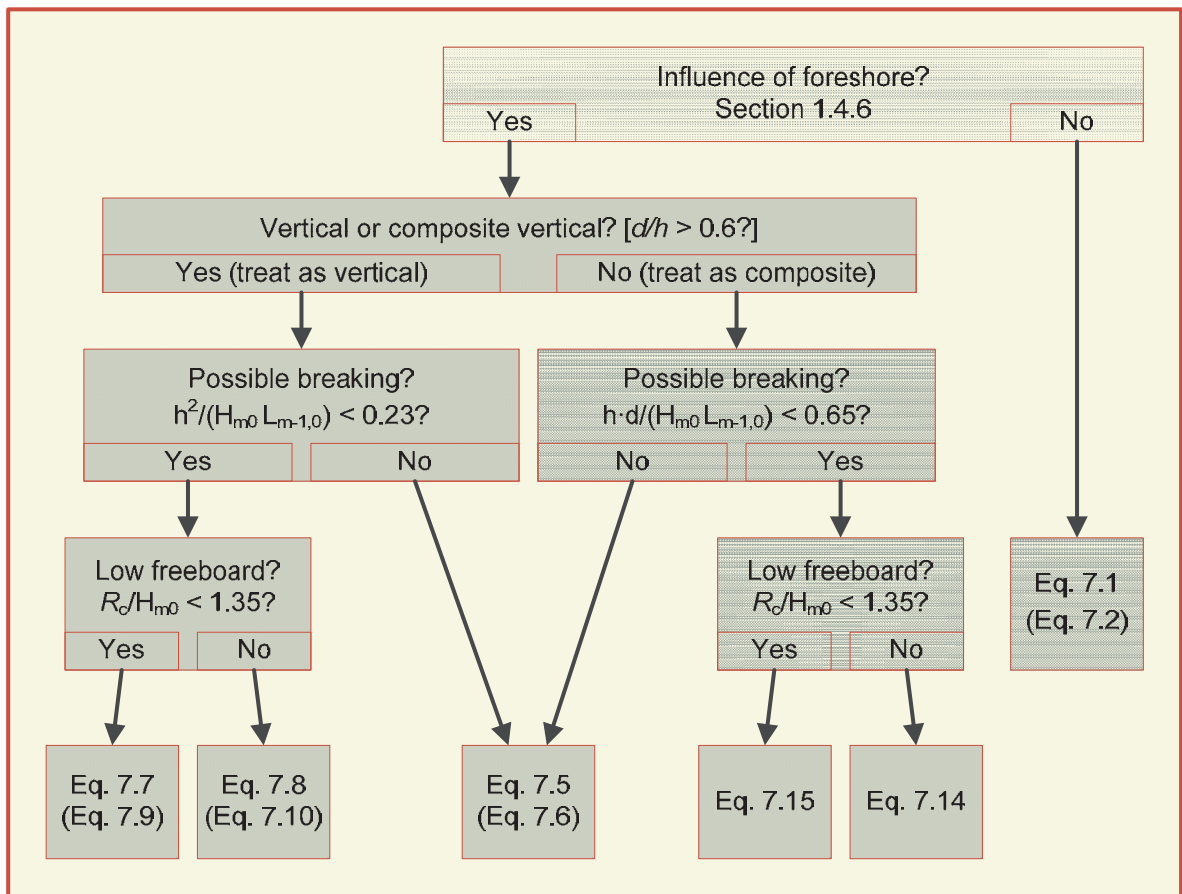
Figure 7.2: Decision chart for prediction of mean discharge at vertical and composite vertical walls. . The equations in brackets give the design and assessment approach

The result is the revised decision chart shown in Figure 7.2 for the prediction of mean overtopping discharges. This in turn means that the major section on mean discharge prediction discussed in Section 7.3 has been organised accordingly.

Table 7.1:   Summary of principal calculation procedures for vertical structures

	Mean value approach		Design approach	
Discrimination – mound influence?	Eq.	7.3	Eq.	7.3
Discrimination – impulsive / non-impulsive regime				
Plain vertical walls	Eq.	7.4	Eq.	7.4
Composite vertical walls	Eq.	7.13	Eq.	7.13
Plain vertical walls; overtopping discharge				
No influencing foreshore	Eq.	7.1 (= Eq. 5.17)	Eq.	7.2
Foreshore; non-impulsive conditions	Eq.	7.5	Eq.	7.6
Foreshore; impulsive conditions	Eqs.	7.7, 7.8	Eqs.	7.9, 7.10
Broken wave conditions (emergent toe)	Figure 7.10			
Steeply-battered walls	Eq.	7.11		
Composite vertical walls				
No influencing foreshore	Eq.	7.1	Eq.	7.2
Foreshore; non-impulsive conditions	Eq.	7.5	Eq.	7.6
Foreshore; impulsive conditions	Eqs.	7.14, 7.15		
Oblique wave attack	Figure 7.17			
Influence of short- vs long-crestedness	Eqs. 7.16, 7.17			
Non-impulsive conditions	Eqs. 7.18, 7.19			
Impulsive conditions			(Eq.	7.20)
Vertical walls with wave return wall / bullnose	Eqs.	7.21 - 7.23; Figure 7.22, Figure 7.23		
Perforated walls	Section 7.3.7 (commentary)			
Proportion of overtopping waves				
Normal wave attack	Eqs.	7.24, 7.25		
Oblique waves, non-impulsive conditions	Eqs.	7.29, 7.30		
Oblique waves, impulsive conditions	Eqs.	7.31 - 7.33		
Individual overtopping volumes	Eqs.	7.26, 7.28; impulsive b = 0.85		
with oblique waves	Eqs.	7.26, 7.28; impulsive b = 0.85 and Table 7.2, with Eqs. 7.31-7.33		
Overtopping velocities	Eq.	7.34		

This chapter follows approximately the same sequence as the preceding two chapters, though certain differences should be noted. In particular, run-up is not addressed, as it is not a measure of physical importance for this class of structure. Indeed, it is not well-defined for cases when the wave breaks, nearly-breaks or is broken when it reaches the structure, under which conditions an up-rushing jet of water is thrown upwards. The qualitative form of the physical processes occurring when the waves reach the wall are described in Section 7.2.

Distinctions drawn between different wave / structure regimes are reflected in the guidance for assessment of mean overtopping discharges given in Section 7.3. The basic assessment tools are presented for plain vertical walls in Section 7.3.1, followed by subsections giving advice on how these basic tools should be adjusted to account for other commonly occurring configurations; battered walls (Section 7.3.3); vertically composite walls (Section 7.3.4); the effect of oblique wave attack (Section 7.3.5); the effect of bull-nose / wave-return walls (Section 0).). The influence of a perforated seawall or breakwater on mean discharge is described in a new Section 7.3.7, and the influence of wind given in Section 7.3.8. Scale and model effects are reviewed in Section 7.3.9.

Methods to assess individual wave overtopping volumes are presented in Section 7.4. The current knowledge and advice on post-overtopping processes including velocities, spatial distributions and post-overtopping loadings are reviewed in Section 7.5. The principal calculation procedures are summarised in Table 7.1

7.2   Wave processes at walls

7.2.1 Overview

In assessing overtopping on sloping structures, it is necessary to distinguish whether waves are in the plunging, collapsing or surging regime (Section 5.3.1). Similarly, for assessment of overtopping at battered and vertical structures, it is generally required to identify the regime of the wave / structure interaction, with quite distinct overtopping responses expected for each regime.

On steep walls (vertical, battered or composite), non-impulsive or pulsating conditions occur when waves are relatively small in relation to the local water depth, and of lower wave steepnesses. In the absence of a foreshore that can affect the waves, these conditions will almost certainly prevail. Under these conditions, waves are not significantly influenced by the structure toe or deeply-submerged foreshore. Overtopping waves run up and over the wall giving rise to fairly smoothly-varying loads and green water overtopping (Figure 7.3 (upper)).

In contrast, impulsive conditions (Figure 7.3 (lower)) occur at vertical or steep walls when waves are larger in relation to local water depths, perhaps shoaling up over a foreshore or structure toe itself. Under these conditions, some waves will break violently against the wall with (short-duration) forces reaching 10 to 40 times greater than for non-impulsive conditions. Overtopping discharge under these conditions is characterised by a violent up-rushing jet of (probably highly aerated) water.
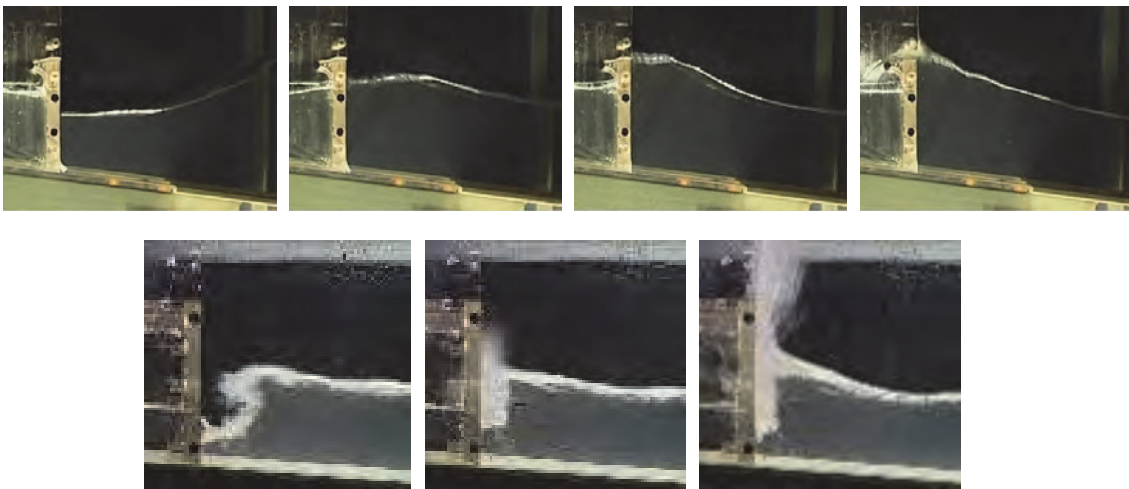
Figure 7.3:   Upper: A non-impulsive (sometimes referred to as "pulsating'" wave condition at a vertical wall, resulting in non-impulsive (or "green water") overtopping. Lower: impulsive (breaking) wave at a vertical wall, resulting in an impulsive (or "violent") overtopping condition

Lying in a narrow band between non-impulsive and impulsive conditions are near-breaking conditions where the overtopping is characterised by suddenness and a high-speed, near vertical up-rushing jet (like impulsive conditions), but where the wave has not quite broken onto the structure and so has not entrained the amount of air associated with fully impulsive conditions. This near-breaking condition is also known as the flip through condition. This condition gives overtopping in line with impulsive (breaking) conditions and is thus not treated separately.

Many seawalls are constructed at the back of a beach such that breaking waves never reach the seawall, at least not during frequent events where overtopping is of primary importance. For these conditions, particularly for typical shallow foreshore slopes of less than (say) 1:30, design wave conditions may be given by waves which start breaking (possibly quite some distance) seaward of the wall. These broken

waves arrive at the wall as a highly-aerated mass of water (Figure 7.4), giving rise to loadings which show the sort of short-duration peak seen under impulsive conditions (as the leading edge of the mass of water arrives at the wall), but smaller in magnitude due to the high level of aeration. For cases where the depth at the wall $h > 0$ m, overtopping can be assessed using the method for impulsive conditions. For conditions where the toe of the wall is emergent ($h \leq 0$ m), these methods can no longer be applied and an alternative is required (Section 7.3.1).
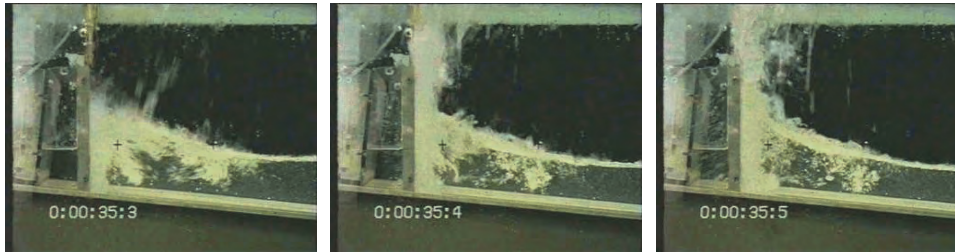
Figure 7.4:   A broken wave at a vertical wall, resulting in a broken wave overtopping condition

In order to proceed with assessment of overtopping, it is therefore necessary first to determine whether there is any influence of the foreshore. If there is foreshore influence, the dominant overtopping regime (impulsive or non-impulsive) must be determined next. No single method gives an impulsive / non-impulsive discriminator which is 100% reliable. The suggested procedure for plain and composite vertical structures includes a transition zone in which there is significant uncertainty in the prediction of the dominant overtopping regime and thus a worst-case is taken.

7.3   Mean overtopping discharges for vertical and very steep walls

7.3.1 Strategy

For plain vertical walls, before describing the detailed methodology, some initial insight into the way in which the methodology is divided-up between distinct settings can be gained from Figure 7.5. The figure shows the relative (non-dimensional) overtopping discharge plotted against the relative freeboard. On this, three regimes can be identified:

(i) The situation for a vertical wall where there is no influence of foreshore, e.g. for relative deep water. For a given relative freeboard, such a setting gives the lowest overtopping. The functional form of the overtopping is well-described by the same formulation as for sloping structures, *viz* a Weibull curve.

(ii) The situation where there is influence of the foreshore, but no wave breaking onto the structure ("non-impulsive" overtopping only). Comparing these situations to (i), it is clear that these give higher overtopping. At lower freeboards, there is hardly difference, but can become quite large for higher freeboards. The overtopping under these situations is well-described by the familiar exponential function (a straight line on a log-linear graph).

(iii) The situation where some waves break at the structure, giving "impulsive" overtopping. For these conditions, the up-rushing water can reach very great heights, and significant overtopping can be expected up to very high relative freeboards, witnessed by the near-horizontal lines extending to the right of the figure. A power-law formulation is used to describe this situation, with the influence of relative depth and wave steepness accounted for in the formulae too (giving the family of curves seen in the figure).

The strategy for assessment of mean overtopping discharge follows the procedures of the decision chart of Figure 7.2. In order to arrive at the most appropriate prediction equation, the following questions may need to be answered:

- Is an influencing foreshore present in front of the structure?
- Is the structure a simple vertical or steep wall, or is there a significant mound present?
- Is the structure likely to experience impulsive (violent, wave-breaking) overtopping?

The following sub-sections take a step-by-step approach through the assessment procedure for plain vertical walls (Section 7.3.2) and for composite vertical structures (Section 7.3.4). Full details of the approach and supporting data and charts can be found in Van der Meer and Bruce (2014).
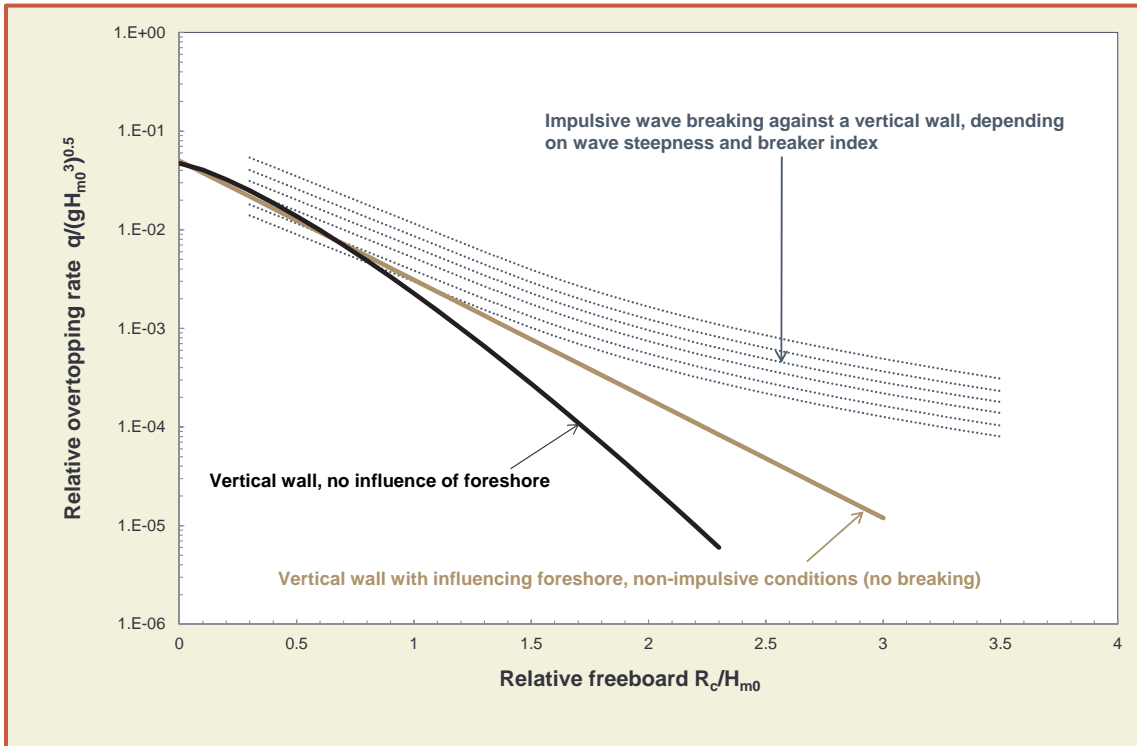
Figure 7.5:   An overview of the regimes of wave overtopping at vertical structures

7.3.2 Plain vertical walls

A definition sketch for the key geometric parameters is given in Figure 7.6.
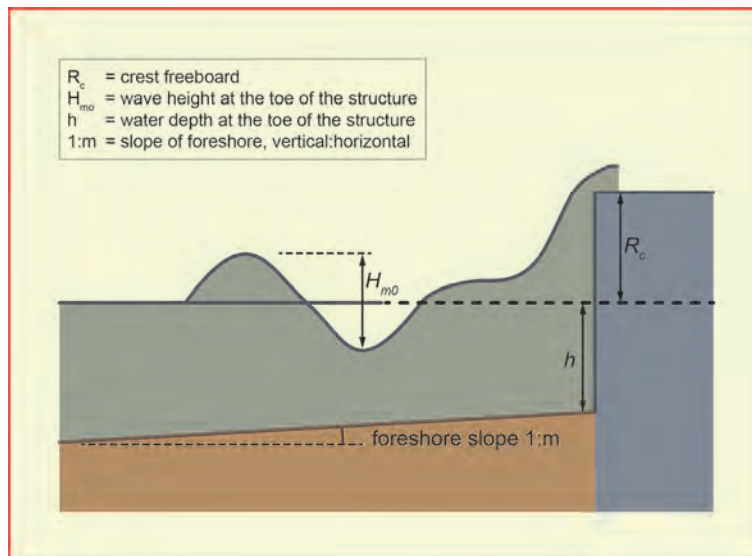
Figure 7.6:   Definition sketch for assessment of overtopping at plain vertical walls

Step 1: Is there an influence of foreshore or not? Analysis of overtopping data indicates that situations in which a foreshore influences the incident waves should be distinguished from situations, such as relative deep water, where this is not the case. A foreshore can have influence by transforming incident wave shape and height through shoaling, steepening and breaking. A practical definition of an influencing

foreshore is shallow or intermediate depth water (i.e. not deep water) at the structure toe, but depends also on whether the foreshore is horizontal or really sloping (1:50 and steeper). See also Section 1.4.6.

If there is an influencing foreshore, then proceed directly to **Step 2**.

For the case of no influencing foreshore, Figure 7.7 shows the CLASH database data for these conditions, see Van der Meer and Bruce (2014) for division in sub-sets. The overtopping is also described by the method of Section 5.3.3, for cot α = 0, where a vertical wall is seen as the steepest slope possible.

To take a mean value approach, Equation 7.1 is derived from measured data and should be used for predictions and comparisons with measurements. This is the same as Equation **5.18** with cot α = 0. The reliability of Equation 7.1 is given by $\sigma(0.047) = 0.007$ and $\sigma(2.35) = 0.23$.

$$\frac{q}{\sqrt{g \cdot H_{m0}^3}} = 0.047 \cdot \exp\left[-\left(2.35\frac{R_C}{H_{m0}}\right)^{1.3}\right] \qquad 7.1$$

For a design or assessment approach, it is strongly recommended to increase the average discharge by about one standard deviation. Thus, Equation 7.2 should be used in design and safety assessments, where the effectiveness and scatter associated with this prediction can be gauged from Figure 7.8:

$$\frac{q}{\sqrt{g \cdot H_{m0}^3}} = 0.054 \cdot \exp\left[-\left(2.12\frac{R_C}{H_{m0}}\right)^{1.3}\right] \qquad 7.2$$
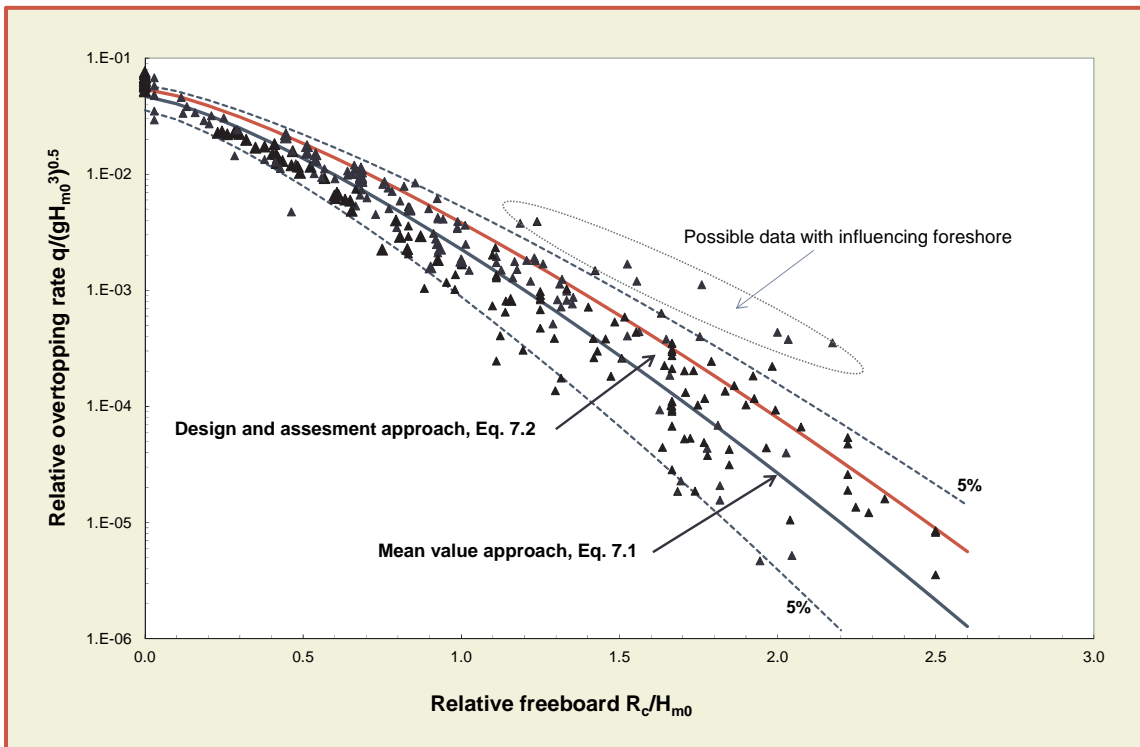
Figure 7.7: CLASH database for vertical walls without influencing foreshore

If the structure has been analysed using the no influencing foreshore method above, then there is no need to proceed further with Section 7.3.2.

Step 2: Is there a significant mound present? This section pertains to vertical or steep structures with a significant or influencing foreshore. Analysis (Van der Meer and Bruce, 2014) shows that a mound, if present in front of the main steep or vertical part of the structure, ceases to influence the overtopping when the water depth over the mound, d, exceeds 60% of the water depth at the toe of the structure, h, *i.e:*

$$d \geq 0.6h \text{ ; mound has no significant influence. Proceed to Step 3.}$$
$$d < 0.6h \text{ ; mound influence significant. Go to Section 7.3.4 (Step 3).} \qquad 7.3$$
$$\text{both assuming that the mound width is } \sim 1 \text{ H}_{m0}, \text{ or smaller.}$$

Note that Equation 7.3 does not account for berm width. There is a paucity of data for the influence of berm width. For practical purposes, it is assumed that the berm, if present, has a width that is of the order of one wave height.

Step 3: Is there a likelihood of impulsive overtopping conditions? This section pertains to vertical or steep structures with an influencing foreshore, but without a significant mound. Under the particular situation in which the toe of the wall is emergent ($h < 0$ m) only broken waves reach the wall, and an example is given at the end of this Section. Under the common conditions where the toe of the wall is submerged ($h > 0$ m; Figure 7.6), whether impulsive overtopping can occur is determined by:

$$\frac{h^2}{H_{m0}L_{m-1,0}} > 0.23 \text{ treat as non-impulsive conditions (Step 4a)}$$

$$\frac{h^2}{H_{m0}L_{m-1,0}} \leq 0.23 \text{ treat as impulsive conditions (Step 4b)} \qquad 7.4$$

Step 4a: Non-impulsive conditions. For the case of simple vertical walls, with influencing foreshore, under non-impulsive conditions, the mean value approach, Equation 7.5, is developed from the averages of the measured data and should be used for predictions and comparisons with measurements. This is the same as the prediction equation originally proposed by Allsop *et al.* (1995) for this class of structure under non-impulsive overtopping conditions.

$$\frac{q}{\sqrt{gH_{m0}^3}} = 0.05 \exp\left(-2.78\frac{R_c}{H_{m0}}\right) \qquad 7.5$$

The reliability of Equation 7.5 can be described by σ(0.05) = 0.012 together with σ(2.78) = 0.17. For a design or assessment approach, it is strongly recommended to increase the average discharge by about one standard deviation. Note that σ = 0.012 should be added to 0.05 and σ = 0.17 should be subtracted from 2.78. Thus, Equation 7.6 should be used in design and safety assessments, where the effectiveness and scatter associated with this prediction can be gauged from Figure 7.8:

$$\frac{q}{\sqrt{gH_{m0}^3}} = 0.062 \exp\left(-2.61\frac{R_c}{H_{m0}}\right) \qquad 7.6$$
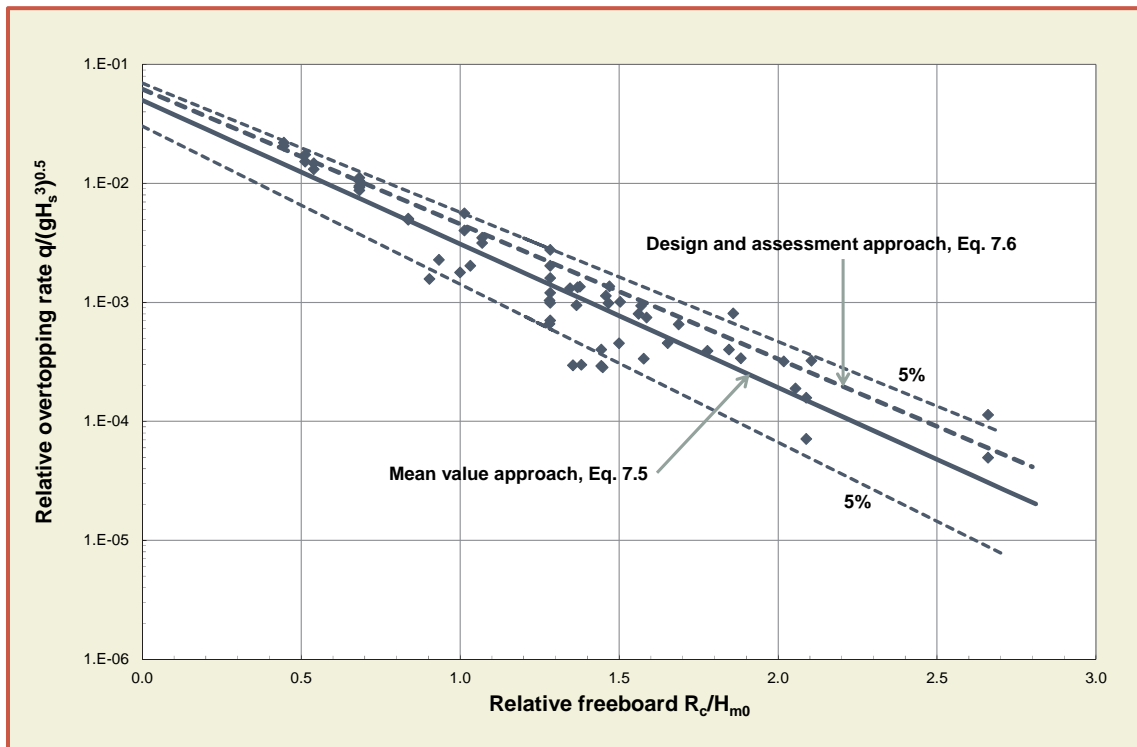
Figure 7.8: Mean overtopping at a plain vertical wall under non-impulsive conditions (Equation 7.5)

Step 4b: Impulsive conditions The mean discharge at vertical walls under conditions where impulsive overtopping is expected are described by two formulae: an exponential formula for lower freeboards, and a power-law formula for the higher freeboards. For the higher freeboards, with impulsive overtopping, there can be overtopping even at very high relative freeboards, so exponential decay is not appropriate and a power-law formula is used instead. But the power law would rise to infinity as relative freeboard approaches zero, which cannot be the case, so an exponential form is used for these lower relative freeboards.

This behaviour can be seen in Figure 7.9, in which discharge is seen to follow a familiar exponential decrease with increasing freeboard for lower values of dimensionless freeboard, before lifting off above this decay line for dimensionless freeboards above 1.35 or so. Note that dataset 107 for zero freeboard shown in Figure 7.9, does not strictly belong on this chart because the conditions are not impulsive, but is plotted to give a sense of the behaviour of the formulae at lowest freeboards in relation to these zero freeboard discharge data.

It should be noted that in contrast to the non-impulsive method, the relative depth and wave steepness at the toe of the structure play a role, and this is reflected in the formulae (Equations 7.7 and 7.8) and in the choice of the non-dimensionalisation used for the mean discharge (y-axis) of Figure 7.9. In addition, the 5% lower and upper confidence limits have been plotted.

For a mean value approach, it is recommended that for lower non-dimensional freeboards $R_c / H_{m0} < 1.35$, Equation 7.7 should be used. The reliability of Equation 7.7 is given by $\sigma(0.011) = 0.0045$.

$$\frac{q}{\sqrt{gH_{m0}^3}} = 0.011 \left(\frac{H_{m0}}{h s_{m-1,0}} \right)^{0.5} \exp\left(-2.2 \frac{R_c}{H_{m0}} \right) \qquad \text{valid for } 0 < R_c/H_{m0} < 1.35 \qquad 7.7$$

For higher non-dimensional freeboards $R_c / H_{m0} \geq 1.35$, Equation 7.8 should be used for a mean value approach. The reliability of Equation 7.8 is given by $\sigma(0.014) = 0.006$.
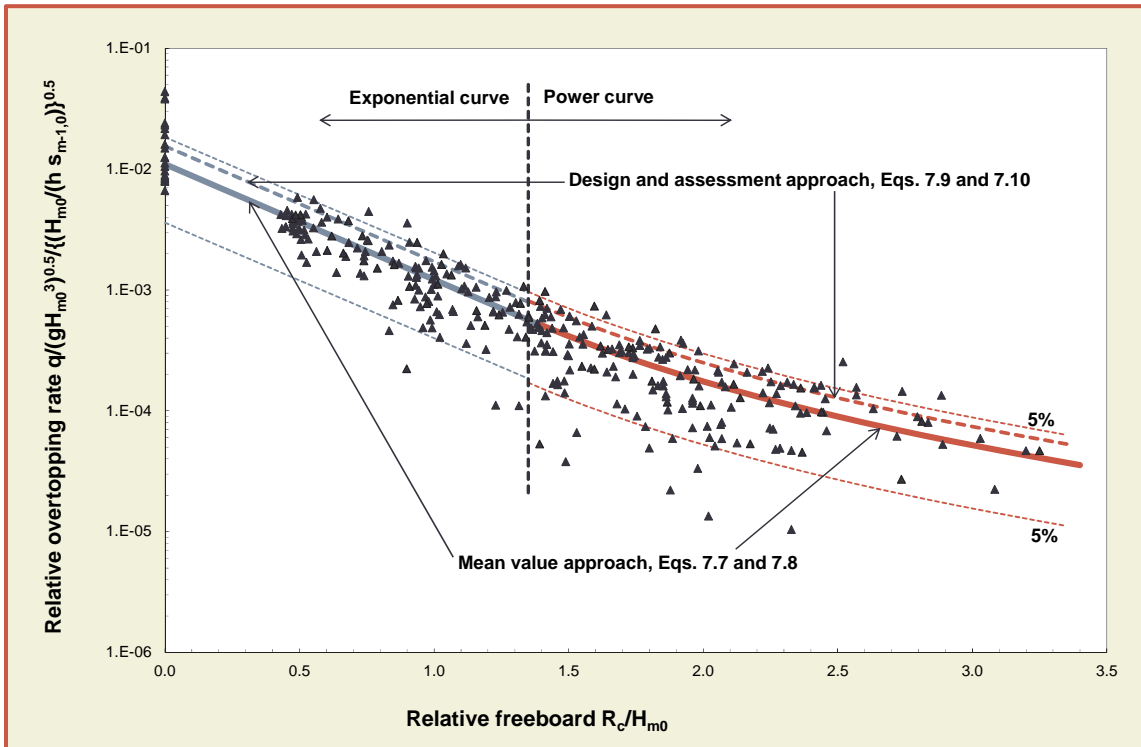
Figure 7.9:   Mean overtopping at a plain vertical wall under impulsive conditions

$$\frac{q}{\sqrt{gH_{m0}^3}} = 0.0014 \left(\frac{H_{m0}}{hs_{m-1,0}} \right)^{0.5} \left(\frac{R_c}{H_{m0}} \right)^{-3} \qquad \text{valid for } R_c/H_{m0} \geq 1.35 \qquad 7.8$$

For a design or assessment approach, it is strongly recommended to increase the average discharge by about one standard deviation. Thus, Equations 7.9 and 7.10 should be used in design and safety assessments.

$$\frac{q}{\sqrt{gH_{m0}^3}} = 0.0155 \left(\frac{H_{m0}}{hs_{m-1,0}} \right)^{0.5} \exp\left(-2.2 \frac{R_c}{H_{m0}} \right) \qquad \text{valid for } 0.1 < R_c/H_{m0} < 1.35 \qquad 7.9$$

$$\frac{q}{\sqrt{gH_{m0}^3}} = 0.0020 \left(\frac{H_{m0}}{hs_{m-1,0}} \right)^{0.5} \left(\frac{R_c}{H_{m0}} \right)^{-3} \qquad \text{valid for } R_c/H_{m0} \geq 1.35 \qquad 7.10$$

Emergent toe: Data for configurations where the toe of the wall is emergent (*i.e.* at or above still water level, $h \leq 0$ m) is limited. Overtopping under emergent toe conditions is illustrated in Figure 7.10. It should be noted that this graph is based upon a limited dataset of small scale tests with a steep 1:10 foreshore only (i.e. cot α = 10) and should not be extrapolated beyond the ranges tested ($s_{m-1,0} \geq 0.03$; $0.55 \leq R_c/H_{m0,deep} \leq 1.6$).

As the foreshore was quite steep, very close to the limit of a gentle sloping structure, the overtopping formula for breaking waves on a gentle slope, Equation 5.10, was used. This means that the wave height

in front of the 1:10 slope was used (and not at the toe of the vertical wall, which is not defined if the toe is emerged) and a slope angle of cot α =10 was used for the data.

Actually, Figure 7.10 shows the effect of a vertical wall, quite close but above the water level, on a slope 1:10, compared to a straight slope 1:10.   A very gentle 1:10 slope with similar crest freeboard as with the vertical wall, shows less overtopping than with the vertical wall, as the data points lie above the prediction line. In that sense a very gentle slope is more effective than a vertical wall, but it also needs a long slope above water to come to the same crest freeboard.

Figure 7.10 shows that overtopping may easily increase by a factor up to 10-100 for small overtopping, compared to a straight gentle smooth slope. This method cannot be applied with foreshores that are gentler than 1:10 as the overtopping formulae for slopes are then not applicable anymore.
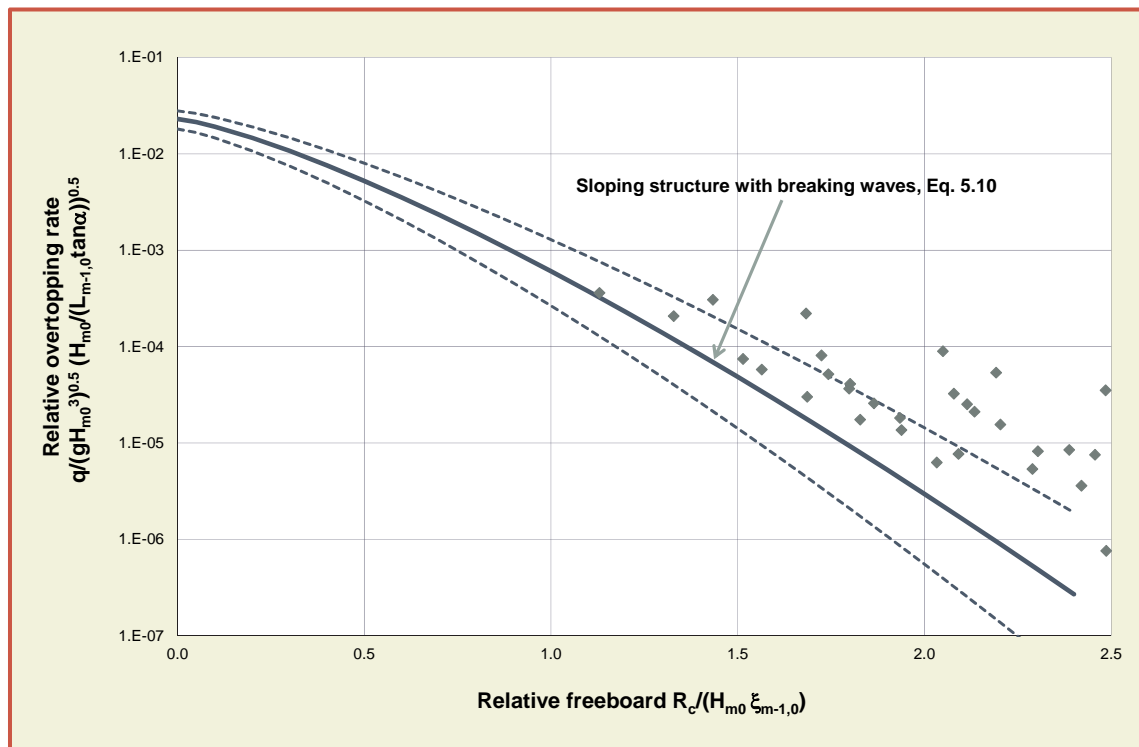
Figure 7.10:   Mean overtopping discharge with emergent toe (h < 0 m) of vertical wall on a foreshore slope 1:10. Data are compared with the formula for sloping structures, using cot α = 10 and deep water wave conditions.

7.3.3 Battered walls

Near-vertical walls, batters such as 5:1 or 10:1 (cot α= 0.2 or 0.1), are found commonly for older UK seawalls and breakwaters (e.g. Figure 7.11).

There is a relative paucity of data on steeply battered walls (cot α ≤ 0.2). Of the two principal datasets, one covers battered walls with no influencing foreshore, and the other covers impulsive conditions (with influencing foreshore).

For the former case of no influencing foreshore, the method of Section 5.3.3 can be applied, using Equation 5.18 with the appropriate choice of cot α. Some sense of the sensitivity of the overtopping to the batter of the wall can be gained from Figure 5.19.

For the latter case of an influencing foreshore, the same procedure as for fully vertical walls (Section 7.3.2) should be followed. If Step 4b from Section 7.3.2 of the procedure is reached (i.e. impulsive overtopping is anticipated at the wall), then Step 4b below should be followed.
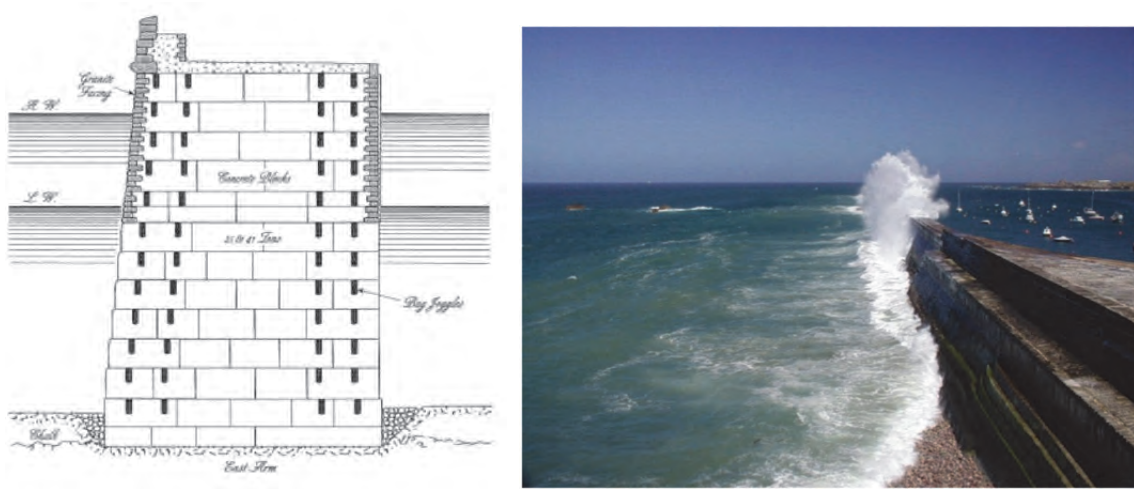
Figure 7.11:   Battered walls: cross-section of a blockwork breakwater (left), and Admiralty Breakwater, Alderney Channel Islands (right, courtesy G. Müller)

Step 4b (battered walls) Mean overtopping discharges for battered walls under impulsive conditions are observed to be slightly in excess of those for a vertical wall over a wide range of dimensionless freeboards. Multiplying factors are given in Equation 7.11.

10:1 battered wall:	$q_{10:1\ batter} = q_{vertical} \times 1.3$	7.11
5:1 battered wall:	$q_{5:1\ batter} = q_{vertical} \times 1.9$	

where $q_{vertical}$ is arrived at from the procedure for fully-vertical walls under impulsive overtopping conditions. These influences are shown in Figure 7.12.   It should be observed that these adjustments are arrived at from a relatively small number of data, and that they represent fairly small changes given the scatter inherent in the underlying prediction methods.
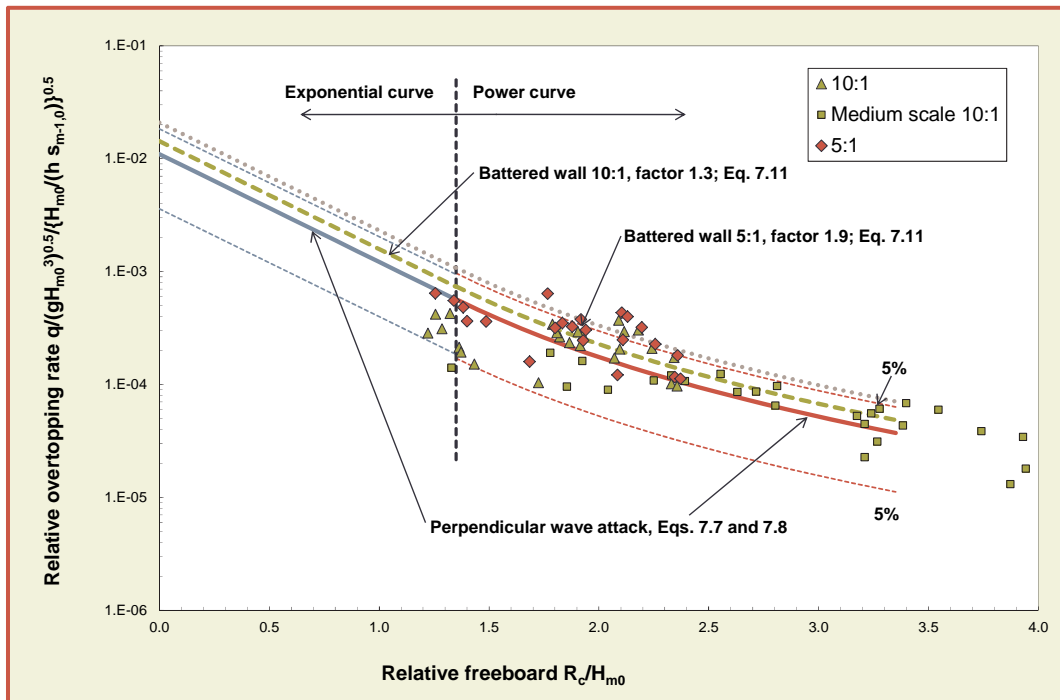
Figure 7.12:   The influence of steeply battered (10:1 and 5:1) walls on wave overtopping, for impulsive conditions

It is informative to compare the order of magnitude of the influence of battered vs. vertical walls suggested by the two schemes, for no foreshore influence (Figure 5.19, with cot α = 0.36 shown in the figure – a batter of approximately 2.8:1) and the influences seen in Figure 7.12.   These influences are comparable in magnitude and not more than a factor of 1.5.

7.3.4 Composite vertical walls

It is well-established that a relatively small toe berm can change wave breaking characteristics, thus significantly altering the type and magnitude of wave loadings. Many vertical seawall walls may be fronted by rock mounds with the intention of protecting the toe of the wall from scour.

Figure 7.13:   Examples of composite vertical structures, Barcelona, Spain (left), Ibiza (Spain) right

The toe configuration can vary considerably, potentially modifying the overtopping behaviour of the structure. Three types of mound can be identified

- Small toe mounds which have an insignificant effect on the waves approaching the wall – here the toe may be ignored and calculations proceed as for simple vertical (or battered) walls.

- Moderate mounds, which significantly affect wave breaking conditions, but are still below water level. Here a modified approach is required. This is the topic of this sub-sub-section.

- Emergent mounds in which the crest of the armour protrudes above still water level. Prediction methods for these structures may be adapted from those for crown walls on a rubble mound (Section 6.3.5), or by application of the EurOtop Artificial Neural Network (ANN).
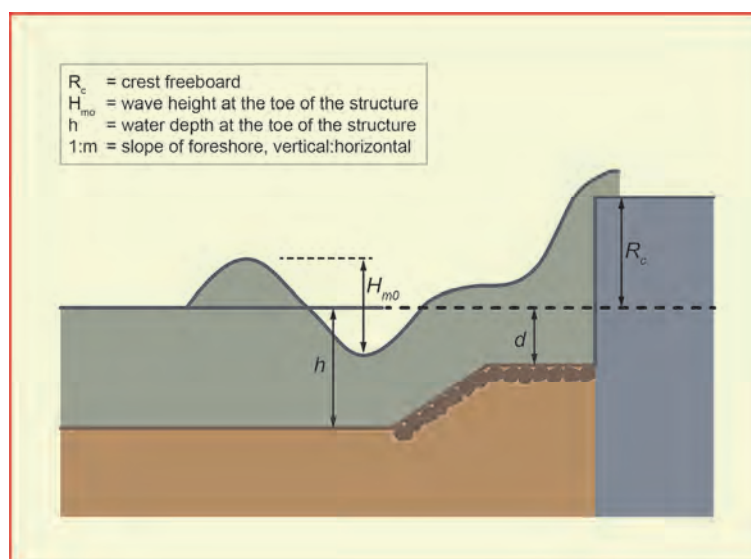
Figure 7.14:   Definition sketch for assessment of overtopping at composite vertical walls.

For assessment of mean overtopping discharge at a composite vertical seawall or breakwater, the same overall strategy is adopted as for plain vertical structures, as set out in Section 7.3.1 and depicted in the decision chart Figure 7.2. The steps down the composite vertical walls branch of the decision chart are set out in steps 1 to 4 below. A definition sketch showing the key parameters is given in Figure 7.14.

Step 1: Is a significant foreshore present or absent? The analysis of overtopping data for plain vertical structures indicates that situations in which a foreshore influences the incident waves should be distinguished from situations, such as relative deep water, where this is not the case. A foreshore can have influence by transforming incident wave shape and height through shoaling, steepening and breaking. A practical definition of an influencing foreshore is a situation with shallow or intermediate depth water (i.e. not deep water) at the structure toe. While there is relatively less data for composite walls without influencing foreshore, the physical rationale for distinguishing cases in which the foreshore does and does not have significant influence applies also to composite vertical walls, and the same distinction is recommended.
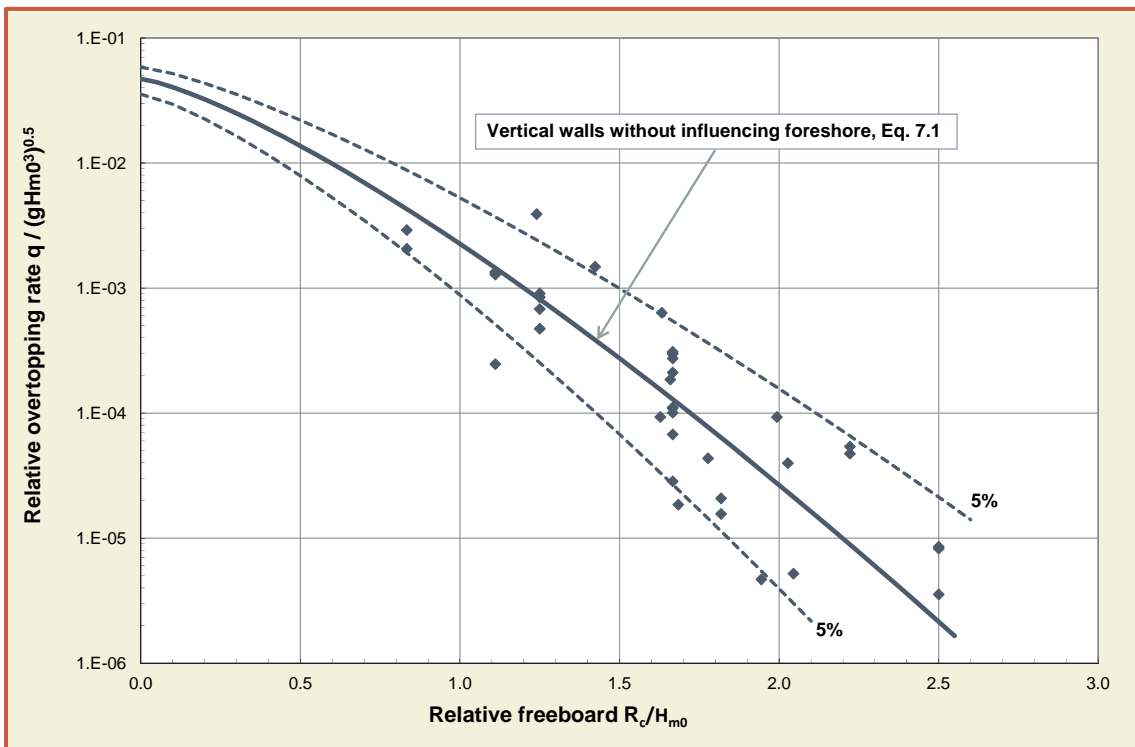
Figure 7.15: Mean discharge at composite vertical walls without influencing foreshore. The data are for composite structures. The prediction line is the same as for plain vertical structures

For no influencing foreshore, the presence of the mound does not appear to influence the overtopping, and the method for plain vertical walls (Section 7.3.2) should be used. For a mean value approach, e.g. for comparisons with measurements, Equation 7.1 should be used. For a design and safety assessment approach, Equation 7.2 is the appropriate choice. The effectiveness of this method for composite structures falling into this category can be gauged from Figure 7.15, which shows all the composite wall data where there is no influencing foreshore, found in the CLASH database.

In the case of no influencing foreshore, there is no need to proceed further with Section 7.3.4. If an influencing foreshore is present, proceed to step 2.

Step 2: Is there a significant mound present? This section pertains to composite vertical structures with a significant foreshore. As noted in the procedure for plain vertical walls (Section 7.3.2), analysis (in Van der Meer and Bruce, 2014) shows that a mound, if present in front of the main steep or vertical part of the structure, begins to affect the overtopping when the water depth over the mound, d, falls below 60% of the water depth at the toe of the structure, h, $i.e.$

$$d \geq 0.6h \text{; mound has no significant influence. Go back to Section 7.3.2 (Step 2)}$$
$$d < 0.6h \text{; mound influence significant. Proceed to Step 3.}$$

7.12

Step 3: Is there a likelihood of impulsive overtopping conditions? This section pertains to composite vertical structures with a significant mound and an influencing foreshore. As for fully-vertical structures, it is now necessary to distinguish whether impulsive overtopping conditions may occur at the structure, although it should be noted that the parameter group used to discriminate between non-impulsive and impulsive conditions differs from that used for fully-vertical structures. Whether impulsive overtopping can occur is determined using Equation 7.13, with parameters defined according to Figure 7.14. Note that the wavelength parameter is calculated for deep water.

$$\frac{d}{H_{m0}} \cdot \frac{h}{L_{m-1,0}} > 0.65 \quad \text{Treat as non-impulsive conditions. Proceed to Step 4a.}$$
$$\frac{d}{H_{m0}} \cdot \frac{h}{L_{m-1,0}} \leq 0.65 \quad \text{Treat as impulsive conditions. Proceed to Step 4b.}$$

7.13

Step 4a: Composite vertical structures; non-impulsive conditions. Actually, there are no data available for composite vertical structures on an influencing foreshore, but with non-impulsive conditions. When non-impulsive conditions prevail, it is proposed that overtopping can be predicted by the standard method given previously for non-impulsive conditions at plain vertical structures: Equation 7.5 for a mean value approach, and Equation 7.6 for a design or assessment approach.

Step 4b: Composite vertical structures; impulsive conditions. For prediction of the mean discharge at composite vertical walls under conditions where impulsive overtopping is expected, a modified version of the impulsive prediction method for plain vertical walls is recommended, accounting for the presence of the mound by use of the ratio of the water depth over the mound to that at the toe of the structure, d / h (see Figure 7.14).

As per the plain vertical wall case, the overtopping response is described by two formulae: an exponential formula is required for lower freeboards in order to offer physically rational behaviour at very low and zero freeboards (a power law would increase towards infinity); and a power-law formula which captures the ability of the violent uprush associated with impulsive events which means there can always be overtopping.

All available CLASH database data for impulsive conditions at composite walls is shown in Figure 7.16. Note that in Figure 7.16 there is a paucity of data for lower freeboard conditions, and that predictions in this zone should be made *as per* a plain vertical wall.

It should be noted that in contrast to the non-impulsive method, the relative depth and wave steepness at the toe of the structure play a role, and this is reflected in the formulae and in the choice of the non-dimensionalisation used for the mean discharge (y-axis) of Figure 7.16. For higher non-dimensional freeboards $R_c / H_{m0} \geq 1.35$, Equation 7.14 should be used.

There is a paucity of data available for lower freeboards $R_c / H_{m0} < 1.35$. Equation 7.15 offers a physically sensible extrapolation to lowest freeboards, based upon the better supported method for plain vertical walls (Equation 7.7). The reliability of the equations is described by $\sigma(0.014) = 0.006$ for Equation 7.14 and $\sigma(0.011) = 0.0045$ for Equation 7.15, which is similar to the equations for impulsive overtopping for plain vertical walls, Equations 7.7 and 7.8.

$$\frac{q}{\sqrt{gH_{m0}^3}} = 1.3 \left(\frac{d}{h}\right)^{0.5} 0.0014 \left(\frac{H_{m0}}{h s_{m-1,0}}\right)^{0.5} \left(\frac{R_c}{H_{m0}}\right)^{-3} \qquad \text{valid for } R_c/H_{m0} \geq 1.35 \qquad 7.14$$

$$\frac{q}{\sqrt{gH_{m0}^3}} = 1.3 \left(\frac{d}{h}\right)^{0.5} 0.0011 \left(\frac{H_{m0}}{h s_{m-1,0}}\right)^{0.5} \exp\left(-2.2 \frac{R_c}{H_{m0}}\right) \qquad \text{valid for } R_c/H_{m0} < 1.35 \qquad 7.15$$

202
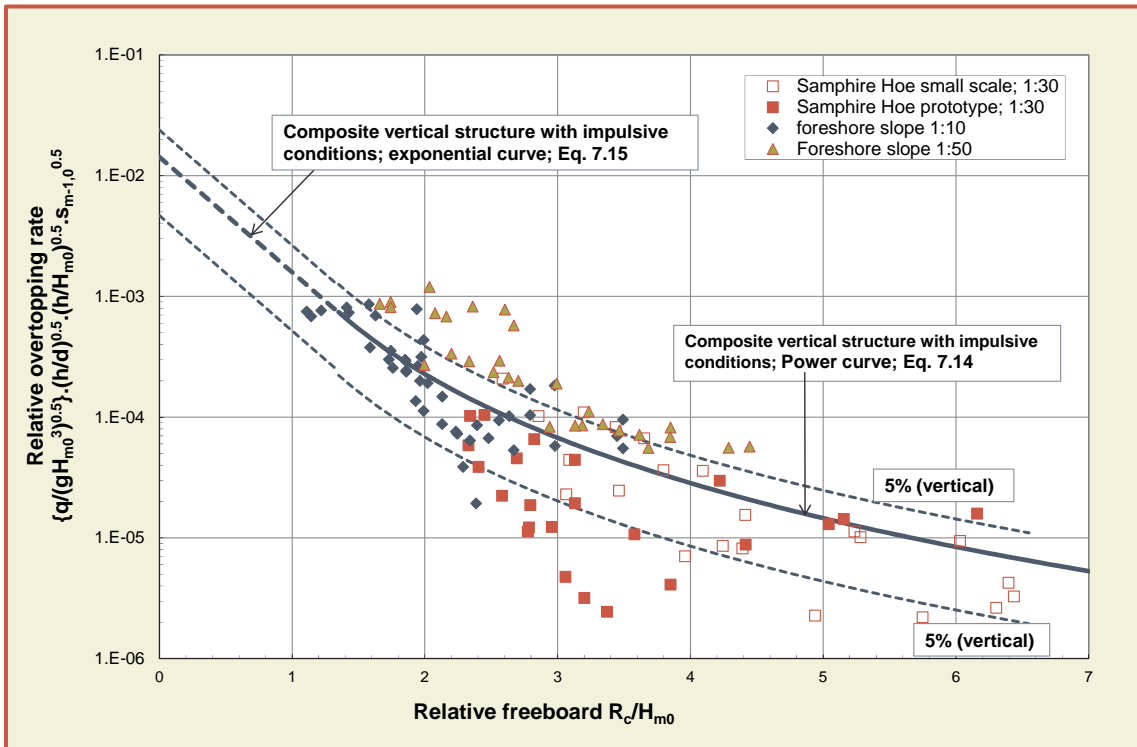
Figure 7.16: Mean overtopping at a composite vertical wall under impulsive conditions. Note that there is a paucity of data for lower freeboard conditions, and that predictions in this zone should be made *as per* a plain vertical wall.

The scatter in Figure 7.16 is considerable. The data for the 1:30 small scale and 1:10 fit reasonably within the 90%-confidence band. But for yet unclear reasons the data of the 1:50 foreshore slope are well above the mean prediction line. The prototype data for Samphire Hoe fall for a large part in the 90%-confidence band, but a number of points fall well below the lower 5%-exceedance line. These points may belong to transition conditions (as the tide varied during the measurements) and may well belong to less impulsive and more non-impulsive conditions.

7.3.5 Effect of oblique waves

Seawalls and breakwaters seldom align perfectly with incoming waves. The assessment methods presented thus far are only valid for shore-normal wave attack. In this subsection, advice is given on how the methods for shore-normal wave attack (obliquity $\beta = 0°$) should be adjusted for oblique wave attack.

Short-crested and long-crested waves. As described for sloping structures in Section 5.4.3, while most laboratory studies have used long-crested waves, the field situation will commonly be characterised by short-crested seas. The greater directional spreading inherent in short-crested seas results in a more

gradual reduction in overtopping with increasing angle of wave attack than is anticipated for long-crested seas.

For normal wave attack, the overtopping response depends upon the presence or absence of an influencing foreshore, and if such a foreshore is present, upon the physical form (or regime) of the wave / wall interaction; non-impulsive or impulsive. As such, the first step is to use the methods given in Section 7.3.2 to determine the form of overtopping for shore-normal. Based upon the outcome of this, guidance under non-impulsive conditions or impulsive conditions should be followed. For **non-impulsive conditions**, an adjusted version of Equation 7.5 should be used (Equation 7.16):

$$\frac{q}{\sqrt{gH_{m0}^3}} = 0.05\exp\left(-\frac{2.78}{\gamma_\beta}\frac{R_c}{H_{m0}}\right)$$

7.16

203

where γ_β is the reduction factor for angle of attack and is given by:

$$\gamma_\beta = 1 - 0.0062\beta \qquad \text{for } 0^0 < \beta < 45°$$
$$\gamma_\beta = 0.72 \qquad \text{for } \beta \geq 45°$$

7.17

and β is the angle of attack relative to the normal, in degrees. The influence of obliquity under non-impulsive wave attack is shown in Figure 7.17. This figure also shows the influence of angle of wave attack for slopes, see Chapter 5. There is a difference between the influence by short-crested or long-crested waves, where short-crested waves show less reduction in overtopping. The reality, certain under storm conditions, is that waves are short-crested. Long-crested waves may be observed for swell-type conditions.
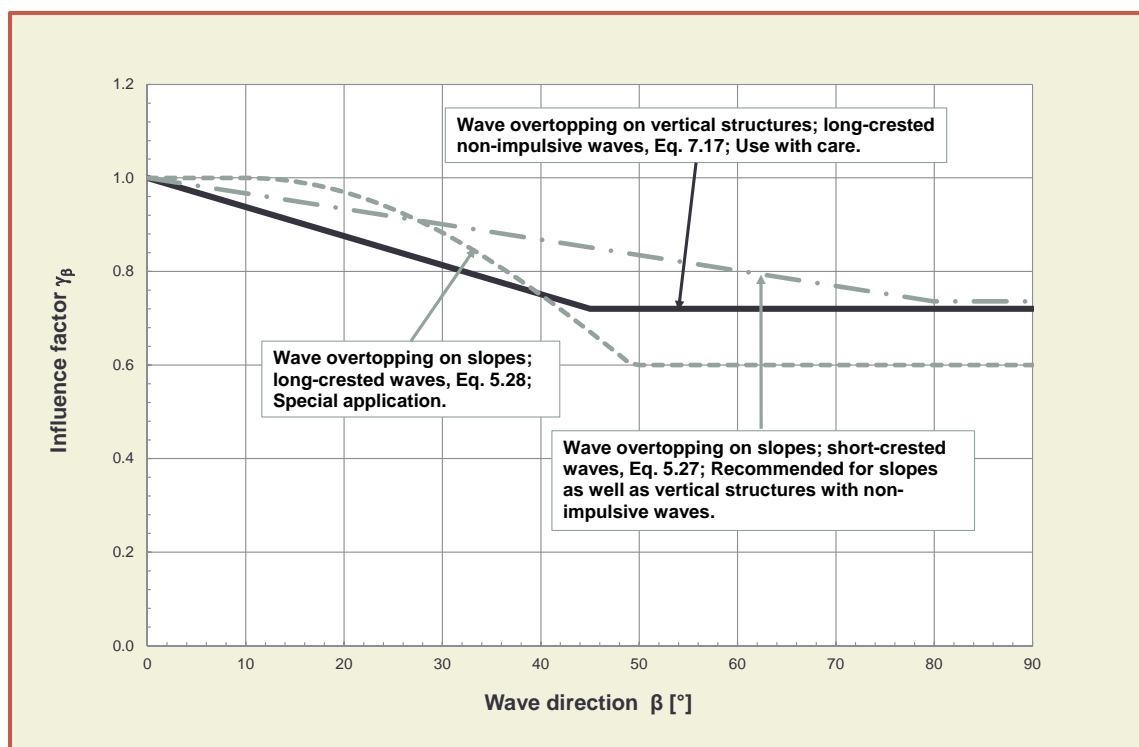
Figure 7.17:   Influence factor γ_β for oblique wave attack, for short- and long-crested waves and compared with sloping structures

It is for this reason that Equation 7.17 should be used with care as it is lower than Equation 5.29 for sloping structures (with short-crested waves). A more cautious approach would be to use Equation 5.29 also for vertical walls under non-impulsive conditions.

For conditions that would be identified as **impulsive** for normal ($\beta = 0°$) wave attack, a more complex picture emerges (Napp *et al.*, 2004). The extent to which the mean discharge is affected by oblique wave attack depends not only upon the angle of obliquity itself, but also upon the impulsiveness of the conditions, characterised by $h^2 / [L_{m-1,0} H_{m0}]$ at $\beta = 0°$. In Figure 7.18, the influence of the oblique wave attack is characterised by an obliquity factor, $k_\beta = q_\beta / q_{\beta=0°}$. Examining Figure 7.18 further, several additional influences can be observed:

- For all cases, the influence of obliquity of wave attack upon mean overtopping discharge increases (i.e the obliquity factor falls further below 1.0) for increasing relative freeboard.

- For a given level of impulsiveness (characterised by $h^2 / [L_{m-1,0} H_{m0}]$ calculated for $\beta = 0°$ conditions), the influence of obliquity increases (k_β decreases) with the magnitude of the obliquity, β, as expected.

- For a given angle of wave obliquity, β, the magnitude of the β influence, as characterised by the obliquity factor, is generally influenced by the level of impulsiveness, as characterised by $h^2 / [L_{m-1,0} H_{m0}]$. At larger obliquities, this influence is felt only above a threshold of impulsiveness.

Example 1: for $h^2 / [L_{m-1,0} H_{m0}] = 0.1$, at $\beta = 15°$, the obliquity factor is well above that for non-impulsive conditions for all freeboards in the applicable range. Moving to $\beta = 30°$, it is observed that the difference between impulsive and non-impulsive conditions only becomes apparent for relative freeboards greater than approximately 3.1.
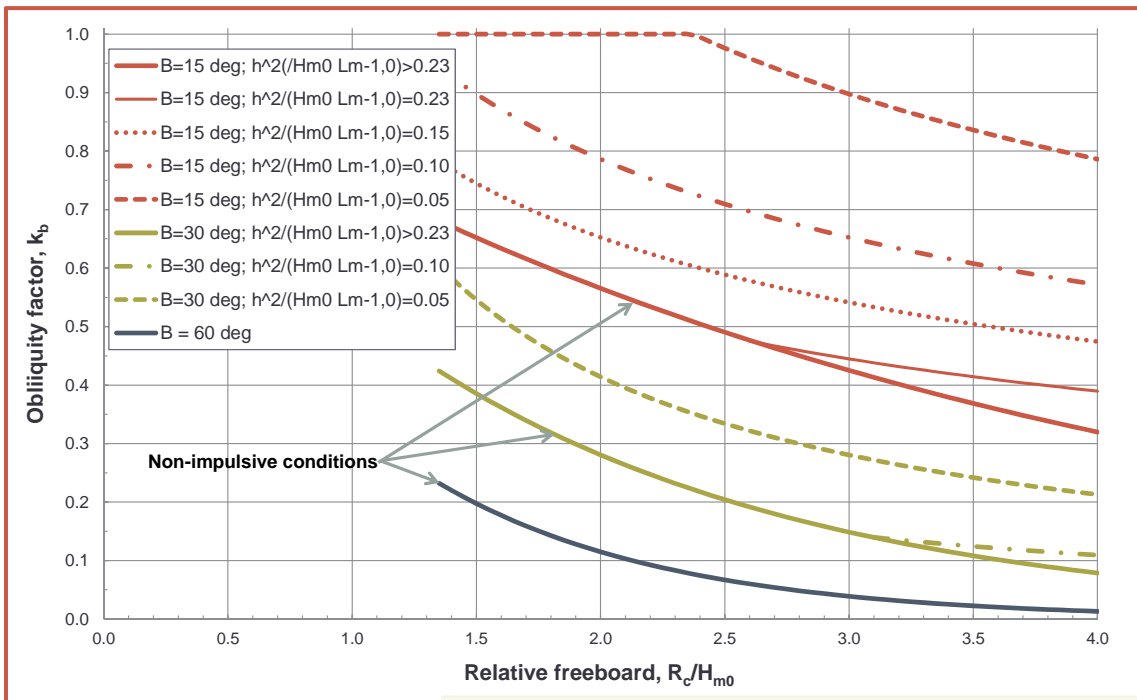
Figure 7.18:   Overtopping of vertical walls under oblique wave attack. The red and green curves are for $\beta = 15°$ and for $\beta = 30°$ respectively. The bold and solid lines show the non-impulsive cases (Equations 7.16, 7.17). The thinner solid line is for the just-impulsive cases ($h^2/[L_{m-1,0} H_{m0}] = 0.23$), with the dotted lines showing increasingly impulsive (lower $h^2/[L_{m-1,0} H_{m0}]$) conditions

Example 2: for $\beta = 15°$, for the most impulsive conditions shown on the graph, $h^2 / [L_{m-1,0} H_{m0}] = 0.05$, it can be seen that the influence of obliquity is not felt except for the highest relative freeboards, $R_c/H_{m0} > 2.4$.

For $\beta \geq 60°$, overtopping is observed to follow the functional form observed for non-impulsive conditions, *i.e.* a move away from a power--law decay such as Equation 7.8 to an exponential form such as Equation 7.5.

For predictions or comparison with measurements, a mean value approach for $1.35 \leq R_c/H_{m0} \leq 4$ (Equations 7.18 and 7.19) should be used. Data only exist for the discrete values of the obliquities shown. For $\beta = 60°$, as per non impulsive $\beta = 60°$ use Equations 7.16 and 7.17.

$$k_{\beta=15°} = \max \begin{cases} 0.375 \left(\dfrac{h^2}{H_{m0} L_{m-1,0}} \cdot \dfrac{R_c}{H_{m0}} \right)^{-0.46} & \text{for } \beta = 15°, \text{ with a maximum of 1.0} \\ \exp\left(-0.267 \dfrac{R_c}{H_{m0}} \right) \end{cases} \qquad 7.18$$

$$k_{\beta=30°} = \max \begin{cases} 0.0454 \left(\dfrac{h^2}{H_{m0} L_{m-1,0}} \cdot \dfrac{R_c}{H_{m0}} \right)^{-0.96} & \text{for } \beta = 30°, \text{ with a maximum of 1.0} \\ \exp\left(-0.495 \dfrac{R_c}{H_{m0}} \right) \end{cases} \qquad 7.19$$

Under oblique wave attack, significant spatial variability of overtopping discharge along a seawall or breakwater is observed in the field and measured in physical model studies. For design or safety assessment**,** a design or assessment approach should be used, Equation 7.20, which gives a prediction of the discharge at worst case (maximum local discharge) locations along the wall.

$$\begin{array}{l} \text{for } \beta = 15° ; \quad \text{as } per \ \beta = 0° \text{ (Eqs. 7.7, 7.8)} \\[1em] \text{for } \beta = 30° ; \quad \text{as } per \ \beta = 15° \text{ (Eq. 7.18)} \\[1em] \text{for } \beta = 60° ; \quad \text{as } per \text{ non-impulsive } \beta = 0° \text{ (Eq. 7.5)} \end{array} \qquad 7.20$$

7.3.6 Effect of bullnose / wave-return walls

Designers of vertical seawalls and breakwaters have often included some form of seaward overhang (recurve / parapet / wave return wall / bullnose) as part of the structure with the design motivation of reducing wave overtopping by deflecting back seaward up-rushing water. In general these designs are often relatively small structures at the top of the wall and they work best if overtopping is not too large. Examples of real structures are shown in Figure 7.19.

The sequence of video frame grabs from a laboratory test with a relatively large wave return wall (Figure 7.20) shows the incoming wave running up the front face of the structure before being projected seaward again by the bullnose or wave return wall.

The mechanisms determining the effectiveness of a bullnose / wave return wall are complex and not yet fully described. The guidance presented here is based upon existing guidance in the Netherlands and physical model studies. The parameters for the assessment of overtopping at structures with bullnose / recurve walls are shown in Figure 7.21.

Figure 7.19: An example of a modern, large vertical breakwater with bull nose (left – Carthagena, Spain) and view on a harbour wall with bullnose under daily conditions (right – Harlingen, NL)

Figure 7.20: A sequence showing the function of a (fairly large) bullnose / wave return wall in reducing overtopping by redirecting the up-rushing water seaward (back to the right)
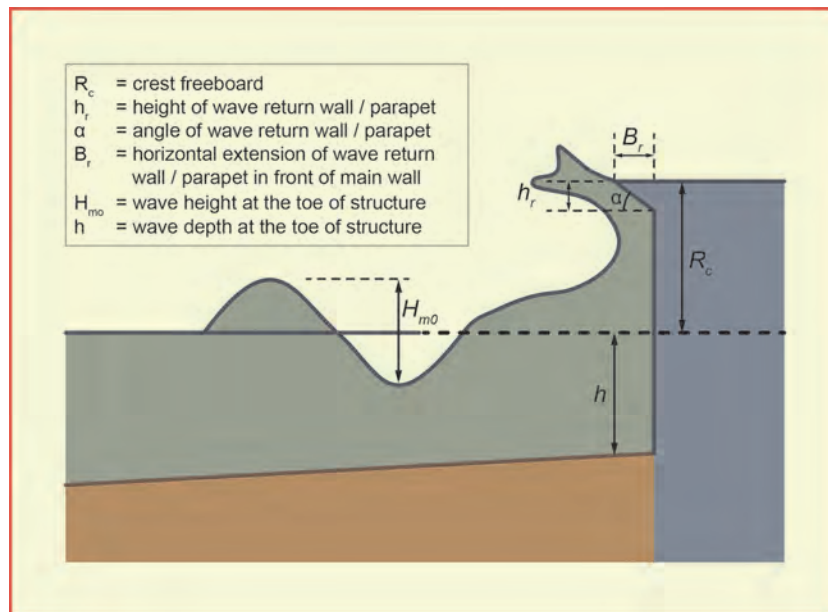
Figure 7.21: Parameter definitions for structures with bullnose / wave return walls. The geometry of the crest detail is in accordance with the idealised geometry used in the physical model studies upon which this guidance is based.

Two conditions are distinguished:

- the familiar case of the bullnose / recurve overhanging seaward (α < 90°), and,

- the case where a wall is chamfered backwards (parapet) at the crest normally *admitting greater overtopping (α > 90°)*. This type of structure is often designed as part of a caisson, see Figure 7.1 – upper left picture.

For the latter, chamfered wall case or parapet, an influence factor $\gamma_{parapet}$ should be applied to the appropriate equation for non-impulsive mean discharge (from Section 7.3.2) with a value of $\gamma_{parapet}$ that is larger than 1 (the overtopping will increase). Cornett *et al.*, 1999 found values between 1.01 and 1.13 for parapet angles between α = 120°-150°, but the trend was not consistent. Based on their tests it is proposed to use the range given in Equation 7.21.

$$\gamma_{parapet} = 1.05 - 1.10 \text{ for } \alpha > 100° \qquad\qquad 7.21$$

For the familiar case of overhanging bullnose / wave return wall, three broad regimes of effectiveness can be defined:

1) a regime in which the bullnose / wave return wall has little or no influence upon the overtopping, with this being typical of lowest relative freeboard conditions, where the bullnose / wave return wall may simple become submerged in the overtopping water;
2) an intermediate regime in which the bullnose / wave return wall is increasingly effective as the relative freeboard increases;
3) a high-relative freeboard regime where the bullnose / wave return wall offers its maximum performance in being successful in deflecting up-rushing water back seawards.

Existing guidance in the Netherlands (TAW, 2003) is shown in Figure 7.22, with the lines described by Equation 7.22. The basic line is overtopping for vertical walls without influencing foreshore (Equation 7.1). The figure clearly shows the three regimes mentioned above.
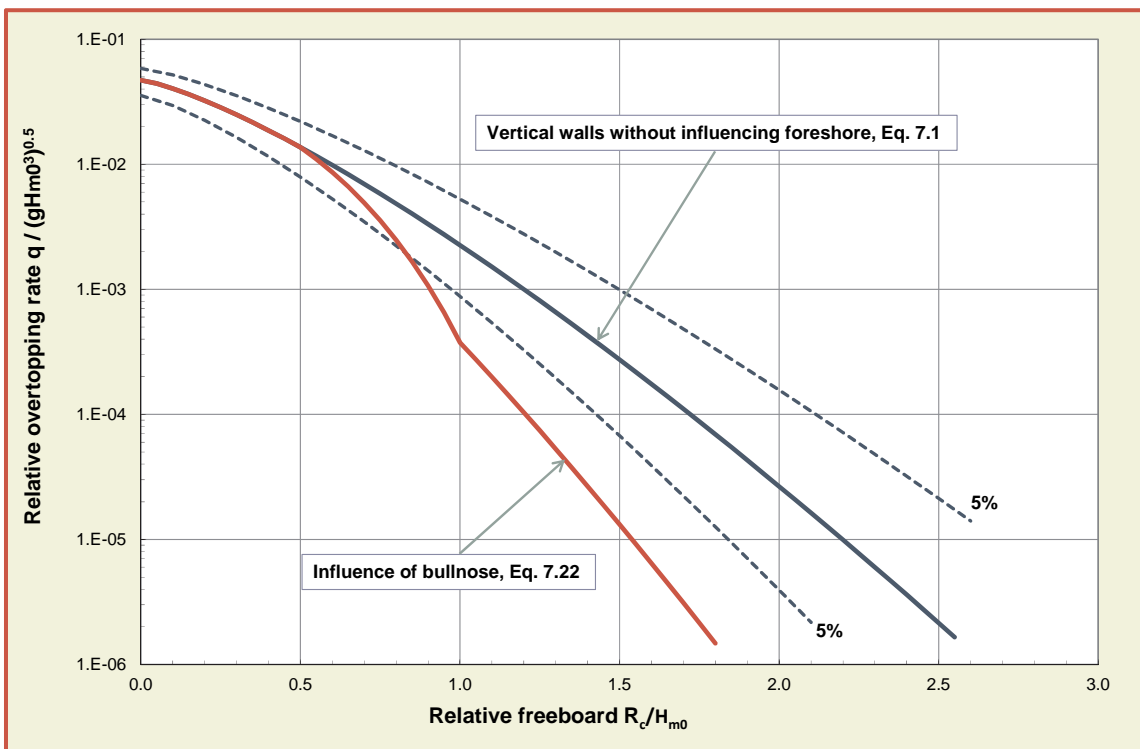
Figure 7.22: Graph showing the three regimes of effectiveness of a bullnose / wave return wall (TAW, 2003)

$$
\begin{aligned}
\gamma &= 1.0 && \text{for } R_c/H_{m0} \leq 0.5 \\
\gamma &= 1.3 - 0.6\, R_c / H_{m0} && \text{for } 0.5 < R_c/H_{m0} \leq 1.0 \qquad\qquad 7.22 \\
\gamma &= 0.7 && \text{for } R_c/H_{m0} > 1.0
\end{aligned}
$$

While Figure 7.22 and Equation 7.22 offer insight and a starting point to gain estimates of possible reductions for a fairly small bullnose, the following method also includes some aspects of (albeit idealised) geometry of the bullnose / wave return wall with larger dimensions and is based on Kortenhaus *et al.* (2003) and Pearson *et al.* (2004).

The effectiveness in reducing overtopping is quantified by a factor k_{bn} defined as:

$$k_{bn} = \frac{q_{with\_bullnose}}{q_{without\_bullnose}}$$

7.23
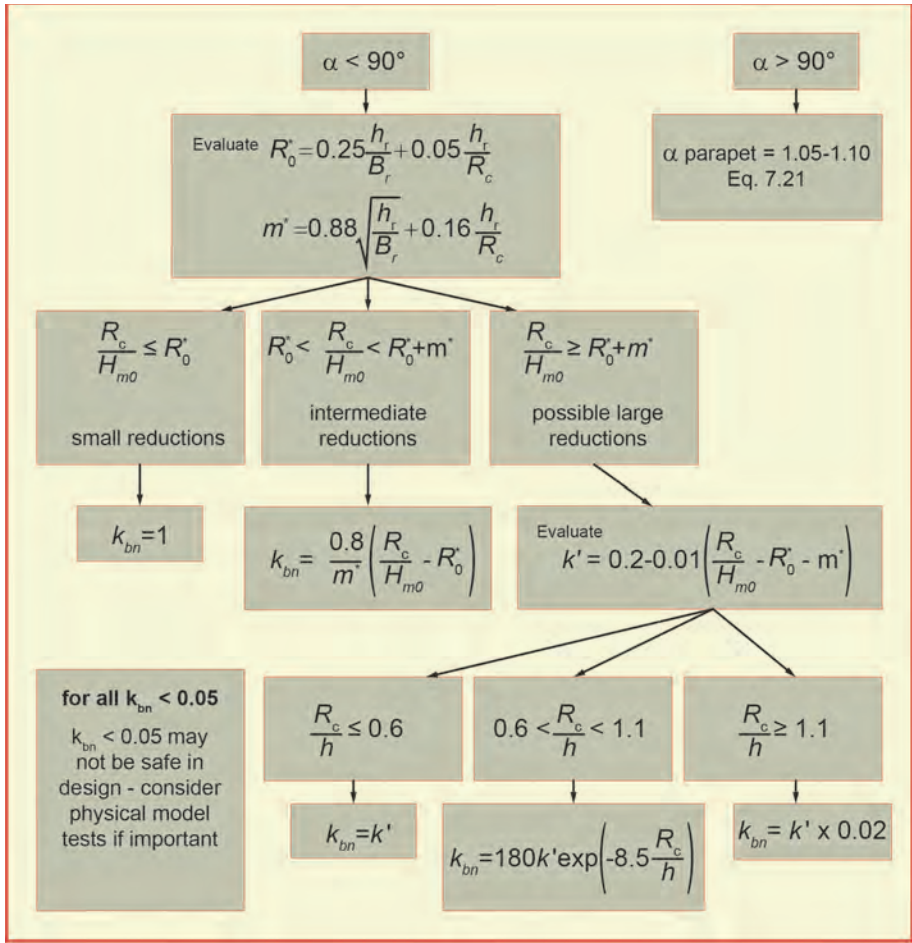
Figure 7.23: Decision chart summarising methodology for tentative guidance for seaward overhanging bullnose/wave return wall. It is important to note, that the symbols R_0^* and m^* shown in Figure 7.23 are only used at intermediate stages of the procedure and are defined in the boxes in row 2 of the figure

The decision chart in Figure 7.23 can then be used to arrive at a value of k_{bn}, which in turn can be applied by multiplication to the mean discharge predicted by the most appropriate method for the plain vertical wall (with the same R_c, h, *etc.*). The decision chart shows three levels of decision:

- Whether the parapet is angled seaward or landward.

- If seaward ($\alpha < 90°$), whether conditions are in the regime of

  o little or no reduction (left box; relative freeboards less than the R_0^* parameter calculated in the procedure),

o   intermediate reductions (middle box; relative freeboards lying between R_0^* and $R_0^* + m^*$, with m* as calculated in the procedure), or

o   large reductions (right box; relative freeboards greater than $R_0^* + m^*$, i.e. lying above the intermediate reductions regime). If in this regime of largest reductions, there is a further step to determine which of three further sub-regimes (for different R_c / h) is appropriate.

Given the level of scatter in the original data and the observation that the methodology is not securely founded on the detailed physical mechanisms / processes, it is suggested that it is impractical to design for $k_{bn} < 0.05$, *i.e.* reductions in mean discharges by factors of greater than 20 cannot be predicted with confidence. If such large (or larger) reductions are required, a detailed physical model study should be considered.

7.3.7   Perforated vertical walls

Perforated caisson breakwaters and perforated seawalls are deployed in order to reduce wave reflection. Examples are shown in Figure 7.24. Although such structures are quite common, especially (e.g.) in Japan, Italy and Spain, few studies exist giving their overtopping response. In general, as compared to plain solid vertical walls, the perforations reduce wave reflection and overtopping.

The overtopping, of perforated walls/caissons depends upon many structural parameters including: the porosity of the walls; the width and height of the absorbing chamber; and the presence of any air vents. Further influences will arise due to detailed conditions including friction, turbulence, resonance and the incident wave conditions, particularly the local wave length and angle of wave attack. It is likely that specific physical model tests are desirable for each case.

Figure 7.24:   Examples of perforated caissons, left Caen, France and right Cardiff Barrage, UK

Some sense of the scale of the influences can be gained from one of the few studies found in the literature (Franco and Franco, 1999) for caisson breakwaters under non-impulsive conditions. Tests reported were for circular and rectangular perforations, with a porosity of 20%. The influence of air venting was also explored.

Tests were performed in a basin with normal and oblique wave attack and with long-crested as well as short-crested waves. The influence factor for short-crested oblique waves was a little larger than for long-crested waves, which is according to what was found for smooth slopes (see Figure 7.17). This suggests that Equation 5.30 is preferred for the influence of oblique short-crested waves on vertical walls. For the circular perforation, rectangular perforation and rectangular perforation with open deck, influence factors of 0.79, 0.72 and 0.58 were found, respectively. These factors may differ for different configuration of the perforation, but at least give some guidance of the effect of perforations on wave overtopping.

7.3.8 Effect of wind

Wind may affect overtopping processes and thus discharges by:

- changing the shape of the incident wave crest at the structure resulting in a possible modification of the dominant regime of wave interaction with the wall;

- blowing up-rushing water over the crest of the structure (for an onshore wind, with the reverse effect for an offshore wind) resulting in possible modification of mean overtopping discharge and wave-by-wave overtopping volumes;

- modifying the physical form of the overtopping volume or jet, especially in terms of its aeration and break-up resulting in possible modification to post-overtopping characteristics such as throw speed, landward distribution of discharge and any resulting post-overtopping loadings (e.g. downfall pressures).

The modelling of any of these effects in small-scale laboratory tests presents very great difficulties owing to fundamental barriers to the simultaneous scaling of the wave-structure and water-air interaction processes. Very little information is available to offer guidance on the effect of the reshaping of the incident waves. Discussion of the modification to overtopping distribution is discussed in Section 7.5.3.

For vertical structures, several investigations have suggested different adjustment multipliers taking values of up to 3 – 4, either using a paddle wheel or large fans to transport up-rushing water over the wall. Tests with the paddle wheel had impulsive conditions and significant overtopping discharges, much larger than a few l/s per m in prototype conditions. A maximum factor of 3 was found for overtopping with and without the paddle wheel, but in this case it is clear that wind is not able to push forward such large volumes of up-rushing water that all this water goes over the crest. In reality the factor will be much smaller than the maximum figures mentioned here. For tests with large fans there is no reliable method to relate the model wind to wind conditions in reality and therefore it is difficult to give good guidance on wind effect based on such tests.

Due to the relative paucity of data, and uncertainty of scale effects, it is not possible to make a general guidance, but it can be observed (i) that the lowest discharges in the field are likely to be the most-influenced, and (ii) that the more impulsive the nature of the overtopping, the greater could be the influence of wind.

The CLASH-project gave prototype measurements for Samphire Hoe, an almost vertical wall, and also 2D and 3D small scale tests of the same prototype conditions, see Pullen *et al.* (2004).. It has been concluded that: "It has been shown that there are no scale effects when the field and laboratory measurements are compared, and that generally the results are in agreement with predictions". This was without making any adjustment for the wind. It should be noted, however, that overtopping discharges in this case were mainly about 1 l/s per m or smaller and that a factor 2 or 3 difference in a graph like Figure 7.16 is hardly noticeable. For impulsive conditions on a vertical wall and relatively small overtopping discharges, smaller than a few l/s per m, there might be a wind effect, but this will be more or less lost in the reliability of the prediction, the 90% confidence band.

7.3.9 Scale and model effect corrections

Overtopping data obtained in a medium-scale wave channel (Pearson *et al.*, 2002) shown in Figure 7.12 show that there are no obvious scale effects in the laboratory setting, going from small to medium scale. These tests were for steeply-battered (10:1 and 5:1) near-vertical walls under impulsive (breaking) conditions where any scale effects would have been expected to be most obvious.

Field measurements (Pullen *et al.*, 2004), Figure 7.16 – the Samphire Hoe prototype data, show rather more scatter, perhaps due to uncertainty of the influence of a possible wind effect, but demonstrate that there are no significant scale effects for these types of structures. The field site was a composite vertical structure subject to impulsive overtopping conditions, but some of the lower points may have been in the transition area to non-impulsive waves.

No information is yet available on the scaling of small-scale data under conditions where broken wave attack dominates. Although the methods presented for the assessment of overtopping discharges under broken wave conditions given in Section 7.3.1 have not been verified at large-scale or in the field, any scale correction is expected to give a *reduction* in predicted discharge.

7.4   Overtopping volumes

7.4.1 Introduction

While the prediction of mean discharge (Section 7.3) offers the information required to assess whether overtopping is slight, moderate or severe, and make a link to any possible hazard that might result, the prediction of the volumes associated with individual wave events can offer an alternative (and often more appropriate) measure for the assessment of tolerable overtopping levels and possible direct hazard, see also Chapter 3. First, a method is given for the prediction of the distribution of individual, wave-by-wave overtopping volumes, (including the maximum event volume) for plain vertical structures under perpendicular wave attack (Section 7.4.2). This method is then extended to composite (toe mound) structures (Section 7.4.3) and to conditions of long-crested, oblique wave attack (Section 7.4.4).

The methods on overtopping volumes given for perpendicular wave attack under non-impulsive conditions, and guidance on adjustment for composite structures and oblique wave attack have not changed and are as *per* EurOtop (2007). Only the procedure for perpendicular wave attack under impulsive conditions is new.

7.4.2 Overtopping volumes at plain vertical walls

Step 1: Number of waves overtopping The first step in the estimation of a maximum expected individual wave overtopping volume is to estimate the proportion of waves overtopping (N_{ow}/N_w) in a sequence of N_w incident waves. For non-impulsive conditions (identified as non-impulsive according to Equation 7.4), this is well-described by Equation 7.24 (Franco *et al.,* 1994). This Rayleigh-distribution of overtopping volumes was originally derived from tests on sloping structures in which situation the number of overtopping waves was directly linked to run-up, which in turn arose from a Rayleigh distributed set of incident wave heights. By applying the Rayleigh-distribution to data of overtopping on vertical structures it was validated that the assumption if this distribution was correct. It is given by:

$$\frac{N_{ow}}{N_w} = \exp\left[-1.21\left(\frac{R_c}{H_{m0}}\right)^2\right] \qquad \text{for non-impulsive conditions} \qquad 7.24$$

Under conditions identified as impulsive according to Equation 7.4, N_{ow} is described by Equation 7.25 (EA / Besley, 1999).

$$\frac{N_{ow}}{N_w} = \max\left\{ \begin{array}{l} \exp\left[-1.21\left(\dfrac{R_c}{H_{m0}}\right)^2\right] \\[2ex] 0.024\left(\dfrac{h^2}{H_{m0}L_{m-1,0}}\dfrac{R_c}{H_{m0}}\right)^{-1} \end{array} \right. \qquad 7.25$$

$$\text{for impulsive conditions}$$

These two formulae are plotted together in Figure 7.25, which shows the effect of the impulsiveness parameter $h^2/(H_{m0} L_{m-1,0})$ (Equation 7.4). The lowest line [$h^2/(H_{m0} L_{m-1,0})$ > 0:23 represents non-impulsive conditions with lower $h^2/(H_{m0} L_{m-1,0})$ conditions becoming increasingly impulsive. The way in which the proportion of waves overtopping for impulsive conditions lifts off from the non-impulsive line for higher

R_c/H_{m0} can be identified clearly, as can the fact that small values of $h^2/(H_{m0} L_{m-1,0})$ give more overtopping waves.
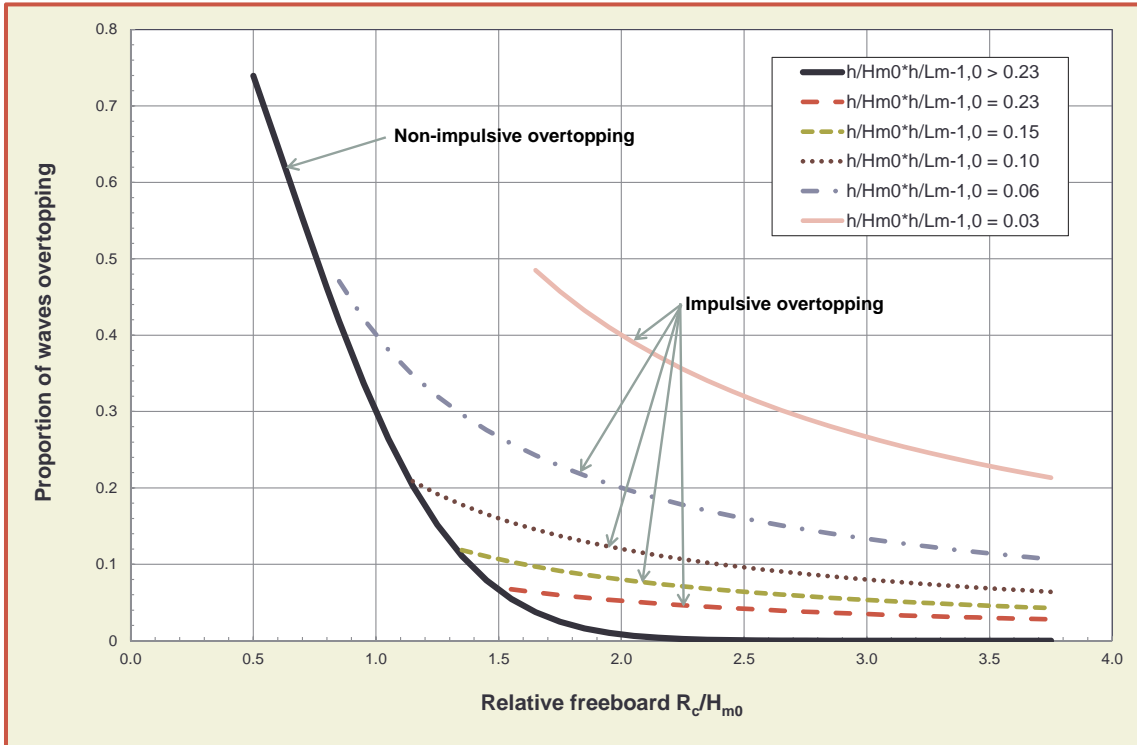
Figure 7.25: Proportion of waves overtopping: non-impulsive and impulsive conditions, showing effect of impulsiveness parameter, $h^2/(H_{m0} L_{m-1,0})$. The solid line $[h^2/(H_{m0} L_{m-1,0}) > 0.23]$ represents non-impulsive conditions; lower $h^2/(H_{m0} L_{m-1,0})$ conditions are increasingly strongly impulsive. Lines for $h^2/(H_{m0} L_{m-1,0}) = 0.06$ and 0.03 terminate according to the range of their validity

Step 2: Distribution of volumes and maximum individual volume. The distribution of individual overtopping volumes in a sequence is generally well-described by a two-parameter Weibull distribution:

$$P_V = 1 - \exp\left\{-\left(\frac{V}{a}\right)^b\right\}$$

7.26

where P_V is the probability that an individual event volume will not exceed V, and a and b are Weibull scale and shape parameters respectively. Weibull-distributions with various shape factors b have been discussed in Section 4.2.4 and given in Figure 4.5. The a-parameter in the Weibull-distribution has been described in depth in Section 5.5.2 and the related mathematical gamma function Γ has been given in Figure 5.57.

To estimate the largest event in a wave sequence predicted to include, for example, $N_{ow} = 200$ overtopping events, V_{max} would be found by taking $P_V = 1/200 = 0.005$. Equation 7.26 can then be rearranged to give Equation 7.27:

$$V_{\max} = a\left(\ln N_{ow}\right)^{1/b}$$

7.27

For non-impulsive conditions, $h^2/(H_{m0} L_{m-1,0}) > 0.23$, there is a weak steepness dependency for the shape parameter (Equation 7.28):

$$b = \begin{cases} 0.66 & \text{for } s_{m-1,0} = 0.02 \\ 0.82 & \text{for } s_{m-1,0} = 0.04 \end{cases} \qquad\qquad 7.28$$

The scale parameter, a, can then be found from Section 5.5.2, Equation 5.53, with the relationship shown in Figure 5.57. Note that for vertical structures, there is not yet an equivalent of Equation 5.54 for the shape parameter b as a function of the mean overtopping discharge and wave characteristics, so the discrete values given in Equation 7.28 should be used.

For impulsive conditions, (EA, 1999 and Pearson *et al.*, 2002) for $h^2/(H_{m0} L_{m-1,0}) \le 0.23$ the value becomes $b = 0.85$.

The effectiveness of the predictor for maximum individual overtopping wave volumes under impulsive conditions can be gauged from Figure 7.26 (Pearson *et al.*, 2002).
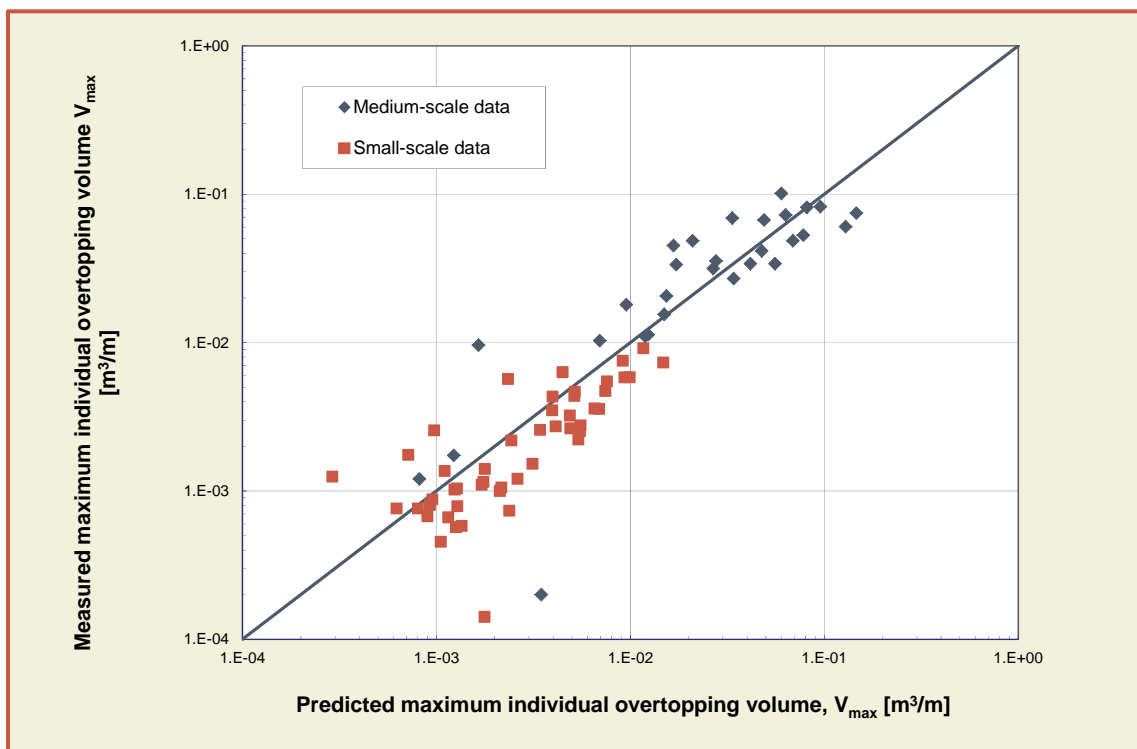
Figure 7.26:   Predicted and measured maximum individual overtopping volumes. Small and medium scale tests (Pearson *et al.*, 2002)

7.4.3 Overtopping volumes at composite (toe mound) structures

There is very little information available specifically addressing wave-by-wave overtopping volumes at composite structures. The guidance offered by EA / Besley (1999), reported in EurOtop (2007), remains the best available. No new formulae or Weibull a, b values are known so, for the purposes of maximum overtopping volume prediction, the methods for plain vertical walls (Section 7.4.2) are used. The key discriminator is that composite structures whose mound is sufficiently small to play little role in the overtopping process are treated as plain vertical, non-impulsive, whereas those with large mounds are treated as plain vertical, impulsive. For this purpose, the significance of the mound is assessed using the impulsiveness parameter group for composite structures, with impulsive conditions anticipated for $(d/H_{m0}) \cdot (h/L_{m-1,0}) < 0.65$ (Equation 7.13).

7.4.4 Overtopping volumes at plain vertical walls under oblique wave attack

For non-impulsive conditions, an adjusted form of Equation 7.24 is suggested (Franco *et al.*, 1994), Equation 7.29.

$$\frac{N_{ow}}{N_w} = \exp\left\{-\frac{1}{C^2}\left(\frac{R_c}{H_{m0}}\right)^2\right\} \qquad \text{for } h^2/(H_{m0}\, L_{m-1,0}) > 0.23 \qquad\qquad 7.29$$

where C is given by Equation 7.30;

$$C = \begin{cases} 0.91 & \text{for } \beta = 0° \\ 0.91\text{-}0.00425\,\beta & \text{for } 0° < \beta < 40° \\ 0.74 & \text{for } \beta \geq 40° \end{cases} \text{ for } h^2/(H_{m0}\, L_{m-1,0}) > 0.23 \qquad\qquad 7.30$$

For impulsive conditions (as determined for perpendicular, $\beta = 0°$, wave attack), the procedure is the same as for perpendicular wave attack, but different formulae should be used for estimating the number of overtopping waves (N_{ow}) and Weibull shape and scale parameters as summarised in Table 7.2 (Napp *et al.*, 2004).

Table 7.2: Summary of prediction formulae proportion of waves overtopping under oblique wave attack. Oblique cases are valid for $0.2 < [h^2/(H_{m0}\, L_{m-1,0})]\, R_c/H_{m0} < 0.65$. For $0.07 < [h^2/(H_{m0}\, L_{m-1,0})]\, R_c/H_{m0} < 0.2$, the $\beta = 0°$ formulae should be used for all β.

$\beta = 15°$	$\beta = 30°$	$\beta = 60°$
Equation 7.31	Equation 7.32	Treat as non-impulsive, Equation 7.33
$a = 1.06\dfrac{qT_mN_w}{N_{ow}}$	$a = 1.04\dfrac{qT_mN_w}{N_{ow}}$	
$b = 1.18$	$b = 1.27$	

The formulae for N_{ow} in Table 7.2 (the same as those presented in EurOtop, 2007) show that the proportion of waves overtopping depends upon the obliquity, upon the freeboard, and upon the impulsiveness of the ($\beta = 0^0$) conditions. These separate influences can be appreciated more clearly in the sequence of graphs in Figure 7.27, which show the influence of obliquity and freeboard for a series of levels of impulsiveness, from $h^2/(H_{m0}\, L_{m-1,0}) = 0.23$ (transition into impulsive conditions) through to highly impulsive conditions ($h^2/[H_{m0}\, L_{m-1,0}] = 0.06$). Figure 7.27 shows the dependence upon obliquity and upon the impulsiveness parameter, $h^2 / (H_{m0}\, L_{m-1,0})$. Conditions (evaluated at $\beta = 0°$) are just impulsive for (a) and increase through (b) and (c) to highly impulsive conditions in (d).

The predictions of Table 7.2 can now be written in a form that ensures the correct handling of the formulae for the different obliquities and wave conditions (impulsive or non-impulsive). Use Equation 7.31 for $\beta = 15°$, Equation 7.32 for $\beta = 30°$ and Equation 7.33 for non-impulsive $\beta = 60°$.
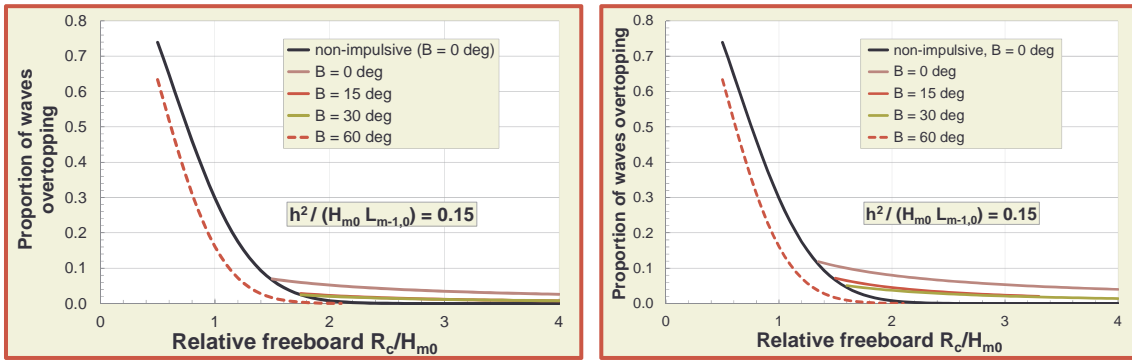
(a) $h^2 / (H_{m0} L_{m-1,0}) = 0.23$ (transition into impulsive)

(b) $h^2 / (H_{m0} L_{m-1,0}) = 0.15$
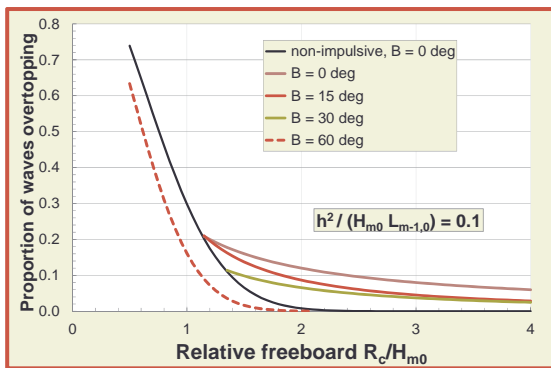
(c) $h^2 / (H_{m0} L_{m-1,0}) = 0.1$
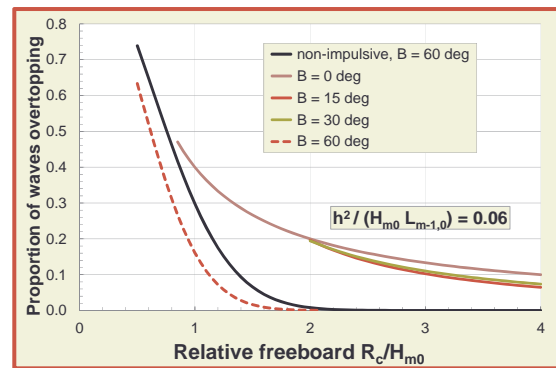
(d) $h^2 / (H_{m0} L_{m-1,0}) = 0.06$ (most impulsive)

Figure 7.27 Proportion of waves overtopping *vs.* freeboard for oblique wave attack

For $\beta = 15°$ and $0.15 \leq [h^2/(H_{m0} L_{m-1,0})] R_c/H_{m0} \leq 0.5$:

$$\frac{N_{ow}}{N_w} = \max \left\{ \begin{array}{l} \exp\left[-1.21\left(\dfrac{R_c}{H_{m0}}\right)^2\right] \\ \min \left\{ \begin{array}{l} 0.024 \left(\dfrac{h^2}{H_{m0}L_{m-1,0}} \cdot \dfrac{R_c}{H_{m0}}\right)^{-1} \\ 0.0066 \left(\dfrac{h^2}{H_{m0}L_{m-1,0}} \cdot \dfrac{R_c}{H_{m0}}\right)^{-1.6} \end{array} \right. \end{array} \right.$$

7.31

For $\beta = 30°$ and $0.15 \leq [h^2/(H_{m0} L_{m-1,0})] R_c/H_{m0} \leq 0.5$:

$$\frac{N_{ow}}{N_w} = \max \left\{ \begin{array}{l} \exp\left[-1.21\left(\dfrac{R_c}{H_{m0}}\right)^2\right] \\ \min \left\{ \begin{array}{l} 0.024 \left(\dfrac{h^2}{H_{m0}L_{m-1,0}} \cdot \dfrac{R_c}{H_{m0}}\right)^{-1} \\ 0.0069 \left(\dfrac{h^2}{H_{m0}L_{m-1,0}} \cdot \dfrac{R_c}{H_{m0}}\right)^{-1.4} \end{array} \right. \end{array} \right.$$

7.32

for β = 60°:

$$\frac{N_{ow}}{N_w} = \exp\left\{-1.83\left(\frac{R_c}{H_{m0}}\right)^2\right\}$$

7.33

7.4.5 Scale effects for individual overtopping volumes

Measurements from large scale laboratory tests indicate that formulae for overtopping volumes, based largely upon small-scale physical model studies, scale well (Figure 7.26) (Pearson *et al.*, 2002). No data from the field is available to support scalability from large-scale laboratory scales to prototype conditions.

216

7.5 Overtopping velocities and distributions

7.5.1 Introduction to post-overtopping processes

There are many design issues for which knowledge of just the mean and / or wave-by-wave overtopping discharges / volumes are not sufficient, for example:

- assessment of direct hazard to people, vehicles and buildings in the zone immediately landward of the seawall;

- assessment of potential for damage to elements of the structure itself (e.g. crown wall; crown deck; secondary defences).

The appreciation of the importance of being able to predict more than overtopping discharges and volumes has led to significant advances in the description and quantification of what can be termed post-overtopping processes. Specifically, the current state of prediction tools for

- the speed of an overtopping jet (or throw velocity);

- the spatial extent reached by (impulsive) overtopping volumes.

7.5.2 Overtopping throw speeds

Studies at small-scale based upon video footage (Bruce *et al.*, 2002), shown in Figure 7.28, suggest that the vertical speed with which the overtopping jet leaves the crest of the structure (u_z) may be estimated according to Equation 7.34.

$$u_z \approx \begin{cases} 2\text{ to }4\times c_i & \text{for non-impulsive conditions} \\ 2\text{ to }10\times c_i & \text{for impulsive conditions – see Figure 7.28} \end{cases}$$

7.34

where $c_i = (gh)^{0.5}$ is the inshore wave celerity.

The medium scale tests in Barcelona in Figure 7.28 are on average a little larger than the small scale tests in Edinburgh and show also more scatter. In general the velocity increases with increasing impulsiveness, i.e., smaller $h^2/(H_{m0} L_{m-1,0})$.
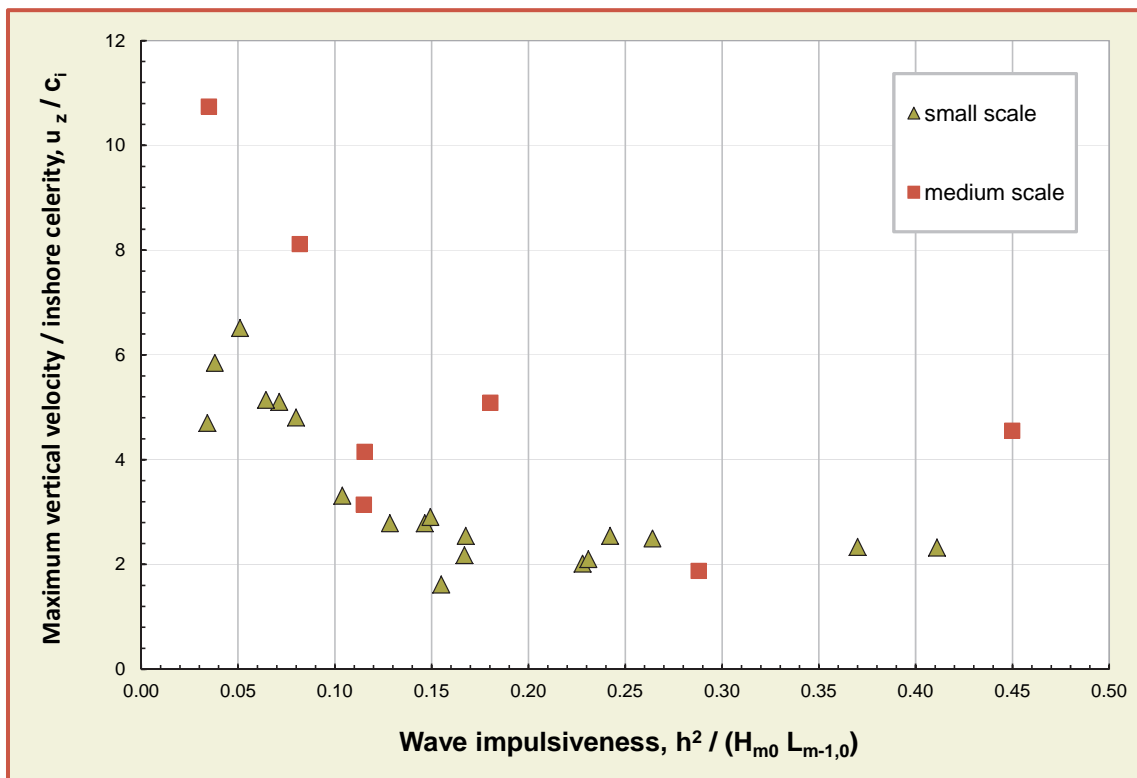
Figure 7.28   Speed of upward projection of overtopping jet past structure crest plotted with "impulsiveness parameter" $h^2 / (H_{m0} L_{m-1,0})$ (after Bruce *et al.*, 2002)

7.5.3   Spatial extent of overtopped discharge

The spatial distribution of overtopped discharge may be of interest in determining zones affected by direct wave overtopping hazard (to people, vehicles, buildings close behind the structure crest, or to elements of the structure itself). Under green water (non-impulsive) conditions, the distribution of overtopped water will depend principally on the form of the area immediately landward of the structures crest (slopes, drainage, obstructions etc.) and no generic guidance can be offered (though see Section 7.5.2 for information of speeds of overtopping jets).

Under violent (impulsive) overtopping conditions, the idea of spatial extent and distribution has a greater physical meaning. That is, where does the airborne overtopping jet come back to the level of the pavement behind the crest? The answer to this question, however, will (in general) depend strongly upon the local wind conditions. Despite the difficulty of directly linking a laboratory wind speed to its prototype equivalent (see Section 7.3.7) laboratory tests have been used to place an upper bound on the possible wind-driven spatial distribution of the fall back to ground footprint of the violently overtopped volumes (Pullen *et al.,* 2004 and Bruce *et al.*, 2005). Tests used large fans to blow air at gale-force speeds (up to 28 m/s) in the laboratory.

The resulting landward distributions for various laboratory wind speeds give the proportion of total overtopping discharge which has landed within a particular distance shoreward of the seaward crest. The lower (conservative) envelope of the data give the approximate guidance that:

- 50% of the violently-overtopped discharge will land within a distance of $0.06 \times L_{m-1,0}$;

- 90% of the violently-overtopped discharge will land within a distance of $0.20 \times L_{m-1,0}$;

- 95% of the violently-overtopped discharge will land within a distance of $0.25 \times L_{m-1,0}$.

8 Case studies

To be implemented in the final version.

List of Figures

221

223

List of Tables

232

Glossary

Armour	Protective layer of rock or concrete units
Artificial Neural Network, ANN	Calculation tool for the mean overtopping rate for all kind of structures, based on 13,000 test data
Bullnose	A relatively small structure at the crest of a seawall, capping wall or storm wall, which is designed to throw back waves
Composite sloped seawall	A sloped seawall whose gradient changes
Composite vertical wall	A structure made up of two component parts, usually a caisson type structure constructed on a rubble mound foundation or a vertical wall against a rubble mound berm
90% Confidence band	Area in a graph between the 5%-exceedance lines
Crest freeboard	The height of the crest above still water level
Crown wall	A concrete super-structure located at the crest of a sloping of vertical seawall
Deep water	Water so deep that the wave height is little affected by the seabed. Generally in this manual, water deeper than 2.5-3 times the significant wave height is considered to be deep
Depth limited waves	Breaking waves whose height is limited by the water depth
Design and assessment approach	Similar to the mean value approach, but now with inclusion of one standard deviation of the uncertainty of the prediction
Impulsive waves	Waves that tend to break onto the seawall
Influencing foreshore	A (mostly sloping) shallow foreshore where waves change over the foreshore and give larger overtopping at vertical walls than at a non-influencing foreshore
Maximum overtopping volume	The largest volume of water passing over the structure in a single wave
Mean overtopping discharge	The average flow rate passing over the coastal structure
Mean value approach	Use of formulae with the mean value of the stochastic parameters that describe the reliability of the formulae. To be used for prediction of or comparison with test data
Mean wave period	The average of the wave periods in a random sea state
Model effects	Model effects occur due to the inappropriate set-up of the model and the incorrect reproduction of the governing forces, the boundary conditions, the measurement system and the data analysis.
Non-impulsive waves	Waves that surge up a vertical structure, not giving impulsive waves
Normal wave attack	Waves that strike the structure normally to its face
Oblique wave attack	Waves that strike the structure at an angle

233

Overflow discharge	The amount of water passing over a structure when the water level in front of the structure is higher than the crest level of the structure
Parapet wall	A relatively small structure at the crest of a seawall, which is designed to throw back waves
PC-Overtopping	Calculation tool for gentle slopes and embankments
Probabilistic approach	Calculation considering all significant stochastic parameters with their standard deviation and assuming a normal or log-normal distribution
Return period	The average length of time between sea states of a given severity
Run-up	The rush of water up a structure or beach as a result of wave action.
Scale effects	Scale effects occur due to the inability to scale all relevant forces from prototype to model scale
Sea dike	Earth structure, sometimes with a sand core covered by clay, and often on the seaward side covered by asphalt or placed concrete block revetments
Shallow Water	Water of such a depth that surface waves are noticeably affected by bottom topography and reduce in height by breaking
Significant wave height	The average height of the highest of one third of the waves in a given sea state. This wave height is NOT used in this manual, but the spectral significant wave height
Spectral wave height	The significant wave height from spectral analysis = $4\sqrt{m_0}$. This is the wave height used in this manual
Stilling wave basin	An area designed in front of the crest or capping wall, where a part of the up-rushing wave may remain without overtopping
Toe	The relatively small mound usually constructed of rock armour to support or key-in armour layer
Tolerable overtopping discharge	The amount of water passing over a structure that is considered safe
Very shallow water	Sloping foreshores with such small water depths that the wave steepness becomes (much) smaller than $s_{m-1,0} = 0.01$ and where long waves determine the wave spectrum
Wave return wall	A wall located at the crest of a seawall, which is designed to throw back the waves
Wave steepness	The ratio of the height of the waves to the wave length
Zero overtopping	The mean overtopping discharge that can in reality be considered as zero overtopping, as it is caused by only one or two waves in a sea state, see also Section 3.3.7

Notation

a	= coefficient	
A_c	= armour crest freeboard of structure	[m]
b	= coefficient or exponent	[-]
b	= shape parameter in the Weibull distribution	[-]
B	= berm width, measured horizontally	[m]
B_r	= width (seaward extension) in front of main vertical wall of recurve / parapet /	
	wave return wall section, see Section 0	[m]
B_t	= width of toe of structure	[m]
c	= wave celerity at structure toe	[m/s]
$c_{g, relative}$	= relative group velocity, Eq. 5.36	[m/s]
$c_{h2\%}$	= coefficient in Eq. 5.59	[-]
$c_{v2\%}$	= coefficient in Eq. 5.58	[-]
CD	= Chart Datum	
CF	= Complexity-Factor of structure section, gives an indication of the complexity	
	of the structure section, can adopt the values 1, 2, 3 or 4	[-]
C_r	= reduction factor for a wide rubble mound crest, see Section 6.3.2	[-]
d	= water depth above a toe mound or berm in front of a vertical or battered seawall	[m]
d	= water depth, Section 5.4.5	[m]
$d_{channel}$	= open volume of a placed block revetment per square metre	[m^3 per m^2]
d_*	= parameter to distinguish impulsive waves for vertical walls with a toe mound	
	or berm, only used in EurOtop (2007)	[-]
D	= weighted average of D_d and D_u	[m]
D(f,θ)	= directional spreading function, defined as:	[°]

$$S(f, \theta) = S(f). \quad D(f,\theta) \text{ with } \int_0^{2\pi} D(f, \theta)d\theta = 0$$

D_d	= average element size at the down slope	[m]
D_n	= nominal diameter of concrete armour unit	[m]
D_{n50}	= nominal diameter of rock	[m]
D_u	= average element size at the upper slope	[m]
f	= frequency	[Hz]

235

f	= friction coefficient for grass in wave overtopping calculations; f = 0.01	[-]
f	= coefficient in Eq. 5.26	[-]
$f(x_i)$	= description of prediction model	[unity of x_i]
f_b	= width of a roughness element (perpendicular to structure axis)	[m]
f_h	= height of a roughness element	[m]
f_L	= centre-to-centre distance between roughness elements	[m]
f_p	= spectral peak frequency	
	= frequency at which $S_\eta(f)$ is a maximum	[Hz]
f_q	= reduction factor for scale and model effects, Eq. 6.13	[-]
$f_{q\,max}$	= maximum reduction factor for scale and model effects, Eq. 6.14	[-]
$f_{q\,max\,red}$	= maximum reduction factor for scale and model effects with $0.7 < \gamma_f < 0.9$, Eq. 6.15	[-]
$F(x,y)$	= spatial distribution of overtopping water traveling through the air, Eq. 6.19	[-]
g	= acceleration due to gravity (= 9,81)	[m/s²]
G_c	= width of structure crest	[m]
h	= water depth in front of toe of structure	[m]
h	= flow thickness of overtopping wave	[m]
$h_{A,2\%}$	= 2%-value of flow thickness at location A on the seaward slope	[m/s]
h_b	= water depth on berm (negative means berm is above SWL)	[m]
h_c	= level of beach crest of a shingle beach profile with respect to SWL	
h_{deep}	= water depth in deep water	[m]
h_n	= height of bullnose	[m]
h_r	= height of recurve / parapet / wave return wall section at top of vertical wall	[m]
h_t	= water depth on toe of structure	[m]
h_{wall}	= height of storm wall on top of slope or at promenade	[m]
h_*	= parameter to distinguish impulsive waves for vertical walls or berm,	
	only used in EurOtop (2007)	[-]
H	= wave height	[m]
H_{m0}	= estimate of significant wave height from spectral analysis = $4\sqrt{m_0}$	[m]
$H_{m0\,deep}$	= H_{m0} determined at deep water	[m]
$H_{m0,\,I}$	= incident wave height	[m]
$H_{m0\,t}$	= H_{m0} determined at toe of structure	[m]
$H_{m0,\,transmitted}$	= transmitted wave height	[m]

H_{rms} = root mean square wave height [m]

H_s = significant wave height defined as highest one-third of wave heights = $H_{1/3}$ [m]

H_{tr} = transition wave height in wave height distribution of Battjes and

Groenendijk (2000) [m]

$H_{x\%}$ = wave height exceeded by x% of all wave heights [m]

$H_{1/x}$ = average of highest 1/x th of wave heights [m]

k = angular wave number (= $2\pi/L$) [rad/m]

k_{bn} = multiplier for mean discharge giving effect of recurve wall (Chapter 7) [-]

k', k_{23} = dimensionless parameters used (only) in intermediate stage of

calculation of reduction factor for recurve walls (Chapter 7) [-]

K_r = average reflection coefficient (= $\sqrt{m_{0,r}}/\sqrt{m_{0,i}}$) [- or %]

K_t = transmission coefficient (= $H_{m0,t}/H_{m0,i}$) [- or %]

$k_{\beta = x°}$ = reduction factor for an angle of wave attack of x° [-]

L_{berm} = horizontal length between two points on slope, 1.0 H_{m0} above and 1.0 H_{m0}

below middle of the berm [m]

L = wave length measured in direction of wave propagation [m]

L_{berm} = horizontal length between two points on slope, 1.0 H_{m0} above and 1.0 H_{m0}

below middle of the berm [m]

L_o = deep water wave length based on $T_{m-1,0}$= $gT^2_{m-1,0}/2\pi$ [m]

$L_{m-1,0}$ = spectral wave length in deep water = $gT^2_{m-1,0}/2\pi$ [m]

L_{op} = peak wave length in deep water = $gT^2_p/2\pi$ [m]

L_{om} = mean wave length in deep water = $gT^2_m/2\pi$ [m]

L_{slope} = horizontal length between two points on slope, $Ru_{2\%}$ above and 1.5 H_{m0}

below S.W.L. [m]

m = slope of the foreshore: 1 unit vertical corresponds to m units horizontal [-]

m = model uncertainty [-]

m^*, m = dimensionless parameters used (only) in intermediate stage of

calculation of reduction factor for recurve walls (Chapter 7) [-]

m_n = $\int_{f_1}^{f_2} f^n S(f)df$ = n^{th} moment of spectral density [m²/s^n]

$m_{n,x}$ = n^{th} moment of x spectral density [m²/s^n]

x may be: i for incident spectrum; r for reflected spectrum

N	= planning period	[years]
N_{ow}	= number of overtopping waves	[-]
N_w	= number of incident waves	[-]
P_{ow}	= probability of overtopping per wave = N_{ow}/ N_w	[-]
P_V	= $P(\underline{V} \geq V)$ = probability of the overtopping volume $\underline{V}$ being larger or equal to V	[-]
$P_{V\%}$	= $P_V \cdot 100\%$	[%]
q	= mean overtopping discharge per meter structure width	[m³/s per m]
$q_{overflow}$	= overtopping discharge when water level is higher than crest freeboard, without effect of waves	[m³/s per m]
q_{us}	= mean overtopping discharge per meter structure width up-scaled to prototype conditions	[m³/s per m]
r_B	= reduction factor for size of berm	[-]
r_{dB}	= reduction factor for level of berm with respect to SWL	[-]
RF	= Reliability-Factor of test, gives an indication of the reliability of the test, can adopt the values 1, 2, 3 or 4	[-]
R_c	= crest freeboard of structure	[m]
R_0^*	= dimensionless length parameter used (only) in intermediate stage of calculation of reduction factor for recurve walls (Chapter 7)	[-]
R_u	= run-up level, vertical measured with respect to the S.W.L.	[m]
$R_{u2\%}$	= run-up level exceeded by 2% of incident waves	[m]
R_{us}	= run-up level exceeded by 13.6% of incident waves	[m]
$R_{u\ max}$	= maximum run-up of all waves in a sea state	[m]
$R_{u\ start}$	= location where the run-down changes into run-up, see Figure 5.61	[m]
$R_{u\ min}$ at $_u{}_{max}$	= lowest location where the velocity is within about 20% of its maximum velocity, see Figure 5.61	[m]
R_u at u_{max}	= location of u_{max}, see Figure 5.61	[m]
$R_{u\ max}$ at $_u{}_{max}$	= highest location where the velocity is within about 20% of its maximum velocity, see Figure 5.61	[m]
$R_{u\ max}$	= the maximum run-up level of a wave, see Figure 5.61	[m]
s	= wave steepness = H/L	[-]
s	= spreading, Eq. 5.27	[-]
$s_{m-1,0}$	= wave steepness with L_o, based on $T_{m-1,0} = H_{m0}/L_{m-1,0} = 2\pi H_{mo}/(gT^2_{m-1,0})$	[-]
s_{om}	= wave steepness with L_o, based on $T_m = H_{m0}/L_{om} = 2\pi H_{mo}/(gT^2_m)$	[-]

s_{op}	= wave steepness with L_o, based on $T_p = H_{m0}/L_{op} = 2\pi H_{mo}/(gT^2_p)$	[-]
SWL	= still water level	[m]
$S(f, \theta)$	= directional spectral density	[(m²/Hz)/]
$S_{\eta,i}(f)$	= incident spectral density	[m²/Hz]
$S_{\eta,r}(f)$	= reflected spectral density	[m²/Hz]
T	= wave period	[s]
$T_{H1/x}$	= average of the periods of the highest 1/x th of wave heights	[s]
T_m	= average wave period defined either as:	
	$\overline{T}$ = average wave period from time-domain analysis	[s]
	$T_{mi,j}$ = average wave period calculated from spectral moments, e.g.:	[s]
$T_{m0,1}$	= average wave period defined by m_0/m_1	[s]
$T_{m0,2}$	= average wave period defined by $\sqrt{m_0/m_2}$	[s]
$T_{m-1,0}$	= spectral wave period defined by m_{-1}/m_0	[s]
$T_{m-1,0\ deep} = T_{m-1,0}$	determined at deep water	[s]
$T_{m-1,0\ toe} = T_{m-1,0}$	determined at the toe of the structure	[s]
$T_{m\ deep}$	= T_m determined at deep water	[s]
$T_{m\ toe}$	= T_m determined at the toe of the structure	[s]
T_p	= spectral peak wave period = $1/f_p$	[s]
$T_{p\ deep}$	= T_p determined at deep water	[s]
$T_{p\ toe}$	= T_p determined at the toe of the structure	[s]
T_R	= record length or return period of event	[s]
T_s	= $T_{H1/3}$ = significant wave period	[s]
U	= velocity of current	[m/s]
U_n	= velocity of current along the angle of wave attack, see Figure 5.38	[m/s]
v	= velocity of overtopping wave	[m/s]
v_{front}	= front velocity of an overtopping wave	[m/s]
V	= volume of overtopping wave per unit crest width	[m³/m]
V_{max}	= maximum individual overtopping wave volume per unit crest width	[m³/m]
x	= horizontal coordinate	[m]
X	= landward distance of falling overtopping jet from rear edge of wall	[m]
X_{max}	= maximum landward distance of falling overtopping jet from rear edge of wall	[m]
X_{qmax}	= landward distance of max mean discharge	[m]

X_{Vmax}	= landward distance of max overtopping volume per wave	[m]
y	= vertical coordinate	[m]
$v_{A,2\%}$	= 2%-value of run-up velocity at location A on the seaward slope	[m/s]
z_A	= location on the seaward slope, measured vertically from SWL	[m]
α	= angle between overall structure slope and horizontal	[°]
α	= angle of parapet / wave return wall above seaward horizontal, Section 0	[°]
α_B	= angle that sloping berm makes with horizontal	[°]
α_d	= angle between structure slope downward berm and horizontal	[°]
α_{excl}	= mean slope of structure calculated without contribution of berm	[°]
α_{incl}	= mean slope of structure calculated with contribution of berm	[°]
α_{sf}	= mean slope of the structure at very shallow water, including a part of the foreshore	[°]
α_u	= angle between structure slope upward berm and horizontal	[°]
α_{wall}	= angle that steep wall makes with horizontal	[°]
β	= angle of wave attack relative to normal on structure	[°]
β_e	= angle of wave energy, see Figure 5.38	[°]
ε	= angle of bullnose, see Section 5.4.7	[°]
γ_b	= influence factor for a berm	[-]
γ_{bn}	= influence factor for a bullnose at a storm wall on slope or promenade	[-]
γ_f	= influence factor for the permeability and roughness of or on the slope	[-]
$\gamma_{parapet}$	= influence factor for a bullnose on a vertical wall	[-]
γ_{prom}	= influence factor for a promenade	[-]
γ_{prom_v}	= influence factor for a storm wall at the end of a promenade	[-]
$\gamma_{prom\_v\_bn}$	= influence factor for a storm wall with bullnose at the end of a promenade	[-]
$\gamma_{s0,\,bn}$	= influence factor of wave steepness for a bullnose at a storm wall on slope or promenade	[-]
γ_v	= influence factor for a vertical wall on the slope	[-]
γ_{BB}	= influence factor for a berm breakwater	[-]
γ_β	= influence factor for oblique wave attack	[-]
γ_ε	= influence factor for angle of a bullnose at a storm wall on slope or promenade	[-]
γ_λ	= influence factor for size of a bullnose at a storm wall on slope or promenade	[-]
γ^*	= overall influence factor for a storm wall on slope or promenade	[-]
$\eta(t)$	= surface elevation with respect to SWL	[m]

λ	= relative size of bullnose, see Section 5.4.7	[-]
$\mu(x)$	= mean of measured parameter x with normal distribution	[unit of x]
θ	= direction of wave propagation	[°]
σ	= spreading function, Eq. 5.27	[-]
σ	= relative frequency, Eq. 5.35	$[s^{-1}]$
$\sigma(x)$	= standard deviation of measured parameter x with normal distribution	[unit of x]
$\sigma'(x)$	= coefficient of variation of measured parameter: $= \sigma(x)/ \mu(x)$	[unit of x]
ω	= angular frequency $= 2\pi/T_{m-1,0}$	[rad/s]
ξ_o	= breaker parameter based on s_o $(= \tan\alpha/s_o^{1/2})$	[-]
ξ_{om}	= breaker parameter based on s_{om}	[-]
ξ_{op}	= breaker parameter based on s_{op}	[-]
$\xi_{m-1,0}$	= breaker parameter based on $s_{m-1,0}$	[-]
Γ	= mathematical gamma function	[-]

242

References

Allsop, N. W. H., Besley, P. & Madurini, L. 1995. Overtopping performance of vertical and composite breakwaters, seawalls and low reflection alternatives. *Paper 4.7 in MCS Project Final Report, University of Hannover.*

Altomare, C., Suzuki, T., Chen, X., Verwaest, T. and Kortenhaus, A. 2016. Wave overtopping of sea dikes with very shallow foreshores. Coastal Engineering *116, 236-257, ISSN 0378-3839, http://dx.doi.org/10.1016/j.coastaleng.2016.07.002.*

Altomare, C., Crespo, A.J.C., Domínguez, J.M., Gómez-Gesteira, M., Suzuki, T. and Verwaest, T. 2015. Applicability of Smoothed Particle Hydrodynamics for estimation of sea wave impact on coastal structures. *Coastal Engineering 96, 1-12.*

AMAZON: Hu, K., Mingham, C.G. and Causon D.M. 2000. Numerical simulation of wave overtopping of coastal structures using the non-linear shallow water equations. *Coastal Engeering, 41, pp. 433-465.*

Aminti, P. and Franco, L. 2001. Performance of overspill basin on top of breakwaters. *Proc. Int. Conf. in Ocean Engineering, Chennai, India, pp.41-46.*

ANEMONE: Dodd, N. 1998. A numerical model of wave run-up, overtopping and regeneration. *ASCE J. Waterw. Port Coast. Ocean Eng., 124 (2), pp. 73–81.*

Asbeck, W. F. Baron van, Ferguson, H. A., & Schoemaker, H. J. 1953. New designs of breakwaters and seawalls with special reference to slope protection. *Proc. 18th Int. Nav. Congress, Rome, Sect. 2, Qu. 1, p. 174.*

Battjes, J. A. & Groenendijk, H. W. 2000. Wave height distributions on shallow foreshores. *Coastal Engineering Vol 40 pp161-182, Elsevier.*

Besley, P. 1999. Overtopping of seawalls – design and assessment manual. *R & D Technical Report W 178, Environment Agency, Bristol, ISBN 1 85705 069 X.*

Brampton A. (Editor) 2002. Coastal defence – ICE design and practice guide. *ISBN 0 7277 3005 3, Thomas Telford, London.*

Briganti R., Dodd, N., Pokrajac D., O'Donoghue T. 2011 Nonlinear shallow water modelling of bore-driven swash: Description of the bottom boundary layer. *Coastal Engineering 58 (6), 463-477*

Bruce, T., Van der Meer, J.W., Franco, L. and Pearson, J.M. 2009. Overtopping performance of different armour units for rubble mound breakwaters. Special Issue of Journal of Coastal Engineering, 56, pp. 166-179.

Bruce, T., Pullen, T., Allsop, W. & Pearson, J. 2005. How far back from a seawall is safe? Spatial distributions of wave overtopping. *Proc. International Conference on Coastlines, Structures and Breakwaters 2005, pp166–176, ICE London, Thomas Telford, ISBN 0 7277 3455 5.*

Bruce, T., Allsop, N. W. H., & Pearson, J. 2002. Hazards at coast and harbour seawalls – velocities and trajectories of violent overtopping jets. *Proc. ICCE, ASCE, pp 2216–2226.*

BS 6349 2000. British Standards. Maritime structures – Part 1: Code of practice for general criteria. ISBN 0 580 33169 5.

Burcharth, H. F., Hawkins, S. J., Zanuttigh, B. & Lamberti, A 2007. Environmental Design Guidelines for Low Crested Coastal Structures. *Elsevier, ISBN-13:978-0-08-044951-7.*

Cavani, A., Franco, L. and Napolitano, M. 1999. Design optimization with model tests for the protection of Gela caisson breakwater. *Proc. Coastal Structures 1999, pp. 927-935.*

Caires, S. and Van Gent, M.R.A. 2012. Wave height distribution in constant and finite depths. *Proc. ICCE, ASCE.*

243

CIRIA / CUR. 1991 Manual on the use of rock in coastal and shoreline engineering. *CIRIA special publication 83, CUR Report 154*, Simm J. D.(Editor), 1991.

CLASH. Crest Level Assessment of coastal Structures by full scale monitoring, neural network prediction and Hazard analysis on permissible wave overtopping. *Fifth Framework Programme of the EU, Contract n. EVK3-CT-2001-00058.* www.clash-eu.org.

Coastal Engineering Manual 2006. *Coastal Engineering Research Centre, Report No. EM 1110-2-1100, US Army Corps of Engineers, Washington DC, USA.*

COBRAS: Liu, P., Lin, P. and Chang, K. and Sakakiyama, T. 1999. Numerical modeling of wave interaction with porous structures. *J. Waterw. Port Coast. Ocean Eng., 125, pp. 322–330.*

ComCoast. COMbined functions in COASTal defence zones. www.comcoast.org.

COMFLOW: Wenneker, I., Wellens, P. and Gervelas, R. 2010. Volume-of-fluid model comflow simulations of wave impacts on a dike. *Proc. ICCE, ASCE.*

CornerDike. Effect of very oblique waves on wave run-up and wave overtopping. *Hydralab project HyIV-DHI-05.*

Cornett, A., Li, Y. & Budvietas, A. 1999. Wave overtopping at chamfered and overhanging vertical structures. *Proc. International Workshop on Natural Disasters by Storm Waves and Their Reproduction in Experimental Basins, Kyoto, Japan.*

Dalrymple, R.A., Knio, O., Cox, D.T., Gomez-Gesteira, M. and Zou, S. 2001. Using a Lagrangian particle method for deck overtopping. *Proc. Waves, ASCE, pp. 1082–1091.*

De Jong, R.J. 1996. Wave transmission at low-crested structures. Stability of tetrapods at front, crest and rear of a low-crested breakwater. *MSc-thesis, Delft University of Technology.*

Del Jesus, Lara, J.L. and Losada I.J. 2012. Three-dimensional interaction of waves and porous coastal structures. Part I: numerical model formulation. *Coastal Engineering, 64, pp. 57–72.*

DELOS. Environmental Design of Low Crested Coastal Defence Structures. *Fifth Framework Programme of the EU, Contract n. EVK3-CT-00041.* www.delos.unibo.it.

EA / Besley, P. 1999 Overtopping of seawalls – design and assessment manual. *R & D Technical Report W 178, Environment Agency, Bristol, ISBN 1 85705 069 X.*

EAK: 2002 Empfehlungen des Arbeitsausschusses Küstenschutzwerke. *Die Küste. H. 65.*

EurOtop 2007. European Manual for the Assessment of Wave Overtopping. Pullen, T, Allsop, N.W.H. Bruce, T. Kortenhaus, A. Schüttrumpf, H. and Van der Meer, J.W. *At: www.overtopping-manual.com.*

FLOODSITE. Integrated Flood Risk Analysis and Management Methodologies. EU 6th Framework programme, Contract Number: GOCE-CT-2004-05420. http://www.floodsite.net/html/project_overview.htm.

FLOW-3D: Vanneste, D and Troch, P. 2015. 2d numerical simulation of large-scale physical model tests of wave interaction with a rubble-mound breakwater. *Coastal Engineering, 103, pp. 22–41.*

FlowDike. Influence of wind and current on wave run-up and wave overtopping. EU-HYDRALAB-III Project and BMBF-KFKI project FlowDike-D, 03KIS075 (IWW), 03KIS076 (IWD).

Formentin, S., Zanuttigh, B. and Van der Meer, J.W. 2016. An advanced neural network tool for predicting the performance parameters of wave-structure interaction. *Coastal Engineering Journal, in press.*

Formentin S. M. and Zanuttigh, B. 2013. Prediction of wave transmission through a new artificial neural network developed for wave reflection, *Proc. 7th International Conference on Coastal Dynamics, Arcachon, 24-28 June 2013, 627-638,* www.coastaldynamics2013.fr/pdf_files/057_Formentin_SaraMizar.pdf

Franco, C. & Franco, L. 1999 Overtopping formulae for caisson breakwaters with non-breaking 3-d waves. *Jo. Waterway, Port, Coastal & Ocean Engineering, Vol 125, No 2, ASCE, New York, pp 98-107.*

Franco, L., Geeraerts, J.,Briganti, R.,Willems, M.,Bellotti, G. and De Rouck, J. 2009. Prototype measurements and small-scale model tests of wave overtopping at shallow rubble mound breakwaters: the Ostia-Rome yacht harbour case. *Coastal Engineering, 56, 154-165.*

Franco, L., de Gerloni, M. & van der Meer, J. W. 1994. Wave overtopping on vertical and composite breakwaters. *Proc. 24th Int. Conf. on Coastal Eng. Kobe pp1030–1044.*

Geeraerts, J., De Rouck, J., Beels, C., Gysens, S., De Wolf, P. 2006. Reduction of wave overtopping at seadikes: stilling wave basin (SWB*). Proc. ICCE, ASCE, pp. 4680–4691.*

Goda, Y. 2000 Random seas and design of maritime structures (2nd edition). *World Scientific, Singapore, ISBN 981-02-3256-X.*

Hirt C.W. and Nichols B.D. 1981. *J. Comp. Phys. Vol. 39, pp. 201-225.*

Holthuijsen, L.H. 2007. Waves in oceanic and coastal waters. *Cambridge University Press.*

Hughes, S.A. 1993. Physical Models and Laboratory Techniques in Coastal Engineering. Advanced Series on Ocean Engineering: Volume 7. World Scientific.

Hughes, S., Thornton, C., Van der Meer, J.W. and Scholl, B. 2012. Improvements in describing wave overtopping processes. *Proc. ICCE, ASCE.*

IH-2VOF: Lara, J.L., Garcia, N. and Losada, I.J. 2006. RANS modelling applied to random wave interaction with submerged permeable structures. *Coastal Engineering, 53, pp. 395–417.*

IHFOAM: Lara, J.L., del Jesus, M. and Losada, I.J. 2012. Three-dimensional interaction of waves and porous structures. Part II: Model validation. *Coastal Engineering, 64, pp. 26–46.*

ISO 2003. Actions from waves and currents. International Standards Organisation *ISO/TC98/SC3/WG8.*

Jensen, B., Jacobsen, N.G. and Christensen, E.D. 2014. Investigations on the porous media equations and resistance coefficients for coastal structures. *Coastal Engineering, 84, pp. 56–72.*

Kortenhaus, A., Pearson, J., Bruce, T., Allsop, N. W. H. & van der Meer, J. W. 2003. Influence of parapets and recurves on wave overtopping and wave loading of complex vertical walls. *Proc 'Coastal Structures 2003', pp 369–381, ASCE, Reston, Virginia, ISBN0-7844-0733-9.*

Lorke, S., Bornschein, A., Schüttrumpf, H. and Pohl, R. 2012. FlowDike-D. Influence of wind and current on wave run-up and wave overtopping. Final report. *EU-HYDRALAB-III Project and BMBF-KFKI project FlowDike-D, 03KIS075 (IWW), 03KIS076 (IWD).*

LVOF: Li, T., Troch, P. and De Rouck, J. 2004. Wave overtopping over a sea dike. *Journal of Computational Physics. 198(2), 686-726.*

Lykke Andersen, T. 2006. Hydraulic response of rubble mound Breakwaters. Scale effects – berm breakwaters. *Ph.D. Thesis, Department of Civil Engineering, Aalborg University, Denmark.*

Lykke Andersen, T. and Burcharth, H.F. 2004a. CLASH D24 Report on additional tests, Part A. . www.clash-eu.org.

Lykke Andersen, T. and Burcharth, H.F. 2004b. CLASH D24 Report on additional tests, Part D. . www.clash-eu.org.

Lynett, P.J., Melby, J.A. and Kim, D.-H. 2010. An application of Boussinesq modeling to hurricane wave overtopping and inundation. *Ocean Eng., 37 (1), pp. 135–153.*

Frostick, L.E., McLelland, S.J. and Mercer, T.G. 2011. Users Guide to Physical Modelling and Experimentation: Experience of the HYDRALAB Network. *IAHR design manual. CRC press.* ISBN 9780415609128

McCabe, M. Stansby, P. and Apsley, D. 2013. Random wave runup and overtopping a steep sea wall: shallow-water and Boussinesq modelling with generalised breaking and wall impact algorithms validated against laboratory and field measurements. *Coastal Engineering, 74, pp. 33–49.*

McConnell K. J. 1998. Revetment systems against wave attack: a design manual. *ISBN 0-7277-2706-0, Thomas Telford, London.*

Molines, J. and Medina, J.R. 2015. Calibration of overtopping roughness factors for concrete armor units in non-breaking conditions using the CLASH database. *Coastal Engineering 96, pp. 62-70.*

Monaghan, J.J. 1992. Smoothed particle hydrodynamics. *Annual Review of Astronomy and Astrophysics 30, pp. 543–574.*

Napp, N., Bruce, T., Pearson, J. and Allsop, N.W.H. 2004. Violent overtopping of vertical seawalls under oblique wave conditions. *Proc. ICCE, ASCE, pp. 4482-4493.*

ODIFLOCS: Van Gent, M.R.A 1994. The modelling of wave action on and in coastal structures. *Coastal Engineering. 22, pp. 311-339.*

OPTICREST. The OPTImisation of CREST level design of sloping coastal structures through prototype monitoring and modelling. *European Union, Contract number: MAS3-CT97-0116.*

Osher, S. and Sethian, J. A. 1988. Fronts propagating with curvature-dependent speed: Algorithms based on Hamilton–Jacobi formulations. *J. Comp. Phys. Vol. 79: pp.12–49.*

Owen, M. W. 1980. Design of seawalls allowing for wave overtopping. *HR Wallingford, Report EX 924.*

Panizzo, A. and Briganti R. 2007. Analysis of wave transmission behind low crested breakwaters using neural networks. *Coastal Engineering, 54, 643–656.*

Pearson, J., Bruce, T., Allsop, N. W. H., Kortenhaus, A. and Van der Meer, J. W. 2004. Effectiveness of recurve wave walls in reducing wave overtopping on seawalls and breakwaters. *Proc. ICCE, ASCE, pp. 4404–4416.*

Pearson, J., Bruce, T., Allsop, N. W. H. & Gironella, X. 2002. Violent wave overtopping – measurements at large and small scale. *Proc. ICCE, ASCE, pp 2227–2238.*

PIANC 1992. Analysis of Rubble mound breakwaters. *Report Working Group 12.*

Pohl, R. Bornschein, A., Schüttrumpf, H. Troch, P., Riha, J., Van der Meer, J.W. and Müller, N. 2014. Effect of very oblique waves on wave run-up and wave overtopping. Final Report. *Hydralab project HyIV-DHI-05.*

Polidori, A., Dornbusch, U. and Pullen, T. 2013. Improved maximum run-up formula for mixed beaches based on field data. *Proc. ICE, Coasts, Marine Structures and Breakwaters 2013, Edinburgh, UK.*

PROVERBS 2001. Probabilistic design tools for vertical breakwaters. H. Oumeraci, A. Kortenhaus, N.W.H. Allsop, M. de Groot, R. Crouch, H. Vrijling and H. Voortman. *Balkema Publishers, ISBN 90 5809 248 8.*

Pullen, T., Allsop, N. W. H., Bruce, T., Pearson, J. and Geeraerts, J. 2004. Violent wave overtopping at Samphire Hoe: field and laboratory measurements. *Proc. ICCE, SCE, pp. 4379–4390.*

RBREAK: Kobayashi, N. and Wurjanto, A. 1989. Wave overtopping on coastal structures. *ASCE J. Waterw. Port Coast. Ocean Eng., 115 (2), pp. 235–251.*

Rock Manual 2007. The Rock Manual. *The use of rock in hydraulic engineering*, CIRIA, CUR, CETMEF.

Romano, A., Bellotti G., Briganti R., Franco L. Uncertainties in the physical modelling of the wave overtopping over a rubble mound breakwater: the role of the seeding number and of the test duration *Coastal Engineering, 103 (2015), 15–21.*

Schüttrumpf, H. & van Gent, M. R. A. 2003. Wave overtopping at seadikes. *ASCE, Proc. Coastal Structures 2003, Portland, USA, pp. 431 – 443.*

Schüttrumpf, H. 2001. Wellenüberlaufströmung bei Seedeichen – Experimentelle und Theoretische Untersuchungen. *PhD-Thesis.*

246

Schüttrumpf, H., Kortenhaus, A., Petes, K. and Fröhle, P. 2006. Expert Judgement of Uncertainties in Coastal Structure design. *Proc. ICCE, ASCE.*

Schüttrumpf, H. and Oumeraci, H. 2005. Scale and Model effects in crest level design. *Proc. 2nd Coastal Symposium. Höfn. Iceland.*

Shao, S. 2010. Incompressible SPH flow model for wave interactions with porous media. Coastal Engineering, 57 (3), pp. 304-316.

Sigurdarson, S. and Van der Meer, J.W. 2012. Wave overtopping at berm breakwaters in line with EurOtop. *Proc. ASCE, ICCE.*

Simm, J. D., Brampton, A. H., Beech, N. W. & Brooke, J. S. 1996. Beach management manual. *Report 153, ISBN: 0-86017 438 7, CIRIA, London.*

SKYLLA: Van der Meer J.W., Petit, H.A.H., Van den Bosch, P., Klopman, G. and Broekens, R.D. 1992. Numerical simulation of wave motion on and in coastal structures. *Proc. ICCE, ASCE, pp. 1772-1784.*

Stansby, P.K. 2003. Solitary wave run-up and overtopping by a semi-implicit finite-volume shallow water Bousinesq model. *J. Hydraul. Res., 41 (6), pp. 639–647.*

Suzuki, T., Altomare, C., Verwaest, T., Trouw, K. and Zijlema, M. 2014. Two-dimensional wave overtopping calculation over a dike in shallow foreshore by SWASH. *Proc. ICCE, ASCE.* doi: http://dx.doi.org/10.9753/icce.v34.structures.3

SWASH: Zijlema, M. and Stelling, G.S. 2011. Swash: an operational public domain code for simulating wave fields and rapidly varied flows in coastal waters. *Coastal Engineering, 58, pp. 92–1012.*

TAW 2003. Guideline wet infrastructure. (In Dutch: Leidraad Kunstwerken). *Technical Advisory Committee for Flood Defence in the Netherlands (TAW). Delft.*

TAW 2002. Technical Report – Wave run-up and wave overtopping at dikes. *Technical Advisory Committee for Flood Defence in the Netherlands (TAW). Delft.*

TAW 1999. Guideline for design of river dikes – Part 2. Downstream area. (In Dutch: Leidraad voor het ontwerpen van rivierdijken. Deel 2 – Benedenrivierengebied). *Technical Advisory Committee for Flood Defence in the Netherlands (TAW). Delft.*

TAW 1997. Technical Report – Erosion Resistance of grassland as dike covering. *Technical Advisory Committee for Flood Defence in the Netherlands (TAW). Delft.*

THESEUS 2014. Coastal risk management in a changing climate. Zanuttigh, B., Nicholls, R., Vanderlinden, J. P., Burcharth, H. F. and Thompson, R. C. – editors. *Elsevier, 671 pp., ISBN 978 0-12-397310-8.*

Tonelli, M. and Petti, M. 2013. Numerical simulation of wave overtopping at coastal dikes and low-crested structures by means of a shock-capturing Boussinesq model. *Coastal Engineering, 79, pp. 75-88.*

Tuan, T.Q. and Oumeraci, H. 2010. A numerical model of wave overtopping on seadikes. *Coastal Engineering, 57, pp. 757-772.*

Van der Meer, J.W. 2011. The Wave Run-up Simulator. Idea, necessity, theoretical background and design. Van der Meer Consulting Report vdm11355, www.vdm-c.nl.

Van der Meer, J.W. 2010. Influence of wind and current on wave run-up and wave overtopping. Detailed analysis on the influence of current on wave overtopping. Van der Meer Consulting Report vdm08310, www.vdm-c.nl

Van der Meer, J.W. and Sigurdarson, S. 2016. Design and Construction of Berm Breakwaters. *World Scientific. Advanced Series on Ocean Engineering, Volume 40. ISBN 978-981-4749-60-2.*

Van der Meer, J.W. and Bruce, T. 2014. New physical insights and design formulas on wave overtopping at sloping and vertical structures. *Journal of Waterway, Port, Coastal and Ocean Engineering, 140.* DOI 10.1061/(ASCE)WW.1943-5460.0000221

247

Van der Meer, J.W., Y. Provoost and Steendam, G.J. 2012. The wave run-up simulator, theory and first pilot test. *ASCE, Proc. ICCE 2012.*

Van der Meer, J.W., Verhaeghe, H. and Steendam, G.J. 2009. The new wave overtopping database for coastal structures. *Coastal Engineering, 56, 108–120.*

Van der Meer, J.W., Briganti, R., Zanuttigh, B. and B. Wang, 2005. Wave transmission and reflection at low crested structures: design formulae, oblique wave attack and spectral change. *Coastal Engineering, 52 (10-11), 915-929.*

Van der Meer, J. W. 1988. Rock slopes and gravel beaches under wave attack. *PhD-Thesis Delft University of Technology. Also Delft Hydraulics Publications. No. 396.*

Van Doorslaer, K. and De Rouck, J. 2016. The reduction of wave overtopping by means of a storm wall. *Proc. ICCE, ASCE, in press.*

Van Doorslaer, K., De Rouck, J., Audenaert, S. and Duquet, V. 2015. Crest modifications to reduce wave overtopping of non-breaking waves over a smooth dike slope. *Coastal Engineering, 101, pp. 69-88.*

Van Gent, M.R.A., van den Boogaard, H.F.P., Pozueta, B. and Medina, J.R. 2007. Neural network modelling of wave overtopping at coastal structures. *Coastal Engineering 54, 586–593.*

Van Gent, M. R. A. 1999. Physical Model Investigations on Coastal Structures with shallow foreshores - 2D model tests with single and double peaked wave energy spectra. *Delft Hydraulics. Report H. 3608.*

Van Gent, M.R.A., Plate, S.E., Berdendsen, E., Spaan, G.B.H., Van der Meer, J.W. and d'Angremond, K. 1999. Single-layer rubble mound breakwaters. *Proc. Coastal Structures 1999.*

Van Oosten, R.P. and Peixò Marco J. 2005. Wave transmission at various types of low-crested structures using neural networks. *MsC Thesis, TU Delft, Faculty of Civil Engineering and Geosciences, Hydraulic Engineering.*

Van Steeg, P., Klein Breteler, M. and Provoost, Y. 2016. Large-scale physical model tests to determine influence factor of roughness for wave run-up of channel shaped block revetments. *Proc. Coastlab16.*

Van Steeg, P. 2014. Residual strength of grass on river dikes under wave attack. Phase 3: Large scale flume model tests on soil and grass of locations Harculo and Oosterbierum. *Deltares Report 1207811-009.*

Verhaeghe, H., De Rouck, J. and Van der Meer, J.W. 2008. Combined classifier–quantifier model: a 2-phases neural model for prediction of wave overtopping at coastal structures. *Coastal Engineering 55, 357–374.*

Victor L. 2012. Optimization of the hydrodynamic performance of overtopping wave energy converters: experimental study of optimal geometry and probability distribution of overtopping volumes. *PhD dissertation, Ghent University, Belgium.*

VOFbreak²: Troch, P. and De Rouck J. 1999. An active wave generating-absorbing boundary condition for VOF type numerical model. *Coastal Engineering, Vol. 38 (4), pp. 223-247.*

VOWS. Violent Overtopping by Waves at Seawalls (VOWS). EPSRC research project.

Big-VOWS. . Violent Overtopping by Waves at Seawalls (VOWS) - Large Scale Tests. EPSRC Reference: GR/R42306/01.

Zanuttigh, B. and Van der Meer, J.W. 2008. Wave reflection from coastal structures in design conditions. *Coastal Engineering, 55 (10), 771-779.*

Zanuttigh, B., Formentin, S. and Van der Meer, J.W. 2016. Prediction of extreme and tolerable wave overtopping discharges through an advanced neural network. *Ocean Engineering 127 (2016) 7-22;* http://dx.doi.org/10.1016/j.oceaneng.2016.09.032.

Zanuttigh, B., Formentin, S. M. and Briganti, R. 2013. A Neural Network for the prediction of wave reflection from coastal and harbour structures. *Coastal Engineering, 80, 49-67.*

Zanuttigh, B., Van der Meer, J.W., Bruce, T. and Hughes, S. 2013. Statistical characterisation of extreme overtopping wave volumes. *Proc. ICE, Coasts, Marine Structures and Breakwaters 2013, Edinburgh, UK.*

249

A   Structure of the EurOtop calculation tool

To be implemented in the final version.

251